

**Lower Passaic River
Contaminant Fate and Transport Model**

**LOWER EIGHT MILES OF THE LOWER PASSAIC RIVER
LOWER PASSAIC RIVER CONTAMINANT FATE AND TRANSPORT MODEL**

TABLE OF CONTENTS

1	Introduction.....	1-1
1.1	Purpose and Objective	1-1
1.2	Modeling Approach	1-1
2	Modeling Framework.....	2-1
2.1	Organic Carbon Production Model.....	2-1
2.1.1	Introduction	2-1
2.1.2	System-Wide Eutrophication Model (SWEM) Background.....	2-2
2.1.3	Incorporating Sediment Transport into SWEM	2-8
2.2	Contaminant Fate and Transport Model	2-23
2.2.1	Introduction	2-23
2.2.2	Interfacing With the Other LPR Sub-Models.....	2-24
2.2.3	RCATOX Bed Structure	2-28
3	Model Inputs	3-1
3.1	Organic Carbon Production Model.....	3-1
3.1.1	Boundary Conditions.....	3-1
3.1.2	Wastewater Treatment Plant Loadings.....	3-3
3.1.3	Stormwater and Combined-sewer Overflows	3-3
3.1.4	Atmospheric Loadings	3-5
3.1.5	Sediment Properties.....	3-6
3.1.6	Parameters and Constants.....	3-7
3.2	Contaminant Fate and Transport Model	3-7
3.2.1	Boundary Conditions.....	3-7

3.2.2	Wastewater Treatment Plant Loadings.....	3-14
3.2.3	Stormwater and Combined-sewer Overflows	3-14
3.2.4	Atmospheric Loadings	3-16
3.2.5	Assignment of Initial Conditions for Sediment Contaminant Concentrations.....	3-17
3.2.6	Parameters and Constants.....	3-27
4	Model Calibration.....	4-1
4.1	Introduction.....	4-1
4.2	Carbon Model Verification.....	4-1
4.3	Contaminant Model Calibration	4-6
4.4	Model Comparisons to Data	4-8
4.4.1	Spatial Transect Plots	4-9
4.4.2	Reach Average Time Series Plots	4-11
4.4.3	Data and Model Scatter Plots	4-14
4.5	Uncertainty.....	4-17
4.6	Summary	4-19
5	Sensitivity Analyses.....	5-1
5.1	Introduction.....	5-1
5.2	Upstream Boundary	5-1
5.3	Partitioning Coefficients	5-3
5.4	Depth of Mixing.....	5-4
5.5	Rate of Mixing	5-5
5.6	One in One Hundred Year Storm.....	5-6
5.7	Sensitivity Summary	5-6
6	Evaluation of Remedial Alternatives	6-1

6.1	Introduction.....	6-1
6.2	Description of Alternatives.....	6-3
6.3	Future Contaminant Concentrations	6-5
6.3.1	2,3,7,8 TCDD Results	6-6
6.3.2	Tetra-PCB Homolog Group Results.....	6-10
6.3.3	Total Mercury Results	6-11
6.4	Net Contaminant Mass Transport	6-12
6.5	Risk Assessment Linkage	6-14
6.6	Uncertainty.....	6-15
7	References.....	7-1

**LOWER EIGHT MILES OF THE LOWER PASSAIC RIVER
LOWER PASSAIC RIVER CONTAMINANT FATE AND TRANSPORT MODEL**

LIST OF TABLES

Table 2-1	24 State Variables Included in SWEM.....	2-4
Table 2-2	Organic Carbon Reaction Equations.....	2-11
Table 2-3	Organic Carbon Forms Included in ST-SWEM.....	2-15
Table 2-4	ECOMSEDZLJS – ST-SWEM Coupling.....	2-19
Table 2-5	Information Passed from ST-SWEM to RCATOX	2-27
Table 3-1	Stormwater and Combined Sewer Concentrations	3-4
Table 3-2	Atmospheric Loads for ST-SWEM	3-6
Table 3-3	RCATOX Head of Tide Concentrations for Measured Tributaries.....	3-11
Table 3-4	Combined Sewer and Storm Water Overflow Concentrations	3-15
Table 3-5	LPR Contaminants of Concern (COPC).....	3-19
Table 3-6	LPR Sediment Investigations.....	3-21
Table 3-7	Chemical Constants	3-27
Table 4-1	LPR Water Column Investigations	4-2
Table 4-2	Model Calibration Results	4-19

**LOWER EIGHT MILES OF THE LOWER PASSAIC
LOWER PASSAIC RIVER CONTAMINANT FATE AND TRANSPORT MODEL
LIST OF FIGURES**

- Figure 1-1 Model Domain
- Figure 2-1 Water Quality Model Phytoplankton Kinetics
- Figure 2-2 RCATOX Bed Structure
- Figure 3-1 Upper Passaic River Total Particulate Organic Carbon (POC) Boundary Condition
- Figure 3-2 Upper Passaic River Algal POC Boundary Condition
- Figure 3-3 Upper Passaic River Dissolved Organic Carbon Boundary Condition
- Figure 3-4 Upper Passaic River Boundary Fraction Organic Carbon (FOC)
- Figure 3-5 Sediment FOC Cycled Initial Condition in the LPR and Interpolated Initial Conditions in Newark Bay
- Figure 3-6 Sediment FOC Cycled Initial Condition in the LPR and Interpolated Initial Conditions in Newark Bay
- Figure 3-7 Upper Passaic River Boundary 2,3,7,8-TCDD
- Figure 3-8 Upper Passaic River Boundary Sum of Tetrachlorobiphenyl PCBs
- Figure 3-9 Upper Passaic River Boundary Total Mercury
- Figure 3-10 Map of the LPR showing sediment sampling points and shaded geomorphic regions
- Figure 3-11 Map of the LPR showing the model grid and shaded geomorphic regions
- Figure 3-12 Map of 2,3,7,8-TCDD Initial Conditions for the Top Six Inches of the LPR
- Figure 3-13 Map of Newark Bay, Arthur Kill and Kill Van Kull Regions
- Figure 3-14 Map of 2,3,7,8-TCDD Initial Conditions for the Top Six Inches of the Newark Bay, the Arthur Kill and the Kill Van Kull

- Figure 3-15 Map of 2,3,7,8-TCDD Initial Conditions for the Top Six Inches Throughout the Model Domain
- Figure 4-1 Legend for Sediment and Water Column Datasets Compared to Model Results
- Figure 4-2 Transect Comparison of Carbon Model Compared to NJHDG Data (June 2011, page 1)
- Figure 4-3 Transect Comparison of Carbon Model Compared to NJHDG Data (June 2011, page 2)
- Figure 4-4 Transect Comparison of Carbon Model Compared to NJHDG Data (May 2007, page 1)
- Figure 4-5 Transect Comparison of Carbon Model Compared to NJHDG Data (May 2007, page 2)
- Figure 4-6 Water Column POC X-Y Scatter Plot
- Figure 4-7 Water Column DOC X-Y Scatter Plot
- Figure 4-8 Sediment FOC X-Y Scatter Plot
- Figure 4-9 Sediment Particle Mixing Rates From Other Studies (Adapted from Boudreau, 1994)
- Figure 4-10 Initial Model Runs to Develop the Starting Point for the Calibration
- Figure 4-11 2,3,7,8-TCDD Surface Sediment Transect Plots (1995, Initial Conditions)
- Figure 4-12 2,3,7,8-TCDD Surface Sediment Transect Plots (1996)
- Figure 4-13 2,3,7,8-TCDD Surface Sediment Transect Plots (1997)
- Figure 4-14 2,3,7,8-TCDD Surface Sediment Transect Plots (1998)
- Figure 4-15 2,3,7,8-TCDD Surface Sediment Transect Plots (1999)
- Figure 4-16 2,3,7,8-TCDD Surface Sediment Transect Plots (2000)
- Figure 4-17 2,3,7,8-TCDD Surface Sediment Transect Plots (2001)

- Figure 4-18 2,3,7,8-TCDD Surface Sediment Transect Plots (2002)
- Figure 4-19 2,3,7,8-TCDD Surface Sediment Transect Plots (2003)
- Figure 4-20 2,3,7,8-TCDD Surface Sediment Transect Plots (2004)
- Figure 4-21 2,3,7,8-TCDD Surface Sediment Transect Plots (2005)
- Figure 4-22 2,3,7,8-TCDD Surface Sediment Transect Plots (2006)
- Figure 4-23 2,3,7,8-TCDD Surface Sediment Transect Plots (2007)
- Figure 4-24 2,3,7,8-TCDD Surface Sediment Transect Plots (2008)
- Figure 4-25 2,3,7,8-TCDD Surface Sediment Transect Plots (2009)
- Figure 4-26 2,3,7,8-TCDD Surface Sediment Transect Plots (2010)
- Figure 4-27 2,3,7,8-TCDD Surface Sediment Transect Plots (2011)
- Figure 4-28 2,3,7,8-TCDD Surface Sediment Transect Plots (2012)
- Figure 4-29 2,3,7,8-TCDD Reach and Sub-reach Sediment Calibration (RM0 to 8.3)
- Figure 4-30 2,3,7,8-TCDD Reach and Sub-reach Sediment Calibration (RM8.3 to 17)
- Figure 4-31 2,3,7,8-TCDD Reach and Sub-reach Sediment Calibration (RM0 to -1.5)
- Figure 4-32 2,3,7,8-TCDD Reach and Sub-reach Sediment Calibration
(RM-1.5 to -2.6)
- Figure 4-33 2,3,7,8-TCDD Reach and Sub-reach Sediment Calibration
(RM-2.6 to -5.25)
- Figure 4-34 2,3,7,8-TCDD Reach Water Column Calibration LPR
- Figure 4-35 2,3,7,8-TCDD Reach Water Column Calibration Newark Bay
- Figure 4-36 Tetrachlorobiphenyl Reach and Sub-reach Sediment Calibration
(RM0 to 8)
- Figure 4-37 Tetrachlorobiphenyl Reach and Sub-reach Sediment Calibration
(RM8.3 to 17)

- Figure 4-38 Tetrachlorobiphenyl Reach and Sub-reach Sediment Calibration (RM0 to -1.5)
- Figure 4-39 Tetrachlorobiphenyl Reach and Sub-reach Sediment Calibration (RM-1.5 to -2.6)
- Figure 4-40 Tetrachlorobiphenyl Reach and Sub-reach Sediment Calibration (RM-2.6 to -5.25)
- Figure 4-41 Tetrachlorobiphenyl Reach Water Column Calibration LPR
- Figure 4-42 Tetrachlorobiphenyl Reach Water Column Calibration Newark Bay
- Figure 4-43 Mercury Reach and Sub-reach Sediment Calibration (RM0 to 8)
- Figure 4-44 Mercury Reach and Sub-reach Sediment Calibration (RM8.3 to 17)
- Figure 4-45 Mercury Reach and Sub-reach Sediment Calibration (RM0 to -1.5)
- Figure 4-46 Mercury Reach and Sub-reach Sediment Calibration (RM-1.5 to -2.6)
- Figure 4-47 Mercury Reach and Sub-reach Sediment Calibration (RM-2.6 to -5.25)
- Figure 4-48 Mercury Reach Water Column Calibration LPR
- Figure 4-49 Mercury Reach Water Column Calibration Newark Bay
- Figure 4-50 2,3,7,8-TCDD Sediment Data and Model Scatter Plots
- Figure 4-51 2,3,7,8-TCDD Water Column Data and Model Scatter Plots
- Figure 4-52 Tetrachlorobiphenyl Sediment Data and Model Scatter Plots
- Figure 4-53 Tetrachlorobiphenyl Water Column Data and Model Scatter Plots
- Figure 4-54 Mercury Sediment Data and Model Scatter Plots
- Figure 4-55 Mercury Water Column Data and Model Scatter Plots
- Figure 5-1 Sediment 2,3,7,8-TCDD Response to Dundee Dam Sensitivity (RM0-8.3)
- Figure 5-2 Sediment 2,3,7,8-TCDD Response to Dundee Dam Sensitivity (RM8.3-17)
- Figure 5-3 Water Column 2,3,7,8-TCDD Response to Dundee Dam Sensitivity

- Figure 5-4 Sediment OCCD Response to Dundee Dam Sensitivity (RM0-8.3)
- Figure 5-5 Sediment OCCD Response to Dundee Dam Sensitivity (RM8.3-17)
- Figure 5-6 Water Column OCCD Response to Dundee Dam Sensitivity
- Figure 5-7 Sediment 2,3,7,8-TCDD Response to Partition Coefficient Sensitivity (RM0-8.3)
- Figure 5-8 Sediment 2,3,7,8-TCDD Response to Partition Coefficient Sensitivity (RM8.3-17)
- Figure 5-9 Water Column 2,3,7,8-TCDD Response to Partition Coefficient Sensitivity
- Figure 5-10 Sediment 2,3,7,8-TCDD Response to Depth of Mixing Sensitivity (RM0-8.3)
- Figure 5-11 Sediment 2,3,7,8-TCDD Response to Depth of Mixing Sensitivity (RM8.3-17)
- Figure 5-12 Water Column 2,3,7,8-TCDD Response to Depth of Mixing Sensitivity
- Figure 5-13 Sediment 2,3,7,8-TCDD Response to Rate of Mixing Sensitivity (RM0-8.3)
- Figure 5-14 Sediment 2,3,7,8-TCDD Response to Rate of Mixing Sensitivity (RM8.3-17)
- Figure 5-15 Water Column 2,3,7,8-TCDD Response to Rate of Mixing Sensitivity
- Figure 5-16 Sediment 2,3,7,8-TCDD Response to One Hundred Year Storm Sensitivity (RM0-8.3)
- Figure 5-17 Sediment 2,3,7,8-TCDD Response to One Hundred Year Storm Sensitivity (RM8.3-17)
- Figure 5-18 Water Column 2,3,7,8-TCDD Response to One Hundred Year Storm Sensitivity
- Figure 6-1 Tierra Removal, Phase 1 and Phase Areas

- Figure 6-2 Areas Capped in Alternative 4 - Focused Capping with Dredging for Flooding
- Figure 6-3 Log Scale Temporal Plots of 2,3,7,8 TCDD sediment concentrations for No Action and Three Remedial Alternatives (RM0-8.3)
- Figure 6-4 Log Scale Temporal Plots of 2,3,7,8 TCDD sediment concentrations for No Action and Three Remedial Alternatives (RM8.3-17)
- Figure 6-5 Log Scale Temporal Plots of 2,3,7,8 TCDD sediment concentrations for No Action and Three Remedial Alternatives (RM0 to -1.5)
- Figure 6-6 Log Scale Temporal Plots of 2,3,7,8 TCDD sediment concentrations for No Action and Three Remedial Alternatives (RM-1.5 to -2.6)
- Figure 6-7 Log Scale Temporal Plots of 2,3,7,8 TCDD sediment concentrations for No Action and Three Remedial Alternatives (RM-2.6 to -5.25)
- Figure 6-8 Spatial Distribution of 2,3,7,8 TCDD in October 1995
- Figure 6-9 Spatial Distribution of 2,3,7,8 TCDD in January 2005
- Figure 6-10 Spatial Distribution of 2,3,7,8 TCDD in January 2012
- Figure 6-11 Spatial Distribution of 2,3,7,8 TCDD in January 2059 - No Action Simulation
- Figure 6-12 Spatial Distribution of 2,3,7,8 TCDD in January 2059 - Deep Dredging Simulation
- Figure 6-13 Spatial Distribution of 2,3,7,8 TCDD in January 2059 - Full Capping Simulation
- Figure 6-14 Spatial Distribution of 2,3,7,8 TCDD in January 2059 - Focused Capping Simulation
- Figure 6-15 Log Scale Temporal Plots of Tetra-PCB Homolog Group sediment concentrations for No Action and Three Remedial Alternatives (RM0-8.3)

- Figure 6-16 Log Scale Temporal Plots of Tetra-PCB Homolog Group sediment concentrations for No Action and Three Remedial Alternatives (RM8.3-17)
- Figure 6-17 Log Scale Temporal Plots of Tetra-PCB Homolog Group sediment concentrations for No Action and Three Remedial Alternatives (RM0 to -1.5)
- Figure 6-18 Log Scale Temporal Plots of Tetra-PCB Homolog Group sediment concentrations for No Action and Three Remedial Alternatives (RM-1.5 to -2.6)
- Figure 6-19 Log Scale Temporal Plots of Tetra-PCB Homolog Group sediment concentrations for No Action and Three Remedial Alternatives (RM-2.6 to -5.25)
- Figure 6-20 Spatial Distribution of Tetra-PCB Homolog Group in October 1995
- Figure 6-21 Spatial Distribution of Tetra-PCB Homolog Group in January 2005
- Figure 6-22 Spatial Distribution of Tetra-PCB Homolog Group in January 2012
- Figure 6-23 Spatial Distribution of Tetra-PCB Homolog Group in January 2059 - No Action Simulation
- Figure 6-24 Spatial Distribution of Tetra-PCB Homolog Group in January 2059 - Deep Dredging Simulation
- Figure 6-25 Spatial Distribution of Tetra-PCB Homolog Group in January 2059 - Full Capping Simulation
- Figure 6-26 Spatial Distribution of Tetra-PCB Homolog Group in January 2059 - Focused Capping Simulation
- Figure 6-27 Log Scale Temporal Plots of Total Mercury sediment concentrations for No Action and Three Remedial Alternatives (RM0-8.3)
- Figure 6-28 Log Scale Temporal Plots of Total Mercury sediment concentrations for No Action and Three Remedial Alternatives (RM8.3-17)

- Figure 6-29 Log Scale Temporal Plots of Total Mercury sediment concentrations for No Action and Three Remedial Alternatives (RM0 to -1.5)
- Figure 6-30 Log Scale Temporal Plots of Total Mercury sediment concentrations for No Action and Three Remedial Alternatives (RM-1.5 to -2.6)
- Figure 6-31 Log Scale Temporal Plots of Total Mercury sediment concentrations for No Action and Three Remedial Alternatives (RM-2.6 to -5.25)
- Figure 6-32 Spatial Distribution of Total Mercury in October 1995
- Figure 6-33 Spatial Distribution of Total Mercury in January 2005
- Figure 6-34 Spatial Distribution of Total Mercury in January 2012
- Figure 6-35 Spatial Distribution of Total Mercury in January 2059 - No Action Simulation
- Figure 6-36 Spatial Distribution of Total Mercury in January 2059 - Deep Dredging Simulation
- Figure 6-37 Spatial Distribution of Total Mercury in January 2059 - Full Capping Simulation
- Figure 6-38 Spatial Distribution of Total Mercury in January 2059 - Focused Capping Simulation
- Figure 6-39 Cumulative (from 2024) Water Column Contaminant Mass Transport at RM 16.7
- Figure 6-40 Cumulative (from 2024) Water Column Contaminant Mass Transport at RM 14.5
- Figure 6-41 Cumulative (from 2024) Water Column Contaminant Mass Transport at RM 12.3
- Figure 6-42 Cumulative (from 2024) Water Column Contaminant Mass Transport at RM 9.8
- Figure 6-43 Cumulative (from 2024) Water Column Contaminant Mass Transport at RM 7.8

- Figure 6-44 Cumulative (from 2024) Water Column Contaminant Mass Transport at RM 5.7
- Figure 6-45 Cumulative (from 2024) Water Column Contaminant Mass Transport at RM 3.1
- Figure 6-46 Cumulative (from 2024) Water Column Contaminant Mass Transport at RM 0.9
- Figure 6-47 Log Scale Temporal Plots of 2,3,7,8 TCDD Sediment Concentrations for No Action and Three Remedial Alternatives (RM0-8.3) with Uncertainty
- Figure 6-48 Log Scale Temporal Plots of Tetra-PCB Sediment Concentrations for No Action and Three Remedial Alternatives (RM0-8.3) with Uncertainty
- Figure 6-49 Log Scale Temporal Plots of Total Mercury Sediment Concentrations for No Action and Three Remedial Alternatives (RM0-8.3) with Uncertainty

**LOWER EIGHT MILES OF THE LOWER PASSAIC
LOWER PASSAIC RIVER CONTAMINANT FATE AND TRANSPORT MODEL
LIST OF ATTACHMENTS**

Attachment A	Carbon Model Transect Plots
Attachment B	Transect Plots
Attachment C-1	LPR Surface Sediment Reach Average Time Series Calibration
Attachment C-2	Newark Bay Surface Sediment Reach Average Time Series Calibration
Attachment C-3	LPR Water Column Reach Average Time Series Calibration
Attachment C-4	Newark Bay Water Column Reach Average Time Series Calibration
Attachment D-1	Surface Sediment X-Y Scatter Plots
Attachment D-2	X-Y Scatter Plots for All Layers
Attachment D-3	Water Column X-Y Scatter Plots For All Layers
Attachment E-1	LPR Surface Sediment Reach Average Time Series Projections
Attachment E-2	Newark Bay Surface Sediment Reach Average Time Series Projections
Attachment E-3	LPR Water Column Reach Average Time Series Projections
Attachment E-4	Newark Bay Water Column Reach Average Time Series Projections
Attachment F	Trajectories with Uncertainty Bounds
Attachment G	Revisions to CARP Loads

1 INTRODUCTION

1.1 PURPOSE AND OBJECTIVE

Contaminant fate and transport modeling of the Lower Passaic River (LPR) was performed as one component in an analysis of potential remedial alternatives for reducing ecological and human health risks posed by contaminated sediments in the lower eight miles of the LPR. The remedial alternatives are being evaluated by the U.S. Environmental Protection Agency (USEPA) under the Comprehensive Environmental Response, Compensation, and Liability Act (CERCLA) as part of a Focused Feasibility Study (FFS) of the lower eight miles of the LPR (FFS Study Area). Results from the sediment transport model (see Appendix BII) provide input to the contaminant fate and transport model, which will in turn provide contaminant exposure concentrations to human health and ecological risk assessments. The objective of the contaminant fate and transport modeling was to develop a mathematical representation of the processes affecting contaminant fate and transport behavior of dissolved and sorbed contaminants based upon the associated sediment transport results. The simulated contaminant results could then be used to assess human health and ecological risk associated with the contaminants of potential concern (COPC) and contaminants of potential ecological concern (COPEC) in the FFS Study Area under various remediation alternatives.

1.2 MODELING APPROACH

The contaminant fate and transport model used for these analyses was based largely on the peer reviewed model developed for NY/NJ Harbor Contaminant Assessment and Reduction Project (CARP) (HydroQual, 2007). The model is composed of two sub-models: the organic carbon production model, ST-SWEM, and the contaminant fate and transport model, RCATOX. The spatial domain is identical to the sediment transport model and extends from the upstream freshwater inputs at Dundee Dam and Oradell Dam on the Passaic and Hackensack Rivers, respectively, to the downstream tidal boundaries at the eastern end of the Kill Van Kull and the southern end of the Arthur Kill (Figure 1-

1). The spatial resolution of the fate and transport model grid, however, is coarser than the sediment transport model grid. To address concerns about model run times, up to three sediment transport model grid cells were combined into a single fate and transport model grid cell along the length of the river. The coarsened grid was developed to account for differences in contaminant transport between the main channel and shoals while still performing the long simulations required for the evaluation of risk reduction.

The model was used to simulate forty-eight of the COPCs and COPECs associated with the FFS Study Area including seven dioxins and ten furans with chlorine substitutions in the 2, 3, 7, and 8 positions, polychlorinated biphenyl (PCB) homologue sums; the twelve PCB congeners which exhibit dioxin like toxicity; dichlorodiphenyltrichloroethane (DDT) and its metabolites dichlorodiphenyldichloroethylene (DDE) and dichlorodiphenyldichloroethane (DDD); copper; and mercury for the time period from October 1, 1995 to September 30, 2059. Model results were compared to sediment contaminant concentrations measured during the period between 1995 and 2010. Carbon and contaminant fresh water head of tide boundary conditions were developed using the approach from the CARP model (HydroQual, 2007). The downstream boundary conditions at the Kills were taken from the larger-domain CARP model (HydroQual, 2007) and were mapped onto the LPR grid, which extends to the ends of the Kills.

Model calibration focused on reproducing observed contaminant concentrations and the rates of change of contaminant concentrations within the bed across the forty-eight contaminants modeled. For the carbon production sub-model all model input rates and constants were used directly from the CARP model without adjustment. For the contaminant sub-model all model input rates and constants were used directly from the CARP model with the exception of rate of mixing within the biologically active surface sediments. This parameter was modified to calibrate the model to the observed rate of sediment recovery under current conditions.

In addition to the steps taken above to improve the calibration of the model, a number of actions were taken based on the recommendations of the peer review conducted in 2013

(HDR|HydroQual, 2013). In particular the sediment transport model has been modified to increase sediment accumulation (infilling) both within the Study Area and throughout the domain. The impact of that change is reflected in the carbon and contaminant model results. The approach to setting contaminant initial conditions has also been modified (Section 3.2.5). Additional analyses have also been included in the sensitivity section of the report including the response of the model to a one in one-hundred year storm event (Section 5). More information about the peer review process, the comments received and how those comments were addressed is provided in a peer review report dated September 2013 (HDR|HQI, 2013).

2 MODELING FRAMEWORK

2.1 ORGANIC CARBON PRODUCTION MODEL

2.1.1 Introduction

Hydrophobic organic contaminants, including some dioxin/furans, PCBs and pesticides, are pollutants that are poorly soluble in water. Partitioning of such contaminants between the dissolved and particulate phases is related to the organic carbon content of the particles (POC) and, to a lesser extent, dissolved organic carbon (DOC) (Karickhoff, 1980, 1984; Di Toro, 1985; Di Toro et al., 1991). Similarly, POC has also been found to be important, as is acid-volatile sulfide, in the binding of ionic metals in sediments (Ankley et al., 1996). Therefore, the fate and transport of organic carbon are important to understanding the fate and transport of these hydrophobic chemicals. This chapter describes the theory of organic carbon production and sediment diagenesis models of the LPR and contiguous waterways. The sediment diagenesis model provides information on redox conditions and sulfide concentrations, important to quantifying the binding of metals to acid-volatile sulfide, and sulfate reduction rates in evaluating the fate and transport of mercury and the production of methyl mercury in sediments.

First, an overview of the carbon production model will be provided, followed by a discussion of the linkage to the hydrodynamic/sediment transport model. The section concludes with a brief discussion of some numerical issues that arose and were addressed during the development and calibration/validation of the carbon model.

Previous organic carbon production modeling of the LPR has been performed as part of larger regional projects. These projects addressed nutrient management issues and toxic contamination. Both prior applications of organic carbon production modeling originate from the calibrated, validated, and peer-reviewed eutrophication model developed by HydroQual as part of the System-Wide Eutrophication Model (SWEM). SWEM has

been used extensively by the New York City Department of Environmental Protection (NYCDEP) and the USEPA NY/NJ Harbor Estuary Program (HEP).

2.1.2 System-Wide Eutrophication Model (SWEM) Background

SWEM was calibrated and validated against observed water and sediment nutrient flux and quality data collected during two full annual cycles, the 12-month periods from October 1, 1994 to September 30, 1995 and from October 1, 1988 to September 30, 1989. The development, calibration, and validation of the SWEM eutrophication model are described in detail in a series of technical reports prepared by HydroQual for NYCDEP. Full citations for these reports are listed in the references section of this report (HydroQual, 1999a, b, c, d, e, f).

The peer-review process for SWEM development and application included oversight by several modeling evaluation groups (MEGs), publication in a peer reviewed edited compilation (Miller and St. John, 2006), and numerous technical presentations at national meetings of several professional societies. The sediment nutrient flux portion of SWEM has also been described previously (Di Toro, 2001). A MEG, comprised of six members from the academic and modeling communities, was convened in 1994 by the USEPA Harbor Estuary Program (HEP). This MEG met on three occasions and provided comprehensive review of the development of the SWEM and the supporting field program as well as the initial calibration of the model in the Harbor portion of the model domain. In 1997, a second MEG was convened by USEPA HEP that consisted of four members. This MEG met on four occasions and provided comprehensive review of the calibration/validation of SWEM over the entire spatial domain. A third MEG was convened by the joint USEPA HEP and Long Island Sound Study Nutrient Work Groups in 1999. This MEG met on four occasions and provided detailed review of the final model calibration/validation. In all three cases, the MEGs also evaluated the SWEM hydrodynamic model and the combined suitability of the hydrodynamic and water quality models for application to address nutrient management actions.

Additional enhancement of the SWEM calibration in the New Jersey tributaries was performed by HydroQual under oversight by New Jersey Department of Environmental Protection (NJDEP) staff. Enhancement to SWEM in the New Jersey tributaries completed in July 2002 included refinements to loadings, vertical mixing coefficients, benthic filtration rates, nitrification rates, vertical light extinction coefficients, and temperature effects on algal growth. The enhancements improved the overall level of calibration and made SWEM more defensible. The enhancements also included refinements to model grid geometry and several hydrodynamic parameters (HydroQual, 2002).

The water quality model source code underlying SWEM is Row Column AESOP (RCA). RCA originates from the Water Analysis Simulation Program (WASP) developed by Hydrosience (HydroQual's predecessor firm) in the 1970's. RCA code has been used to develop numerous models outside of the NY/NJ Harbor region. The code has been constantly refined and upgraded to include both more realistic representations of the chemical and biological processes associated with eutrophication, and more robust numerical solution techniques.

The initial version of SWEM, developed for the NYCDEP, contained 24 water quality or state-variables as listed in Table 2-1.

Table 2-1. 24 State Variables Included in SWEM

salinity (Sal)
winter phytoplankton carbon (PC ₁)
summer phytoplankton carbon (PC ₂)
refractory particulate organic phosphorus (RPOP)
labile particulate organic phosphorus (LPOP)
refractory dissolved organic phosphorus (RDOP)
labile dissolved organic phosphorus (LDOP)
dissolved inorganic phosphorus (DIP)
refractory particulate organic nitrogen (RPON)
labile particulate organic nitrogen (LPON)
refractory dissolved organic nitrogen (RDON)
labile dissolved organic nitrogen (LDON)
ammonium nitrogen (NH ₄)
nitrate and nitrite nitrogen (NO ₂ +NO ₃)
biogenic silica (BSi)
available silica (DSi)
refractory particulate organic carbon (RPOC)
labile particulate organic carbon (LPOC)
refractory dissolved organic carbon (RDOC)
labile dissolved organic carbon (LDOC)
reactive dissolved organic carbon (ReDOC)
algal exudates dissolved organic carbon (ExDOC)
dissolved oxygen (DO)
equivalent of aqueous DO demand (i.e., H ₂ S) (O _{2eq})

Figure 2-1 is a simplified diagrammatic representation of the principal eutrophication kinetics and water column-sediment interactions included in the original SWEM. The kinetics shown in Figure 2-1 have been described in detail (Meyers et al. 2000; HydroQual, 1999). Brief descriptions of the key features of primary production and sediment nutrient flux kinetics as shown in Figure 2-1 are presented.

2.1.2.1 Algal Growth

Phytoplankton growth in NY/NJ Harbor and Long Island Sound has been modeled for two functional groups or assemblages: winter diatoms and summer flagellates. It is likely that the phytoplankton of the LPR may also be characterized as two assemblages. The reason phytoplankton are considered as assemblages rather than as individual species is that at any particular time of the year there are literally tens of individual algal species present within the water column of the study domain. It is currently beyond the state-of-the-science in eutrophication modeling to include state-variables for each algal species since the growth rate of an individual population of phytoplankton in a natural environment is a complicated function of the species present and their differing reactions to solar radiation, temperature, and the balance between nutrient requirements and nutrient availability. This type of information is generally not known for many of the algal species present within New York/New Jersey Harbor waters.

2.1.2.2 Nutrient and Organic Carbon Cycling

Five forms of phosphorus, six forms of nitrogen, two forms of silica and six forms of organic carbon are included in the nutrient and carbon formulations in the original SWEM (for ST-SWEM, which was used for the FFS, additional forms are included) as schematically shown on Figure 2-1. Inorganic phosphorus is utilized by phytoplankton for growth and is returned to various organic and inorganic forms via respiration and predation. A fraction of the phosphorus released during phytoplankton respiration and predation is in the inorganic form and is readily available for uptake by other viable phytoplankton. The remaining fraction is released in the dissolved and particulate organic forms. The organic phosphorus must undergo a mineralization or bacterial decomposition into inorganic phosphorous before it can be used by other viable phytoplankton.

During algal respiration and death, a fraction of the algal cellular nitrogen is returned to the inorganic pool in the form of ammonia. The remaining fraction is recycled to the dissolved and particulate organic nitrogen pools. Organic nitrogen undergoes a bacterial decomposition, the end product of which is ammonia. Ammonia nitrogen, in the presence

of nitrifying bacteria and oxygen, is converted to nitrite nitrogen and subsequently nitrate nitrogen (nitrification). Both ammonia and nitrate are available for uptake and use in cell growth by phytoplankton; however, for physiological reasons, the preferred form is ammonia.

Two silica forms are considered. Available silica is dissolved and is utilized by diatoms during growth for their cell structure. Unavailable or particulate biogenic silica is produced from diatom respiration and diatom grazing by zooplankton. Particulate biogenic silica undergoes mineralization to available silica or settles to the sediment from the water column.

Pools of dissolved and particulate organic carbon are established on the basis of timescale for oxidation or decomposition. Zooplankton consume algae and take up and redistribute algal carbon to the organic carbon pools via grazing, assimilation, respiration, and excretion. Since zooplankton are not directly included in the SWEM kinetics, the redistribution of algal carbon to the organic carbon pools by zooplankton is simulated by empirical distribution coefficients. An additional term, representing the excretion of dissolved organic carbon by phytoplankton during photosynthesis, is included in SWEM. This algal exudate is very reactive. The decomposition of organic carbon is assumed to be temperature and bacterial biomass-mediated. Since bacterial biomass is not directly included within the SWEM framework, phytoplankton biomass is used as a surrogate variable. An additional loss mechanism of particulate organic matter (POM) is that due to filtration by benthic bivalves. This loss is handled in SWEM kinetics by increasing the deposition of non-algal particulate organic carbon from the water column to the sediment.

Although the number of dissolved and particulate pools of organic matter (including organic carbon) may appear greater than necessary for the purposes of modeling the fate and transport of hydrophobic contaminants, implementing SWEM as it is currently calibrated, rather than starting over with a new modeling framework, fulfilled the objectives of this FFS modeling effort and preserves the various reactivity pools of organic matter that are essential to the framework incorporated in the sediment diagenesis

/nutrient flux sub-model, the output of which is key to modeling rates of mercury methylation (King, 1999).

2.1.2.3 Dissolved Oxygen Balance

The dissolved oxygen balance includes both sources and sinks. Algal growth provides two of the sources: the production of dissolved oxygen from photosynthetic carbon fixation and an additional source of oxygen from algal growth when nitrate rather than ammonia is utilized. Atmospheric reaeration may be another source of dissolved oxygen, if the concentration of water column oxygen is less than dissolved oxygen saturation. Sinks of dissolved oxygen include algal respiration, nitrification, the oxidation of carbonaceous material, sediment oxygen demand (SOD) and atmospheric reaeration when dissolved oxygen saturation is exceeded. SOD is the quantity of oxygen transferred from the water column to the sediment bed that is necessary to satisfy the oxygen requirements of bacteria in the sediment as they decompose previously deposited organic matter.

2.1.2.4 Sediment Diagenesis and Nutrient Flux Dynamics

The mass balance equations of the SWEM sediment kinetics account for changes in POM (carbon, nitrogen, phosphorus, and silica) in the sediments due to deposition from the overlying water column, sedimentation, and decay or diagenesis. The decay of POM follows first-order kinetics as described by Berner (1971, 1974, and 1980) and is often referred to as the G model. The end products of diagenesis or decay of the POM include ammonia nitrogen, dissolved inorganic phosphorus and dissolved inorganic silica. These end products can undergo additional biological, chemical, and physical processing within the sediment layer such as nitrification, sorption, and exchange with the overlying water column. Of particular importance to the overlying water column is the calculation of SOD. A more complete development of the SWEM sediment diagenesis model theory is presented elsewhere (Di Toro and Fitzpatrick, 1993; Di Toro, 2001). The sediment kinetics state variables include: temperature, labile (G1) particulate organic phosphorus (POP), refractory (G2) POP, slow refractory (G3) POP, labile particulate organic nitrogen

(PON), refractory PON, slow refractory PON, labile particulate organic carbon (POC), refractory POC, slow refractory POC, biogenic silica, ammonia nitrogen, nitrate nitrogen, inorganic phosphorus, dissolved silica, and hydrogen sulfide. The latter variable considers sulfate reduction and is important to determining rates of mercury methylation (King, 1999).

2.1.3 Incorporating Sediment Transport into SWEM

2.1.3.1 Addition of New State-Variables

The original SWEM model did not fully consider resuspension and erosion processes for POM on a time-variable basis. Rather, SWEM utilized constant sediment burial rates (~ 2.5 cm/yr ~ 1.0 in/yr) and varied the net deposition rate by considering areas subject to high bottom shear due to high bottom velocity and wind-induced resuspension in shallow areas of the NY/NJ Harbor complex. The net deposition rates were further adjusted and calibrated against SOD and water and sediment concentrations of POM. In modifying the SWEM eutrophication model for use in the NY/NJ Harbor CARP (HydroQual, 2007), the SWEM eutrophication model was modified to:

- Include a more deterministic sediment transport modeling framework, which included formulations for settling (a non-linear function of solids concentration and depth), resuspension (a function of bottom shear stress calculated directly from the hydrodynamic flow field and the bottom roughness) and the structure of the sediment bed (a 0-0.2 cm (0.08 in) fluff layer used to simulate tidal resuspension and deposition and a 9.9 cm (3.9 in) sediment layer, which represented previously deposited material that had undergone consolidation and which required a higher value of the critical shear stress for sediment resuspension), and
- An expansion of the water column state-variables to include the inert forms of sediment particulate organic matter (carbon, phosphorus and nitrogen, the G3 components of sediment POM).

For purposes of the CARP sediment transport/organic carbon production sub-model, settling, resuspension and burial of particulate organic carbon, nitrogen and phosphorus were incorporated directly in SWEM rather than being driven by an external hydrodynamic/sediment transport model. Calculated settling rates were applied to both inorganic solids (cohesive solids) and POM (particulate carbon, nitrogen, phosphorus, and silica). Using this approach, it was assumed that inorganic solids and POM aggregate in the water column and settle at a concentration and salinity dependent flocculation settling rate. The settling velocities for algae, however, were set independently due to their low rates of aggregation, i.e., low collision efficiencies. Time-variable resuspension and burial rates of bed material were also applied equally to inorganic and organic matter. In the present application of the organic carbon model for the LPR, settling of inorganic and non-algal organic matter is computed based on information (settling fluxes and deposition and resuspension rates) calculated by a separate hydrodynamic/sediment transport model (ECOMSEDZLJS) developed specifically for the LPR (Appendix BII).

The LPR eutrophication-sediment model (ST-SWEM) now includes ten (10) rather than six (6) organic carbon state-variables in the water column to accommodate a detailed consideration of resuspension and erosion processes. The ten organic carbon state variables considered in ST-SWEM include the original six state-variables contained in SWEM: RPOC, LPOC, RDOC, LDOC, ReDOC, and ExDOC, as well as the four new state-variables: inert particulate organic carbon (IPOC) and the three G forms of sediment organic carbon resuspended from the sediment bed (SG1C, SG2C, and SG3C). (Note: analogous state-variables have also been included for phosphorus, nitrogen and particulate silica). An additional state-variable representing inert cohesive suspended solids has also been added to ensure that information passed forward from the sediment transport model to the organic carbon model has not been “lost” via temporal or spatial averaging. This is similar to the inclusion of salinity in the water quality model to insure that advective and dispersive information computed by the hydrodynamic model is not “lost” via temporal and spatial averaging of hydrodynamic model outputs. This will be discussed in more detail below.

The original SWEM model did not have an inert or G3 carbon, nitrogen, or phosphorus fraction in the water column. Instead when the refractory fraction settled to the sediment it was split between the G2 and G3 fractions, with about 57% in the G2 fraction and 43% in the G3 fraction. This split was based on the original calibration of the sediment flux sub-model developed for Chesapeake Bay (Di Toro and Fitzpatrick, 1993; Di Toro, 2001). This code was removed as it would re-split the refractory fraction each time organic matter was resuspended and redeposited driving most of the material into the G3 or inert fraction. Removing this code required the addition of the inert fraction to the particulate organic loads in order to maintain a source of the G3 fraction to the sediment. This is discussed further in the carbon model inputs section (Section 3.1).

Reactive, labile, refractory, and inert distinctions are based upon the time-scales of oxidation or decomposition. In the water column, reactive organic carbon originating from CSOs is assumed to decompose on a time scale of days to one to two weeks. Water column labile organic carbon decomposes on a time scale of several weeks to one to two months, while refractory organic carbon decomposes over a timescale of a few months to a year. In the sediment bed, labile organic carbon is assumed to decompose on the order of a few months, while refractory organic carbon will require several years to decompose. Inert particulate organic carbon is assumed to be conservative, its only loss pathways being either burial or resuspension and transport out of the model domain. Inert organic carbon dominates the carbon present in sediments.

Table 2-2 presents the reaction rate terms for each of the organic carbon pools considered in the ST-SWEM framework. An additional loss mechanism of POM from the water column due to filtration by benthic bivalves has been removed for the LPR model, due to a lack of information concerning benthic filtration rates for suspension feeding species present in the river. Table 2-3 presents a summary overview of the organic carbon pools considered in ST-SWEM.

Table 2-2. Organic Carbon Reaction Equations

Labile Particulate Organic Carbon (LPOC)

$$\text{LPOC} = f_{\text{LPOC}} \cdot k_{\text{grz}}(T) \cdot P_c - k_{5,7} \theta_{5,7}^{T-20} \cdot \text{LPOC} \cdot \frac{P_c + \text{ReDOC} + \text{ExDOC}}{K_{\text{mP}_c} + P_c + \text{ReDOC} + \text{ExDOC}} - \frac{v_5}{H} \cdot \text{LPOC} + \frac{r_5}{H_{\text{sed}}} \cdot \text{G1C}$$

(Note: Last term above applies only to layer 10)

Refractory Particulate Organic Carbon (RPOC)

$$\text{RPOC} = f_{\text{RPOC}} \cdot k_{\text{grz}}(T) \cdot P_c - \frac{v_6}{H} \cdot \text{RPOC} - k_{6,8} \theta_{6,8}^{T-20} \cdot \text{RPOC} \cdot \frac{P_c + \text{ReDOC} + \text{ExDOC}}{K_{\text{mP}_c} + P_c + \text{ReDOC} + \text{ExDOC}} + \frac{r_6}{H_{\text{sed}}} \cdot \text{G2C}$$

(Note: Last term above applies only to layer 10)

Inert Particulate Organic Carbon (IPOC)

$$\text{IPOC} = -\frac{v_7}{H} \cdot \text{IPOC} + \frac{r_7}{H_{\text{sed}}} \cdot \text{G3C}$$

(Note: Last term above applies only to layer 10)

Labile Dissolved Organic Carbon (LDOC)

$$\begin{aligned} \text{LDOC} = & f_{\text{LDOC}} \cdot k_{\text{grz}}(T) \cdot P_c + k_{5,7} \theta_{5,7}^{T-20} \cdot \text{LPOC} \cdot \frac{P_c + \text{ReDOC} + \text{ExDOC}}{K_{mP_c} + P_c + \text{ReDOC} + \text{ExDOC}} \\ & - k_{7,0} \theta_{7,0}^{T-20} \cdot \text{LDOC} \cdot \frac{\text{LDOC}}{K_{m\text{LDOC}} + \text{LDOC}} \cdot \frac{\text{DO}}{k_{\text{DO}} + \text{DO}} \cdot \frac{P_c + \text{ReDOC} + \text{ExDOC}}{K_{mP_c} + P_c + \text{ReDOC} + \text{ExDOC}} \\ & - \frac{5}{4} \cdot \frac{12}{14} \cdot K_{\text{DN}} \theta_{\text{DN}} \cdot \text{NO}_x \cdot \frac{K_{\text{NOX}}}{K_{\text{NOX}} + \text{DO}} \cdot \frac{\text{LDOC}}{K_{m\text{LDOC}} + \text{LDOC}} \end{aligned}$$

Refractory Dissolved Organic Carbon (RDOC)

$$\begin{aligned} \text{RDOC} = & f_{\text{RDOC}} \cdot k_{\text{grz}}(T) \cdot P_c - k_{8,0} \theta_{8,0}^{T-20} \cdot \text{RDOC} \cdot \frac{P_c + \text{ReDOC} + \text{ExDOC}}{K_{mP_c} + P_c} \cdot \frac{\text{DO}}{K_{\text{DO}} + \text{DO}} \\ & + k_{6,8} \theta_{6,8}^{T-20} \cdot \text{RPOC} \cdot \frac{P_c + \text{ReDOC} + \text{ExDOC}}{K_{mP_c} + P_c + \text{ReDOC} + \text{ExDOC}} \end{aligned}$$

Reactive Dissolved Organic Carbon (ReDOC)

$$\text{ReDOC} = -k_{9,0} \theta_{9,0}^{T-20} \cdot \text{ReDOC} \cdot \frac{\text{ReDOC}}{K_{m\text{LDOC}} + \text{ReDOC}} \cdot \frac{\text{DO}}{K_{\text{DO}} + \text{DO}} \cdot \frac{P_c + \text{ReDOC} + \text{ExDOC}}{K_{mP_c} + P_c + \text{ReDOC} + \text{ExDOC}}$$

Algal Exudate Dissolved Organic Carbon (ExDOC)

$$\begin{aligned} \text{ExDOC} = & f_{\text{ExPP}} \cdot G_p \cdot P_c \\ & - k_{10,0} \theta_{10,0}^{T-20} \cdot \text{ExDOC} \cdot \frac{\text{ExDOC}}{K_{m\text{LDOC}} + \text{ExDOC}} \cdot \frac{\text{DO}}{K_{\text{DO}} + \text{DO}} \cdot \frac{P_c + \text{ReDOC} + \text{ExDOC}}{K_{mP_c} + P_c + \text{ReDOC} + \text{ExDOC}} \end{aligned}$$

Table 2-2. Organic Carbon Reaction Equations(Continued)

Description	Notation	Value	Units
Phytoplankton Biomass	P_c	-	mgC/L
Specific Phytoplankton Growth Rate	G_p	Eq. 11	day ⁻¹
Half Saturation Constant for Phytoplankton Limitation	K_{mPc}	0.0	mgC/L
Half Saturation Constant for LDOC	K_{mLDOC}	0.0	mgC/L
Fraction of Grazed Organic Carbon Recycled to:			
the LPOC pool	f_{LPOC}	0.40	
the RPOC pool	f_{RPOC}	0.025	
the IPOC pool	f_{IPOC}	0.025	
the LDOC pool	f_{LDOC}	0.45	
the RDOC pool	f_{RDOC}	0.10	
Fraction of Primary Productivity Going to the Algal Exudate DOC pool	f_{ExpP}	0.20	
Hydrolysis Rate for RPOC	$k_{6,8}$	0.01	day ⁻¹
Temperature Coefficient	$\theta_{6,8}$	1.08	
Hydrolysis Rate for LPOC	$k_{5,7}$	0.20	day ⁻¹
Temperature Coefficient	$\theta_{5,7}$	1.08	
Settling Rate of LPOC	v_5	Eq.4	m/day
Settling Rate of RPOC	v_6	Eq.4	m/day
Settling Rate of IPOC	v_7	Eq.4	m/day
Resuspension Rate of G1C	r_5	Eq.9	m/day
Resuspension Rate of G2C	r_6	Eq.9	m/day
Resuspension Rate of G3C	r_7	Eq.9	m/day
Water Column Segment Depth	H	-	m
Sediment Segment Depth	H_{SED}	-	m
Oxidation Rate of LDOC	$k_{7,0}$	0.15	day ⁻¹
Temperature Coefficient	$\theta_{7,0}$	1.08	
Oxidation Rate of RDOC	$k_{8,0}$	0.008	day ⁻¹
Temperature Coefficient	$\theta_{8,0}$	1.08	

Table 2-2. Organic Carbon Reaction Equations(Continued)

Description	Notation	Value	Units
Oxidation Rate of ReDOC	$k_{9,0}$	0.3	day^{-1}
Temperature Coefficient	$\theta_{9,0}$	1.047	
Oxidation Rate of ExDOC	$k_{10,0}$	0.1	day^{-1}
Temperature Coefficient	$\theta_{10,0}$	1.08	
Half Saturation for Oxygen Limitation	K_{DO}	0.2	mgO_2/L
Dissolved Oxygen	DO	-	mgO_2/L
Denitrification Rate	K_{DN}	0.05	day^{-1}
Temperature Coefficient	θ_{DN}	1.045	
Nitrate + Nitrite	NOX	-	mgN/L
Half Saturation Constant for Denitrification	K_{NOX}	0.10	mgO_2/L

Table 2-3. Organic Carbon Forms Included in ST-SWEM

		WATER COLUMN		SEDIMENT BED	
PHASE	POOL	SOURCES	SINKS	SOURCES	SINKS
Living Algae	Diatoms	external sources growth	Settling Respiration zooplankton grazing benthic filtration	NA	NA
	Greens	external sources growth	Settling Respiration zooplankton grazing benthic filtration	NA	NA
POC	Inert G3	Resuspension grazed algae	Settling benthic filtration	Settling benthic filtration 15% of dead algae/POM deposition	Resuspension Burial mineralization/diagenesis
	Refractory G2	external loadings grazed algae resuspension	hydrolysis to DOC settling benthic filtration	settling benthic filtration 20% of dead algae/POM deposition	resuspension burial mineralization/diagenesis
	Labile G1	external loadings grazed algae resuspension	hydrolysis to DOC settling benthic filtration	settling benthic filtration 65% of dead algae/POM deposition	resuspension burial mineralization/diagenesis
DOC	Refractory	external loadings grazed algae from refractory POC	oxidation	NA	NA
	Labile I	external loadings grazed algae from labile POC	Oxidation denitrification	NA	NA
	Labile II	external loadings	oxidation	NA	NA
	Exudate	algal exudation	oxidation	NA	NA

2.1.3.2 Necessity for Use of Grid Aggregation for ST-SWEM and RCATOX

The original model grid developed for SWEM included the LPR, Hackensack River (HR) and Newark Bay (NB), and also included all of Long Island Sound, the New York Bight Apex, and a significant portion of the Mid-Atlantic Bight. However, the original segmentation for the LPR, HR, and NB is too spatially coarse for the needs of this FFS assessment. Therefore, a new high resolution grid was developed for this study. This grid, referred to as the truncated LPR grid, includes the LPR, HR and NB as well as the Kill van Kull (KVK) and the Arthur Kill (AK). The high resolution grid contains 243x44x10 cells and requires approximately one day to simulate one year of time for the hydrodynamic transport and up to three days to simulate one year of sediment transport due, in part, to the small time-steps required to maintain computational stability. Taking advantage of a specialized numerical integration algorithm developed for the generalized RCA computer code, which is the computational framework, underlying both ST-STEM and RCATOX, it was projected that it would take 16-20 hours to simulate one-year of time in ST-SWEM (with similar estimates of time to run contaminants in RCATOX). Since the FFS evaluations required simulations of 60 years for the No Action scenario and 37 years for other management scenarios, No Action would have taken ~50 days and the other alternatives would have taken ~30 days to run. Therefore, a scheme involving the use of grid aggregation to shorten run times was selected. This scheme has been demonstrated to perform well in a previous modeling study of Massachusetts and Cape Cod Bays (HydroQual, 2000). The underlying principle of this scheme is take a 2x2 (or larger) group of cells and spatially aggregate (or collapse) them into 1 cell. If for example, a 2x2 grid aggregation is performed there is a run time reduction of a factor of four, since the number of grid cells has been reduced by a factor of four. In addition, another factor of two reduction in computational time usually results, since with the larger grid cells the time-step required for computational stability is often doubled. Thus the overall time to complete a one year simulation is reduced by a factor of about eight. However, in the case of the LPR, it is important to maintain spatial resolution/definition of the channels versus the shoals. Therefore, grid aggregation was only implemented

along the “length” of the LPR and NB, i.e., grid aggregations of 2x1, or 3x1 (or “X”x1) were performed. As a result run times were reduced to about 6 hours/year of simulation, allowing a No Action simulation to be completed in about 15 days.

2.1.3.3 Information Transfer between ECOMSEDZLJS and ST-SWEM

ECOMSEDZLJS computes the fate and transport of cohesive and non-cohesive solids. Information computed by ECOMSEDZLJS that is of importance to the fate and transport of organic carbon computed within ST-SWEM includes: settling rates of cohesive solids, deposition of cohesive solids, resuspension of cohesive solids, and the bulk density of the sediment bed. Table 2-4 presents a summary of the parameter/processes generated in ECOMSEDZLJS that are passed forward to the grid aggregation processor and then forward to ST-SWEM and describes how this information is used within ST-SWEM. The following notation is used in Table 2-4:

- COH(K) – concentration of cohesive solids in layer K of the water column, ($M L^{-3}$),
- $V_{SCOH}(K)$ – cohesive solids’ settling velocity between layer K and K+1 of the water column, ($L T^{-1}$),
- NZ – number of vertical layers in the water column (NZ=10),
- NCOH(K) - concentration of non-cohesive solids in layer K of the water column, ($M L^{-3}$),
- $V_{SNCOH}(K)$ – non-cohesive solids’ settling velocity between layer K and K+1 of the water column, ($L T^{-1}$),
- ΔZ – change in thickness of the active layer in the ST-SWEM sediment bed, (L),
- ΔT – time-step of the ST-SWEM water quality model, (T),

- D_{COH}, D_{NCOH} – cohesive/non-cohesive solids' deposition flux rate (+ \rightarrow increases ΔZ), ($M L^{-2} T^{-1}$),
- R_{COH}, R_{NCOH} – cohesive/non-cohesive solids' resuspension flux rate (- \rightarrow decreases ΔZ), ($M L^{-2} T^{-1}$),
- ρ_{COH}, ρ_{NCOH} – density of cohesive/non-cohesive bed solids, ($M L^{-3}$),
- H_{bed} – depth of active layer in ST-SWEM bed, (L),
- H_{bedMAX}, H_{bedMIN} – maximum and minimum depths of ST-SWEM bed (L).

Table 2-4. ECOMSEDZLJS – ST-SWEM Coupling

Parameter/Process	ECOMSEDZLJS Output	Grid Aggregation	ST-SWEM
Settling and Deposition	<p>Cohesives: concentrations COH(K) and settling velocities $V_{SCOH}(K+1)$, $K=1,NZ$; $V_{SCOH}(NZ)$ is the deposition velocity</p> <p>Non-cohesives: total concentrations of NCOH(K) summed over the non-cohesive size classes and the flux-weighted settling velocities $V_{SNCOH}(K+1)$, $K=1,NZ$</p> <p>Deposition velocity includes adjustment by deposition coefficient</p>	<p>Cohesives: volume weighted average concentrations and flux-weighted settling velocities</p> <p>Non-cohesives: volume weighted average concentrations and flux-weighted settling velocities</p>	<p>Apply spatially aggregated ECOMSEDZLJS cohesive settling velocities (V_{SCOH}) to ST-SWEM non-algal POM and inorganic cohesives</p> <p>Water Column non-cohesives not currently included in ST-SWEM model</p>
Resuspension	<p>Cohesives: concentration of COH in the top 10 cm of the ECOMSEDZLJS sediment bed and the gross resuspension flux ($M L^{-2} T^{-1}$)</p> <p>Non-cohesives: total concentration of NCOH, summed over the non-cohesive size classes in the top 10 cm of the sediment bed and the average NCOH net resuspension flux ($M L^{-2} T^{-1}$)</p>	<p>Cohesives: Area-weighted average gross resuspension flux and bed COH concentration.</p> <p>Non-cohesives: Area-weighted average net resuspension flux</p>	<p>Resuspension velocities calculated from spatially aggregated flux and concentration applied to applied to ST-SWEM sediment organic and inorganic variables.</p> <p>Water Column non-cohesives not currently included in ST-SWEM model</p>
Burial/Erosive exchange between ST-SWEM active (10 cm) and archive layers	Output initial mass ($M L^{-2}$) of cohesive and non-cohesive solids in the top 10 cm (active layer) and the remainder of the bed (archive layer) of the ECOMSEDZLJS sediment bed and deposition and resuspension fluxes ($M L^{-2} T^{-1}$) of cohesive and non-cohesive solids	Area-weighted average mass for COH and NCOH and area-weighted deposition/ resuspension fluxes	Use bulk density and deposition and resuspension fluxes to calculate the change in the active layer thickness: $\Delta Z = \Delta T \cdot (+/- (D/R)_{COH} / \rho_{COH} +/- (D/R)_{NCOH} / \rho_{NCOH})$ If $H_{bed} + \Delta Z > H_{bedMAX}$ (burial) or $< H_{bedMIN}$ (erosion), calculate active-archive layer exchange of COH and NCOH solids

2.1.3.4 ST-SWEM Bed Structure

The bed structure employed within ST-SWEM assumes that it is modeling the depth of the biologically active zone (BAZ), i.e., the depth to which benthic organisms induce particle mixing or bioturbation. Active layer depths of 5 to 15 cm (~2 to ~6 in) have been reported for estuaries (Aller, 1982). Boudreau (1998) developed a theoretical model based on the assumption that the particle mixing diffusion coefficient is proportional to the available food, which yielded an active layer depth of 9.7 cm (3.8 in). An accompanying statistical analysis of reported values from widely varying locations – from shallow waters to water depths of > 5000 m – yielded a mean \pm standard deviation of 9.8 ± 4.5 cm (3.9 ± 2.1 in). The development and calibration of the sediment nutrient flux model for Chesapeake Bay (Di Toro and Fitzpatrick, 1993) assumed an active layer depth of 10 cm (~4 in). This depth is consistent with recently reported analyses of sediment profile images (SPI) of surficial sediments in Newark Bay, which yielded estimates of BAZ depths that were typically in the range of 5 – 15 cm (Diaz and Arcadis, 2008).

ST-SWEM uses an active layer of 10 ± 0.1 cm and a deeper archive layer. The active layer depth is further sub-divided, based on redox chemistry (i.e., aerobic and anaerobic layers) and erodibility. From the redox chemistry perspective, the aerobic and anaerobic regions of the 9.9 to 10.1 cm active layer are allowed to vary as depth of oxygen penetration changes (usually on the order of several millimeters over a yearly cycle), but the depths of the aerobic and anaerobic regions must always sum in the 9.9 to 10.1 cm range. From the erodibility perspective, the original ST-SWEM model (HydroQual, 2007), did not make use of a full sediment transport model based on first principles. Rather, relatively simple sediment transport algorithms were developed and coded into ST-SWEM. Specifically, calculated settling rates were applied to both organic and inorganic particulate matter (or state-variables). It was assumed that organic and inorganic particulate matter aggregate in the water column and are removed at similar rates as the floc settles. Settling velocities for phytoplankton, however, were set independently due to their low rates of aggregation (i.e., low collision efficiencies). In the original ST-SWEM model the bed was broken into two layers a 0.2 cm “fluff” layer with a lower

critical shear stress to represent recently deposited material, and the remainder of the bed with a higher critical shear stress. Rates of resuspension were based on bottom shear stresses computed by the hydrodynamic model and critical shear stresses for resuspension were arrived at by calibration to observed concentrations of suspended solids in the water column. In the current LPR version of ST-SWEM, the same bed structure has been maintained (i.e., an active layer of 10 ± 0.1 cm that includes up to a 0.2 cm “fluff” layer and a deeper archive layer), but the resuspension rates are determined by the ECOMSEDZLJS sediment transport model. The inclusion of the “fluff” layer significantly reduces artificial or numerical mixing problems in the underlying active and archive layers during frequent resuspension and deposition that occurs on a tidal cycle basis. The archive layer is of variable depth and is dependent on computations derived from ECOMSEDZLJS in each model grid cell.

2.1.3.5 Numerical Considerations

The algorithm for numerical integration in ST-SWEM uses operator-splitting, wherein during one time-step, the concentrations for each state-variable are solved by separating the terms associated with vertical dispersion/diffusion from the rest of the advective/dispersion terms. During the first part of the time-step, state-variable derivatives are computed based on biogeochemical processes (i.e., reaction kinetics, such as listed for organic carbon in Table 2-2), advective transport in the horizontal and vertical planes of the model grid and dispersive transport in the horizontal plane of the model grid, as per equation 2-1:

$$\begin{aligned} \frac{dC_{ijk}^n}{dt} = & (Q_{xijk}c_{i-1jk}^n - Q_{xi+1jk}c_{ijk}^n + Q_{yijk}c_{ij-1k}^n - Q_{yij+1k}c_{ijk}^n + Q_{zijk}c_{ijk+1}^n - \\ & Q_{zijk-1}c_{ijk}^n + R_{xijk}c_{i-1jk}^n - R_{xijk}c_{ijk}^n + R_{xi+1jk}c_{i+1jk}^n - R_{xi+1jk}c_{ijk}^n + \\ & R_{yijk}c_{ij-1k}^n - R_{yijk}c_{ijk}^n + R_{yij+1k}c_{ij+1k}^n - R_{yij+1k}c_{ijk}^n \pm k_{ijk}c_{ijk}^n V_{ijk} + \\ & W_{ijk}) / V_{ijk} \end{aligned} \quad (2-1)$$

for all Q_x , Q_y and $Q_z > 0$

Where:

- c_{ijk}^n = the concentration at grid cell i,j,k at time n,
- t = time
- Q_{xijk} = the advective flow between grid cell i,j,k and grid cell i+1,j,k,
- R_{xijk} = the bulk exchange (diffusion) between grid cell i-1,j,k and grid cell i,j,k
- k_{ijk} = the reaction rate of the water quality concentration in grid cell i,j,k,
- V_{ijk} = the volume of grid cell i,j,k, and
- W_{ijk} = the input loading of the water quality variable or state-variable to grid cell i,j,k.

Then an intermediate concentration is computed, using the explicit integration Euler algorithm, represented in equation 2-2:

$$c_{ijk}^{n+1*} = c_{ijk}^n + \Delta t \frac{dc_{ijk}^n}{dt} \quad (2-2)$$

The time-step integration is completed, using an implicit integration algorithm for dispersive transport in the vertical plane of the model grid, presented in equations 2-3 and 2-4:

$$c_{ijk}^{n+1} = c_{ijk}^{n+1*} + \Delta t \frac{dc_{ijk}^{n+1}}{dt} \quad (2-3)$$

Where:

$$\frac{dc_{ijk}^{n+1}}{dt} = (R_{zijk}c_{ijk-1}^{n+1} - R_{zijk}c_{ijk}^{n+1} + R_{zjk+1}c_{ijk+1}^{n+1} - R_{zjk+1}c_{ijk}^{n+1})/V_{ijk} \quad (2-4)$$

The need to utilize the implicit integration solver presented in equations 2-3 and 2-4 is due to the stability requirements for explicit integration schemes that result from

potentially large vertical mixing coefficients and small volumes (or vertical depths) in the shallower portions of the LPR, HR, and NB (see equation 2-5).

$$\Delta t \leq \text{Min}\left(\frac{V_{ijk}}{R_{zijk} + R_{zijk+1}}\right) \quad (2-5)$$

The use of the implicit scheme removes the time-step limitation and permits the model to use larger time-steps and reduce the time required to complete a model run.

With the introduction of sediment transport within the ST-SWEM model, the associated high rates of settling for water column POM and the high rates of settling for resuspended G-class POM from the sediment bed (especially in the shallow shoal areas of the model domain), it was necessary to include the transport due to vertical settling into equation 2-4, as follows:

$$\frac{c_{ijk}^{n+1}}{dt} = (R_{zijk}c_{ijk-1}^{n+1} - R_{zijk}c_{ijk}^{n+1} + R_{zjk+1}c_{ijk+1}^{n+1} - R_{zjk+1}c_{ijk}^{n+1} + v_{sijk}c_{ijk-1}^{n+1} - v_{sijk+1}c_{ijk}^{n+1})/V_{ijk}$$

2.2 CONTAMINANT FATE AND TRANSPORT MODEL

This section of the report focuses on the computational framework of the contaminant fate and transport model, RCATOX. The first part of this section will describe the approach towards the transport of toxic contaminants (hydrophobic organic contaminants and metals), including linkages between the hydrodynamic, sediment transport and organic carbon models and the RCATOX model, while the second part of this section will focus on the contaminant kinetics used in this study.

2.2.1 Introduction

RCATOX includes the ability to represent numerous hydrophobic organic contaminant (HOC) and metals-associated processes in the water column and sediment bed, including: partitioning of HOCs and metals to dissolved and particulate organic carbon, settling and

resuspension of particle associated contaminants, diffusive and mixing exchanges across the water column and sediment bed interface, and volatilization of HOCs and elemental mercury across the water-air interface. RCATOX also has the capability to consider, photolysis, dechlorination, and other degradation processes; however, absent strong evidence indicating that these processes are occurring in the study area for the HOCs of concern, these model features were not implemented.

2.2.1.1 Three Phase Partitioning To Organic Carbon

For purposes of hydrophobic organic contaminants, three contaminant phases are modeled: freely dissolved (C_D), DOC-complexed dissolved (C_{DOC}), and POC-complexed (C_{POC}):

$$C_T = C_D + C_{DOC} + C_{POC} \quad (2-6)$$

In order to model the three phases, partition coefficients, K_{POC} and K_{DOC} , are used to express the relationship between POC-complexed contaminant (C_{POC}) and freely dissolved contaminant (C_D), and between DOC-complexed contaminant (C_{DOC}) and freely dissolved (C_D) contaminant. Following the approach of Burkhard (2000), K_{DOC} is equal to the contaminant specific octanol-water partition coefficient (K_{OW}) times a scale factor (A_{DOC}) to account for the more hydrophilic nature and lower binding affinity of contaminants to DOC. Substituting the relationships for K_{POC} and K_{DOC} into equation 2-6 yields the following expression:

$$C_T = C_D + C_D \cdot DOC \cdot A_{DOC} \cdot K_{OW} + C_D \cdot POC \cdot K_{POC} \quad (2-7)$$

2.2.2 Interfacing With the Other LPR Sub-Models

In order to compute the fate and transport of hydrophobic organic and metal contaminants, the RCATOX model utilizes information generated by the hydrodynamic and sediment transport sub-model (ECOMSEDZLJS) and the organic carbon production model (ST-SWEM). In general, the hydrodynamic sub-model calculates water

circulation and transport patterns, while the sediment transport model computes water column and sediment bed concentrations of cohesive and non-cohesive solids, water column settling rates, and deposition and resuspension of solids between the water column and sediment bed. The organic carbon production model calculates the concentrations of particulate and dissolved organic carbon over time and space, both in the water column and sediment bed and the concentrations of hydrogen sulfide and rates of sulfate reduction in the sediment bed, which are important to determining the bioavailable fractions of metals in the sediment and rates of mercury methylation in the sediment bed, respectively.

2.2.2.1 General Hydrodynamic Information Passed from ECOMSEDZLJS to the LPR RCATOX Model

The LPR hydrodynamic sub-model produces an output file (gcm_tran) that includes, as time histories in three dimensions, the calculated (i.e., one hour average) water depths and the rate of change in water depths, advective transport rates, dispersions, salt concentrations, and temperatures. The advective transport rates and dispersions are reported in both horizontal directions (x- and y-directions or longitudinal and lateral direction) and the vertical direction (z-direction). Calculated water depths and associated changes in water depths (or derivatives) are tracked as changes in elevation over time. Salinity information is used by RCATOX to make ionic strength corrections for metals partitioning in the water column and the sediment bed. Information generated by the sediment transport sub-model is not directly passed to RCATOX via the gcm_sedtran file, but rather the required information, having been read and utilized by ST-SWEM, is packaged together with the appropriate information generated by the organic carbon production model, and passed forward to RCATOX in a file known as the RCACRBFLXS file.

2.2.2.2 General Organic Carbon Information Passed from ST-SWEM to the LRP RCATOX Model

The same information, i.e., volume, the 3-D advective and dispersive transport fields, and salinity and temperature, generated by the LPR hydrodynamic field that is used by the organic carbon production model is also used by the RCATOX model. The RCATOX model grid is the same as used for the organic carbon production model (i.e., using the same spatially aggregated grid) and, therefore using the same `gcm_tran` file as described in Section 2.1. The organic carbon production sub-model calculates concentrations of particulate organic carbon and dissolved organic carbon over time and space in ten vertical layers of the water column. The carbon production model also computes the vertical distribution of particulate organic carbon in the sediment bed in the active (bioturbated) layer and archive (deep bed layer). The carbon is type-identified based on its reactivity (i.e., the G₁, G₂, G₃ classes of organic matter described previously in Section 2.1).

The LPR organic carbon production sub-model produces an output file called `RCAFCRBFLXS` containing all of the relevant information required by the RCATOX model. The output file is quite large (i.e., approximately 7.4 gigabytes per year), as it contains time histories (averaged over 15 minute intervals) for all of the relevant variables, in three dimensions in the water column and two dimensions in the sediment. The water column variables include the calculated phytoplankton biomass and settling rates, particulate organic carbon (POC) concentrations and settling rates, dissolved organic carbon (DOC) concentrations, average light intensity, and hydrogen sulfide concentrations.

For the sediment, the output file includes diffusive and particle mixing rates, resuspension and burial rates for the active sediment bed, erosion rates from the sediment bed archival stack to the active sediment bed, depths and rates of change of the depth of the active and archive sediment bed, the concentrations of labile, refractory and inert (also referred to as G₁, G₂, and G₃ carbon) in the active and archive layer of the

sediment bed, and the active and archive layer cohesive and non-cohesive sediment bed concentrations. This output file is utilized by RCATOX for both hydrophobic organic chemicals (HOCs) and metals. The detailed list of variables included in the RCAFCRBFLXS file is provided in Table 2-3.

Table 2-5. Information Passed from ST-SWEM to RCATOX

Variable Name	Description	Units
<u>3-D Fields</u>		
VSALG1	settling rate of phytoplankton group 1	m/day
PHYTC1	phytoplankton group 1 carbon	mg C/L
VSALG2	settling rate of phytoplankton group 2	m/day
PHYTC2	phytoplankton group 2 carbon	mg C/L
TPOC	water column total particulate organic carbon	mg C/L
RDOC	water column total dissolved organic carbon	mg C/L
AVGLIGHT	average light in the water segment	langleys
VSRESSCOAG	settling rate of resuspended material with coagulation	m/day
O2EQ	water column oxygen equivalents to be used as H ₂ S	mg-O ₂ /L
TSS	total suspended sediment	mg/L
<u>2-D Fields</u>		
VSMIX	sediment-water column dissolved mixing rate	m ² /day
VDMIX	sediment-sediment dissolved mixing rate	m ² /day
VPMIX	sediment-sediment particulate mixing rate	m ² /day
HAEROFLX	sediment aerobic layer thickness	m
SEDSMIX	sediment-water column dissolved mixing rate	m/day
SEDKL12MIX	sediment-sediment dissolved mixing rate	m/day
SEDW12MIX	sediment-sediment particulate mixing rate	m/day
VRESUSPC	resuspension velocity for bed carbon	m/day
VBURIALC	bed accretion or burial velocity	m/day
VARCH2ACTC	rate of active layer replenishment from archive	m/day
HSEDCRB	active sediment layer thickness	m
DHSEDDTCRB	active sediment layer thickness rate of change	m/d
SG1C	active sediment bed G1 (labile) carbon	mg/L

Table 2-5. Information Passed from ST-SWEM to RCATOX

Variable Name	Description	Units
SG2C	active sediment bed G2 (refractory) carbon	mg/L
SG3C	active sediment bed G3 (inert) carbon	mg/L
HSEDCRBA	archive sediment layer thickness	m
DHSEDDTCRBA	archive sediment layer thickness rate of change	m/d
SG1CA	archive sediment bed G1 (labile) carbon	mg/L
SG2CA	archive sediment bed G2 (refractory) carbon	mg/L
SG3CA	archive sediment bed G3 (inert) carbon	mg/L
CCOH10	active layer cohesives	gm/cm ²
CNCOH10	active layer non-cohesives	gm/cm ²
CCOHAR	archive layer cohesives	gm/cm ²
CNCOHAR	archive layer non-cohesives	gm/cm ²

2.2.3 RCATOX Bed Structure

The ST-SWEM organic carbon production sub-model follows the bed structure used in the original CARP model (HydroQual, 2007). The ST-SWEM bed structure is represented by a 10±0.1 cm active layer and a deeper completely mixed archive layer. The allowable variation in the active layer thickness in the original CARP model was used to simulate tidal resuspension and re-deposition of a 0-0.2 cm “fluff” layer, so as to minimize artificial or numerical mixing through the underlying sediment. For purposes of the LPR contaminant fate and transport sub-model, the 10±0.1 cm active sediment bed layer from the organic carbon production sub-model is broken out into ten 1 cm chemical layers. In the early application of the RCATOX model, it was found that using a completely mixed archive layer for the sediment bed resulted in significant artificial or numerical mixing between the active layer and the archive layer. Therefore, it was decided to re-code the original CARP fate and transport contaminant model and utilize an archive stack (i.e., a vertically segmented sediment bed) and a completely mixed deep-bed archive layer. Therefore, the current bed structure used in the LPR RCATOX model includes:

- an active layer, which is comprised of 10 vertical slices, with the surface slice permitted to vary between 0.5 cm to 2 cm (more about this below) and the next 9 slices all being 1 cm thick, wherein bioturbation (particle mixing by benthic organisms) takes place,
- an archival stack, which is comprised of 97 vertical slices with each slice being 1 cm thick, and
- a deep-bed archival layer, which is initially assumed to be 0.61 m (2 feet) thick, but which can vary over time and space in response to temporal and spatial patterns of deposition and erosion, as computed by the sediment transport model, ECOMSEDZLJS.

The rationale for choosing this bed layering approach is based on the following:

- The 10 cm active (~4 in) layer is assumed to represent the biologically active zone (BAZ) and is consistent with the 10 cm depth used to represent biogeochemical processes in the organic carbon production model's sediment nutrient flux model.
- Dividing the active layer into 10 vertical slices each of 1 cm (~0.4 in) thickness (except for the surface layer which is permitted to vary between 0.5 cm to 2 cm in thickness) significantly reduces artificial or numerical mixing of contaminants due to tidally induced resuspension and re-deposition.
- Most of the available sediment contaminant data were obtained from sediment cores that were vertically sliced and underwent chemical analysis. The depth intervals of the vertical slices were 0-0.5 ft, 0.5-1.5 ft, 1.5-2.5 ft, 2.5-3.5 ft and 3.5-5.5 ft (with some cores analyzed to deeper depth intervals). An archival stack of ninety-seven (97) 1 cm thick slices together with the 10 cm active layer, represents a total depth of 107 cm or ~3.5 feet, which bounded the expected maximum depth of bed erosion computed by the sediment transport model, and permitted the available historical data to be used readily to assign sediment bed initial conditions, and which represented a balance between detailed vertical resolution and computational resource.
- The deep-archive layer (0.6 m or 2 ft) was used to represent the 3.5-5.5 foot slice of a sediment core which represented the maximum depth used for contaminant analysis for many of the available cores.

For both the ST-SWEM and RCATOX applications the mass of solids eroded and deposited are passed from the ECOMSEDZLJS computation. Because of the complexity of the bulk density calculation in ECOMSEDZLJS, which varies in four dimensions in the bed (X, Y, Z, and time), the bulk density of sediments eroded and deposited were approximated for purposes of the ST-SWEM and RCATOX models. For each cell an equilibrium cohesive and non-cohesive bulk density was assigned based on the ECOMSEDZLJS values and the bulk density is computed as a weighted average of those values. Bed elevation changes were then computed based on the ECOMSEDZLJS solids fluxes and the approximated bulk density values in ST-SWEM and passed to RCATOX.

As mentioned above, the surface slice of the active layer is allowed to vary between 0.5 and 2 cm in thickness. This represents the minimum and maximum depths permitted before slices are either combined or divided to form a new surface layer. In a situation where resuspension of bed solids results in the surface slice thickness decreasing to 0.5 cm, the surface slice and the slice immediately below it (active layer slice 2) are combined into a single 1.5 cm slice. The new contaminant concentration is the depth-weighted average of the two original slices. The remaining slices in the active layer and the archive stack are then moved up one layer. The deep-bed archive layer thickness is reduced by 1 cm, and its corresponding contaminant concentration is assigned to layer 97 of the archive stack (Figure 2-2). On the other hand, if deposition of water column suspended solids to the sediment bed results in the thickness of the surface slice of the active layer to increasing to 2 cm in thickness (the bed solids density is kept constant) then the surface slice is divided into two 1 cm slices. The bottom 1 cm becomes slice 2 of the active layer and the remaining slices of the active layer and archive stack are moved downwards 1 cm. The bottom 1 cm slice of the archive stack (i.e., slice 97) is added to the deep-bed archive layer. The new archive layer concentration is set equal to the depth weighted average of the concentrations in slice 97 of the archive stack and the deep bed archive layer (Figure 2-2). The deep bed archive layer is initially 60 cm (~2 ft) thick and can increase or decrease in thickness by 1 cm increments with deposition or erosion. Since, there is no vertical mixing between layers of the archive stack and since no biochemical reactions are assumed to occur in the archive stack, then the slices in the

archive stack are not actively involved in the model computations. This allows RCATOX to maintain improved vertical resolution of contaminant profiles in the sediment bed without having a significant effect on computational runtime requirements for the model.

3 MODEL INPUTS

The following sections describe inputs for the contaminant fate and transport sub-models. These include boundary conditions at the upstream freshwater boundaries, open-water tidal boundaries, loadings from wastewater treatment plants, loadings from SWOs and CSOs, atmospheric loadings, and sediment bed properties.

3.1 ORGANIC CARBON PRODUCTION MODEL

The inputs for the carbon production sub-model were copied directly from the CARP model and only modified to accommodate the higher spatial resolution of the LPR model grid and to incorporate an inert fraction in the POM state variables.

3.1.1 Boundary Conditions

3.1.1.1 Freshwater Boundaries

Freshwater boundaries were copied over from CARP for the tributaries included in both models as head of tide inputs: the Passaic, Saddle, and Hackensack Rivers. The other tributaries included as heads of tide in the LPR model (Second and Third Rivers, and MacDonald Brook) were assigned the storm water concentrations developed for the SWEM model. These smaller tributaries were not measured as part of the SWEM program, but given the limited area that they drain they are likely dominated by stormwater runoff.

Following the same approach used in the CARP model, monthly values based on the SWEM 1994-1995 sampling program were used for all years. For the LPR project:

- Monthly total POC values were replaced with daily POC values estimated as a function of flow.

- POC values were estimated using the Normalized POC Loading Function (NPL) analogous to the Normalized Sediment Loading Function (NSL), both described in the CARP model reports (HydroQual, 2007).
- As discussed in Section 2.1.3.1 the addition of resuspension to the carbon model made it necessary to add a source of G3 or inert carbon to the model.
- The distribution between the model non-algal POC state variables was modified to incorporate inert POC.
- The labile fraction remained ¼ of the non-algal POC.
- The refractory POC fraction was split to create an inert POC fraction with about 43% of the refractory carbon replaced with inert carbon. The inert fraction of 43% was based on the way RPOC was split between the G2 and G3 fractions when settling to the bed in the original application of the sediment flux sub-model in Chesapeake Bay, and later in SWEM. This split was calibrated as part of Chesapeake Bay modeling study (Di Toro and Fitzpatrick, 1993; Di Toro, 2001).
- An inert fraction was added for particulate organic phosphorus (POP) and particulate organic nitrogen (PON) in the same fashion.
- In addition to using the NPL estimated POC to define the POC boundaries the other particulate organic state variables were scaled on a daily basis in proportion to the POC to maintain the same stoichiometry (e.g. for refractory particulate organic phosphorus (RPOP), $RPOP_{LPR} = RPOP_{SWEM} * TPOC_{NPL} / TPOC_{SWEM}$).

The other smaller tributaries that were not included in the CARP model or measured during the original SWEM sampling program were assigned the stormwater state variable concentrations (Table 3-1) which were also modified to incorporate a fraction of inert organic material.

Figures 3-1 through 3-4 present the Upper Passaic River boundary conditions at Dundee Dam for total POC, algal POC, DOC, and fraction organic carbon (FOC) respectively. Each figure has three panels. The top panel is the flow at Dundee Dam, the middle panel is the concentration at Dundee Dam and the bottom panel is the load coming over Dundee Dam. Figures 3-2 and 3-3 reflect the repeating monthly values for algal POC

and DOC derived from the 1994-1995 SWEM dataset. The combination of the solids boundary from the ECOM-SEDZLJS model with the POC boundary from the ST-SWEM model results in the FOC time history presented in Figure 3-4. The FOC values at Dundee Dam average 11.5 % and range from approximately 2% to 40% (note that the POC load from Figure 3-1 is repeated on the last panel of Figure 3-4).

3.1.1.2 Open Water Tidal Boundaries

The open water tidal boundaries at the Kill Van Kull and Arthur Kill were assigned monthly average concentrations based on CARP model outputs for the CARP model grid cells closest to the LPR truncated grid boundary cells. These values were used directly without being modified.

3.1.2 Wastewater Treatment Plant Loadings

Although there are no wastewater treatment plants within the LPR itself, there are a number of plants that discharge within the domain of the model. The Bergen County Utility Authority and the Town of Secaucus discharge to the Hackensack River, the Port Richmond Water Pollution Control Plant (WPCP) discharges to the Kill Van Kull, and the Essex and Union County Joint Meeting Sewage Treatment Plant (STP), the Linden Roselle Sewerage Authority STP, and the Rahway Valley Sewerage Authority STP discharge to the Arthur Kill. The loads for these discharges were copied over from the CARP model and mapped to the appropriate grid cells on the LPR grid. Similar to the loadings associated with head of tide boundaries (Section 3.1.1.1), about 43% of the refractory POM was treated as inert POM.

3.1.3 Stormwater and Combined-sewer Overflows

SWO and CSO loads were developed using the same approach as the CARP model. Time variable hourly flows for both CSOs and SWOs were developed based on landside watersheds and sewershed models together with rainfall records for the period from 1995 through 2010. The watershed models compute stormwater and sanitary overflow volumes. The landside models are discussed in further detail in the Final Hydrodynamic

Modeling Report (HydroQual, 2008). These flows were then assigned temporally constant concentrations based on the values developed for the SWEM model (Table 3-1). Similar to the other loads about 43% of the refractory POM was replaced with inert POM.

Table 3-1. Stormwater and Combined Sewer Concentrations

System	Variable	CSO (mg/L)	SWO (mg/L)
1	SALINITY	0	0
2	PHYT1-C	0	0
3	PHYT2-C	0	0
4	RPOP	0.199	0.036
5	LPOP	0.349	0.027
6	RDOP	0.065	0.0133
7	LDOP	0.065	0.0057
8	DIP	0.596	0.084
9	RPON	1.08	0.186
10	LPON	1.51	0.112
11	RDON	0.813	0.283
12	LDON	0.813	0.121
13	NH4	4.44	0.236
14	NO ₂ +NO ₃	0.492	0.765
15	BSI	0	0
16	DSI	1.71	1.77
17	RPOC	11.8	2.93
18	LPOC	20.7	2.2
19	RDOC	9.35	6.16
20	LDOC	4.68	1.32
21	REDOC	4.68	1.32
22	EXDOC	0	0
23	O2EQ	0	0

Table 3-1. Stormwater and Combined Sewer Concentrations

System	Variable	CSO (mg/L)	SWO (mg/L)
24	O2	3.81	6.33
25	IPOC	8.88	2.2
26	IPON	0.431	0.0744
27	IPOP	0.149	0.027
28	SG1C	0	0
29	SG2C	0	0
30	SG3C	0	0
31	SG1N	0	0
32	SG2N	0	0
33	SG3N	0	0
34	SG1P	0	0
35	SG2P	0	0
36	SG3P	0	0
37	SPSI	0	0
38	COSS	202	27

3.1.4 Atmospheric Loadings

Atmospheric loads were copied directly from CARP which were in turn copied from SWEM. These values remained unmodified for the LPR model application. The atmospheric loads from the original SWEM model are spatially constant and vary on a monthly basis. The systems which receive atmospheric loads are LDOP, DIP, LDON, NH4, NO2+NO3, Total Silica (Si), LDOC, and REDOC. The monthly values for the atmospheric loads copied from SWEM are tabulated in Table 3-2.

<i>Month</i>	<i>LDOP</i>	<i>DIP</i>	<i>LDON</i>	<i>NH4</i>	<i>NO₂+NO₃</i>	<i>Si</i>	<i>LDOC</i>	<i>REDOC</i>
October	1.76E-08	8.19E-09	1.65E-07	4.99E-07	1.32E-06	3.86E-08	1.05E-06	1.05E-06
November	3.67E-09	1.47E-08	3.85E-07	7.86E-07	2.09E-06	7.71E-08	2.81E-06	2.81E-06
December	5.47E-08	1.19E-08	1.50E-07	4.30E-07	1.39E-06	6.66E-08	1.64E-06	1.64E-06
January	0.00E+00	1.98E-08	2.64E-08	2.47E-07	1.12E-06	6.60E-08	1.15E-06	1.15E-06
February	2.84E-09	1.14E-08	2.53E-07	1.06E-06	2.24E-06	6.25E-08	2.04E-06	2.04E-06
March	2.06E-09	7.21E-09	7.83E-08	3.49E-07	1.14E-06	2.78E-08	7.43E-07	7.43E-07
April	1.94E-08	4.27E-08	5.16E-07	1.68E-06	2.90E-06	5.43E-08	3.80E-06	3.80E-06
May	1.40E-08	1.40E-08	5.73E-07	9.49E-07	2.02E-06	1.31E-07	2.45E-06	2.45E-06
June	5.31E-09	5.31E-09	1.75E-07	5.22E-07	1.48E-06	7.08E-08	1.51E-06	1.51E-06
July	7.53E-08	3.51E-08	7.08E-07	1.84E-06	3.44E-06	1.66E-07	4.48E-06	4.48E-06
August	2.25E-09	1.05E-09	2.12E-08	1.44E-07	7.58E-07	4.95E-09	1.34E-07	1.34E-07
September	3.86E-08	1.80E-08	3.62E-07	9.86E-07	2.09E-06	8.48E-08	2.30E-06	2.30E-06

3.1.5 Sediment Properties

Sediment bed initial conditions evolved over the course of the development of the LPR version of the ST-SWEM model. Earlier runs were done on the CARP model grid incorporating the changes in the loads described above, and cycling the model through a number of years, until the state-variables in the sediment reached a quasi-equilibrium. These results were copied from the CARP grid to the LPR grid and used to set the sediment bed initial conditions for the carbon model.

The datasets used to set contaminant initial conditions within the LPR, particularly the 1995 RI dataset¹, included unrealistically high values for FOC. For this reason those values were not used to set sediment organic carbon initial conditions within the LPR. The Newark Bay sediment datasets used to generate sediment initial conditions (Table 3-6) were not affected by this issue and were therefore used with the same approach as the

¹ Lower Passaic River and Newark Bay-specific datasets are described in Table 3-6.

contaminants to set initial conditions for sediment organic carbon in Newark Bay. This approach is discussed further in section 3.2.5. Figures 3-5 and 3-6 present the combined surface FOC for the model including the values generated by cycling the model in the LPR and Interpolating FOC data within Newark Bay.

3.1.6 Parameters and Constants

Model rate coefficients and constants for all reactions in both the water column and sediment were copied directly from the CARP model and were not altered for application to the LPR model.

3.2 CONTAMINANT FATE AND TRANSPORT MODEL

The contaminant fate and transport model inputs were based either directly on those developed for the CARP model (HydroQual, 2007), or followed the approach used for the CARP model incorporating additional data collected for the FFS or 17-mile Remedial Investigation and Feasibility Study (RI/FS) at the Passaic and Saddle River heads of tide. The one exception to this was the development of sediment initial conditions for the contaminants. These were developed using an approach developed specifically for the FFS described below.

3.2.1 Boundary Conditions

3.2.1.1 Freshwater Boundaries

Similar to the organic carbon production model, the freshwater boundaries used in CARP were also used for the LPR contaminant model, i.e., the Passaic, Saddle, and Hackensack Rivers. The other tributaries included as heads of tide in the LPR model (Second and Third Rivers, and MacDonald Brook) were assigned the storm water contaminant concentrations developed for the CARP model. Two additional tributaries were measured as part of the CARP sampling program: the Elizabeth and Rahway Rivers, but not included in the LPR model as heads of tide. Loads for these two rivers were

incorporated in the model using a similar approach to that used for the other measured heads of tide. The RCA model framework requires inputs for the head of tide boundaries as concentrations, and combines those concentrations with flow information passed from the hydrodynamic model to calculate loads. Because the Elizabeth and Rahway Rivers were not represented in the hydrodynamic model, and therefore there are no flows in the file passed from the hydrodynamic model to RCATOX, the loads for these tributaries had to be calculated separately. The other forcing function input files, for treatment plants, CSO, and SWO, are input as loads in units of Kg/day. Once the loads were calculated they were combined with wastewater treatment plant loads described below in a single input file.

The CARP data collected at the boundaries showed less variability in dissolved and carbon normalized particulate concentrations than total concentrations. Based on that observation, dissolved and particulate concentrations were used to develop the head of tide loads for the CARP model (HydroQual, 2007). Median dissolved and median carbon normalized particulate concentrations were calculated from data and total contaminant concentrations were calculated based on those values along with NPL-calculated POC loads. Contaminant loads were calculated as the sum of the median of measured dissolved concentrations plus the product of NPL POC and median measured organic carbon-normalized particulate concentrations.

As part of the FFS, the concentrations from the CARP model were reviewed for a handful of contaminants and some values were modified to incorporate additional analyses and additional data. These modifications to CARP values are discussed in further detail in Attachment G, Revisions to CARP Loads. Attachment G includes analyses of the loads entering the Lower Passaic River at the heads of tide at Dundee Dam from the Upper Passaic River, and the Saddle, Second, and Third Rivers. The MacDonald Brook was not re-evaluated, due to its small size and the lack of new data for that tributary.

There are twelve PCB congeners that display dioxin like toxicity. These congeners each have a Toxic Equivalency Factor (TEF) used to normalize their toxicity relative to

2,3,7,8-TCDD. The CARP model did not include the twelve PCB congeners that display dioxin like toxicity (TEF-PCBs) which were considered in the FFS; however boundary concentrations for the twelve congeners were measured as part of the CARP sampling program. The CARP data were used to develop boundary concentrations for these chemicals using the same approach used in the CARP model.

Based on head of tide sampling results there were a number of assumptions necessary to complete the calculation of heads of tide loads:

- As part of the CARP project head of tide measurements for the New Jersey tributaries were reported for the homologues trichlorobiphenyl through octachlorobiphenyl. The monochlorobiphenyl, dichlorobiphenyl, nonachlorobiphenyl, and decachlorobiphenyl data were reported as mono+di and nona+deca respectively. Concentrations were split equally between the two homologues reported as a pair.
- Total dissolved (free + DOC-complexed) concentrations were not reported for the New Jersey heads of tide for dioxins and furans as part of CARP. Values from the Mohawk River were used for the dissolved phase for the tributaries. The Mohawk was chosen during the development of the CARP model because it had the lowest concentrations out of the tributaries that were measured for that study.
- The Saddle River was not measured during the CARP sampling program. When available, data from the Hackensack (the New Jersey tributary with the lowest concentrations) were used for the Saddle River. If data were unavailable for the Hackensack River, then data from the Mohawk River were used.

The head of tide dissolved and particulate contaminant concentrations used in the LPR RCATOX model are tabulated in Table 3-3. Footnotes on the table indicate where values from the Hackensack or Mohawk Rivers were substituted for unavailable data during the CARP project. The concentrations that were modified as part of the LPR modeling effort are also noted.

Figures 3-7 through 3-9 present the Upper Passaic River boundary conditions at Dundee Dam for 2,3,7,8-TCDD, the sum of tetrachlorobiphenyl PCBs, and total mercury respectively. Each figure has three panels. The top panel is the flow at Dundee Dam, the middle panel is the concentration at Dundee Dam and the bottom panel is the load coming over Dundee Dam. Although the loads are computed as dissolved and particulate, they are input into the model as a total concentration, and the model computes the distribution of the chemical based on equilibrium partitioning to the POC and DOC concentrations for the cell immediately inside of the boundary. For the projection runs the time history for the period of time from October 1, 1995 through September 30, 2010 is repeated in a cycle from October 1, 2012 through September 30, 2059.

Table 3-3. RCATOX Head of Tide Concentrations for Measured Tributaries

Chemical	Passaic		Saddle		Hackensack		Elizabeth		Rahway	
	Diss. (ng/L)	Part. (µg/g-OC)	Diss. (ng/L)	Part. (µg/g-OC)	Diss. (ng/L)	Part. (µg/g-OC)	Diss. (ng/L)	Part. (µg/g-OC)	Diss. (ng/L)	Part. (µg/g-OC)
2,3,7,8-TCDD	8.00E-07 ³	4.41E-05 ³	4.46E-05 ³	3.00E-05 ³	1.13E-05 ²	7.62E-06	1.13E-05 ²	7.62E-06	1.13E-05 ²	7.62E-06
1,2,3,4,7,8-HxCDD	6.62E-06 ²	1.11E-04	6.62E-09 ²	3.42E-08 ¹	6.62E-06 ²	3.42E-05	6.62E-06 ²	1.47E-04	6.62E-06 ²	8.96E-05
1,2,3,6,7,8-HxCDD	4.10E-06 ²	3.07E-04	4.10E-09 ²	7.98E-08 ¹	4.10E-06 ²	7.98E-05	4.10E-06 ²	3.94E-04	4.10E-06 ²	2.02E-04
1,2,3,7,8,9-HxCDD	2.73E-06 ²	2.53E-04	2.73E-09 ²	7.05E-08 ¹	2.73E-06 ²	7.05E-05	2.73E-06 ²	4.95E-04	2.73E-06 ²	2.11E-04
1,2,3,4,6,7,8-HpCDD	7.34E-04 ²	7.11E-03	7.34E-07 ²	1.94E-06 ¹	7.34E-04 ²	1.94E-03	7.34E-04 ²	7.79E-03	7.34E-04 ²	5.08E-03
OCDD	1.82E-03 ²	1.28E-01	1.82E-06 ²	2.40E-05 ¹	1.82E-03 ²	2.40E-02	1.82E-03 ²	8.71E-02	1.82E-03 ²	8.21E-02
1,2,3,7,8-PeCDD	4.45E-06 ²	7.11E-05	4.45E-09 ²	1.23E-08 ¹	4.45E-06 ²	1.23E-05	4.45E-06 ²	1.66E-04	4.45E-06 ²	6.60E-05
1,2,3,7,8-PeCDF	3.74E-06 ²	1.56E-04	3.74E-09 ²	9.91E-09 ¹	3.74E-06 ²	9.91E-06	3.74E-06 ²	1.87E-04	3.74E-06 ²	1.84E-04
1,2,3,7,8,9-HxCDF	6.00E-06 ²	1.56E-05	6.00E-09 ²	3.88E-09 ¹	6.00E-06 ²	3.88E-06	6.00E-06 ²	3.88E-06	6.00E-06 ²	3.88E-06
2,3,4,6,7,8-HxCDF	2.06E-06 ²	1.22E-04	2.06E-09 ²	3.65E-08 ¹	2.06E-06 ²	3.65E-05	2.06E-06 ²	2.11E-04	2.06E-06 ²	1.04E-04
1,2,3,4,7,8,9-HpCDF	1.41E-06 ²	2.24E-04	1.41E-09 ²	4.56E-08 ¹	1.41E-06 ²	4.56E-05	1.41E-06 ²	3.65E-04	1.41E-06 ²	8.30E-05
2,3,7,8-TCDF	1.10E-05 ²	3.73E-04	1.10E-08 ²	7.44E-08 ¹	1.10E-05 ²	7.44E-05	1.10E-05 ²	3.48E-04	1.10E-05 ²	2.33E-04
2,3,4,7,8-PeCDF	1.50E-05 ²	1.25E-04	3.62E-05 ³	7.00E-05 ³	1.50E-05 ²	2.90E-05	1.50E-05 ²	4.38E-04	1.50E-05 ²	8.46E-05
1,2,3,4,7,8-HxCDF	5.15E-06 ²	2.50E-04	5.15E-09 ²	1.02E-07 ¹	5.15E-06 ²	1.02E-04	5.15E-06 ²	4.86E-04	5.15E-06 ²	2.14E-04
1,2,3,6,7,8-HxCDF	1.90E-06 ²	3.46E-04	1.90E-09 ²	6.26E-08 ¹	1.90E-06 ²	6.26E-05	1.90E-06 ²	5.96E-04	1.90E-06 ²	2.16E-04
1,2,3,4,6,7,8-HpCDF	2.17E-04 ²	2.41E-03	2.17E-07 ²	6.57E-07 ¹	2.17E-04 ²	6.57E-04	2.17E-04 ²	3.02E-03	2.17E-04 ²	1.63E-03
OCDF	2.42E-05 ²	8.52E-03	2.42E-08 ²	1.34E-06 ¹	2.42E-05 ²	1.34E-03	2.42E-05 ²	4.77E-03	2.42E-05 ²	2.98E-03
di-PCB	3.05E-01 ³	1.33E-01 ³	1.03E-01 ³	8.64E-02 ³	7.50E-03	6.35E-03	1.18E+00	1.29E-01	2.93E-02	9.15E-03

Table 3-3. RCATOX Head of Tide Concentrations for Measured Tributaries

Chemical	Passaic		Saddle		Hackensack		Elizabeth		Rahway	
	Diss. (ng/L)	Part. (µg/g-OC)	Diss. (ng/L)	Part. (µg/g-OC)	Diss. (ng/L)	Part. (µg/g-OC)	Diss. (ng/L)	Part. (µg/g-OC)	Diss. (ng/L)	Part. (µg/g-OC)
tri-PCB	5.68E-01	4.60E-01	9.01E-02 ¹	1.78E-02 ¹	9.01E-02	1.78E-02	2.42E+00	1.44E+00	3.09E-01	1.74E-01
tetra-PCB	7.08E-01 ³	1.46E+00 ³	6.94E-01 ³	5.00E-01 ³	1.30E-01	9.36E-02	1.01E+00	2.11E+00	4.20E-01	5.81E-01
penta-PCB	1.95E-01	1.43E+00	5.39E-02 ¹	1.92E-01 ¹	5.39E-02	1.92E-01	3.64E-01	1.69E+00	2.90E-01	1.37E+00
hexa-PCB	7.52E-02 ³	1.32E+00 ³	9.27E-02 ³	7.00E-01 ³	1.67E-02	1.26E-01	3.03E-01	2.85E+00	9.81E-02	7.04E-01
mono-PCB	8.35E-02	3.65E-02	7.50E-03 ¹	6.35E-03 ¹	7.50E-03	6.35E-03	1.18E+00	1.29E-01	2.93E-02	9.15E-03
hepta-PCB	9.23E-03	3.40E-01	4.69E-03 ¹	6.19E-02 ¹	4.69E-03	6.19E-02	1.16E-01	2.32E+00	2.43E-02	3.15E-01
octa-PCB	2.10E-03 ³	1.97E-01 ³	5.59E-02 ³	8.00E-02 ³	1.37E-02	1.96E-02	1.71E-02	6.06E-01	3.89E-03	1.01E-01
nona-PCB	3.31E-03 ¹	2.96E-02	3.31E-03 ¹	3.35E-03 ¹	3.31E-03	3.35E-03	9.50E-04	6.65E-02	3.53E-04	1.33E-02
deca-PCB	3.31E-03 ¹	2.96E-02	3.31E-03 ¹	3.35E-03 ¹	3.31E-03	3.35E-03	9.50E-04	6.65E-02	3.53E-04	1.33E-02
BZ#77	3.24E-03	2.05E-02	1.04E-03 ¹	1.26E-03 ¹	1.04E-03	1.26E-03	5.12E-03	3.02E-02	3.38E-03	7.20E-03
BZ#81	9.44E-04	8.18E-04	1.60E-03 ¹	2.67E-04 ¹	1.60E-03	2.67E-04	1.64E-03	1.06E-03	1.56E-03	1.84E-04
BZ#105	1.00E-02	7.74E-02	4.38E-03 ¹	8.42E-03 ¹	4.38E-03	8.42E-03	1.21E-02	1.21E-01	1.03E-02	4.04E-02
BZ#114	1.02E-03	6.91E-03	6.84E-04 ¹	7.04E-04 ¹	6.84E-04	7.04E-04	1.47E-03	7.11E-03	1.09E-03	3.62E-03
BZ#118	2.26E-02	1.55E-01	1.02E-02 ¹	2.03E-02 ¹	1.02E-02	2.03E-02	2.79E-02	2.83E-01	2.26E-02	9.83E-02
BZ#123	9.57E-04	3.47E-03	6.95E-04 ¹	5.27E-04 ¹	6.95E-04	5.27E-04	1.39E-03	5.09E-03	7.79E-04	2.29E-03
BZ#126	9.72E-04	1.35E-03	6.90E-04 ¹	4.98E-04 ¹	6.90E-04	4.98E-04	1.53E-03	3.91E-03	1.02E-03	5.29E-04
BZ#156	8.35E-04	1.72E-02	1.34E-03 ¹	2.60E-03 ¹	1.34E-03	2.60E-03	2.28E-03	7.28E-02	1.69E-03	1.26E-02
BZ#157	1.12E-03	4.26E-03	1.41E-03 ¹	6.08E-04 ¹	1.41E-03	6.08E-04	1.49E-03	5.25E-03	7.77E-04	2.55E-03

Table 3-3. RCATOX Head of Tide Concentrations for Measured Tributaries

Chemical	Passaic		Saddle		Hackensack		Elizabeth		Rahway	
	Diss. (ng/L)	Part. (µg/g-OC)	Diss. (ng/L)	Part. (µg/g-OC)	Diss. (ng/L)	Part. (µg/g-OC)	Diss. (ng/L)	Part. (µg/g-OC)	Diss. (ng/L)	Part. (µg/g-OC)
BZ#167	5.13E-04	7.70E-03	1.43E-03 ¹	1.21E-03 ¹	1.43E-03	1.21E-03	1.73E-03	3.62E-02	9.18E-04	6.16E-03
BZ#169	1.19E-03	1.32E-03	1.56E-03 ¹	4.58E-04 ¹	1.56E-03	4.58E-04	1.53E-03	2.66E-03	9.31E-04	2.73E-04
BZ#189	7.32E-04	1.53E-03	1.23E-03 ¹	5.42E-04 ¹	1.23E-03	5.42E-04	1.01E-03	1.47E-02	8.68E-04	1.28E-03
2,4'-DDD	5.00E-02	1.80E-01	3.40E+01 ¹	2.60E-02 ¹	3.40E-02	2.60E-02	1.30E-01	2.90E-01	1.90E-01	2.40E-01
2,4'-DDE	2.40E-03	7.50E-02	7.30E+00 ¹	1.30E-02 ¹	7.30E-03	1.30E-02	1.50E-02	4.60E-02	1.20E-02	2.30E-02
2,4'-DDT	2.60E-02	1.80E-01	4.00E+01 ¹	3.60E-02 ¹	4.00E-02	3.60E-02	5.60E-02	1.90E-01	3.00E-02	7.80E-02
4,4'-DDD	4.80E-02	2.00E-01	3.00E+01 ¹	4.00E-02 ¹	3.00E-02	4.00E-02	3.40E-01	7.50E-01	2.10E-01	8.10E-01
4,4'-DDE	6.90E-02	3.30E-01	1.00E+02 ¹	6.10E-02 ¹	1.00E-01	6.10E-02	1.30E-01	5.90E-01	1.80E-01	5.00E-01
4,4'-DDT	2.30E-02	4.10E-01	1.50E+01 ¹	6.20E-02 ¹	1.50E-02	6.20E-02	1.90E-01	7.40E-01	7.80E-02	3.90E-01
Cd	5.41E+01	3.70E+01	7.30E+00 ²	1.72E+01 ²	7.30E+00 ²	1.72E+01 ²	1.01E+02	7.47E+01	2.53E+01	2.47E+01
Hg	1.08E+00	6.55E+00	6.40E-01 ¹	1.89E+00 ¹	6.40E-01	1.89E+00	8.05E+00	1.12E+01	3.65E+00	5.22E+00
MeHg	5.80E-02	0.00E+00	1.40E-02 ¹	0.00E+00 ¹	1.40E-02	0.00E+00	2.81E-02	0.00E+00	8.95E-02	0.00E+00

1. Hackensack Substituted
2. Mohawk Substituted
3. Revised for FFS

3.2.1.2 Open Water Tidal Boundaries

Similar to the carbon model, the open water tidal boundaries at the Kill Van Kull and Arthur Kill were assigned monthly average concentrations based on CARP model outputs for the CARP model grid cells closest to the LPR truncated grid boundary cells. The CARP model was run to predict future concentrations at boundary locations. These values were saved on a monthly basis for use as inputs to the LPR RCATOX model. These values were used directly without being modified.

Once the forcing functions were developed for the TEF-PCBs the model was run on the CARP grid to develop open water boundaries for those contaminants in the same fashion as for contaminants modeled as part of the CARP.

3.2.2 Wastewater Treatment Plant Loadings

Wastewater treatment plant loadings were developed using the same approach as the CARP model. Treatment plant specific median measured concentrations from the CARP model were applied to the time variable monthly treatment plant flows for each treatment plant included in the LPR model.

3.2.3 Stormwater and Combined-Sewer Overflows

SWO and CSO concentrations from CARP were used along with hourly time variable flows calculated by models of the watersheds and sewersheds draining to the model domain. The CARP concentrations were developed as the median of measured data. As part of the FFS modeling effort some of these values were adjusted to incorporate new analyses and additional data. These modifications to the CARP values are discussed in further detail in Attachment G, Revisions to CARP Loads.

Similar to the other forcing functions, concentrations of the TEF-PCBs were developed using the median of concentrations measured as part of the CARP sampling program.

**Table 3-4 Combined Sewer and Storm Water Overflow
Concentrations**

<i>Chemical</i>	<i>CSO (ng/L)</i>	<i>SWO (ng/L)</i>
2,3,7,8-TCDD	3.20E-04	3.30E-03
1,2,3,4,7,8-HxCDD	1.91E-03	4.50E-03
1,2,3,6,7,8-HxCDD	5.38E-03	9.70E-03
1,2,3,7,8,9-HxCDD	4.91E-03	8.30E-03
1,2,3,4,6,7,8-HpCDD	1.55E-01	1.90E-01
OCDD	1.58E+00	2.70E+00
1,2,3,7,8-PeCDD	1.38E-03	6.60E-03
1,2,3,7,8-PeCDF	1.25E-03	8.00E-03
1,2,3,7,8,9-HxCDF	3.10E-03	1.30E-02
2,3,4,6,7,8-HxCDF	2.37E-03	7.20E-03
1,2,3,4,7,8,9-HpCDF	3.57E-03	9.30E-03
2,3,7,8-TCDF	1.23E-03	3.00E-03
2,3,4,7,8-PeCDF	1.59E-03	7.40E-03
1,2,3,4,7,8-HxCDF	4.21E-03	1.60E-02
1,2,3,6,7,8-HxCDF	1.39E-04	1.20E-02
1,2,3,4,6,7,8-HpCDF	4.48E-02	1.20E-01
OCDF	9.34E-02	2.30E-01
di-PCB	4.11E-01 - 2.71E+00	6.07E-01
tri-PCB	1.60E+00 - 7.66E+00	2.21E+00
tetra-PCB	4.92E+00 - 1.81E+01	7.07E+00
penta-PCB	7.60E+00 - 3.95E+01	1.11E+01
hexa-PCB	6.73E+00 - 4.02E+01	8.81E+00
mono-PCB	4.63E-02 - 3.73E-01	1.08E-01
hepta-PCB	3.42E+00 - 1.70E+01	3.66E+00
octa-PCB	1.20E+00 - 5.62E+00	1.09E+00
nona-PCB	4.04E-01 - 1.58E+00	3.07E-01
deca-PCB	1.78E-01 - 3.70E-01	1.49E-01

**Table 3-4 Combined Sewer and Storm Water Overflow
Concentrations**

<i>Chemical</i>	<i>CSO (ng/L)</i>	<i>SWO (ng/L)</i>
BZ#77	8.42E-02 - 2.53E-01	1.07E-01
BZ#81	1.15E-02 - 1.26E-01	1.11E-01
BZ#105	7.25E-01 - 2.79E+00	7.12E-01
BZ#114	3.68E-02 - 1.44E-01	5.10E-02
BZ#118	1.58E+00 - 6.12E+00	1.61E+00
BZ#123	1.27E-01	0.00E+00
BZ#126	3.54E-02 - 9.84E-02	8.75E-02
BZ#156	2.80E-01 - 1.24E+00	2.54E-01
BZ#157	0.00E+00	0.00E+00
BZ#167	8.96E-02 - 3.79E-01	8.34E-02
BZ#169	6.14E-03 - 1.10E-01	1.19E-01
BZ#189	2.87E-02 - 7.70E-02	3.40E-02
2,4'-DDD	7.29E-01	1.02E+00
2,4'-DDE	1.88E-01	2.36E-01
2,4'-DDT	2.03E+00	2.30E+00
4,4'-DDD	1.77E+00	2.50E+00
4,4'-DDE	3.92E+00	3.78E+00
4,4'-DDT	9.27E+00	7.42E+00
Cd	5.18E+02	6.59E+02
Hg	3.30E+02	1.16E+02
MeHg	9.55E-01	4.65E-01

3.2.4 Atmospheric Loadings

Atmospheric loads were also developed using the same approach used in CARP. Data from the New Jersey Atmospheric Deposition Network (NJADN) were used to define atmospheric loads of contaminants in the gas, particle and precipitation phases.

Calculations required to convert measured data into atmospheric loads are discussed in further detail in the CARP report (HydroQual, 2007) as well as the NJADN protocol cited by CARP (Totten et al., 2004).

Atmospheric loads of the TEF-PCB congeners were not developed as part of CARP. However, Rutgers used the same approach used in CARP to provide estimates of atmospheric loads for these contaminants (Rodenburg, 2008).

3.2.5 Assignment of Initial Conditions for Sediment Contaminant Concentrations

Forty-eight COPCs and COPECs in the LPR were tracked by the RCATOX Contaminant Fate and Transport Model (Table 3-5). Initial sediment concentrations for these contaminants were based on historical data; however, data sampling was not distributed uniformly over the model domain (Figure 3-10). To overcome this limitation, the following procedure was used to assign characteristic initial concentrations throughout the model domain.

3.2.5.1 Assignment of Initial Conditions within the Lower Passaic River

The COPCs and COPECs of the LPR are generally characterized as persistent, particle-reactive contaminants. Therefore, it is reasonable to expect that patterns of contemporary COPC and COPEC concentrations in sediments of the LPR will reflect both proximity to and magnitude of contaminant sources and the influence of physical processes that transport particle-sorbed contaminants. In light of this expectation, a first step in assigning initial COPC and COPEC concentrations was to characterize the bed as geomorphic regions that reflect time-averaged and quasi-steady conditions of sediment transport. High-resolution multi-beam survey data from the November 2008, Cooperating Parties Group (CPG²) - Multi-Beam and Single-Beam Bathymetry (GBA,

² The CPG is a group of potentially responsible parties who signed an agreement with USEPA to perform the 17-mile Lower Passaic River Study Area Remedial Investigation and Feasibility Study (RI/FS), under USEPA oversight.

2009) were used to characterize finer-scale morphological features, partitioning the river bed into seven morphological categories (Figure 3-10):

1. Abutment – Hard structures such as bridge piers or scour protection in the vicinity of bridges that can alter flow and create local scour.
2. Abutment Scour – Readily identifiable scour due to proximity to abutments.
3. Broad Shoal – Broad mudflats and/or point bars typically located on the inside of river bends.
4. Island – Islands emerge from water in upstream sections of the river.
5. Margins – Broad channel margins near the shoreline that are often similar to the broad shoals but can also be anthropogenic shoreline features.
6. Smooth Channel – Broad relatively flat central channel that is present throughout much of the river. Although there are bathymetric perturbations, the overall feature is considered smooth.
7. Deep Scoured Channel – Channel regions that occur typically on the outside of river bends, where enhanced currents and boundary shear stress tend to create and preserve a deeper scoured channel. However, some sections of deep scoured channel may represent channel modifications due to dredging.

Historical sediment-sampling data and delineated geomorphic regions were combined within a GIS framework. The datasets used throughout the river for purposes of setting initial sediment concentrations included the 1995 RI Sampling Program dataset as well as others listed in Table 3-6. The interpolation within the River Mile (RM) 1 to RM 7 reach of the LPR relied mainly on the 1995 RI dataset. The organic carbon data included in this dataset contained a number of unrealistically high values (as high as 46%), which made setting initial conditions based on organic carbon normalized values infeasible. Instead dry weight values from all datasets were used to interpolate sediment initial conditions. For the stretch of the LPR from RM 7 to RM 17 data from the 1995 time period were too sparse to use to set initial conditions. For this section of the river the 2008 CPG Low Resolution Sediment Coring data were used to set initial conditions for the model calibration period. All sediment contaminant data collected within each

geomorphic region were averaged to characterize a representative concentration for that region (Figure 3-10).

Table 3-5. LPR Contaminants of Concern (COPC)

S No	Chemical Abbreviation	Chemical Full Name	Unit	CAS
1	DIOXIN1-1 pcd2378	2,3,7,8-TCDD (Dioxin)	(µg/kg)	1746-01-6
2	DIOXIN1-2 pcd123478	1,2,3,4,7,8-Hexachlorodibenzo-p-dioxin	(µg/kg)	39227-28-6
3	DIOXIN1-3 pcd123678	1,2,3,6,7,8-Hexachlorodibenzo-p-dioxin	(µg/kg)	57653-85-7
4	DIOXIN1-4 pcd123789	1,2,3,7,8,9-Hexachlorodibenzo-p-dioxin	(µg/kg)	19408-74-3
5	DIOXIN1-5 pcd1234678	1,2,3,4,6,7,8-Heptachlorodibenzo-p-dioxin	(µg/kg)	35822-46-9
6	DIOXIN1-6 pcd_t8	Octachlorodibenzo-p-dioxin	(µg/kg)	3268-87-9
7	DIOXIN2-1 pcd12378	1,2,3,7,8-Pentachlorodibenzo-p-dioxin	(µg/kg)	40321-76-4
8	DIOXIN2-2 pcf12378	1,2,3,7,8-Pentachlorodibenzofuran	(µg/kg)	57117-41-6
9	DIOXIN2-3 pcf123789	1,2,3,7,8,9-Hexachlorodibenzofuran	(µg/kg)	72918-21-9
10	DIOXIN2-4 pcf234678	2,3,4,6,7,8-Hexachlorodibenzofuran	(µg/kg)	60851-34-5
11	DIOXIN2-5 pcf1234789	1,2,3,4,7,8,9-Heptachlorodibenzofuran	(µg/kg)	55673-89-7
12	DIOXIN3-1 pcf2378	2,3,7,8-TCDF (Tetrachlorodibenzofuran)	(µg/kg)	51207-31-9
13	DIOXIN3-2 pcf23478	2,3,4,7,8-Pentachlorodibenzofuran	(µg/kg)	57117-31-4
14	DIOXIN3-3 pcf123478	1,2,3,4,7,8-Hexachlorodibenzofuran	(µg/kg)	70648-26-9
15	DIOXIN3-4 pcf123678	1,2,3,6,7,8-Hexachlorodibenzofuran	(µg/kg)	57117-44-9
16	DIOXIN3-5 pcf1234678	1,2,3,4,6,7,8-Heptachlorodibenzofuran	(µg/kg)	67562-39-4
17	DIOXIN3-6 pcf_t8	Octachlorodibenzofuran	(µg/kg)	39001-02-0
18	PCB1-1 pcbs_cl2	PCBs, sum of dichloro biphenyl congeners	(µg/kg)	25512-42-9
19	PCB1-2 pcbs_cl3	PCBs, sum of trichloro biphenyl congeners	(µg/kg)	25323-68-6
20	PCB1-3 pcbs_cl4	PCBs, sum of tetrachloro biphenyl congeners	(µg/kg)	26914-33-0
21	PCB1-4 pcbs_cl5	PCBs, sum of pentachloro biphenyl congeners	(µg/kg)	25429-29-2
22	PCB1-5 pcbs_cl6	PCBs, sum of hexachloro biphenyl congeners	(µg/kg)	26601-64-9
23	PCB2-1 pcbs_cl1	PCBs, sum of monochloro biphenyl congeners	(µg/kg)	27323-18-8
24	PCB2-2 pcbs_cl7	PCBs, sum of heptachloro biphenyl congeners	(µg/kg)	28655-71-2
25	PCB2-3 pcbs_cl8	PCBs, sum of octachloro biphenyl congeners	(µg/kg)	55722-26-4
26	PCB2-4 pcbs_cl9	PCBs, sum of nonachloro biphenyl congeners	(µg/kg)	53742-07-7
27	PCB2-5 pcbs_cl10	PCBs, sum of decachloro biphenyl congeners	(µg/kg)	2051-24-3
28	PCB-TEF1-1 pcb077	BZ#077	(µg/kg)	32598-13-3
29	PCB-TEF1-2 pcb081	BZ#081	(µg/kg)	70362-50-4

Table 3-5. LPR Contaminants of Concern (COPC)

S No	Chemical Abbreviation	Chemical Full Name	Unit	CAS
30	PCB-TEF1-3 pcb105	BZ#105	(µg/kg)	32598-14-4
31	PCB-TEF1-4 pcb114	BZ#114	(µg/kg)	74472-37-0
32	PCB-TEF1-5 pcb118	BZ#118	(µg/kg)	31508-00-6
33	PCB-TEF1-6 pcb123	BZ#123	(µg/kg)	65510-44-3
34	PCB-TEF2-1 pcb126	BZ#126	(µg/kg)	57465-28-8
35	PCB-TEF2-2 pcb156	BZ#156	(µg/kg)	38380-08-4
36	PCB-TEF2-3 pcb157	BZ#157	(µg/kg)	69782-90-7
37	PCB-TEF2-4 pcb167	BZ#167	(µg/kg)	52663-72-6
38	PCB-TEF2-5 pcb169	BZ#169	(µg/kg)	32774-16-6
39	PCB-TEF2-6 pcb189	BZ#189	(µg/kg)	39635-31-9
40	PEST1-1 op_ddd	2,4-DDD	(µg/kg)	53-19-0
41	PEST1-2 op_dde	2,4-DDE	(µg/kg)	3424-82-6
42	PEST1-3 op_ddt	2,4-DDT	(µg/kg)	789-02-6
43	PEST1-4 pp_ddd	4,4-DDD	(µg/kg)	72-54-8
44	PEST1-5 pp_dde	4,4-DDE	(µg/kg)	72-55-9
45	PEST1-6 pp_ddt	4,4-DDT	(µg/kg)	50-29-3
46	METALS-1 cadmium	Cadmium	(µg/kg)	7440-43-9
47	METALS-2 mercury	Mercury	(µg/kg)	7439-97-6
48	METALS-3 methyl_hg	Methyl mercury	(µg/kg)	22967-92-6

Table 3-6. LPR Sediment Investigations

Year	Study Name	Surveying Agency	Survey Extent (RM)	Initial Conditions
1990	1990 Surficial Sediment Investigation	USEPA	RM 0 to RM 17	Yes
1990	EPA EMAP 90-92	USEPA	RM 0 to RM 6	Yes
1991	1991 Core Sediment Investigation	USEPA	RM -5 to RM 17	Yes
1991	NOAA NS&T Hudson-Raritan Phase I, 1991	NOAA	RM -5 to RM 15.5	Yes
1992	1992 Core Sediment Investigation	USEPA	RM -4 to RM 15	Yes
1993	1993 Core Sediment Investigation - 01 (March)	USEPA	RM -5 to RM 11	Yes
1993	1993 Core Sediment Investigation - 02 (July)	USEPA	RM 0 to RM 7	Yes
1993	1993 USEPA Surficial Sediment Program	USEPA	RM 2.5 to RM 7	Yes
1993	NOAA NS&T Hudson-Raritan Phase II, 1993	NOAA	RM -5 to RM 11.5	Yes
1993	REMAP, 1993	USEPA	RM -5 to RM 15.5	Yes
1994	1994 Surficial Sediment Investigation	USEPA	RM 3.5 to RM 8	Yes
1994	REMAP, 1994	USEPA	RM -5 to RM 15.5	Yes
1995	1995 RI Sampling Program	USEPA	RM 1 to RM 6.5	Yes
1995	1995 Sediment Grab Sampling Program	USEPA	RM 2.5	Yes
1995	1995 USACE Minish Park Investigation	USACE	RM 4 to RM 5.5	Yes

Table 3-6. LPR Sediment Investigations

Year	Study Name	Surveying Agency	Survey Extent (RM)	Initial Conditions
1996	1996 Newark Bay Reach A Sediment Sampling Program	USEPA	RM -1.5	No
1997	1997 Newark Bay Reach B,C,D Sampling Program	USEPA	RM -4 to RM -2	No
1997	1997 Outfall Sampling Program	USEPA	RM 1.5 to RM 5.5	No
1998	1998 Newark Bay Elizabeth Channel Sampling Program	USEPA	RM -2.5	No
1998	REMAP, 1998	USEPA	RM -5 to RM 15.5	No
1999	1999 Late Summer/Early Fall ESP Sampling Program	USEPA	RM 1 to RM 7	No
1999	1999 Newark Bay Reach ABCD Baseline Sampling Program	USEPA	RM -4 to RM -1.5	No
1999	1999 Sediment Sampling Program	USEPA	RM -2 to RM 6	No
1999	1999 Prelim Toxicity Identification Eval			No
1999	1999/2000 Minish Park Monitoring Program	USACE	RM 5	No
2000	2000 BioGenesis Sediment Collection Program	NJDOT-USACE	RM 4.5	No
2000	2000 Spring ESP Sampling Program	USEPA	RM 1 to RM 7	No
2000	2000 Toxicity Identification Evaluation			No
2005	2005 MPI - Newark Bay Phase I Oversight	USEPA	RM -7.5 to RM 0	No
2005	2005 Newark Bay RIWP Phase I Sediment Investigation	USEPA	RM -7.5 to RM 0	No

Table 3-6. LPR Sediment Investigations

Year	Study Name	Surveying Agency	Survey Extent (RM)	Initial Conditions
2005	2005 USEPA-MPI High Res Sediment Core	USEPA	RM 0 to RM 15	No
2006	2006 HRSA RI Sampling Program	USEPA	Hackensack River	No
1999-2006	1999-2006 Honeywell Intl Sampling		Hackensack River	No
2006	2006 USEPA-MPI Low Resolution Core	USEPA	RM 0 to RM 7	No
2007	2007 USEPA-MPI Dundee High Res Core	USEPA	Above Dundee Dam	No
2007	2007 MPI - Newark Bay Phase II Oversight	USEPA	RM -9.5 to RM 0	No
2007	2007 USEPA-MPI-EMBM Sediment Samples	USEPA	Upper Passaic	No
2008	2007 Newark Bay Phase II TSI Sediment Samples	USEPA	RM -9.5 to RM 0	No
2008	2008 CPG Low Resolution Sediment Coring	USEPA	RM 0 to RM 17	RM 7-17
2008	2008 USEPA-MPI Low Resolution Core Oversight	USEPA	RM 0 to RM 17	No
2009	2009 CPG Benthic Sediment Study	USEPA	RM 0 to RM 17	No
2009	2009 Tierra Phase I Removal design cores	USEPA	RM 3	No
2009	2009 USEPA-MPI Benthic Oversight	USEPA	RM 0 to RM 17	No
2010	2010 CPG Benthic Sediment Sampling	USEPA	RM 0 to RM 17	No

Table 3-6. LPR Sediment Investigations

Year	Study Name	Surveying Agency	Survey Extent (RM)	Initial Conditions
2010	2010 USEPA-CDM Benthic Oversight	USEPA	RM 0 to RM 17	No
2011	2011 CPG River Mile 10.9 Data	USEPA	RM10.5 to RM 11	Yes
2012	2012 CDMSmith Background BenthicSediment	USEPA	Above Dundee Dam	No
2012	2012 CDMSmith LowRes Coring Supplemental	USEPA	RM 0 to RM 17	No
2012	2012 CPG Background Benthic Sediment	USEPA	Above Dundee Dam	No
2012	2012 CPG Low Resolution Coring Supplemental	USEPA	RM 0 to RM 17	No
2012	2012 CPG River Mile 10.9 Data	USEPA	RM 10.9	No

CDM: CDM Smith

EMAP: Environmental Monitoring and Assessment Program

EMBM: Empirical Mass Balance Model

ESP: Ecological Sampling Plan

HRSA: Hackensack River Study Area

MPI: Malcolm Pirnie, Inc.

NS&T: National Status and Trends

REMAP: Regional Environmental Monitoring and Assessment Program

RIWP: Remedial Investigation Work Plan

Sediment contaminant data within an undivided geomorphic region were segregated by vertical layer within the sediment (0.0–0.5 ft, 0.5–1.5 ft, 1.5–2.5 ft, 2.5–3.5 ft, and 3.5–5.5 ft), and average concentrations were determined separately for each layer. The depth intervals for vertical slices were determined based on intervals reported for the majority of the data. No contaminant data were available for several small geomorphic regions, and therefore other methods for establishing initial contaminant concentrations were required. Deep scoured regions without historical sampling data were assigned concentration averages of the contiguous upstream and/or downstream smooth channel regions. Margin and broad shoal regions without historical sampling data were handled similarly; however, in these few cases, concentration averages were taken from the nearest upstream and/or downstream margin or broad shoal regions along the same bank of the river as the region without historical data. The reason for distinguishing between river banks in these cases is that localized contaminant sources and hot zones may occur along one or the other bank of several river reaches, but do not necessarily occur along both banks simultaneously within the same reach.

Once average initial contaminant concentrations (for all five sediment layers) were assigned to each geomorphic region, the LPR model grid was laid over the geomorphic regions. As presented in Figure 3-11, multiple geomorphic regions typically fall within each model grid cell. Characteristic initial contaminant concentrations for each grid cell were derived by taking a spatially weighted average of the contaminant concentrations assigned to each geomorphic region present in the grid cell. This process was repeated separately for each of the five sediment layers. Figure 3-12 shows the final interpolated 2,3,7,8-TCDD concentrations for the top six inches of sediment for each geomorphic region within the LPR.

3.2.5.2 Assignment of Initial Conditions within Newark Bay, the Arthur Kill, and the Kill Van Kull

Newark Bay, the Arthur Kill, and the Kill Van Kull were broken into 15 regions based on geographic location and water depth similar to the geomorphic region approach used to

develop sediment initial conditions for the LPR. The first fourteen of these regions represent the shoals throughout the Newark Bay, Arthur Kill, and Kill Van Kull portions of the model domain, and the final region represents the channel in those areas (Figure 3-13).

Within each of the regions an inverse distance weighted average of the data falling within the region was used. Unlike the 1995 RI dataset in the LPR, the Newark Bay datasets did not suffer from artificially high organic carbon values. All of the organic carbon data from the incorporated datasets was interpolated for each of the regions. Then for each of the modeled chemicals the data was organic carbon normalized, interpolated for each region, and then converted back to dry weight concentrations by multiplying by the interpolated organic carbon values. This process was repeated for organic carbon and each of the contaminants for each of the five layers generated for the LPR. Figure 3-14 shows the final interpolated 2,3,7,8-TCDD concentrations for the top six inches of sediment for each grid cell within Newark Bay, the Arthur Kill, and the Kill Van Kull.

3.2.5.3 Combined Initial Conditions for the Complete Domain

In addition to the surfaces developed for the LPR, Newark Bay and the Kills, values within the Hackensack River were interpolated throughout the river using an inverse distance weighted average of the organic carbon normalized data. The three surfaces resulting from the previous steps were then combined to generate a continuous surface. In locations where the surfaces intersect the LPR surface values superseded the Newark Bay values, and the Newark Bay values superseded the Hackensack River values. The result is one continuous surface for the entire domain for each chemical for each layer. Figure 3-15 shows the final combined interpolated 2,3,7,8-TCDD concentrations for the top six inches of sediment for each grid cell within the model domain.

Attachment B, Transect Plots, displays initial COPC and COPEC concentrations for all five sediment layers versus distance from the head of tide at Dundee Dam to the Southern end of Newark Bay.

3.2.6 Parameters and Constants

Model rate coefficients and constants for all reactions in both the water column and sediment were the same as those used in CARP model and were not altered for application to the LPR model with two exceptions: sediment mixing rates calculated by ST-SWEM were modified for purposes of calibration, and since the TEF-PCB congeners were not included in CARP these chemical specific inputs were developed using the same approach used in the CARP model.

The chemical specific information required for the contaminant model includes the molecular weight, K_{OW} , K_{POC} , A_{DOC} , ΔH_{OW} , K^{salt} , Henry's constant, and ΔH_{AW} . Table 3-7 lists the constants used for each chemical in the model including those developed for the TEF-PCB congeners.

Table 3-7. Chemical Constants								
<i>Name</i>	<i>Molecular Weight</i> (gm/mole)	<i>Log K_{OW}</i> (L/Kg)	<i>Log K_{OC}</i> (L/Kg)	<i>A_{DOC}</i>	<i>Δ H_{OW}</i> (KJ/mole)	<i>K^{salt}</i>	<i>Henry's Constant</i> (Pa m ³ /mole)	<i>Δ H_{AW}</i> (KJ/mole)
2378-TCDD	322.0	6.65	6.81	0.08	0.0	0.35	1.42	0
123478-HxCDD	390.9	8.12	8.20	0.08	0.0	0.35	1.28	0
123678-HxCDD	390.9	8.09	8.53	0.08	0.0	0.35	1.35	0
123789-HxCDD	390.9	8.10	8.59	0.08	0.0	0.35	1.26	0
1234678-HpCDD	425.3	8.82	9.89	0.08	0.0	0.35	1.23	0
OCDD	459.8	9.57	10.9 0	0.08	0.0	0.35	1.21	0
12378-PeCDD	356.4	7.37	7.18	0.08	0.0	0.35	1.38	0
12378-PeCDF	340.4	7.25	7.28	0.08	0.0	0.35	2.18	0
123789-HxCDF	374.9	7.95	6.97	0.08	0.0	0.35	1.98	0
234678-HxCDF	374.9	7.96	8.04	0.08	0.0	0.35	1.93	0

Table 3-7. Chemical Constants								
<i>Name</i>	<i>Molecular Weight</i> (gm/mole)	<i>Log K_{OW}</i> (L/Kg)	<i>Log K_{OC}</i> (L/Kg)	<i>A_{DOC}</i>	<i>Δ H_{OW}</i> (KJ/mole)	<i>K^{salt}</i>	<i>Henry's Constant</i> (Pa m ³ /mole)	<i>Δ H_{AW}</i> (KJ/mole)
1234789-HpCDF	409.3	8.67	8.74	0.08	0.0	0.35	1.75	0
2378-TCDF	306.0	6.54	6.87	0.08	0.0	0.35	2.49	0
23478-PeCDF	340.4	7.23	7.38	0.08	0.0	0.35	2.36	0
123478-HxCDF	374.9	7.96	7.97	0.08	0.0	0.35	2.01	0
123678-HxCDF	374.9	7.95	8.16	0.08	0.0	0.35	2.06	0
1234678-HpCDF	409.3	8.67	9.37	0.08	0.0	0.35	1.75	0
OCDF	443.8	9.37	10.3 0	0.08	0.0	0.35	1.6	0
Di-CB	223.1	5.00	6.04	0.08	-23.5	0.35	23.8	48.7
Tri-CB	257.5	5.60	6.20	0.08	-24.2	0.35	28.1	42.5
Tetra-CB	292.0	6.00	6.27	0.08	-24.9	0.35	36	27.7
Penta-CB	326.4	6.45	6.62	0.08	-25.7	0.35	45.2	33.5
Hexa-CB	360.9	6.85	7.15	0.08	-26.8	0.35	57.5	67.3
Mono-CB	188.7	4.63	6.39	0.08	-22.9	0.35	20.4	50.7
Hepta-CB	395.3	7.22	7.75	0.08	-27.6	0.35	58.1	111
Octa-CB	429.8	7.63	8.21	0.08	-28.4	0.35	40.8	160
Nona-CB	464.2	7.99	8.72	0.08	-29.3	0.35	63.8	154
Deca-CB	498.7	8.18	9.01	0.08	-29.9	0.35	97.5	145
BZ#77	292.0	6.36	7.46	0.08	-28.2	0.35	16.7	57.5
BZ#81	292.0	6.36	6.69	0.08	-28.2	0.35	25.8	57.5
BZ#105	326.4	6.65	7.64	0.08	-27.9	0.35	33.9	59.5
BZ#114	326.4	6.65	7.57	0.08	-27.9	0.35	36.7	59.5
BZ#118	326.4	6.74	7.65	0.08	-27.9	0.35	36.3	59.5
BZ#123	326.4	6.74	7.34	0.08	-27.9	0.35	36.7	59.5
BZ#126	326.4	6.89	7.42	0.08	-29.8	0.35	21.3	60.5
BZ#156	360.9	7.18	8.37	0.08	-29.4	0.35	37	62.4

Table 3-7. Chemical Constants								
<i>Name</i>	<i>Molecular Weight</i> (gm/mole)	<i>Log K_{OW}</i> (L/Kg)	<i>Log K_{OC}</i> (L/Kg)	<i>A_{DOC}</i>	<i>Δ H_{OW}</i> (KJ/mole)	<i>K^{salt}</i>	<i>Henry's Constant</i> (Pa m ³ /mole)	<i>Δ H_{AW}</i> (KJ/mole)
BZ#157	360.9	7.18	8.37	0.08	-29.4	0.35	37	62.4
BZ#167	360.9	7.27	8.44	0.08	-29.4	0.35	39.2	62.4
BZ#169	360.9	7.42	7.35	0.08	-31.3	0.35	23.4	63.4
BZ#189	395.3	7.71	8.33	0.08	-31.0	0.35	28.8	65.3
2,4'-DDD	320.1	6.08	6.41	0.08	0.0	0	0.85	0
2,4'-DDE	318.0	6.72	7.07	0.08	0.0	0	4.61	0
2,4'-DDT	354.5	6.60	6.85	0.08	0.0	0	2.86	0
4,4'-DDD	320.1	6.18	6.42	0.08	0.0	0	0.74	0
4,4'-DDE	318.0	6.79	7.26	0.08	0.0	0	4.63	0
4,4'-DDT	354.5	6.73	7.38	0.08	0.0	0	2.36	0
Cd	112.4	-	-	-	0.0	0	0.000329	0
Hg	200.6	-	-	-	0.0	0	729	0
MeHg	215.6	-	-	-	0.0	0	0.000329	0

Note: Metals (Cd, Hg, MeHg) partitioning is computed by the speciation model

4 MODEL CALIBRATION

4.1 INTRODUCTION

The model simulation period used to calibrate the contaminant fate and transport model was the same period used for the hydrodynamic and sediment transport models, beginning in October of 1995 and running through September of 2012. Model results for all forty-eight of the individual contaminants modeled were compared to the sediment data collected during the calibration period. Particular attention was given to the most extensive datasets: the 1995 RI data which was used to set initial conditions, and the later datasets including the 2008 CPG Low Resolution Sediment Coring, 2009-2010 Benthic Sediment Investigations, and the 2012 CPG Low Resolution Coring Supplemental datasets near the end of the calibration period. These datasets were the most extensive with respect to the quantity of data collected and spatial coverage. Model results were also compared to the CPG chemical water column monitoring (CWCM) data collected during the period between the August of 2011 and October 2012. The complete list of sediment datasets considered is presented in Table 3-6. The water column datasets considered are listed below in Table 4-1. For the sake of consistency individual datasets were plotted using the same symbol throughout the calibration, sensitivity, and projection sections of the report unless otherwise stated. The plotting symbols used are presented in Figure 4-1 for the sediment and water column datasets. Given the size of this legend it is not presented on all figures where data are included.

4.2 CARBON MODEL VERIFICATION

There are a number of datasets available for comparison to the carbon model although none of them provide a complete set of parameters for comparison. The New Jersey Harbor Discharges Group (NJHDG) routinely collects water quality samples at seven stations between Dundee Dam and the southern end of Newark Bay, in addition to a station just above Dundee Dam. This dataset includes measurements of dissolved oxygen, nutrients, chlorophyll-a, 5-day carbonaceous biochemical oxygen demand

(CBOD-5), and DOC, but it does not include measurements of water column particulate organic carbon or of sediment FOC. Numerous other datasets collected as part of other investigations have collected either water column POC and DOC measurements, or sediment FOC measurements. The water column datasets used for comparison to the model are listed in Table 4-1, and the Sediment datasets used for comparison are listed in Table 3-6.

Table 4-1. LPR Water Column Investigations

Year	Study Name	Surveying Agency	Survey Extent (RM)
2000-2002	Passaic Valley Sewerage Commissioners	PVSC	RM -5 to RM 17
2003-2012	New Jersey Harbor Dischargers Group	USEPA	RM -5 to RM 17
2009-2010	2009-2010 CPG Physical Water Column Monitoring	USEPA	RMs 1.4, 4.2, 6.7, 10.2 and 13.5
1993-1996	1993-1997 USACE - DMDAT	USACE	RM -2.7 to RM -2.7
1995-1996	1995-96 Passaic Study RI/FS Sed Mobility	USEPA	RM 0.6 to RM 7.9
1997	1997 Outfall Sampling Program		RM 2.2 to RM 6.9
1998-2000	1998-2001 CARP Database		RM -2.5 to RM 10.4
1999	1999 Newark Bay Reach A Monitoring		RM -1.6 to RM -1.6
1999	1999 Newark Bay Reach ABCD Baseline Sampling		RM -3.3 to RM -1.6
1999	1999 USACE Drift Removal Monitoring	USACE	RM 6.4 to RM 7.5
2003-2006	1999-2006 Honeywell Intl Sampling		RM -0.2 to RM 1
2000	2000 Toxicity Identification Evaluation		RM 1.1 to RM 6.9
2004-2005	2005 Hydrodynamic Mooring	USEPA	RM 8.6 to RM 11.5
2005	2005 MPI SPMD Deployment	USEPA	RM 2.5 to RM 10.5
2005	2005 USEPA-MPI High Flow Water Column	USEPA	RM 4.4 to RM 17
2005	2005 USEPA-MPI Large Volume Study	USEPA	RM 2.7 to RM 2.7

Table 4-1. LPR Water Column Investigations

Year	Study Name	Surveying Agency	Survey Extent (RM)
2005	2005 USEPA-MPI Small Volume Water Column	USEPA	RM 1 to RM 10.6
2005	2005 USEPA-MPI Water Column Above RM 8.5	USEPA	RM 8.6 to RM 15
2008	2007 USEPA-MPI-EMBM Water Column Sample	USEPA	RM 3.9 to RM 10.4
2009	2009 CPG LPR Water Column Monitoring DEC	USEPA	RM 1.5 to RM 13.5
2010	2010 CPG LPR-NB PWCM Field Measurements	USEPA	RM -4.3 to RM 17
2010	2010 CPG LPR-NB PWCM Sample Dataset	USEPA	RM -3.9 to RM 17
2010	2010 USEPA LBG-CDM PWCM Oversight	USEPA	RM -3.9 to RM 17
2011	2011 CDM Smith CWCM Sampling Data	USEPA	RM 1.4 to RM 10.2
2011	2011 CPG CWCM Sampling Data	USEPA	RM -3.9 to RM 10.2
2012	2012 CDM Smith CWCM Sampling - Round 2	USEPA	RM 1.4 to RM 10.2
2012	2012 CDM Smith CWCM Sampling - Round 3	USEPA	RM 0.1 to RM 10.2
2012	2012 CDM Smith CWCM Sampling - Round 4	USEPA	RM 0.1 to RM 10.2
2012	2012 CDM Smith CWCM Sampling - Round 5	USEPA	RM 0.1 to RM 10.2
2012	2012 CDM Smith CWCM Sampling Round - 6	USEPA	RM 1.4 to RM 10.2
2012	2012 CPG CWCM Sampling – Low Flow	USEPA	RM 0.1 to RM 10.2
2012	2012 CPG CWCM Sampling – Round 2	USEPA	RM -3.9 to RM 10.2
2012	2012 CPG CWCM Sampling – Round 3	USEPA	RM -3.9 to RM 10.2
2012	2012 CPG CWCM Sampling – Round 4	USEPA	RM -3.9 to RM 10.2

The water column results were compared qualitatively to the NJHDG data by comparing computed and measured values for the parameters included in the model. Some examples of these comparisons are presented in Figures 4-2 through 4-5. The model

results and data were plotted on transects for periods when data were collected. For each time period plotted there are two figures and each figure has nine panels with different variables plotted. In general the model compares well to the observed spatial and temporal patterns in the data. There are however many times, locations, and individual variables where the model and data do not match particularly well. Most of the instances where the comparison is poor appear to be related to the external boundaries rather than the internally computed organic carbon dynamics. This is likely related to the use of the SWEM 1994-1995 water year boundary and loading concentrations for all years. While the monthly values from SWEM account for seasonal variations in external loads they do not account for the impact of variations in hydrology between years or reductions to external sources that may have been implemented over time. SWEM's computations are based on organic carbon, and unfortunately the vast majority of the available datasets do not measure particulate organic carbon. This would make it difficult to generate a more accurate time history for the external loads to the LPR model domain from the more recent datasets such as the NJHDG data. The complete set of transect plots for the NJHDG data is presented in Attachment A Carbon Model Transect Plots.

Water column and sediment data and model results were plotted on X-Y scatter plots for a point by point comparison. Comparisons were made for three variables: water column POC, water column DOC and sediment FOC in Figures 4-6 through 4-8. The data are plotted on five panels representing five reaches: RM 8-17, RM 0-8, RM 0 to -1.5 (the mouth of the LPR to Port Newark), RM -15 to -2.6 (Port Newark to Port Elizabeth), and RM -2.6 to -5.25 (south of Port Newark). The source dataset and year for each point is indicated in the legend. For the water column each data point was paired with the hourly average model result corresponding to the time and model cell where the sample was collected, and for the sediment each data point was paired with the corresponding 30 day average model result for the location where it was collected. In the top left of each panel, the figures also include the overall average of all of the data and model values presented within that panel.

For water column POC (Figure 4-6) and DOC (Figure 4-7) the model reproduces both the average and range of the data with some scatter about the 1 to 1 line. Despite the amount of scatter, overall the average of the model results compares well with the average of the POC data without a bias toward being high or low. The predicted DOC compares favorably to the data as well. The DOC is biased somewhat high, but falls within the variability in the data.

The sediment X-Y scatter comparison for the FOC data (Figure 4-8) shows a great deal of scatter. This scatter is the result of a number of factors. There is considerable heterogeneity of the FOC in the sediment data. For cells where multiple samples were taken in the same month the FOC varied on average by a factor of 30 from the minimum value to the maximum value. Upstream of approximately RM 8 the composition of the bed of the LPR is characterized by an increase in the fraction of non-cohesive sediments. In addition to the natural heterogeneity, sampling in the RM 8-17 reach may be biased toward cohesive sediments with higher organic fractions than the reach average. This is particularly true in the case of the studies which collected cores where it may not have been possible to get samples in areas with non-cohesive sediments. The overall average of the model tends to be slightly below the average of the sediment FOC data (Figure 4-8). Because of this bias it was decided to test the sensitivity of the contaminant model to this parameter, but due to the relatively high KPOC of the COPCs and COPECs modeled, doubling the sediment FOC did not significantly affect the fraction of the contaminant sorbed to the organic carbon, and therefore did not impact the computed contaminant fate and transport.

Overall the ST-SWEM model roughly reproduces the average of the observed organic carbon data within the LPR and Newark Bay across a variety of studies and over the duration of the calibration period. Although the model reproduces the average, there is a great deal of scatter around the average of the model and data associated with temporal and spatial heterogeneity in the organic carbon in the system.

4.3 CONTAMINANT MODEL CALIBRATION

The model was run initially using the ST-SWEM and CARP inputs as is. These results showed a fairly rapid initial decline in concentrations in the sediment bed between 1995 and the end of 1998 that did not correspond to the data. To address this issue a number of options were considered, including equilibrium partitioning effects and rates of sediment particle mixing. Because of the magnitude of the partition coefficients, increasing them had little impact on the behavior of contaminants in the sediment. The higher partition coefficients did result in more re-deposition of resuspended contaminants, and a slower rate of decline in sediment concentrations, but the response was not great enough to justify the large change in the partition coefficients. The sensitivity of the model to the partitioning coefficients is presented in further detail in the sensitivity section (Section 5). Ultimately the only parameter adjusted as part of the calibration was the rate of particle mixing in the sediment. The model was run for a range of values for the particle mixing rates, including the ST-SWEM values, the ST-SWEM values scaled down by a factor of 10, 120 cm²/year (18.6 in²/yr), 40 cm²/year (6.2 in²/yr), 10 cm²/year (1.6 in²/yr), 3.15 cm²/year (0.5 in²/yr). Ultimately, the mixing rate of 10 cm²/year was chosen as the value that provided the best simulation of the rate of decline exhibited by the data. It was also in keeping with mixing coefficients evaluated for use in other studies. Figure 4-9, adapted from Boudreau, 1994, shows the particle mixing rates from a number of studies along with the range of values computed by ST-SWEM, values from the Housatonic River study, and values tested as part of the calibration. The ST-SWEM, Housatonic, and calibration mixing values are plotted in the range of 1-2 cm/year (0.4 – 0.8 in/yr) of burial as an order of magnitude approximation for LPR average burial rates. The rate of 10 cm²/year was kept for the present series of model runs, and an analysis of the sensitivity of the model to both the depth and rate of particle mixing in the bed is presented in the discussion of model sensitivity (Section 5).

The RCATOX model surface sediment initial conditions were developed using data that were mostly from the depth interval of 0.0 - 0.5 ft. The initial condition was first assigned as a uniform concentration over this surface sediment layer. After running the

model initially for the period through 2008, the sediments developed a gradient over the top 15 cm (~6 in) . This gradient is controlled mainly by the rate of particle mixing within the bed. As the model develops this gradient from lower concentrations at the surface of the sediments to higher concentrations in the bulk of the sediment it results in an artificially rapid decline in surface sediment concentrations. To compensate for this initial condition data resolution artifact, the model was then restarted from 1995 with the same average concentration but with the vertical distribution computed by the model after running through 2008.

In the portion of the River above RM 7, data for the time period around 1995-1996 were sparse. Because of this, the model was run using initial conditions based on 2008 data for that portion of the domain. Previous runs had reset the bed concentrations in 2008 to the values from the interpolated 2008 data. In response to comments made during the 2013 peer review of the model (HDR|HydroQual, 2013), the reset in the middle of the model simulation was eliminated by adjusting the initial conditions used upstream of RM7. The initial conditions developed after applying the vertical gradient to the top 15 cm (~6 in) were used starting in 1995 and running through 2008 again. The concentrations in the portion of the domain where initial conditions were based on the 2008 data were then scaled up based on the decline during that period. A reach average scale factor was used to prevent artifacts of localized deposition, or erosion into more highly contaminated sediments from producing unreasonably large scale factors.

Finally this adjusted set of initial conditions incorporating a gradient in the surface sediment concentrations and scaled to compensate for the use of 2008 data to set 1995 sediment concentrations where appropriate, were used as the starting point for all calibration and projection scenarios starting in October 1995.

Figure 4-10 shows a high level summary comparison of the model results run initially to develop a gradient in the surface sediment concentrations, then run again to develop the scale factor to apply above RM 7, and then run as the calibration for the model. This figure has three panels for different reaches of the LPR. The top panel is RM0 through

RM8.3, the extent of the Study Area. The middle panel is RM1 through RM7, and roughly represents the extent of the 1995 RI dataset (the most extensive dataset available for the time period of the initial conditions). This panel is a subset of the top panel. The final bottom panel is RM8.3 through 17. The data plotted on these figures is the arithmetic average of measured concentrations from each study (plus or minus two standard errors). It is worth noting that the bars representing plus or minus two standard errors approximate the 95% confidence limit on the mean. Given that the data vary by orders of magnitude these confidence limits can be quite large. Each mean plotted has a number of samples noted next to it. This was done in order to distinguish between the more extensive data sets and others where only a few localized samples were taken. In addition each of the sediment studies noted had a different extent and objectives, which should be considered when looking at the comparison between the model and data. On these figures the black line represents the initial spin-up of the model starting with vertically constant sediment concentrations and running through 2008. The lighter blue line is the result starting again in 1995 with a gradient applied to the initial conditions, but with the same average concentration over the top 15 cm (~6 in). By applying the gradient computed by the model to the initial conditions the initially rapid rate of decline, an artifact of the vertical resolution of the data used to develop the initial conditions, is reduced. The darker blue line is the model result starting again in 1995 and scaling the initial conditions above RM7 based on the change between 1995 and 2008 computed by the previous run. This line was used as the model calibration, and the starting point for all projections.

4.4 MODEL COMPARISONS TO DATA

Model results were compared to sediment data, for all forty-eight contaminants modeled, using a variety of formats: (1) model results and data were plotted as spatial transects from Dundee Dam to the southern end of Newark Bay and are compared at several different points in time, (2) model results and data were averaged over selected LPR (RM 1-7, 0-8, and 8-17) and Newark Bay reaches (RM 0 to -1.5, -1.5 to -2.6, and -2.6 to -5.25) and compared as time series plots for each reach, and (3) data and model results were

plotted as X-Y scatter plots. The LPR reaches for the second type of plot represent the portion of the river where the 1995 RI dataset was collected (RM 1-7), the extent of the FFS Study Area (RM 0-8), and the remainder of the river (RM 8-17), and the Newark Bay reaches represent the portions of the Bay North of the Port Newark Channel (RM0 to -1.5, labeled RM0 to -2), the portion of the Bay from the Port Newark Channel through the Port Elizabeth Channel (RM-1.5 to -2.6, labeled RM-2 to -3), and the portion of the Bay South of Port Elizabeth (RM-2.6 to -5.25, labeled RM-3 to -5).

Model and data comparisons are discussed in detail for three of the forty-eight contaminants modeled. The three contaminants were chosen to demonstrate model performance for different groups of contaminants: 2,3,7,8-TCDD was chosen to represent hydrophobic COPCs and COPECs that originate largely from within the LPR, tetra-PCB was chosen to represent hydrophobic COPCs and COPECs that are more widespread in the environment, and mercury was chosen to represent the metals. Figures presenting the model results for the full suite of chemicals modeled are presented in the attachments to this appendix.

4.4.1 Spatial Transect Plots

Simulated model results and data are compared along plotting transects that are parallel to the longitudinal axis of the river and which extend from as far upstream as the head of tide at Dundee Dam (~ RM 17) to the southern end of Newark Bay (RM -5.0) (Figures 4-11 through 4-28). Each of these figures includes two panels to display results along transects for the channel (upper panel) and shoals (bottom panel) Each figure shows the computed sediment concentration for a given year along with all data collected in that year. The plots show the years starting in 1995 with the initial conditions and go through the end of the 2012 water year. Data values reported as non-detects are plotted at the detection limit.

Figures 4-11 through 4-28 show transects for 2,3,7,8-TCDD. There are a few patterns that are evident when looking at the transect plots. First, the initial condition

concentrations used by the model are not nearly as variable as the data. This is due to the spatial distribution of the data, the model grid and the geomorphic zones. Measured concentrations in the sediments can vary by orders of magnitude within any one of the geomorphic zones used to evaluate a single average value that is used by the model. Additionally, based on the approach used to develop initial conditions, there can only be one concentration assigned per geomorphic zone and, based on model grid resolution, there can be only one concentration assigned within a model cell. This is in contrast to the measured concentrations which may vary considerably within the limits of any individual model grid cell. A second pattern that emerges from the model results is that concentrations simulated through 2010 have tended to decrease throughout the LPR and Newark Bay relative to the initial conditions. The data collected over this time period show do not show a significant trend with similar median concentrations in 1995 and 2008 through 2012. Given the variability in the data, however, the model results and data are still in reasonable agreement in most areas. In the final two calibration years 2011 and 2012 the model shows an increase due to some relatively high flows. In these final two years the 2011 CPG River Mile 10.9 Data, 2012 CPG River Mile 10.9 Data, and the 2012 CPG Low Resolution Coring Supplemental data show just how variable the data can be at small scales. The model does a fairly good job of going through the middle of the range of the data, but cannot reproduce the observed sub-grid scale variability. It is important to note that, with the exception of the 1995 RI Sampling Program, the various sampling programs were not designed to collect data that were spatially representative of the sediment bed.

Overall, the model results tend to be consistent with the generally observed spatial pattern of the data and are within the limits of variability of the observations. Similar plots for the remainder of the chemicals that were simulated are included in Attachment B (Transect Plots).

4.4.2 Reach Average Time Series Plots

Reach-average time series model results and data are compared on Figures 4-29 through 4-49 for 2,3,7,8-TCDD, tetrachlorobiphenyl and mercury, respectively. There are seven figures for each of the selected contaminants. The first figure includes three panels to display results for the RM 0-8.3: reach total, channel, and shoals. The top panel is the overall reach average, the middle panel is the average for the channel and the bottom panel is the average for the shoals. On the bottom two panels there is a light grey line that represents the overall reach average from the top panel as a reference for comparison. The data plotted on these figures is the arithmetic average of measured concentrations from each study (plus or minus two standard errors). Given that the data vary by orders of magnitude it is worth noting that the bars representing plus or minus two standard errors approximate the 95% confidence limit on the mean. Each mean plotted has a number of samples noted next to it. This was done in order to distinguish between the more extensive data sets and others where only a few localized samples were taken. The changes in the mean of the data between datasets tend to be much smaller than the uncertainty around the mean of any given dataset. All of the available datasets are plotted with more weight given those data sets with the greatest number of samples and most extensive spatial coverage. Given that the number of samples is relatively low for some years (1997, 1998 and 2000), it is appropriate to give more weight to the 1995, 1999, and 2008-2012 datasets. In addition each of the sediment studies noted had a different spatial extent and objectives, which should be considered when looking at the comparison between the model and data. The model results presented are approximately monthly (30 day averages) area weighted average concentrations for the top 15 cm (~0.5 ft) over either the reach or sub-reach and the data presented are for the corresponding area and the surface sediment data were generally collected from the same depth interval of 0-0.5 ft. Note that these figures are a fairly high level summary of both the model results and data, and the different extents of the datasets and model make an absolute one to one comparison between the points and each other or the line inappropriate.

The next four figures incorporate the same layout and present sediment results for RM8.3 to 17, 0 to -1.5, -1.5 to -2.6, and -2.6 to -5.25. The final two figures for 2,3,7,8-TCDD present the water column results for the LPR and Newark Bay on a reach basis. Water column comparisons were not plotted separately for the channel and shoals as the water column concentration would not be expected to vary significantly over the width of the river.

It is evident from inspection of Figures 4-29 through 4-49 that the October 1995 initial conditions may not exactly match the average of the data used to develop the initial conditions due to differences in areal contributions of each of the geomorphic zones to the total area within a reach. For example, in RM0-8.3, the value plotted for the data average weights all points equally, while the geomorphic zones for RM0-8.3 would give the most weight to the zones with the largest portion of the area (broad shoals, and smooth channel, Figure 3-10). The 2,3,7,8-TCDD model results in the LPR are within the 95% confidence limits of the mean of the data for the larger datasets (1995, 1999, 2008, 2009, and 2012) (Figures 4-29 and 4-30). Some of the datasets with fewer points tend to show trends that are inconsistent with the larger datasets. Because of the limited sample sizes and heterogeneity in spatial distribution of the samples from the smaller datasets, they are not likely to provide an accurate representation of the average concentrations over the larger reaches plotted here. These data are included for purposes of completeness and in order to avoid subjectivity in the process of censoring data. The comparison in Newark Bay (Figures 4-31, 4-32, and 4-33) does not achieve the same level of fit with the data. The large area of Newark Bay along with the relatively small number of samples may influence the ability to compare the model and data. There are also processes occurring in Newark Bay that are not represented in the contaminant model, particularly capital and maintenance dredging and the resuspension resulting from shipping traffic. The X-Y model-data results presented in Section 4.4.3 suggest a better fit of the Newark Bay data than the transect plots represent. Figures 4-34 and 4-35 present the comparison between the model results and water column data for the LPR and Newark Bay respectively. For a number of reaches and sampling events, the model falls within the 95% confidence limits of the mean of the data, but the model over predicts

total water column concentrations measured during a number of the CWCM sampling events particularly within the Study Area. This is related to the response of the model to the high flows in 2007, 2010, and 2011, and particularly Hurricane Irene in 2011. The high flows result in erosion in a small number of cells to a depth that exposes fairly elevated contaminant concentrations to the water column, and the model computed water column concentrations do not recover as quickly as the data suggests.

The datasets collected between 1995 and 2008 did not report homologue sums for PCBs. Because of this the only points available for comparison between the model and data for the PCB homologues are the averages from 2008 on. The tetrachlorobiphenyl model results match the 2008 LPR data quite well (Figures 4-36 and 4-37). The model results fall well with the 95% confidence limits of the mean of the data. For Newark Bay (Figures 4-38, 4-39, and 4-40) there are far fewer data points with reported tetrachlorobiphenyl concentrations to make any conclusions about the model results. Figures 4-41 and 4-42 present the comparison between the model results and water column data for the LPR and Newark Bay respectively. Similar to the TCDD results the model tends to over predict observed concentrations of tetrachlorobiphenyl in the water column. The over estimate of water column concentrations is again related to the response of the model to the high flows in the 2007 through 2011 time period.

Figures 4-43 through 4-48 present the reach average time series comparisons for mercury in the LPR and Newark Bay surface sediments and water column. Again the results compare favorably with the larger datasets in 1995, 1999, 2008, and 2009. The model results generally fall within the 95% confidence limits of the means for the LPR data and do particularly well for the larger datasets (i.e., years 1999, 2008, 2009, and 2012). For Newark Bay the X-Y plots presented below suggest a better fit of the data than the reach time series for the same reasons noted for 2,3,7,8-TCDD. The water column mercury does not show as large of a response to the high flows between 2007 and 2011 and therefore does a better job of reproducing the observed water column concentration. The difference in response from TCDD and Tetra PCB is related to the different patterns in

location and depth of mercury contamination based on the interpolation of the initial condition data.

Reach average time series plots for all forty-eight of the chemicals modeled are included in Attachment C-1 (LPR Surface Sediment Reach and Sub-Reach Average Time Series Calibration), Attachment C-2 (Newark Bay Surface Sediment Reach and Sub-Reach Average Time Series Calibration), Attachment C-3 (LPR Water Column Reach and Sub-Reach Average Time Series Calibration, and Attachment C-4 (Newark Bay Water Column Reach and Sub-Reach Average Time Series Calibration. The results plotted in Attachments C-1 through C-4 show similar fits to the measured data for the other forty-five model contaminant calculations.

4.4.3 Data and Model Scatter Plots

Data and model results were plotted on X-Y scatter plots for a point by point comparison. Each sediment sample was paired with the corresponding 30-day average model result for the cell where the sample was collected, and each water column sample was paired with the corresponding 1 hour average model result for the cell where the sample was collected. Figures 4-50 through 4-55 show surface sediment (15 cm or ~6 in), and water column results for 2,3,7,8-TCDD, tetrachlorobiphenyl and mercury, respectively. The data are plotted on five panels representing five reaches: RM8.3 to 17, RM0 to 8.3, RM 0 to -1.5 (the mouth of the LPR to Port Newark), RM -1.5 to -2.6 (Port Newark to Port Elizabeth), and RM -2.6 to -5.25 (south of Port Newark). The source dataset and year for each point is indicated in the legend. Data values are shown on the X-axis and model values on the Y-axis. The diagonal lines from the lower left corner to the upper right corner represent the one-to-one line (a perfect match) in the middle plus or minus a factor of five ($\pm 5x$; outer dotted lines). The percentage of samples within the \pm factor of 5 on each graph is noted in the lower right corner. Table 4-2 lists the percentage of data falling within the factor of five lines for the FFS Study Area and for all data within the domain.

In keeping with the previously described results of the spatial transect and time series comparisons for 2,3,7,8-TCDD, the cross-plots of the surface sediment model results with the data indicate that reasonable agreement has been achieved by the model. Both the model and data vary over about a 5 order of magnitude range and overall 67.5% of the calculated 2,3,7,8-TCDD concentrations (Figure 4-50) are within a factor of +/- 5x of the measurements. For the FFS Study Area, 81.6% of the data falls within the +/- 5x envelope. In addition, for data points that fall outside of the +/- 5x envelope, there does not appear to be a distinct bias towards over- or under-prediction of the data. It should be recognized that this reasonably good agreement is in part a reflection of use of site data to set the initial conditions, in combination with the relatively slow response time of sediment COPC and COPEC concentrations to natural attenuation processes within the system.

The water column 2,3,7,8-TCDD model results do not compare as favorably with the data. The concentration in the water column is overpredicted for most of the water column datasets, particularly the later datasets south of RM8.3. As described above in the reach average time series discussion, this is related to the response of the model to the high flows in 2007, 2010, and 2011, and particularly Hurricane Irene in 2011. The high flows result in erosion in a small number of cells to a depth that exposes fairly elevated contaminant concentrations to the water column, and the model computed water column concentrations do not recover as quickly as the data suggests. Overall 49.1% of the calculated 2,3,7,8-TCDD concentrations (Figure 4-51) are within a factor of +/- 5x of the measurements. For the FFS Study Area, 35.9% of the data falls within the +/- 5x envelope.

The X-Y model-data comparison for surface sediment tetrachlorobiphenyl (Figure 4-52) shows a degree of agreement between model and data that is comparable to the TCDD results. That is, 64.1% overall and 80.4% of the FFS Study Area data points are within the +/-5x envelope. However, the overall concentration range represented by the data is relatively limited in comparison to the dioxin results, about 3 orders of magnitude in this case. The model tends to overpredict some of the measured values, particularly the lower

concentrations measured as part of the 2011 RM 10.9 data collection effort and the Honeywell data in northern Newark Bay. These lower concentrations often co-occur in grid cells where high concentrations were also measured. In such cases the average concentrations within a grid cell would likely be in better agreement with the model than would the individual sample results.

The X-Y model data comparison for water column tetrachlorobiphenyl suffers from the same issue as the TCDD, with elevated concentrations following Hurricane Irene and a slow rate of decline afterwards. Overall 50.8% of the calculated tetrachlorobiphenyl concentrations (Figure 4-53) are within a factor of +/- 5x of the measurements. For the FFS Study Area, 45.5% of the data falls within the +/- 5x envelope.

The X-Y model-data comparison for sediment mercury (Figure 4-54) is comparable to what was achieved for Tetra-PCBs and TCDD. The scatter of the data about the line of perfect agreement is in part a residual effect of the variability of the data that was not readily represented by the assignment of initial conditions. Even so, the majority of the results cluster about the one-to-one line, with a limited fraction of the data falling well outside of the +/-5x envelope. Overall 63.6% of the points fall within the factor of +/- 5x envelope with 77% of the points within the FFS Study Area falling within the +/- 5x envelope. On this figure the majority of the data fall within or close to the factor of 5 envelope with the exception of a cluster of points in both the RM8.3 to 17, RM0 to 8.3, and RM0 to -2 reaches from the 2012 CPG Low Resolution Coring Supplemental data set, and 1996-2006 Honeywell Intl Sampling data sets. This data looks suspect and should be evaluated further, as the low values occur alongside the values that compare favorably with the model.

The X-Y model data comparison to mercury in the water column fairs better than the TCDD and Tetra PCB results with 61.7% overall and 68.6 % of the predictions within the Study Area falling within the factor of 5 envelope (Figure 4-55). The response of the mercury concentrations to the high flows between 2007 and 2011 were less than TCDD

and Tetra-PCB based on the spatial and vertical distribution of mercury within the bed, specified as initial conditions.

Attachment D-1 includes the X-Y scatter plots for all forty-eight contaminants for the surface sediments. Attachment D-2 includes the same figures with comparisons over the full model depth. Attachment D-3 includes the same figures with comparisons for the water column. These results are similar to the three results included in the text.

Attachment D-2 has the same plots for all five of the sediment output layers: ~0-0.5 ft, 0.5-1.5 ft, 1.5-2.5 ft, 2.5-3.5 ft and 3.5-5.5 ft. The general behavior in the other layers is similar to that of the surface sediments, but there is a larger degree of variability in both the model and data.

4.5 UNCERTAINTY

Computed model results have inherent uncertainty associated with the data used to specify inputs to the model, the model's representation of physical, biological and chemical processes and the scale of the model in both time and space. Model uncertainty can be evaluated using quantitative approaches such as Monte Carlo Analyses for models requiring limited computational resources and short simulation times. Efforts to address model uncertainty for computationally intensive models are much more of a challenge. Uncertainty analyses were performed for the Lower Duwamish Waterway's sediment transport model (Quantitative Environmental Analysis, 2008). These involved developing upper and lower bound estimates for selected model inputs and running 6-years with permutations of the upper and lower bound values for the selected parameters, requiring $2n$ simulations, where n is the number of parameters included in the analysis (i.e. 32 simulations for 5 parameters). Results from the simulations were compared to the calibration results to identify upper and lower bound sets of parameters which were then used in long-term simulations (21 years). This approach was considered for the FFS modeling, which includes hydrodynamics and sediment transport, a eutrophication model, and a contaminant fate and transport model. The time required to implement a

similar approach and include each of these components was estimated 6 to 9 months, even with a dedicated bank of computers.

As an alternative, an approach discussed in USEPA's 2005 Contaminated Sediment Remediation Guidance for Hazardous Waste Sites, which relies on consideration of residuals between model results and data (Connolly and Tonelli, 1985) was adopted. The uncertainty propagated through the models is being evaluated using this approach with the exposure concentrations generated by the fate and transport model and passed to the risk assessment. The uncertainty values computed represent a lower bound on the uncertainty in the RM 0 to 8.3 averages passed to the risk assessment.

To account for the large degree of variability in the data the results were first averaged prior to computing relative errors. The process also included steps to account for the spatial extent and number of samples in each dataset. The calculation involved the following steps.

- Compute an arithmetic average of the data within the Study Area from each dataset.
- Compute an area weighted average of the model cells within the Study Area where data were collected for each dataset. This approach accounts for the different spatial extents of the various datasets.
- Compute the absolute relative error between the data and model averages computed in the first two steps.
- Compute the median of the relative errors weighed by the number of samples in each dataset. This approach accounts for the number of samples associated with each of the datasets.

Median relative error values were computed for the predicted water column POC, DOC, sediment FOC, sediment COPC/COPEC, and water column COPC/COPEC data. The resulting computed median relative error values are presented in Table 4-2.

4.6 SUMMARY

Model results for the forty-eight COPCs and COPECs simulated were compared to sediment and water column data on a spatial, temporal and point by point basis.

Although both model and data show considerable amounts of variability within the FFS Study Area, overall the model compares favorably with the data across a wide range of modeled contaminants, locations, and years. The modeled rate of change in average sediment concentrations from the beginning of the calculation in 1995 through the time of the 2012 data collection, generally falls within the range of the averages of the data and matches well with the 2008 through 2012 data.

The water column model calculations tend to overpredict the response of the water column to the high flow events between 2007 and 2011 (except for mercury, where model results compared well with data), in particular, the rate of decline in water column concentrations suggested by the CWCM data collected between 2011 and 2012. This result is related to the response of the model to high flows resulting in erosion in a small number of cells to a depth that exposes fairly elevated contaminant concentrations to the water column.

Table 4-2. Model Calibration Results

Name	River Mile 0-8						All Data			
	Sediment Top 15cm			Water Column			Sediment Top 15cm		Water Column	
	N	Percent of Samples w/in factor of 5	Median Relative Error	N	Percent of Samples w/in factor of 5	Median Relative Error	N	Percent of Samples w/in factor of 5	N	Percent of Samples w/in factor of 5
2378-TCDD	304	81.6	35	198	35.9	525	812	67.5	436	49.1
123478-HxCDD	304	91.4	17	198	69.2	86	802	83.4	435	53.1
123678-HxCDD	304	91.1	23	198	93.9	42	812	78.6	435	86.7
123789-HxCDD	304	92.1	27	198	86.9	64	806	83.6	435	76.1
1234678-HpCDD	304	90.1	20	198	83.3	68	815	78.7	437	90.4
OCDD	304	91.8	18	198	77.8	78	816	79.9	437	86.3
12378-PeCDD	304	90.1	28	198	71.2	77	801	80.6	435	54.9
12378-PeCDF	291	91.4	13	198	87.9	72	794	79.6	435	73.1
123789-HxCDF	262	67.9	179	198	72.7	76	707	75	435	59.5
234678-HxCDF	304	90.5	22	198	92.4	49	810	78	435	84.8
1234789-HpCDF	304	89.1	11	198	85.4	62	808	78.1	435	74.5
2378-TCDF	304	90.1	25	198	87.9	57	812	75.2	435	92
23478-PeCDF	291	89	22	198	92.4	51	793	76	435	88.7

Table 4-2. Model Calibration Results

Name	River Mile 0-8						All Data			
	Sediment Top 15cm			Water Column			Sediment Top 15cm		Water Column	
	N	Percent of Samples w/in factor of 5	Median Relative Error	N	Percent of Samples w/in factor of 5	Median Relative Error	N	Percent of Samples w/in factor of 5	N	Percent of Samples w/in factor of 5
123478-HxCDF	304	80.6	30	198	87.9	95	816	70.1	435	91.7
123678-HxCDF	304	88.5	10	198	93.4	36	811	76.8	435	90.1
1234678-HpCDF	304	86.5	21	198	79.3	97	816	74	436	86.7
OCDF	303	85.1	31	198	76.8	98	815	74	436	86.2
Di-CB	235	78.7	110	191	41.9	292	524	63.4	413	46
Tri-CB	235	77.9	64	191	48.7	270	524	61.5	413	61
Tetra-CB	235	80.4	67	191	45	279	524	64.1	413	50.8
Penta-CB	235	87.2	27	191	42.4	296	568	65.8	413	41.9
Hexa-CB	235	85.5	20	191	52.4	200	568	65.5	413	47.5
Mono-CB	235	79.1	83	191	20.4	588	524	66.2	412	16.3
Hepta-CB	230	85.7	20	191	46.1	247	563	66.4	413	39
Octa-CB	230	86.1	7	191	38.7	311	563	66.4	413	31.5
Nona-CB	230	83.5	42	191	33	305	519	71.7	413	36.6
Deca-CB	222	84.7	51	197	69	137	653	72	435	74.7
BZ#77	237	81.9	30	206	28.6	443	702	66.2	469	27.1

Table 4-2. Model Calibration Results

Name	River Mile 0-8						All Data			
	Sediment Top 15cm			Water Column			Sediment Top 15cm		Water Column	
	N	Percent of Samples w/in factor of 5	Median Relative Error	N	Percent of Samples w/in factor of 5	Median Relative Error	N	Percent of Samples w/in factor of 5	N	Percent of Samples w/in factor of 5
BZ#81	232	83.6	38	199	27.6	486	662	68.1	462	32.5
BZ#105	232	86.2	32	206	38.3	411	698	67.5	469	35.2
BZ#114	232	82.3	20	199	29.6	498	690	62	462	25.5
BZ#118	234	86.3	22	206	42.2	414	456	73.9	469	39.4
BZ#123	232	74.1	77	199	21.6	604	689	58.3	462	22.1
BZ#126	228	83.8	86	206	20.4	613	676	57.8	469	24.7
BZ#156	237	84	33	206	16	684	701	65	469	16
BZ#157	75	76	70	188	61.2	306	399	57.6	410	61.2
BZ#167	237	57	236	199	11.1	1457	699	50.4	462	15.6
BZ#169	149	79.9	69	206	67	99	495	67.5	469	69.3
BZ#189		237	86.1	20	199	36.2	415	692	66	462
2,4'-DDD		227	80.6	47	126	61.9	363	504	73.4	307
2,4'-DDE		227	77.1	32	126	63.5	123	498	68.9	307
2,4'-DDT		222	39.6	686	126	22.2	813	487	54.2	307
4,4'-DDD		240	85.4	33	129	72.1	297	773	70.9	313
4,4'-DDE		306	87.3	34	129	66.7	182	844	71.8	313
4,4'-DDT		302	64.2	94	130	23.1	1038	804	61.1	314

Table 4-2. Model Calibration Results

Name	River Mile 0-8						All Data			
	Sediment Top 15cm			Water Column			Sediment Top 15cm		Water Column	
	N	Percent of Samples w/in factor of 5	Median Relative Error	N	Percent of Samples w/in factor of 5	Median Relative Error	N	Percent of Samples w/in factor of 5	N	Percent of Samples w/in factor of 5
Cd		389	76.3	52	172	86.6	256	1018	61.1	457
Hg		395	77	44	204	68.6	117	1075	63.6	496
MeHg		79	62	414	119	83.2	51	149	44.3	260
POC					361	94.7	32			1022
DOC					332	97.9	45			975
FOC		277	88.1	67				981	73	

5 SENSITIVITY ANALYSES

5.1 INTRODUCTION

As part of the FFS contaminant modeling effort, the sensitivity of the model to a number of important model input parameters was investigated. A “No Action” simulation consisting of the calibration simulation (water years 1996 through 2059) served as the base case run to which other sensitivity runs were compared. The four model sensitivity runs that were performed were: the upstream boundary condition, partition coefficients, depth of particle mixing, and rate of particle mixing. In addition the sensitivity of the model to a one in one hundred year storm after completion of deep dredging was also simulated for all remedial scenarios (in response to the 2013 peer review comments (HDR|HydroQual, 2013)). All of the sensitivities were run for the group of contaminants including 2,3,7,8-TCDD, and five other dioxins. The other COPCs and COPECs, although not simulated, would be expected to behave similarly to 2,3,7,8-TCDD due to their persistent and particle reactive nature.

The sensitivity results are presented on a reach average time series basis for sub-reaches from RM0-8.3, and RM8.3-17 for sediments, as well as on a reach basis for water column concentrations. The calibration result on the figures is plotted in blue, the results of increasing a parameter is plotted in red, and decreases are plotted in green.

5.2 UPSTREAM BOUNDARY

Given the relatively small number of samples available for use when specifying external loads there is uncertainty associated with those values. To test the relative importance of the external load coming over Dundee Dam, a simulation was conducted to test the sensitivity of the model to the specified boundary load. The sensitivity of the model to the upstream boundary condition coming over Dundee Dam was simulated by increasing and decreasing the boundary concentration by a factor of two. If the sediment and water column response of the model were controlled by the Dundee Dam boundary

concentrations, the model would show a noticeable response to this change in concentration.

Figures 5-1 through 5-3 show the responses in RM0-8.3 and RM8.3-17 for the sediment and water column 2,3,7,8-TCDD concentrations to the changes in the upstream boundary. Because the 2,3,7,8-TCDD boundary concentrations are so low relative to the ambient concentrations within the river, the change in the concentration is too small to see a difference between the response across the range of boundary concentrations simulated.

Figures 5-4 through 5-6 show the responses in RM0-8.3 and RM8.3-17 for the sediment and water column OCDD concentrations to the changes in the upstream boundary. In this case the changes are large enough to perceive on the plots, but remain relatively small compared to the change in the boundary concentration. This suggests that the boundary concentration for OCDD is more important in controlling concentrations within the LPR than the boundary concentration of 2,3,7,8-TCDD. The response is greatest in the water column in RM8.3-17 as expected, but beyond that remains relatively small.

The incorporation of additional data into the analyses of the boundary concentrations would help improve the confidence in those values, but would not be likely to have a large impact on computed concentrations. Because none of the remedial alternatives considered in the FFS include changes to conditions above the heads of tide, the head of tide boundary concentrations are consistent among all alternatives. As a result, changes in the boundary concentrations would not change the relative order of the alternatives considered, but would to some extent impact the absolute amount of recovery or recontamination in the future. The degree to which the boundary concentration could impact the computed concentrations is dependent on the magnitude of the boundary concentration relative to the concentrations in the LPR, Newark Bay and in other sources. The approach used to develop the boundary concentrations used for the calibration and projections represent a best estimate of the concentration based on the available data.

5.3 PARTITIONING COEFFICIENTS

To test the models sensitivity to the specified partitioning coefficients two simulations were conducted. The first simulation increased the partitioning coefficient to all POC (KPOC) by a factor of 1000. The second simulation both increased the KPOC used for detrital organic carbon by a factor of 1000 and decreased the KPOC used for phytoplankton carbon to be equal to the DOC partitioning coefficient (KDOC).

Figures 5-7 through 5-9 present the partition coefficient sensitivity results for both the sediment and water column. Because of the relatively high partitioning coefficient for 2,3,7,8-TCDD simply increasing it further does not have a large impact on the distribution between the freely dissolved, DOC bound, detrital POC, and algal POC bound phases. The second simulation was conducted recognizing that the detrital POC in the model settles at a faster rate than the phytoplankton POC and has a relatively short residence time in the water column. By increasing the partitioning to the detrital POC and reducing the partitioning to phytoplankton POC the second simulation approximates a condition where the contaminant is irreversibly sorbed to the detrital POC. The response of the sediment in the second sensitivity shows similar behavior under erosional conditions when the concentrations in the sediment are increasing, but a slower rate of decrease under normal conditions.

While the first sensitivity shows little response to the increase in partition coefficient the second does suggest that the distribution of the contaminant between the different types of POC represented by the model may be a factor in the model's behavior. Given the large changes in parameter values used in this sensitivity and the relatively small response in computed concentrations a more subtle change in partitioning, within the range of measured values, would not result in appreciably different results from the calibration.

5.4 DEPTH OF MIXING

Among other factors, the rate of recovery of the LPR is dependent upon the total amount of contaminated sediment which can interact with the surface of the sediment and the water column. Generally, the larger the volume of sediment that is available to interact with the water column, the longer it will take for the sediment concentration to increase or decrease in response to changes in external loads. If the sediment response in the model were controlled by diffusive processes, and did not include deposition and resuspension, doubling the depth of particle mixing in the sediment would double the amount of time that the sediment would take to respond, and halving that depth would in turn halve the amount of time the sediment would take to respond. The amount of tidal and event driven sediment resuspension in the LPR as well as the interactions between sediments of different concentrations from different areas of the river generate a less predictable result. The process of particle mixing within the sediment in the model represents a combination of both biological and physical processes that mix the sediments over a given depth.

To test the sensitivity of the model to the depth of mixing, simulations were done where the calibration depth of mixing of 10 cm (~3.9 in) was doubled and halved. Note that this is the depth over which mixing can occur at the modeled rate of $10 \text{ cm}^2/\text{year}$ (~1.6 in²/yr), rather than the depth of a completely mixed layer. The sediment and water column results for the depth of mixing sensitivity are presented in Figures 5-10 through 5-12. Note that while the depth of mixing has changed between runs the plots are all showing the top 15 cm (~6 in) of sediment. Both sets of results show a slower sediment response than the calibration run. This is because in the case where the depth of mixing has been increased more contaminated sediments below the 15 cm (~6 in) horizon are now mixed with the shallower sediments. In the 5 cm (~2 in) mixing depth sensitivity the sediments below 5 cm no longer mix with the sediments above. This results in the sediments between 5 and 15 cm maintaining higher concentrations, and a slower response of the 15 cm average despite the faster rate of decrease in the top 5 cm. The sediment in the 20 cm (~8 in) depth of mixing simulation also shows a larger response to high flows as erosion

into the bed allows deeper sediments with more elevated concentrations to interact with sediments within the top 15 centimeters.

The water column however does not show the same response. As contaminant from deeper in the bed is allowed to mix with the surface sediments and in turn the water column in the 20 cm (~8 in) mixing depth run, the water column concentration increases. On the other hand in the 5 cm (~2 in) run the contaminant below 5 cm (~2 in) is isolated from the water column resulting in a more rapid decline in water column concentrations.

The model shows the greatest response to increases in the depth of mixing. Measured sediment bed and water column concentration data indicate that the assigned depth of mixing of 10 cm is a reasonable value.

5.5 RATE OF MIXING

In addition to the depth of mixing, the rate of sediment mixing will also influence the rate of recovery of the LPR based on the rate at which contaminant can mix from below the surface and replenish the contaminants on the particles in the top 0.5 to 2 cm (~0.2 to 0.8 in) which interact with the water column. To test the model sensitivity to the rate of sediment mixing the calibration rate was both increased and decreased by a factor of 10.

Figures 5-13 through 5-15 present the sediment and water column response of the model to the rate of sediment particle mixing sensitivity. The slower rate of mixing results in a slower rate of decline in sediment concentrations along with generally lower water column concentrations as the contaminant in the sub surface sediments is more isolated from the surface sediments, and interaction with the water column. With the higher rate of particle mixing the sediments decline more quickly, and water column concentrations increase, as the contaminant at depth interacts more with the surface of the sediment and subsequently the water column.

As part of the model calibration effort a number of sediment mixing rates were tested in the model. Ultimately, the mixing rate of $10 \text{ cm}^2/\text{year}$ ($\sim 1.6 \text{ in}^2/\text{yr}$) was chosen as the

value that provided the best simulation of the rate of decline exhibited by the surface sediment data.

5.6 ONE IN ONE HUNDRED YEAR STORM

The sensitivity of the model to large storms was assessed by running a simulation of a one in one hundred year storm. The time period chosen was starting October 1, 2029 and running through the subsequent 3 years. This time period follows the completion of the Deep Dredging remedial alternative, which is the longest duration of the simulated remedies. Beginning the simulation at this point allows a comparison of the impact of an extreme flow with all of the alternatives in place. The run was completed for all four remedial alternatives discussed in further detail in Section 6. Unlike the sensitivities above, which were only run by modifying the contaminant fate and transport model, this sensitivity was simulated using all three models. The sensitivity was simulated in the hydrodynamic and sediment transport (Appendix BII) and the results were used as an input to the organic carbon and contaminant fate and transport models.

Figures 5-16 through 5-18 present the sediment and water column response of the model to the one hundred year storm sensitivity. The hydrograph used for the projection simulations repeats the flows from October 1995 through September 2010 into the future. This series of flows include high flows from 2007 repeated in 2024 and 2039, and from 2010 repeated in 2027 and 2042. The RM8.3-17 reach response to the one hundred year storm sensitivity shows a similar response in the water column and sediment to the other storms. The response in RM0-8.3 in the water column is also similar to the response to the other high flows. The response in the sediments of RM0-8.3 is nearly two times greater than the other high flow periods. While the response to the one hundred year storm is significant it does not change the relative order of the remedial alternatives.

5.7 SENSITIVITY SUMMARY

The model sensitivity calculations showed varied responses to the different sensitivities that were simulated. The model does show significant responses to variations in

parameters, particularly those related to the quantity of contaminated sediments available and rate at which contaminant can migrate to the surface of the sediment and subsequently be transported through the water column to other locations. The sensitivities also show that erosion predicted by the sediment transport model along with the specification of elevated concentrations at depth in the bed can be an equalizing factor which tends to reset the surface sediment concentrations and reduce the differences between the simulations using different parameters for bed processes. Overall the parameter values chosen for the calibration and projection scenarios provide the best reproduction of the observed data out of the values tested in the model.

6 EVALUATION OF REMEDIAL ALTERNATIVES

6.1 INTRODUCTION

Future contaminant concentrations after implementation of the four remedial alternatives developed in the FFS were evaluated through a series of contaminant fate and transport model simulations. The alternatives simulated were:

- Alternative 1 – No Action
- Alternative 2 – Deep Dredging with Backfill (Deep Dredging)
- Alternative 3 – Capping with Dredging for Flooding and Navigation (Full Capping)
- Alternative 4 – Focused Capping with Dredging for Flooding (Focused Capping)

Future conditions simulations begin at the end of the 1995-2012 calibration period. Between 1995 and 2010, bathymetry in Newark Bay was adjusted in four steps to account for progress in the Harbor Deepening Project (HDP) [see Appendix BII, Section 1.1]. Bathymetry associated with completion of the HDP was assigned at the start of the future conditions simulations. The hydrographs (and other tidal forcing) for the period October 1995 – October 2010 (water years 1996-2010) were repeated in 15-year cycles to simulate conditions into the future to October 2059, which is 30 years after remedy-related construction is completed. (Although the calibration simulations included a 17-year period from 1995-2012, the hydrodynamic transport from only the first 15 years was used, to avoid repeating the 90-year return frequency flow associated with Hurricane Irene in the repeating cycle.) Model simulation input and results for the period from the start of the calibration period in October 1995 through the beginning of construction of the remedial alternatives in March 2018 are common to all alternatives. Boundary conditions for contaminants were developed as a function of river flow, and not changed over time into the future.

For all alternatives involving net changes in bathymetry due to dredging, the bathymetry used in the hydrodynamic model was adjusted each timestep during the dredging period to account for the depth changes in the individual grid cell where dredging was being simulated at an average production rate. By applying the small changes in depth with each timestep, any numerical stability issues associated with instantaneously changing the cell depth to the dredged depth were prevented. The alternative would be to adjust the cell depths either prior to or after the completion of dredging. Adjusting depths of the dredged cells prior to dredging results in the release of solids to an artificially deep water column and excessively rapid accumulation of released solids. Adjusting depths upon completion of dredging results in the release of solids to an artificially shallow water column and transport of solids over greater distances than would be expected. Either of these approaches would result in a misrepresentation of the fate of the released solids. In locations where sediment removal and cap placement are designed to bring the river bed back to original grade, bathymetric changes were not included in the hydrodynamic model, but releases related to dredging were included. The bed composition was modified at the completion of dredging and backfilling in each grid cell to reflect the higher sand content of the cap/backfill.

Releases of solids, carbon and contaminants are represented in the three models for each alternative where dredging is represented without the construction of a coffer dam or sheet-pile enclosure. In these cases, remediation was simulated in the model by setting duration and volume of sediment removal in each grid box. Simulation of losses during dredging required mass to be dredged, duration, and loss rate. The mass of solids, POM, and contaminant in the specified volume was summed for each cell to be dredged. The solids concentrations and POM concentrations from the deepest layer were used for the concentration in deeper sediments in cases where dredging occurred deeper than the model's representation of the bed. For contaminants a concentration was specified in the dredging inputs for the sediments deeper than the modeled sediments. The total mass of solids, POM, and contaminant in the sediments to be dredged from a given cell multiplied by a loss rate was then released to the water column over the duration of dredging in that cell. The loss rate specified in the model was set to 3% based on data from the 2005

Environmental Dredging Pilot Study (LBG, 2012) and data from other sediment sites. Losses during dredging were simulated in the model split equally between layer 10, the sediment water interface, and layer 1, the air water interface. These are the two points in the dredging operation where the greatest losses are expected. The contaminants were released to the water column during dredging as a total mass and allowed to partition according to the equilibrium partition coefficient along with the calculated organic carbon concentrations, which also account for the releases during dredging. Conditions specific to each of the alternatives are described below.

6.2 DESCRIPTION OF ALTERNATIVES

Alternative 1 – No Action – Simulations include the Tierra Removal, Phase 1 and Phase 2³ (see Figure 6-1). Removal of Phase 1 occurs between March and August 2012 and removal of Phase 2 is assumed to occur between March and September 2016. Phase 1 and 2 solids and contaminant releases during dredging are not simulated because the removals occur behind a coffer dam, although the structure of the cofferdam is not represented in the model. The removal and capping of approximately 20,000 CY from a 5.6 acre near-shore sediment deposit near RM10.9 from June through September of 2013 is also represented, along with the associated releases of sediment, organic carbon, and contaminants⁴. These removals are common to all alternatives.

Alternative 2 – Deep Dredging with Backfill (bank to bank) – Dredging of the FFS Study Area begins in March 2018 and is completed in 2029 progressing from upstream at RM 8

³ In June 2008, USEPA, Occidental Chemical Corporation and TSI signed an administrative order on consent (AOC) for TSI to remove 200,000 cubic yards (cy) of contaminated sediment from the river adjacent to the former Diamond Alkali facility at 80-120 Lister Avenue, Newark, NJ (RM 2.6-3.6) [“Tierra Removal”]. Phase 1 of the Tierra Removal (40,000 cy) was completed in 2012. The AOC contemplates that Phase 2 (160,000 cy) will undergo a separate engineering study and proposal that will be submitted to the public for review and comment at a later date.

⁴ The CPG is implementing the RM10.9 Removal under an agreement signed with USEPA in 2012. When the FFS model runs were performed, the RM10.9 Removal was on-going, so assumptions were made relating to the final dredging volume and construction duration.

downstream to RM 0. The simulation includes the removals from the No Action run with the same schedule and assumptions.

Alternative 3 – Capping with Dredging for Flooding and Navigation (bank to bank) – For Alternative 3, dredging of the FFS Study Area begins in March 2018 and is completed in 2023. Dredging of the federally-authorized navigation channel progresses from RM 0 upstream to RM 2.2. Then, dredging for flooding progressing from RM 8 downstream to RM 2.2, followed by restoration of the Kearny flats near RM 0. Alternative 3 includes the removals from the No Action run with the same schedule and assumptions. Similar to Alternative 2, contaminant concentrations are reset to zero in each grid box following completion of sediment removal in the particular grid box in the contaminant model.

Alternative 4 – Focused Capping with Dredging for Flooding – For the simulation of Alternative 4, dredging of the FFS Study Area begins in March 2018 and is completed in 2019. Dredging progresses from upstream near RM8.3 to downstream near RM 0, addressing selected cells targeted for remediation. As with Alternatives 2 and 3, Alternative 4 includes the removals from the No Action run with the same schedule and assumptions.

Model grid cells were selected for Focused Capping based on the gross and net contaminant resuspension per unit area from each grid cell. For each grid cell, a normalized gross and net resuspension was calculated as the ratio of the cell's gross (or net) contaminant resuspension to the RM 0-8.3 maximum gross (or net) resuspension. The sum of each grid cell's normalized gross and net resuspension was sorted from high to low, and cells were selected for Focused Capping based on a knee of the curve analysis. The selected cells represent approximately 33% of the RM 0-8 surface area (Figure 6-2).

Releases during dredging were simulated in the models for Alternative 4 in the same fashion as Alternatives 2 and 3.

The sequencing of construction described above is assumed for FFS evaluation purposes only; optimal sequencing will be determined in remedial design, after selection of a remedy.

6.3 FUTURE CONTAMINANT CONCENTRATIONS

Changes in contaminant concentrations are summarized with temporal plots of reach average sediment concentrations, maps showing spatial distributions of sediment concentrations at selected points in time, and as tabulations of contaminant concentrations at the end of the simulation. Model results for 2,3,7,8-TCDD, the sum of tetrachlorobiphenyl congeners, and mercury are discussed below; temporal plots for each of the 48 contaminants modeled are included in Attachment E-1 through E-4.

Model projections are discussed in detail for three of the forty-eight contaminants modeled. The three contaminants were chosen to demonstrate model performance for different groups of contaminants: 2,3,7,8-TCDD was chosen to represent hydrophobic COPCs and COPECs that originate largely from within the LPR, tetra-PCB was chosen to represent hydrophobic COPCs and COPECs that are more widespread in the environment, and mercury was chosen to represent the metals. Figures presenting the model results for the full suite of chemicals modeled are presented in the attachments to this appendix.

As discussed previously in Section 4.5, there is uncertainty associated with the concentrations computed by the model. The model computes a best estimate of future concentrations, but when the uncertainty associated with those estimates is accounted for the result is a best estimate, with a range around it. Section 6.3 presents the best estimates of future concentrations computed by the model under the four FFS alternative conditions. The uncertainty associated with the best estimate values is discussed further in Section 6.6.

6.3.1 2,3,7,8 TCDD Results

Reach Average Trajectories

Reach-average sediment concentrations of 2,3,7,8 TCDD are presented for the FFS Study Area (Figure 6-3), the reach upstream of RM8.3 to Dundee Dam (Figure 6-4) and three subsections of Newark Bay (Figures 6-5 to 6-7). Within each reach, reach averages are presented for the entire reach (top panel) and separately for the channel (middle panel) and shoals (bottom panel). For the Newark Bay reaches, the shoal areas to the east and west of the navigation channel are presented separately, as labeled. The overall reach-average concentration for No Action is repeated for comparison purposes, as a gray line, on the panels with the results for channels and shoals. In the reach between Dundee Dam and RM 8.3 (Figure 6-4) 2,3,7,8-TCDD concentrations in the shoals are higher than the reach average, and concentrations in the channel are lower than the reach average. This pattern is related to the coarser, less-organic substrate in the channel relative to the shoals in this reach. This pattern is reversed in the FFS area because of higher silt and organic carbon content in the channel relative to the upstream reach (Figure 6-3).

The results show a reduction in the variability in concentrations simulated within the FFS Study Area for the Deep Dredging, Full Capping, and Focused Capping alternatives compared to the variability in the No Action simulation, due to a reduction in erosion of contaminated sediment from within the FFS Study Area⁵. This variability is further reduced in the Deep Dredging and Full Capping results because the backfill and capping material contains less particulate organic carbon than native sediment. As a result, the remedial alternatives that include backfill or capping (both sand) include less intratidal resuspension of silt and particulate organic carbon (POC) that can sorb contaminants from the water column and transport sorbed contaminants back to the sediment with redeposited POC.

⁵ Note that the results are plotted on a log scale, so that while the Deep Dredging and Full Capping lines appear more variable visually, all of the alternatives vary over a range of approximately 0.1 ug/kg in response to the high flow events in 2039 and 2054.

The effect of cycling the 15-year hydrograph is evident in the results throughout the system, although to a lesser extent in the eastern shoals of Newark Bay. The effect of the April 2007 and March 2010 high flows (both over 15,000 cfs at Little Falls) is evident as they are repeated in years 2024 and 2027, 2039 and 2042, as the 15-year hydrograph is cycled. Attention to the log-scales is required to evaluate the relative response to the high flows among the alternatives. While the high flow conditions appear to have the most substantial effect on the Alternative 2 and 3 results in the FFS Study Area (Figure 6-3), the response is visually exaggerated because small changes to the lower concentrations preceding the high flow events appear to be larger increases on the log scale. The log scale, however, is helpful for seeing temporal changes in the results for each alternative, and for comparisons among alternatives.

Evaluating the effect of storms during the active remediation period is complicated by the fraction of the remediation completed and the locations that are still unremediated when the storms occur. Sediment removal and capping begin in March 2018 in the three active remedial alternatives. Because of the different volumes of sediment removed in each alternative, the remedies are completed at different times: 2019 for the Focused Capping, 2023 for the Full Capping, and 2029 for the Deep Dredging alternatives. The location of areas remediated and unremediated during the storms is also affected by the different spatial sequence in Alternative 2 versus 3, with Deep Dredging beginning at RM8.3 and progressing downstream, while in Alternative 3, RM0 to 2.2 is remediated first, before relocating to RM 8.3 and progressing downstream. After completion of the construction in all alternatives, the response to the 2039 high flow (2007 hydrograph) is more pronounced in the Deep Dredging alternative than the Full Capping alternative due to changes in hydrodynamics in the section of the river between RM8.3 and Dundee Dam. The post-remedy bathymetry for the Full Capping and Focused Capping alternatives is the same as the No Action bathymetry from RM 2.2 to 8.3; however, the Deep Dredging alternative results in deeper water depths up to RM 8.3, and the deeper bathymetry affects the transport upstream of RM 8.3. The deeper bathymetry results in somewhat higher velocities and shear stresses upstream of RM 8.3 (compared to the three other simulations) and additional erosion occurs. The deeper bathymetry in the FFS Study

Area also allows more of the eroded sediment to deposit in the FFS Study Area, resulting in a greater increase in the FFS Study Area average, as seen in Figure 6-3. When all of the remediation is completed in year 2029, the reach average concentrations in FFS Study Area are approximately 0.4 ug/Kg (ppb) for No Action, about a factor of 2 less for the Focused Capping alternative, and about a factor of 20 less for the Deep Dredging and Full Capping Alternatives. For the last twenty years, the reach averages in the FFS Study Area for the Deep Dredging and Full Capping alternatives cross numerous times, with one alternative higher for periods and then falling below the other. In 2059, simulated concentrations have declined to 0.35 ug/Kg for No Action, 0.18 ug/Kg for Focused Capping, 0.012 ug/Kg for Full Capping and to 0.09 ug/Kg for the Deep Dredging. Comparing the Deep Dredging and Full Capping results at the end of the simulation, the relationship between the channel and shoals is reversed. In the channel, the Deep dredging average is higher than the Full Capping results, and in the shoals the Deep Dredging average is lower than the Full Capping results.

In the reach upstream of the FFS Study Area (Figure 6-4), the results for No Action, Full Capping and Focused Capping track each other more so than the results for the Deep Dredging alternative, particularly in the shoal areas (Figure 6-4, bottom panel). At the beginning of active remediation, concentrations in the RM8.3-17 reach increase in the Deep Dredging alternative as sediment removal begins near RM 8.3. Following the high flow events in 2024 and 2027 (2007 and 2010 hydrographs), 2,3,7,8-TCDD concentrations in the shoals for the Deep Dredging alternative diverge downward from the other alternatives, although the gap varies over time.

Model results for 2,3,7,8-TCDD for Newark Bay are summarized for the reach north of Port Newark (Figure 6-5), from the northern side of Port Newark to the southern side of Port Elizabeth (Figure 6-6) and south of Port Elizabeth to the confluence with the Kill Van Kull and Arthur Kill (Figure 6-7). The most noticeable response in Newark Bay is the increase in concentrations associated with the period of dredging for the Deep Dredging alternative, although this elevated concentration declines over time. At the end of the simulation, concentrations in the channels for the Deep Dredging Alternative are

between 20% and 25% lower than the No Action results. For the Full Capping Alternative, the reduction in the channel is between 15% and 22%. For the Deep Dredging and Full Capping alternatives, with the exception of the shoals on the western side of the bay north of Port Elizabeth, where year 2059 concentrations are 20% to 34% lower than the No Action results, the reductions in the shoals are generally half of the reduction in the adjacent channel. The response in Newark Bay to the Focused Capping alternative is generally less than a 10% change.

Spatial Patterns of 2,3,7,8-TCDD Concentrations

The temporal variations in reach average concentrations, shown on Figures 6-3 through 6-7 are in response to erosion and deposition of contaminated and new cleaner solids. Maps showing the spatial distribution of 0-15 cm (~6 in) average 2,3,7,8 TCDD concentrations from the No Action simulation are shown for four time periods on Figures 6-8 through 6-11. Initial conditions estimated for October 1995 (Figure 6-8) show the general pattern of lower contaminant concentrations upstream, and increasing downstream of RM 13, with numerous areas of elevated concentrations (e.g. RM 11, 7.5-6.5, 4, and 3.5-2.5). Between October 1995 and January 2005, flows at Little Falls exceeded 10,000 cfs only one time, when Tropical Storm Floyd moved through the area in September 1999. Surface concentrations of 2,3,7,8 TCDD generally decreased during this period (Figure 6-9) but increased again in many areas as a result of the high flows in 2007, 2010 and 2011, as seen in the concentrations at the end of September, 2012 (Figure 6-10). By the end of the No Action simulation in 2059 (Figure 6-11) concentrations in many areas decreased somewhat, and gradients in surface concentrations are generally decreased.

The No Action simulation includes the implementation of remediation at RM10.9, in 2013. The extent of the removal action falls within the orange area adjacent to the RM10.9 label on Figure 6-11.

Figures 6-12 through 6-14 show the spatial variation in 2,3,7,8 TCDD concentrations at the end of the Deep Dredging, Full Capping, and Focused Capping simulations,

respectively. The greatest spatial variation among these three alternatives is seen in the Focused Capping results (Figure 6-14), which is consistent with only 33% of the FFS Study Area being capped. The spatial variation in the Deep Dredging alternative results (Figure 6-12) is contributed to by spatial variations in the contaminant concentrations released during dredging (based on 3% loss of removed solids) and the changes in hydrodynamics upstream of RM 8.3 resulting from deepening the river between RM 0 and 8.3. In addition, the Deep Dredging simulation results in deeper bathymetry and a corresponding decrease in velocity, which would result in higher rates of deposition than the Full Capping simulation (Figure 6-13).

6.3.2 Tetra-PCB Homolog Group Results

Reach average sediment concentrations for the sum of tetra-PCBs are presented on Figure 6-15 to 6-19 for the same five reaches presented above for dioxin. PCB concentrations are less variable spatially than the 2,3,7,8 dioxin concentrations, which leads to smaller spikes in reach average concentrations, as sediments erode and deposit during storms. This is true for both upstream and downstream of RM 8.3. The temporal patterns of tetra-PCB concentrations are more typical of the other contaminants (see Attachment E-1 through E-4), which generally show much less spatial and temporal variability than 2,3,7,8, dioxin. The relative differences in the sum of tetra-PCBs among the alternatives are similar to the differences noted for 2,3,7,8 TCDD. Responses in Newark Bay to the releases during dredging for the Deep Dredging and Full Capping simulations are much less than seen for 2,3,7,8-TCDD because the tetra-PCB spatial gradients between the LPR and Newark Bay are much less than for 2,3,7,8-TCDD. Remediation within the LPR has little effect on the long-term trends in Tetra-PCB concentrations in Newark Bay.

PCB concentrations in the tetra-homolog group at the start of the simulation (October 1995) are shown on Figure 6-20. Between 1995 and 2005 (Figure 6-21), simulated concentrations in some areas decreased somewhat, which introduces more variability than is seen in the initial conditions. Concentrations simulated in 2012 (Figure 6-22) following the high flows in 2007, 2010 and 2011 show increased concentrations in many areas, particularly around the outside bends in the lower 7 miles.

At the end of the No Action simulation (Figure 6-23) the number of areas with elevated concentrations and the magnitude of the elevated concentrations are reduced. Figures 6-24 through 6-26 show the spatial variation in concentration of the sum of the tetra-PCBs homolog group at the end of the Deep Dredging, Full Capping, and Focused Capping simulations, respectively. Concentrations at the end of the Deep Dredging alternative simulation (Figure 6-24) show most of the RM 0-8 reach with concentrations in .001 to .05 mg/Kg range (1-50 ppb), and several areas of lower concentration on the outside of the bends between RM 3.2 and 4.2. At the end of the Full Capping alternative simulation (Figure 6-25), recontamination of the cap occurs on the south side of the river between RM 3.3 and RM 4.5. The Focused Capping results (Figure 6-26) show a fair amount of recontamination of capped areas, and concentrations in uncapped areas above 0.5 mg/kg (ppm) in several locations.

6.3.3 Total Mercury Results

Reach average sediment mercury concentrations are presented on Figure 6-27 to 6-31 for the same five reaches presented above for dioxin and tetra-PCBs. The temporal patterns of mercury results are similar to the patterns in the Tetra PCB results for both the No Action alternative and the active remedial alternatives. In the FFS Study Area at the end of the period of remediation, which is completed by 2029 for all alternatives, the reach-average concentration for the Deep Dredging and Full Capping alternatives are between 10 and 15% of the No Action average at that time. In comparison, the Focused Capping average is approximately two-thirds (or 75-80%) of the No Action average. At the end of the simulation (2059) the averages for the Deep Dredging and Full Capping alternatives are between 5 and 10% of the No Action average, while the reach average for the Focused Capping alternative is approximately two-thirds (or 75-80%) of the No Action average. For the RM8.3-17 reach and the three reaches in Newark Bay, the three alternatives show little response compared to the No Action simulation.

Maps showing the spatial distribution of total mercury concentrations indicate generally small changes between 1995 and 2005 (Figure 6-32 and 6-33) with some areas increasing

and others decreasing in concentration. Following the high flows in 2007, 2010, and 2011, several areas in 2012 (Figure 6-34) show substantially higher concentrations than in 2005. By 2059 (Figure 6-35), noticeable cross-river gradients develop in the No Action simulation as along-river gradients become smoother. The along-river concentration gradients for mercury are smoother than for tetra-PCBs or for 2,3,7,8 TCDD. Concentrations at the end of the Deep Dredging simulation fall into the range of 0.1 to 0.5 mg/Kg (ppm) (100-500 ppb) over much of the FFS Study Area, with the exception of areas on the outsides of bends, which generally have concentrations less than 0.05 mg/Kg (50 ppb) (Figure 6-36). In the Full Capping run (Figure 6-37), surface sediment mercury concentrations in the majority of the FFS Study Area are in the range of less than 0.05 mg/Kg (ppm) (50 ppb). In shoals areas between RM 2.2 and 3.3 and downstream of RM 1.5, concentrations are between 0.1 and 0.5 mg/Kg (ppm) (100-500 ppb). Concentrations in the FFS Study Area at the end of the Focused Capping simulation (Figure 6-38) show considerable spatial variability, with a considerable number of cells with concentrations in the range of 1.0-2.5 mg/kg (ppm) (1000-2500 ppb), another sizable fraction with concentrations between 0.1 and 0.5 mg/Kg (100-500 ppb) and a limited number of areas with concentrations less than 0.05 mg/Kg (50 ppb).

6.4 NET CONTAMINANT MASS TRANSPORT

Contaminant mass transported in the water column was evaluated at eight transects across the river, ranging from RM 16.7 to 0.9 at approximately 2.2 mile intervals. Cumulative mass transported in the water column was calculated for the period following completion of remediation of all alternatives (2029-2059). Cumulative mass transport for No Action and the three active remedial alternatives are plotted together to facilitate comparison among the alternatives. Figures 6-39 through 6-41 show cumulative mass transport at RM 16.7, RM 14.5, and RM 12.3, respectively, for (from top to bottom panel) 2,3,7,8 TCDD, tetra-PCBs and mercury. There are only minor differences in contaminant mass transport among the alternatives at these locations.

At RM 9.8 (Figure 6-42) contaminant mass transport for all alternatives and contaminants show gradual increases over time, with step increases associated with high flow

conditions in 2039 and 2054, which is when the April 2007 high flow occurs in the 15-year repeating hydrograph. Smaller steps are also noted in 2042 and 2057 when the 2010 high flow occurs in the 15-year cycle. For each contaminant shown, the simulated mass transport for the No Action, Full Capping and Focused Capping alternatives are very similar over the entire 2029 through 2059 period. Differences are seen in the mass transport, however, for the Deep Dredging simulation, with greater steps in the mass transport compared to No Action and the other two alternatives due to a more-substantial response to the high flow in early 2039 and again in 2054 when the 2007 flow is repeated in the 15-year cycle. The increase in cumulative mass transport in the Deep Dredging alternative compared to the other three alternatives is due to additional erosion upstream caused by changes in the hydrodynamics resulting from the deeper bathymetry downstream.

Patterns in cumulative mass transport of 2,3,7,8 TCDD at RM 7.8 (Figure 6-43) are similar to those at RM 9.8, although with more pronounced differences between the Deep Dredging and the other three alternatives. At RM7.8 small differences between the Deep Dredging and the other three alternatives are noticeable before 2039 for tetra-PCBs and mercury, which was not the case at RM 9.8. For 2,3,7,8-TCDD the gap between the Deep Dredging and the other three alternatives remains fairly constant between the steps in 2039 and 2054, while for the other contaminants/groups the gap increases over time.

At RM5.7 (Figure 6-44), the mass transport for each contaminant/group for the Deep Dredging alternative is less than was calculated at RM 7.8 (Figure 6-43), indicating substantial deposition in this reach due to the deepened bathymetry in Alternative 2. For 2,3,7,8-TCDD this is the first station, moving from upstream to downstream, where the cumulative flux under No Action conditions exceeds the other remedial alternatives. The differences between No Action and the other alternatives show the reduction in transport achieved by each alternative. For 2,3,7,8-TCDD, the deposition in the reach between RM7.8 and 5.7 eliminates most of the difference in mass transport among the alternatives. For tetra-PCBs and mercury the deposition partially closes the gap between the Deep Dredging and the other alternatives. For mercury small differences between No

Action and the two capping alternatives begin to be noticeable following the high flow in 2054.

At RM 3.1 (Figure 6-45), the mass transport for each contaminant/group for the Deep Dredging alternative decreases again compared to the previous upstream transect at RM 5.7 (Figure 6-44), indicating additional deposition in this reach due to the deepened bathymetry in Alternative 2. Deposition upstream of RM 3.1 results in the Deep Dredging alternative having the smallest mass transport for 2,3,7,8-TCDD among the alternatives, with the Full Capping alternative having the next smallest mass transport for these contaminants. For tetra-PCBs and mercury, the mass transport for the Full Capping alternative is at the low end of the range of mass transport among the alternatives and the Focused Capping alternative is at the upper end.

At RM 0.8, where the river widens on the approach to Newark Bay, the separation among the alternatives is more pronounced (Figure 6-46) than at any of the locations previously presented. For each contaminant/group the No Action and Focused Capping result are close and both are greater than the mass transport for the Full Capping and Deep Dredging. Except for tetra-PCBs, for which the mass transport for the Full Capping and Deep Dredging are essentially the same by 2059, the mass transport for the Deep Dredging alternative is less than the other alternatives at RM0.9.

The reach-average contaminant results for the FFS Study Area show that the Deep Dredging and Full Capping concentrations produce substantial reductions in contaminant concentrations within the FFS Study Area, with smaller effects both upstream in the LPR and downstream in Newark Bay. The mass transport comparisons show that the Deep Dredging and Full Capping alternatives reduce the transport of 2,3,7,8-TCDD, tetra-PCBs and mercury to Newark Bay by one third or less.

6.5 RISK ASSESSMENT LINKAGE

Contaminant concentrations in water and sediment computed for each alternative were averaged in several ways, both spatially and temporally, to provide exposure

concentrations to both ecological and human health risk assessments. The risk assessments will provide a quantitative basis for evaluating future risk for each of the alternatives.

6.6 UNCERTAINTY

The median relative error uncertainty values computed in section 4.5 were applied to the FFS study Area reach average top-15cm (~6 in) sediment concentrations for the four modeled alternatives. These results are presented in Figures 6-47 through 6-49 for 2,3,7,8-TCDD, tetrachlorobiphenyl, and mercury respectively. The solid lines are the same area weighted full reach averages presented in section 6.3 on the top panels of Figures 6-3, 6-15, and 6-27. The dashed lines represent the uncertainty bounds based on the median relative error analysis.

The 2,3,7,8-TCDD area weighted average concentrations for the Focused Capping alternative are lower than the No Action results for the entire period after completion of the remedy (Figure 6-47); however, the lower uncertainty bound for No Action overlaps the upper uncertainty bound for the Focused Capping. In the case of the Full Capping and Deep Dredging results the area weighed averages and uncertainty bounds overlap each other for the period after completion of the Deep Dredging remedy, and these results only overlap the results for the No Action and Focused Capping alternatives for limited periods of time. At times when the 2007 high flow condition is repeated in the hydrograph in 2039 and 2054, the upper uncertainty bound on the Deep Dredging result overlaps the lower bound on the Focused Capping result, but the two results diverge after a couple of months to about a year. For the remainder of the time after all of the remedies are completed in 2029 the Deep Dredging and Focused Capping results including the uncertainty bounds are noticeably lower than the No Action and Focused Capping results.

Results for tetra-PCB (Figure 6-48) are similar to those for 2,3,7,8-TCDD in that although the area weighted average for the Focused Capping alternative is lower than the area weighted average for No Action, the area weighted average and lower uncertainty

bound for No Action overlap the area weighted average and upper uncertainty bound for the Focused Capping alternative for the entire period after completion of the Focused Capping remedy. In the case of the Full Capping and Deep Dredging results the area weighed averages and uncertainty bounds overlap each other for the period after completion of the Deep Dredging remedy, with Deep Dredging being somewhat higher. The tetra-PCB Deep Dredging and Full Capping results do not follow each other as closely as the 2,3,7,8-TCDD results. Under the 2007 high flow condition, repeated in the hydrograph in 2039 and 2054, the upper uncertainty bound on the Deep Dredging result overlaps the lower bound on the Focused Capping result, but the two results diverge after a couple of months to about a year. For the remainder of the time after all of the remedies are completed in 2029 the Deep Dredging and Focused Capping results including the uncertainty bounds are noticeably lower than the No Action and Focused Capping results.

For total Mercury (Figure 6-49) the lower uncertainty bound for No Action overlaps the upper uncertainty bound for the Focused Capping result for the entire period after completion of the Focused Capping remedy, again with the area weighted average for Focused Capping lower than the area weighted average for No Action. In the case of the Full Capping and Deep Dredging results the area weighed averages and uncertainty bounds overlap each other for the period after completion of the Deep Dredging remedy, with Deep Dredging being somewhat higher. The total mercury Deep Dredging and Full Capping results follow a similar pattern to the tetra-PCB results. Under the 2007 high flow condition, repeated in the hydrograph in 2039 and 2054, the upper uncertainty bound on the Deep Dredging result approaches the lower bound on the focused capping result, but the two do not overlap. For the remainder of the time after all of the remedies are completed in 2029 the Deep Dredging and Full Capping results, including the uncertainty bounds, are noticeably lower than the No Action and Focused Capping results.

For the majority of the remainder of the contaminants (Attachment F) the contaminants show similar patterns, with the No Action and Focused Capping results overlapping each

other, and the Deep Dredging and Full Capping results overlapping each other, but the two groups of results remaining separate. Some exceptions include 1,2,3,7,8,9-hexachlorodibenzofuran, BZ#123, BZ#126, BZ#167, BZ#169, 2,4'-DDT, 4,4'-DDT, and methyl-mercury (more overlap), and mono-PCBs, di-PCBs and tri-PCBs, deca-PCBs, cadmium (more overlap under high flow conditions).

7 REFERENCES

Aller, R.C., 1982. The effects of macrobenthos on chemical properties of marine sediment and overlying water. In *Animal-Sediment Relations. The Biogenic Alteration of Sediments*. P. McCall and M. Tevesz, editors. pp 53-102. Plenum Press, New York, NY.

Ankley, G.T., D.M. Di Toro, D.J. Hansen, and W.J. Berry, 1996. Technical basis and proposal for deriving sediment quality criteria for metals. *Environ. Toxicol. Chem.* 15(12): 2056-2066.

Berner, R.A., 1971. *Principles of Chemical Sedimentology*. McGraw-Hill, New York, New York.

Berner, R.A., 1974. Kinetic models for the early diagenesis of nitrogen, sulfur, phosphorus and silicon in anoxic marine sediment. In E. Goldberg, editor, *The Sea*, vol. 5, pp. 427-450. John Wiley & Sons, New York, New York.

Berner, R.A., 1980. A rate model for organic matter decomposition during bacterial sulfate reduction in marine sediments. In *Biogeochemistry of Organic Matter at the Sediment-Water Interface*, pp. 35-44. Comm. Natl. Recherche Scientific, France.

Boudreau, B.P., 1994. Is burial velocity a master parameter for bioturbation? *Geochimica et Cosmochimica Acta*, Vol. 58, No. 4, pp.1243-1249

Boudreau, B.P., 1998. Mean mixed depth of sediments: The wherefore and the why. *Limnol. Oceanogr.* 43: 524-526.

Burkhard, L. P., 2000. "Estimating Dissolved Organic Carbon Partition Coefficients for Nonionic Organic Chemicals," *Environmental Science and Technology*, 34(22): 4663-4668.

Connolly, J.P., and R. Tonelli, 1985. Modeling Kepone in the Striped Bass Food Chain of the James River Estuary. *Estuarine Coastal and Shelf Science* (20), pp 349-366, 1988.

Di Toro, D.M. and J.J. Fitzpatrick, 1993. Chesapeake Bay sediment flux model. HydroQual, Inc. Mahwah, NJ. Prepared for the USACE Waterways Experiment Station, Vicksburg, MS. Contract Report EL-93-2.

DiToro, D. M. "A Particle Interaction Model of Reversible Organic Chemical Sorption" (1985). *Chemosphere* 14 (10): 1503-1538

Di Toro, D.M., 2001. *Sediment Flux Modeling*. John Wiley & Sons, New York, New York.

Di Toro, D.M., C.S. Zarba, D.J., Hansen, W.J. Berry, R.C. Swartz, C.E. Cowan, S.P. Pavlou, H.E. Allen, N.A. Thomas, P.R. Paquin, 1991. Technical basis for establishing sediment criteria for nonionic organic chemical using equilibrium partitioning. *Environ. Toxicol. Chem.* 10: 1541-1583.

Diaz, R., and Arcadis, 2008. "Estimation of the Biologically Active Zone, Newark Bay, NJ," prepared for USEPA, Region II.

ENSR. 2008. Quality Assurance Project Plan RI Low Resolution Coring/Sediment Sampling Lower Passaic River Restoration Project Newark, New Jersey. May 2, 2008. Revision 1 July 18, 2008; 2 July 24, 2008; 3, July 29, 2008; and 4 October 20, 2008.

Gahagan & Bryant Associates, Inc. (GBA), 2009. Submission of Required Deliverables for the Multi Beam Portion of the referenced Hydrographic Survey conducted upon the Passaic River, Vicinity of Newark, N.J. February 2009

HDR|HydroQual, 2013. Lower Passaic River, Lower Eight Miles Focused Feasibility Study, Report of the Peer Review of Sediment Transport, Organic Carbon and Contaminant Fate and Transport Model. prepared for USEPA, Region II.

HydroQual, Inc., 1999. Newton Creek Water Pollution Control Project East River Water Quality Plan, Report to NYCDEP. Task 10.0 System-Wide Eutrophication Model (SWEM) Sub-task 10.1 Construct SWEM. Prepared under subcontract to Greeley and Hansen, New York, NY.

HydroQual, Inc., 1999. Newton Creek Water Pollution Control Project East River Water Quality Plan, Report to NYCDEP. Task 10.0 System-Wide Eutrophication Model (SWEM) Sub-task 10.2 Obtain and Reduce Loading/Water Quality Data. Prepared under subcontract to Greeley and Hansen, New York, NY.

HydroQual, Inc., 1999. Newton Creek Water Pollution Control Project East River Water Quality Plan, Report to NYCDEP. Task 10.0 System-Wide Eutrophication Model (SWEM) Sub-task 10.4 Calibrate SWEM Water Quality. Sub-task 10.6 Validate SWEM Water Quality. Prepared under subcontract to Greeley and Hansen, New York, NY.

HydroQual, Inc., 1999. Newton Creek Water Pollution Control Project East River Water Quality Plan, Report to NYCDEP. Task 10.0 System-Wide Eutrophication Model (SWEM) Sub-task 10.5 Apply SWEM for Preliminary Facility Design. Prepared under subcontract to Greeley and Hansen, New York, NY.

HydroQual, Inc., 1999. Newton Creek Water Pollution Control Project East River Water Quality Plan, Report to NYCDEP. Task 10.0 System-Wide Eutrophication Model (SWEM) Sub-task 10.7 Final Facility Design. Prepared under subcontract to Greeley and Hansen, New York, NY.

HydroQual, Inc., 1999. Newton Creek Water Pollution Control Project East River Water Quality Plan, Report to NYCDEP. Task 10.0 System-Wide Eutrophication Model

(SWEM) Sub-task 10.6 Validate SWEM Hydrodynamics. Prepared under subcontract to Greeley and Hansen, New York, NY.

HydroQual, Inc., 2000. Bays Eutrophication Model (BEM): Modeling analysis for the period 1992-1994. Final report prepared for the Massachusetts Water Resources Authority, Environmental Quality Department. Report ENQUAD 2000-02.

HydroQual, Inc., 2000. Bays Eutrophication Model (BEM): Modeling analysis for the period 1992-1994. Final report prepared for the Massachusetts Water Resources Authority, Environmental Quality Department. Report ENQUAD 2000-02

HydroQual, Inc., 2002. Calibration Enhancement of the System-Wide Eutrophication Model (SWEM) in the New Jersey Tributaries, Report to NJDEP. Final Technical Report April 23, 2001 through July 31, 2002. Prepared under subcontract to Passaic Valley Sewerage Commissioners, Newark, NJ.

HydroQual, 2007. A model for the evaluation and management of contaminants of concern in water, sediment and biota in the NY/NJ Harbor Estuary: Contaminant fate & transport & bioaccumulation sub-models. Prepared for the Contamination Assessment and Reduction Project (CARP) Management Committee. HydroQual, Inc., Mahwah, NJ, 07430.

HydroQual, 2008. Lower Passaic River, Final Hydrodynamic Modeling Report. prepared for USEPA, Region II.

King, J., Saunders, F., Lee, R. and Jahnke, R., 1999. Coupling Mercury Methylation Rates to Sulfate Reduction Rates in Marine Sediments. Environmental Toxicology and Chemistry. 18(7): 1362-1369.

Karickhoff, S.W., 1980. Sorption Kinetics of Hydrophobic Pollutants in Natural Sediments. Contaminants and Sediments, Vol. 2, (ed. R.A. Baker) Ann Arbor Sci Publ. Ann Arbor, Mich., pp. 193-205

Karickhoff, S.W., 1984. Organic Pollutant Sorption in Aquatic Systems. J. Hydraulic Div. ASCE, Vol. 110, No. 6, pp. 707-735

Louis Berger Group, Inc. (LBG), 2012. "Environmental Dredging Pilot Study Report." Prepared for USACE New York District. July 2012.

Meyers, M.B., D.M, Di Toro, and S.A. Lowe, 2000. Coupling suspension feeders to the Chesapeake Bay Eutrophication Model. Water Quality and Ecosystem Modeling. Vol. 1(1-4): 123-140

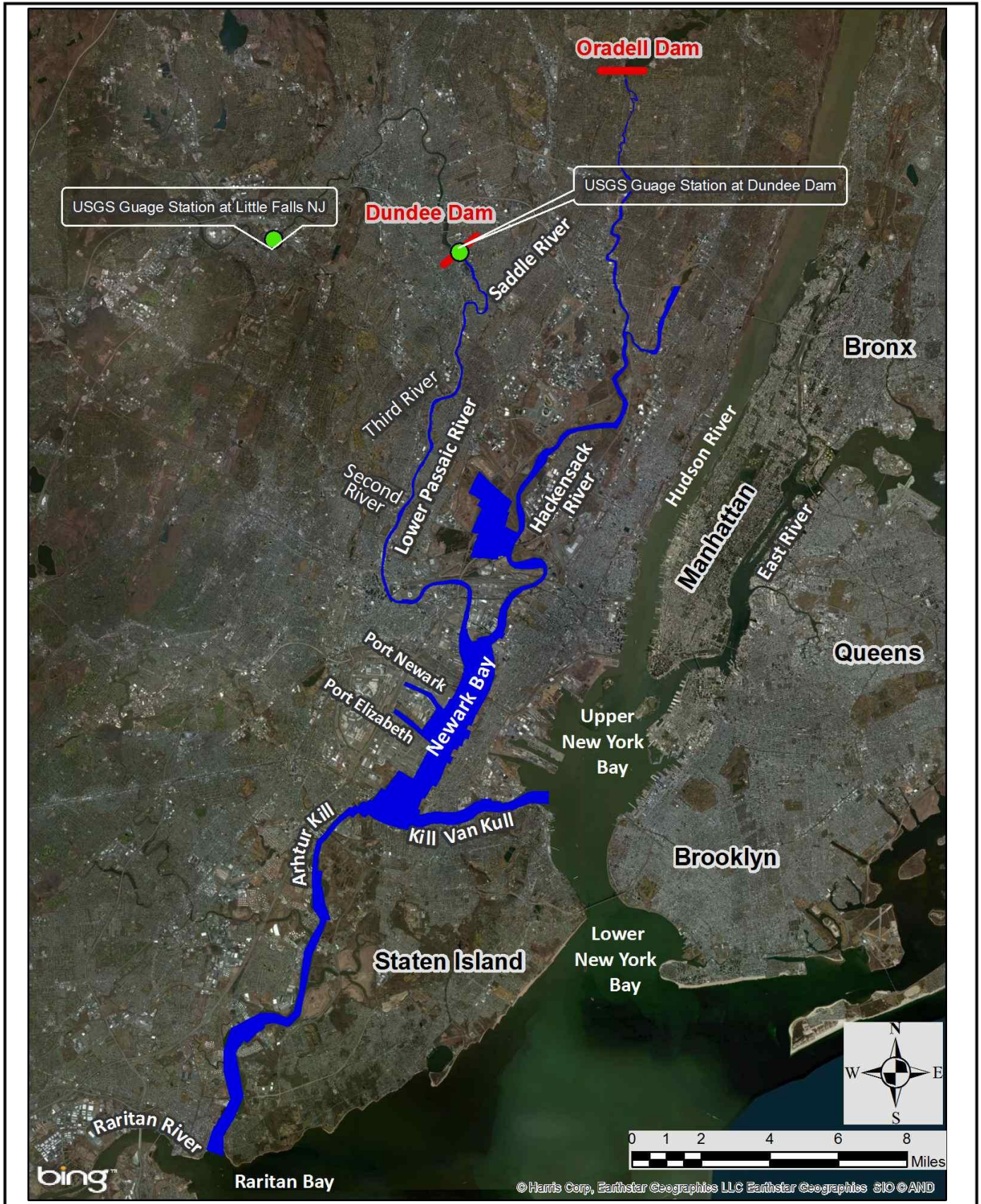
Miller, R. L. and J. P. St. John (2006). Modeling Primary Production in the Lower Hudson River Estuary. Chapter 11. The Hudson River Estuary. J. S. Levinton and J. R. Waldman, editors. pp. 140-153. Cambridge University Press. New York, NY.

Quantitative Environmental Analysis, 2008. Lower Duwamish Waterway Sediment Transport Modeling Report –Final. Prepared for:U.S. Environmental Protection Agency Region 10 Seattle, WA and Washington State Department of Ecology Northwest Regional Office Bellevue, WA. October 2008.

Rodenburg, L.A., 2008. "OCB atmospheric depositional fluxes to NY/NJ Harbor". Personal Communication.

Tierra Solutions, Inc. (TSI). 2009. Hydrodynamic Assessment Plan – Phase I Removal Action, Quality Assurance Project Plan (QAPP3) for CERCLA Non-Time Critical Removal Action, Lower Passaic River Study Area, Revision 2. July 2009.

Totten, L.A., et al., 2004. Atmospheric Concentrations and Deposition of Polychlorinated Biphenyls to the Hudson River Estuary. *Environ. Sci. Technol.*, 38 (9): 2568–2573.



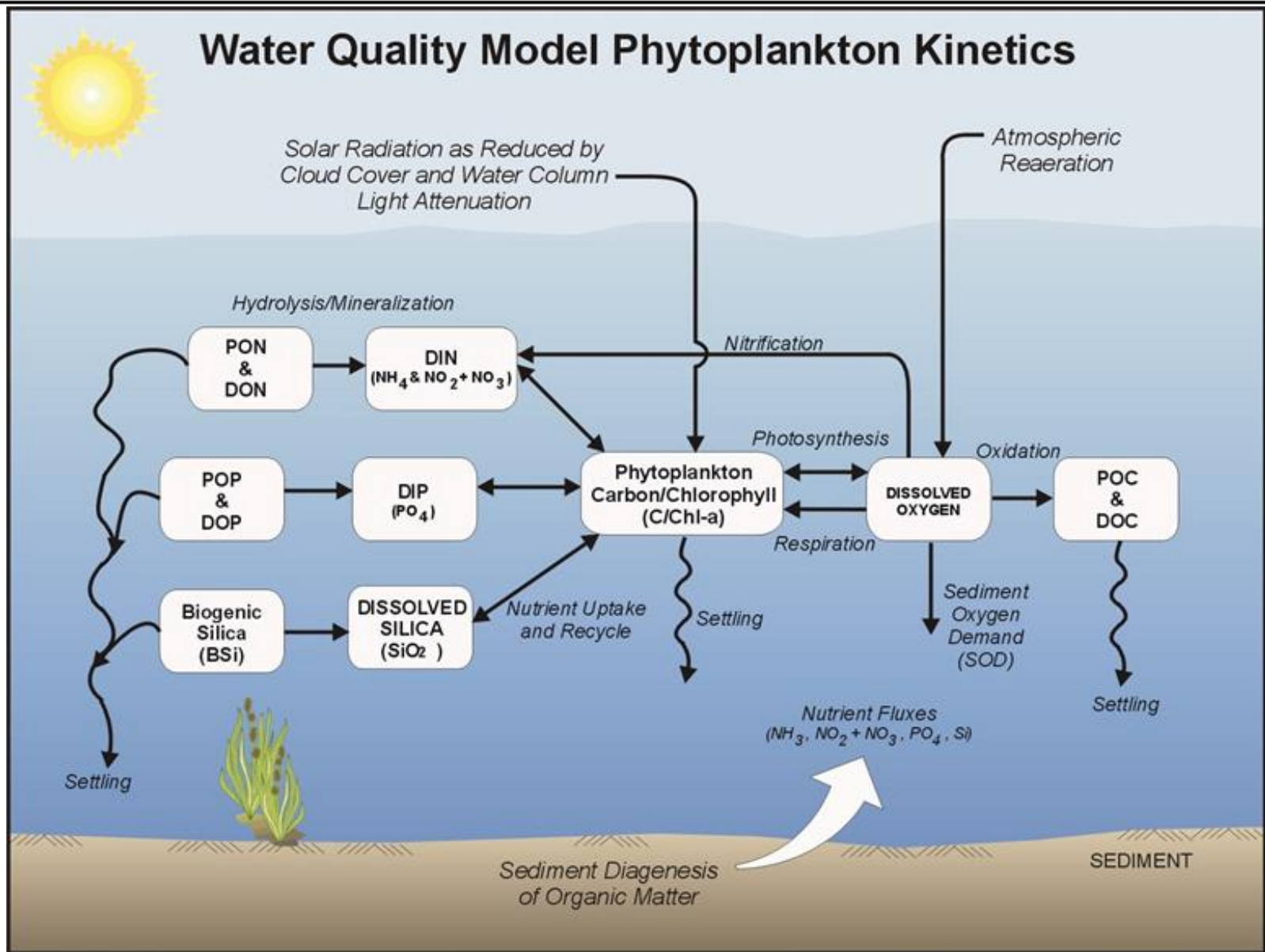
Model Domain

Figure 1-1

Lower Eight Miles of the Lower Passaic River

2014

Water Quality Model Phytoplankton Kinetics



Water Quality Model Phytoplankton Kinetics

Figure 2-1

Lower Eight Miles of the Lower Passaic River

2014

	Bed		Erosion				Deposition			
	Layer Number	Thickness (cm)	Thickness (cm)	Conc	Thickness (cm)	Conc	Thickness (cm)	Conc	Thickness (cm)	Conc
Active Layer	1	0.5-2	0.5	A	1.5	$(0.5 \cdot A + B) / 1.5$	2	A	1	A
	2	1	1	B	1	C	1	B	1	A
	3	1	1	C	1	D	1	C	1	B
	4	1	1	D	1	E	1	D	1	C
	5	1	1	E	1	F	1	E	1	D
	6	1	1	F	1	G	1	F	1	E
	7	1	1	G	1	H	1	G	1	F
	8	1	1	H	1	I	1	H	1	G
	9	1	1	I	1	J	1	I	1	H
	10	1	1	J	1	K	1	J	1	I
Archive Layer	1	1*	1	K	1	L	1	K	1	J
	2	1*	1	L	1	M	1	L	1	K

	96	1*	1	X	1	Y	1	X	1	W
	97	1*	1	Y	1	Z	1	Y	1	X
Deep Bed	1	60**	60	Z	59	Z	60	Z	61	$(60 \cdot Z + Y) / 61$

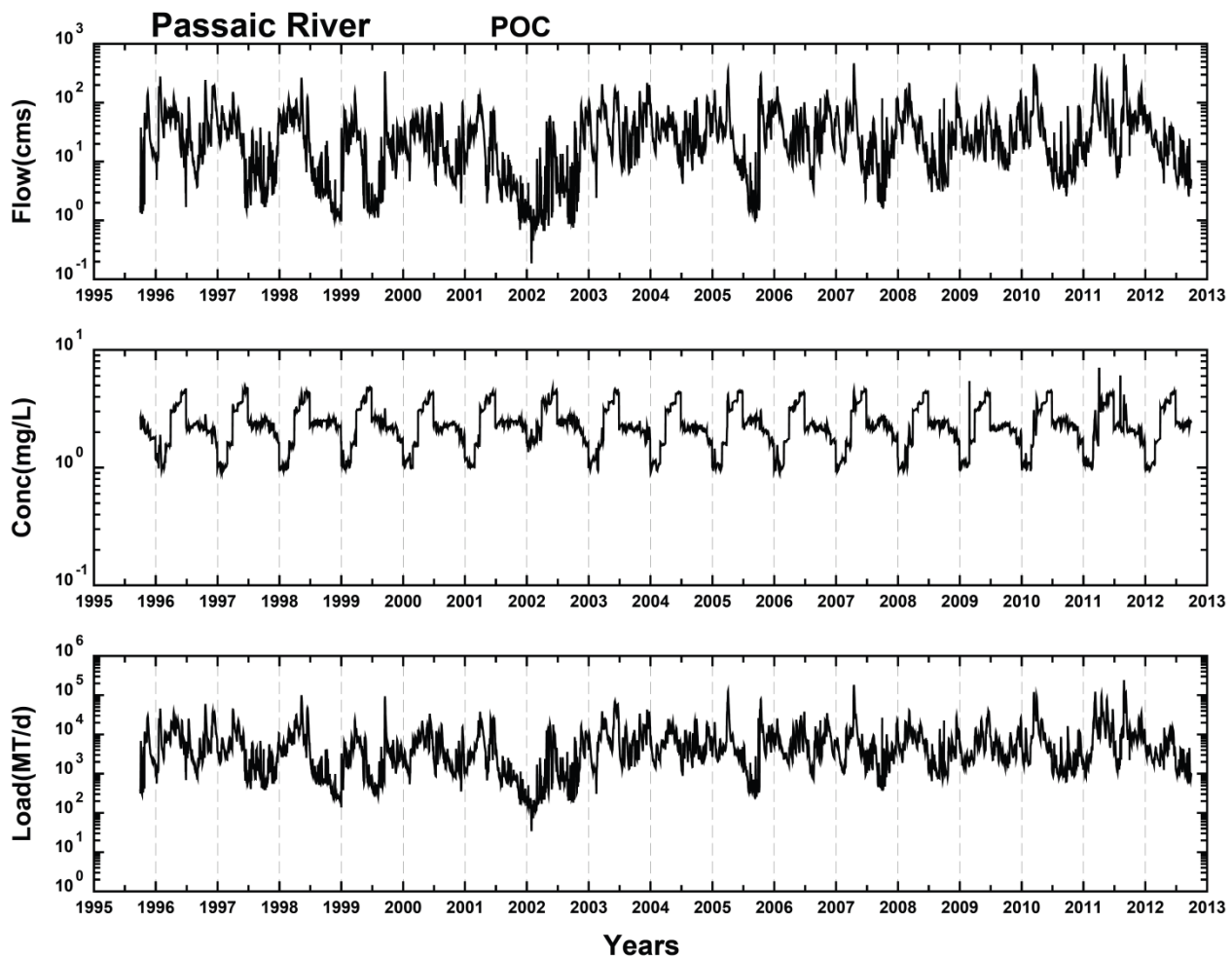
*Archive stack layers are 1 cm if present.
 **Deep bed archive is initially 60cm. It can decrease in 1 cm increments to 0 cm with erosion or increase in 1 cm increments with deposition.

RCATOX Bed Structure

Figure 2-2

Lower Eight Miles of the Lower Passaic River

2014

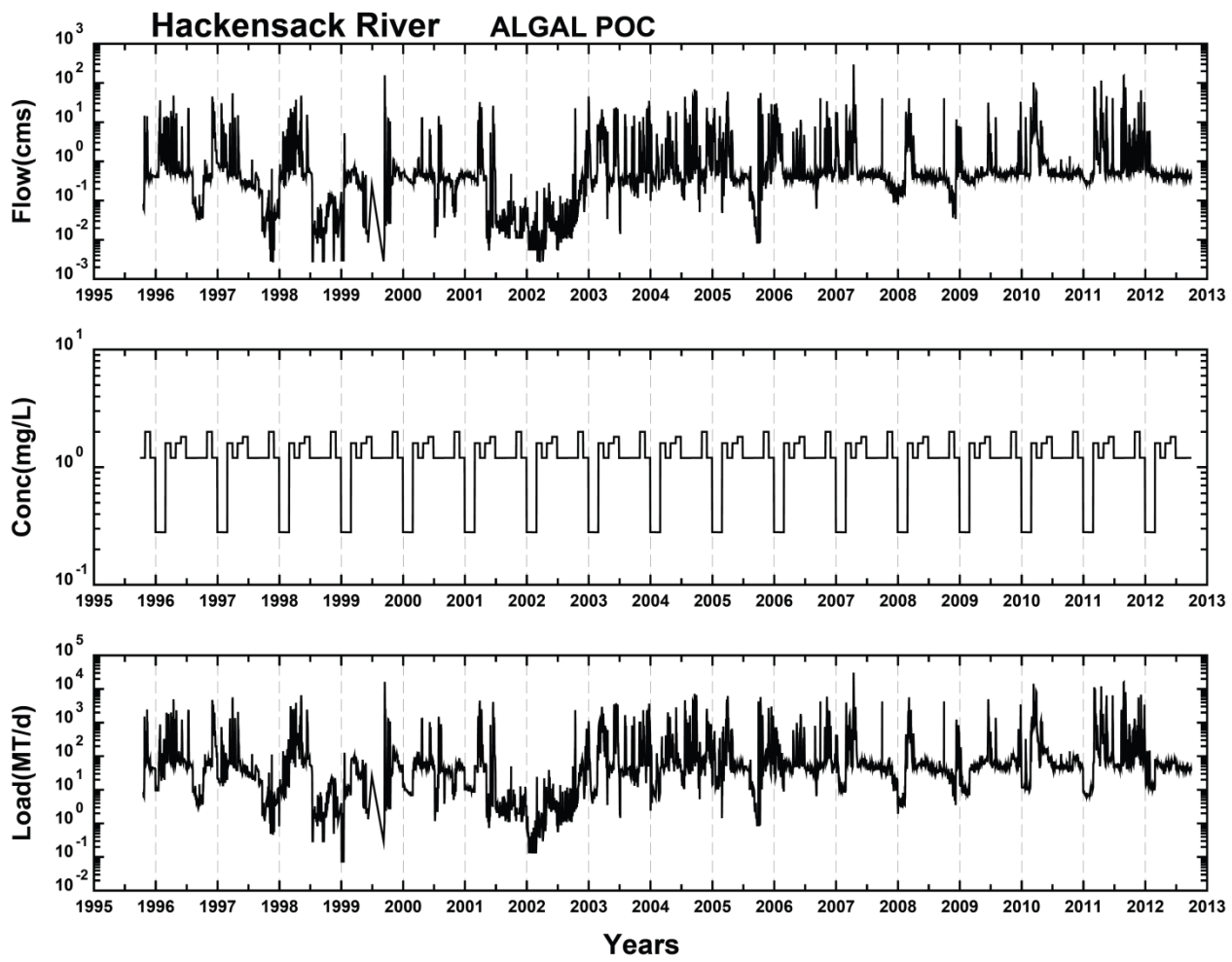


Upper Passaic River Total Particulate Organic Carbon (POC) Boundary Condition

Figure 3-1

Lower Eight Miles of the Lower Passaic River

2014

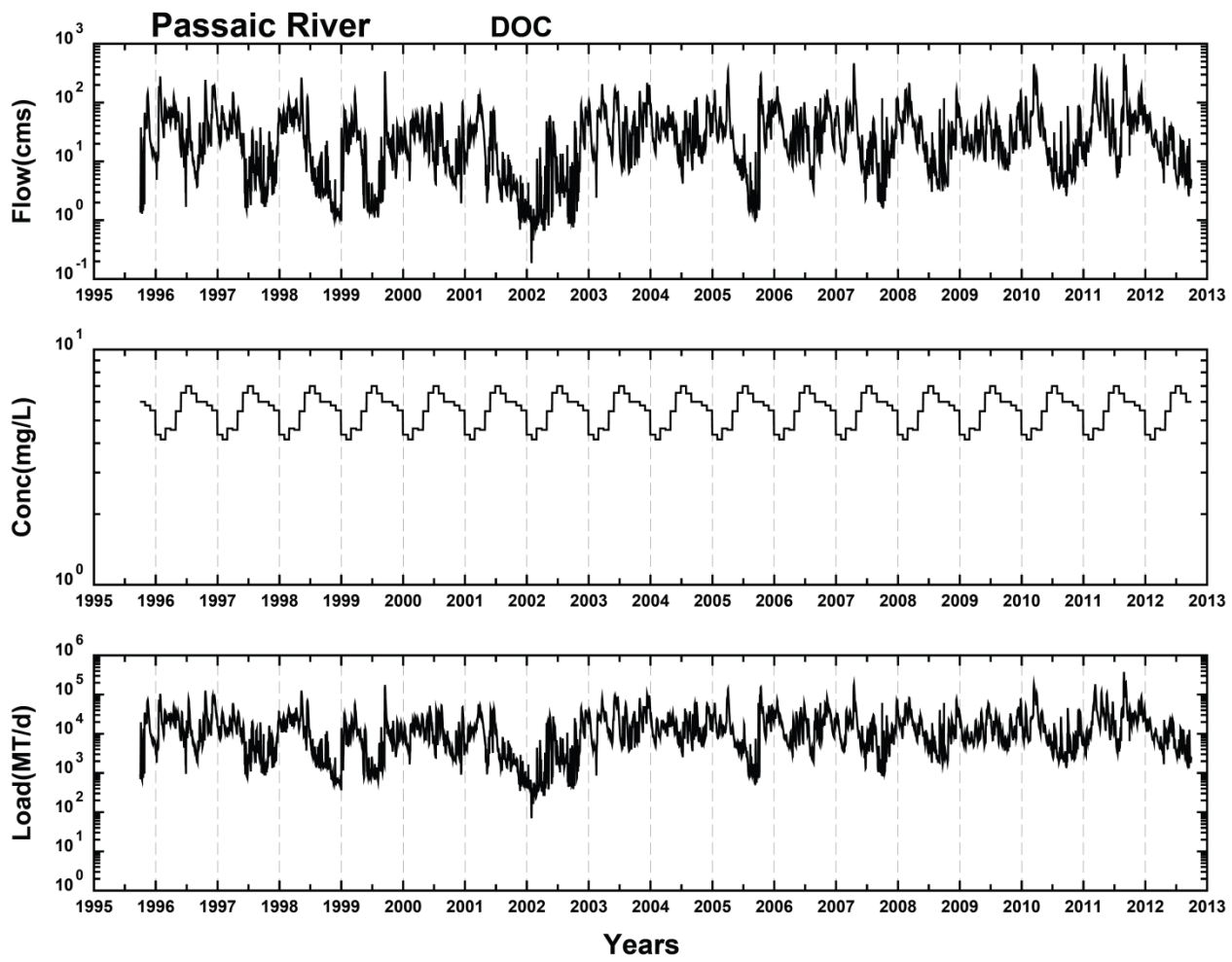


Upper Passaic River Algal POC Boundary Condition

Lower Eight Miles of the Lower Passaic River

Figure 3-2

2014

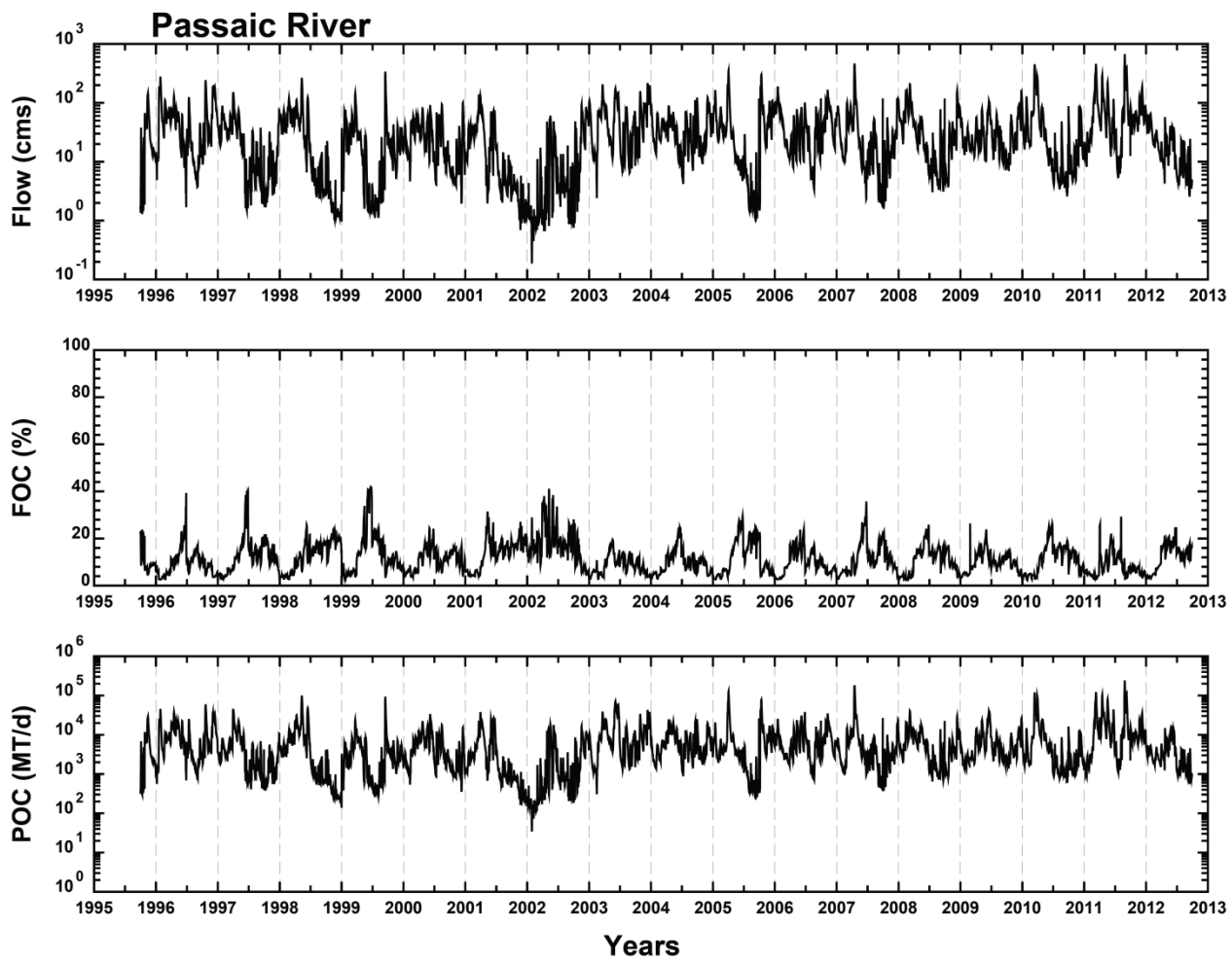


Upper Passaic River Dissolved Organic Carbon Boundary Condition

Figure 3-3

Lower Eight Miles of the Lower Passaic River

2014



Upper Passaic River Boundary Fraction Organic Carbon (FOC)

Figure 3-4

Lower Eight Miles of the Lower Passaic River

2014

No Action
Top 15 cm FOC(%) in yr: 1995.75



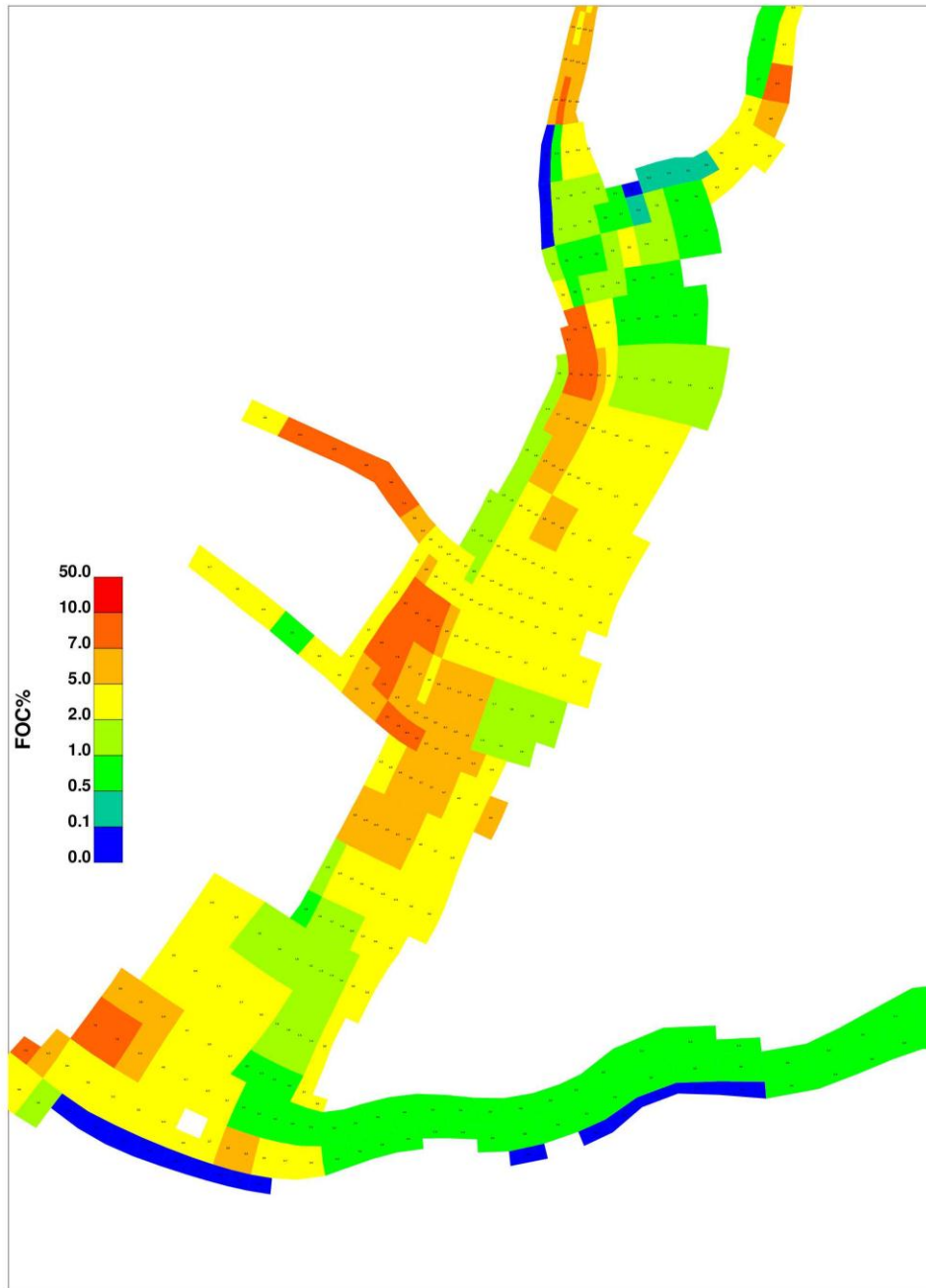
Sediment FOC Cycled Initial Condition in the LPR and Interpolated Initial Conditions in Newark Bay

Lower Eight Miles of the Lower Passaic River

Figure 3-5

2014

No Action
Top 15 cm FOC(%) in yr: 1995.75

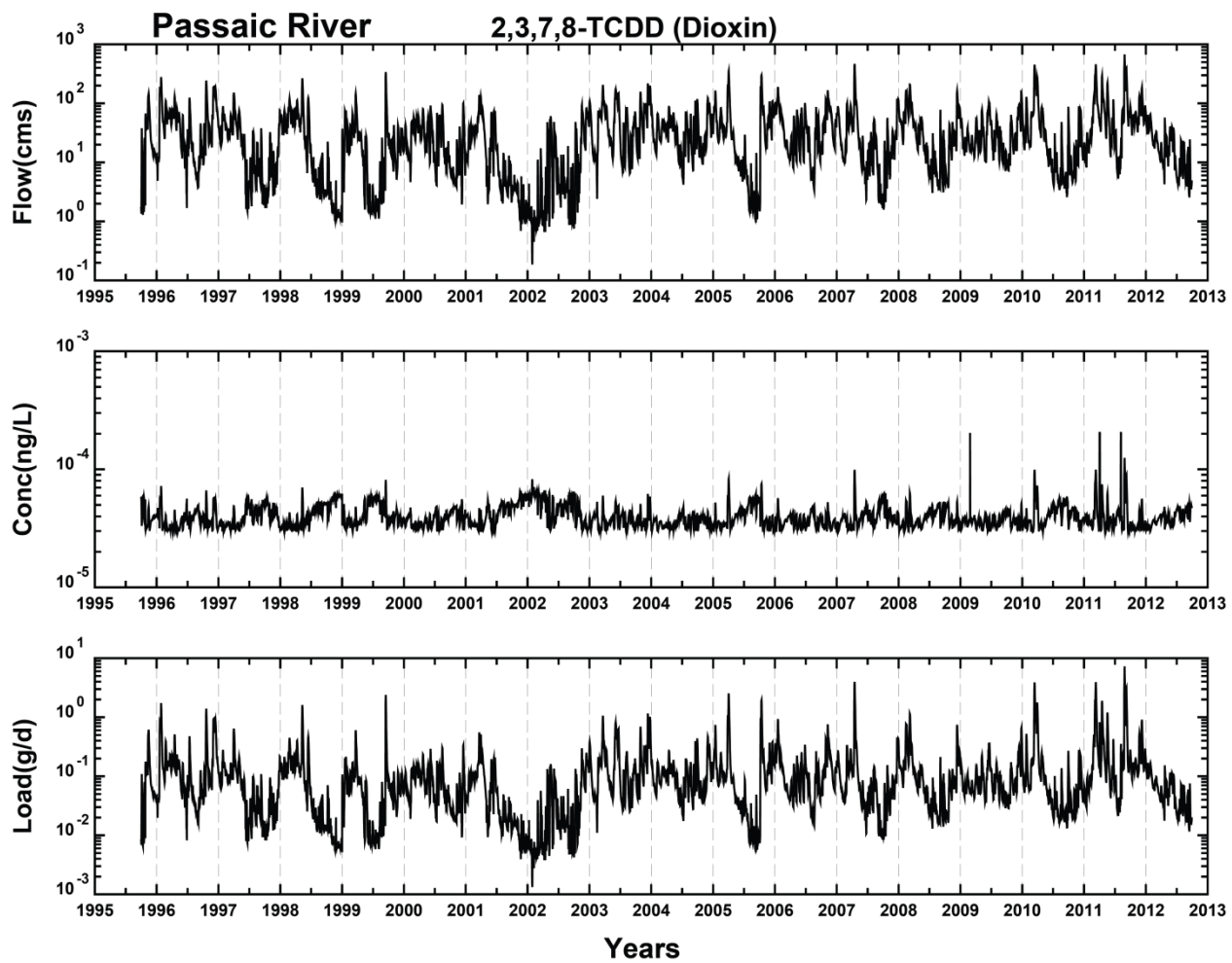


Sediment FOC Cycled Initial Condition in the LPR and Interpolated
Initial Conditions in Newark Bay

Lower Eight Miles of the Lower Passaic River

Figure 3-6

2014

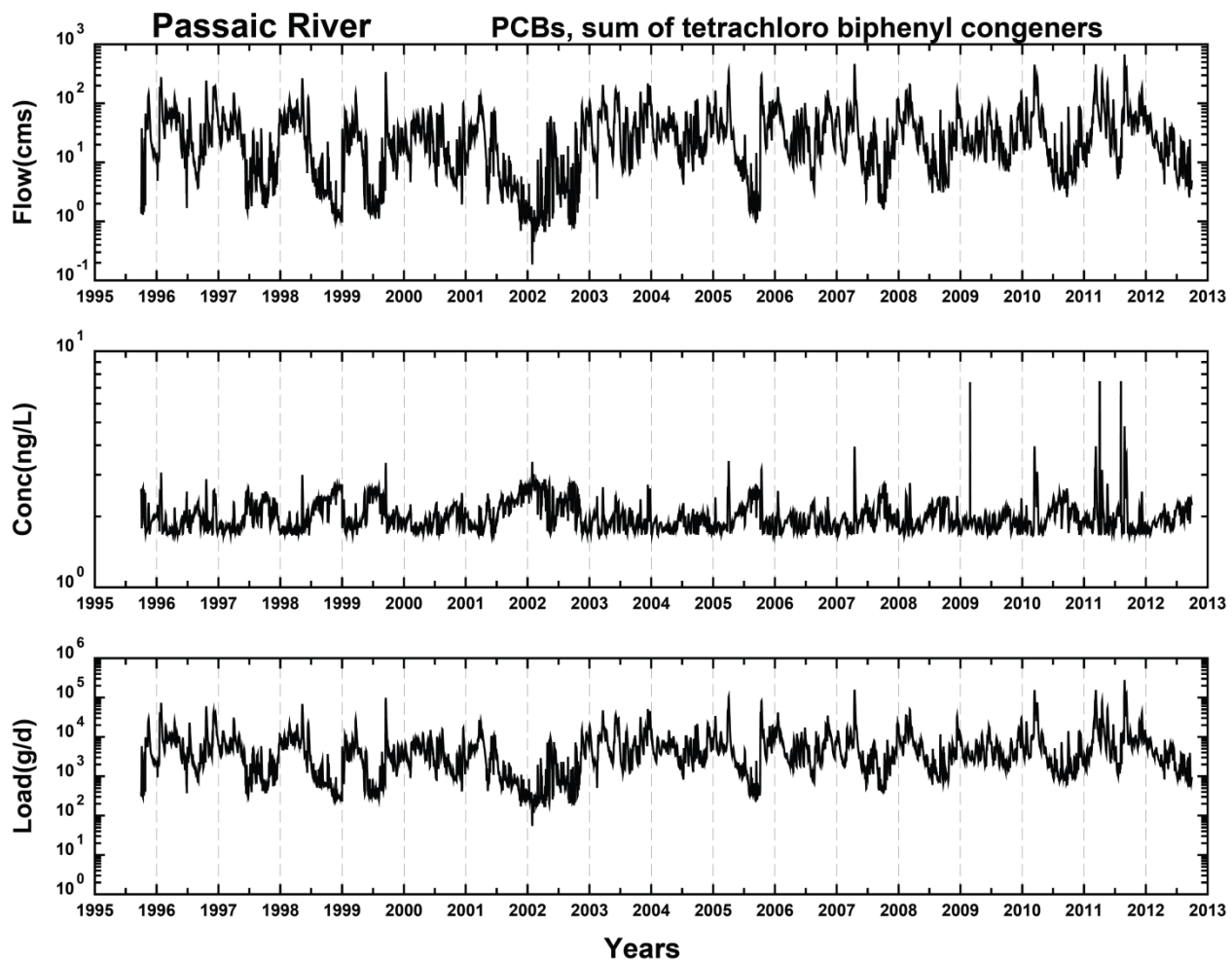


Upper Passaic River Boundary 2,3,7,8-TCDD

Lower Eight Miles of the Lower Passaic River

Figure 3-7

2014

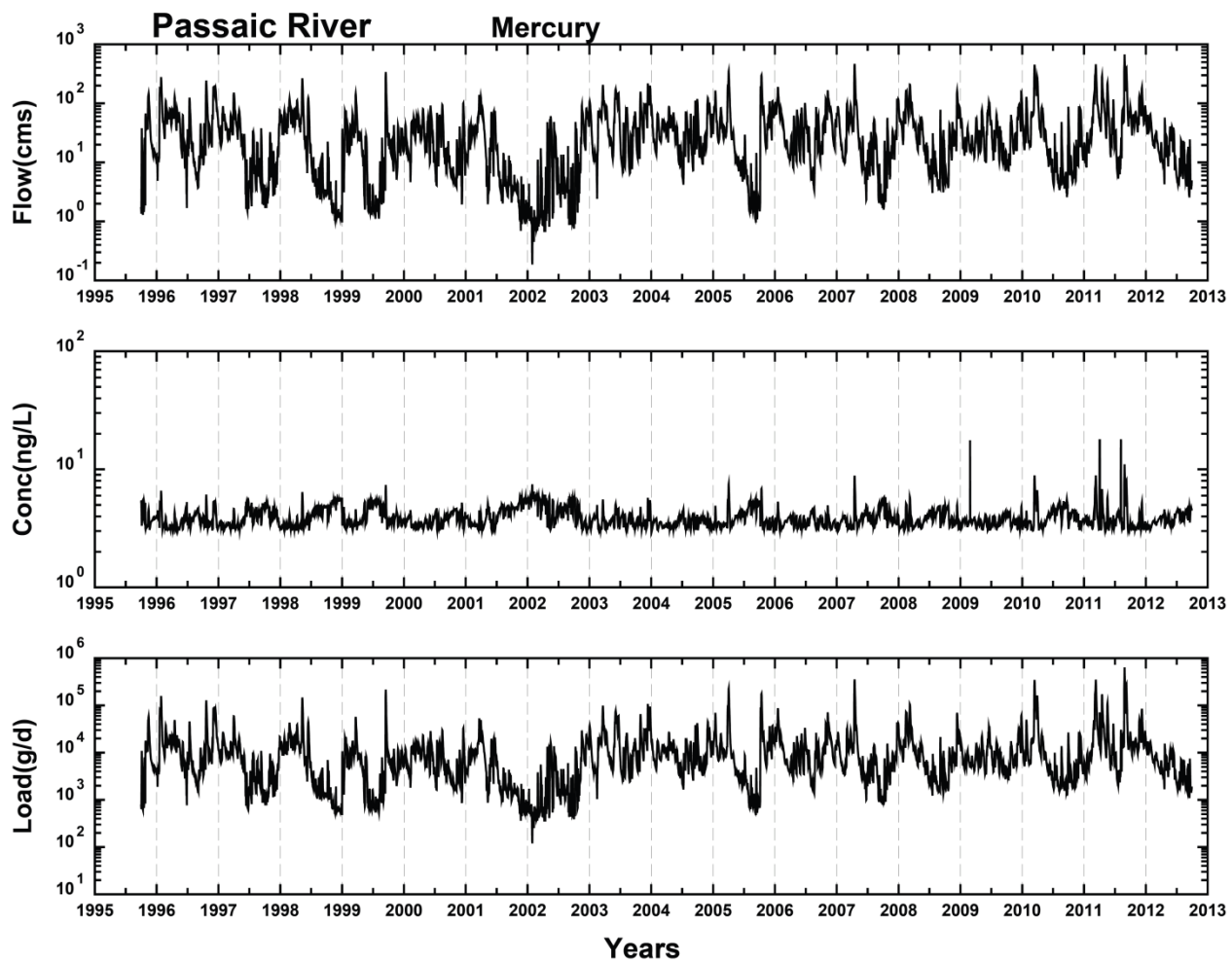


Upper Passaic River Boundary Sum of Tetrachlorobiphenyl PCBs

Lower Eight Miles of the Lower Passaic River

Figure 3-8

2014

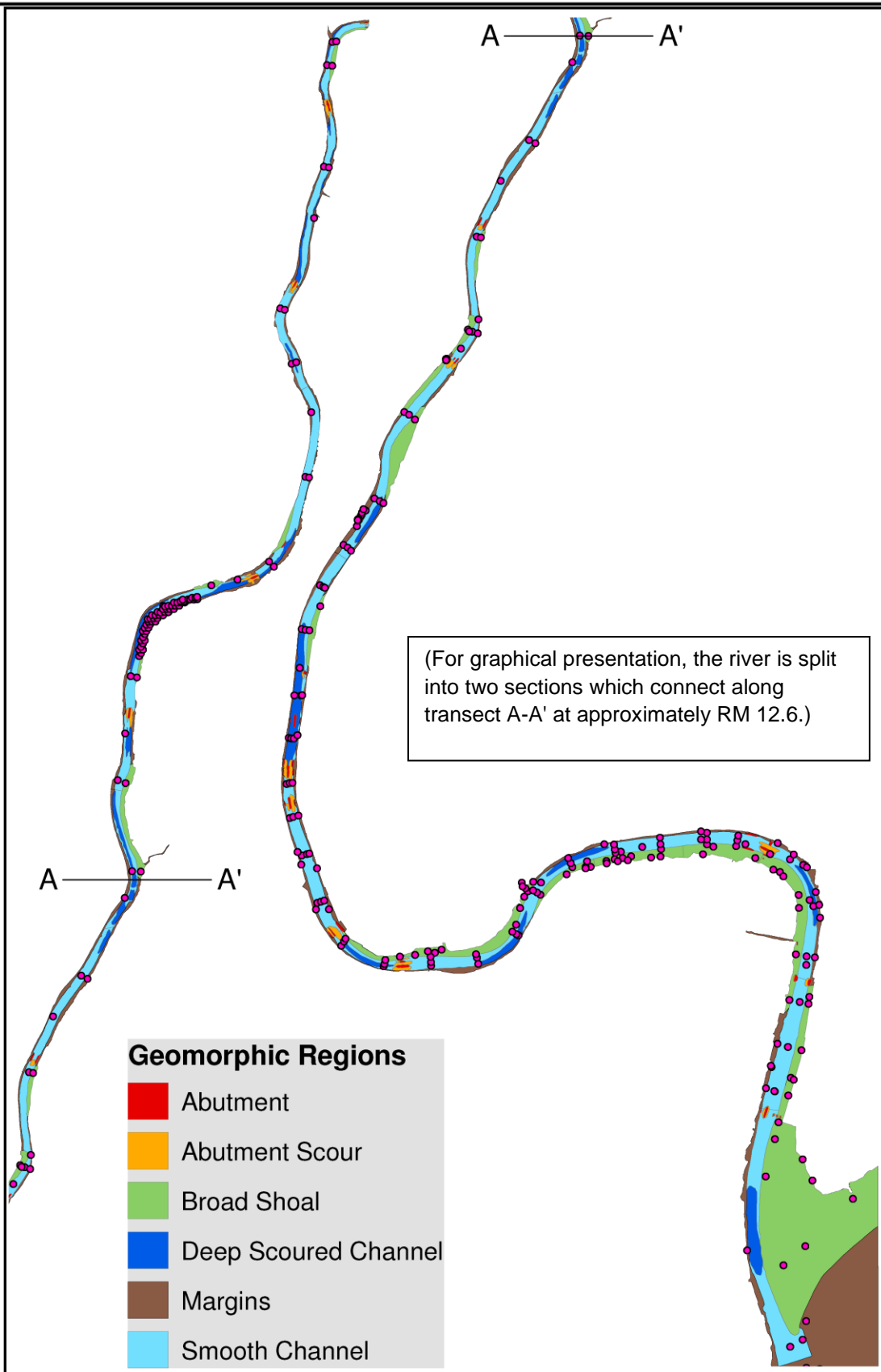


Upper Passaic River Boundary Total Mercury

Lower Eight Miles of the Lower Passaic River

Figure 3-9

2014

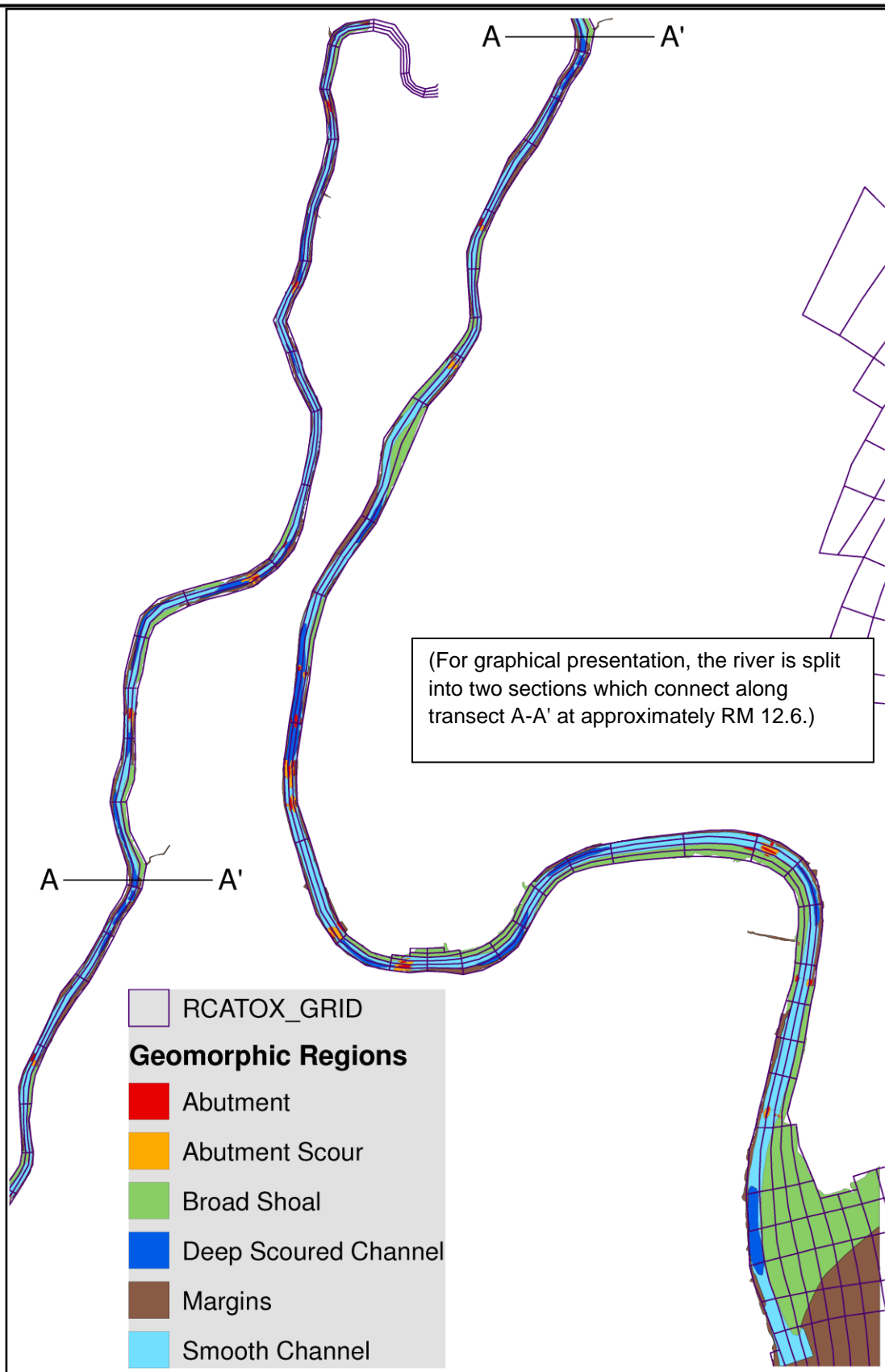


Map of the LPR Showing Sediment Sampling Points and Shaded Geomorphic Regions.

Lower Eight Miles of the Lower Passaic River

Figure 3-10

2014



Map of the LPR Showing the Model Grid and Shaded Geomorphic Regions.

Lower Eight Miles of the Lower Passaic River

Figure 3-11

2014

Layer1 2378TCDD including RM10.9 Data



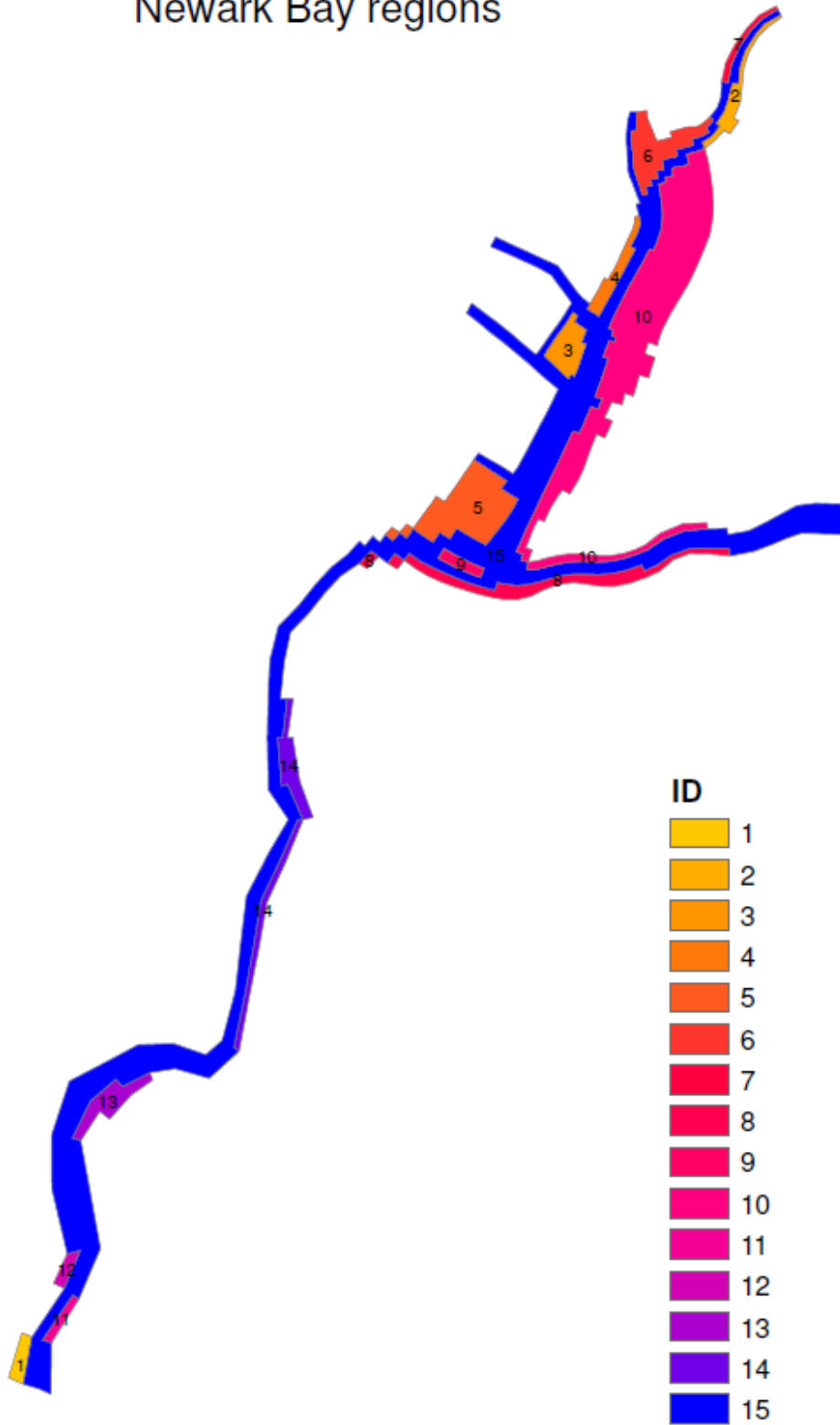
Map of 2,3,7,8-TCDD Initial Conditions for the Top Six Inches of the LPR

Lower Eight Miles of the Lower Passaic River

Figure 3-12

2014

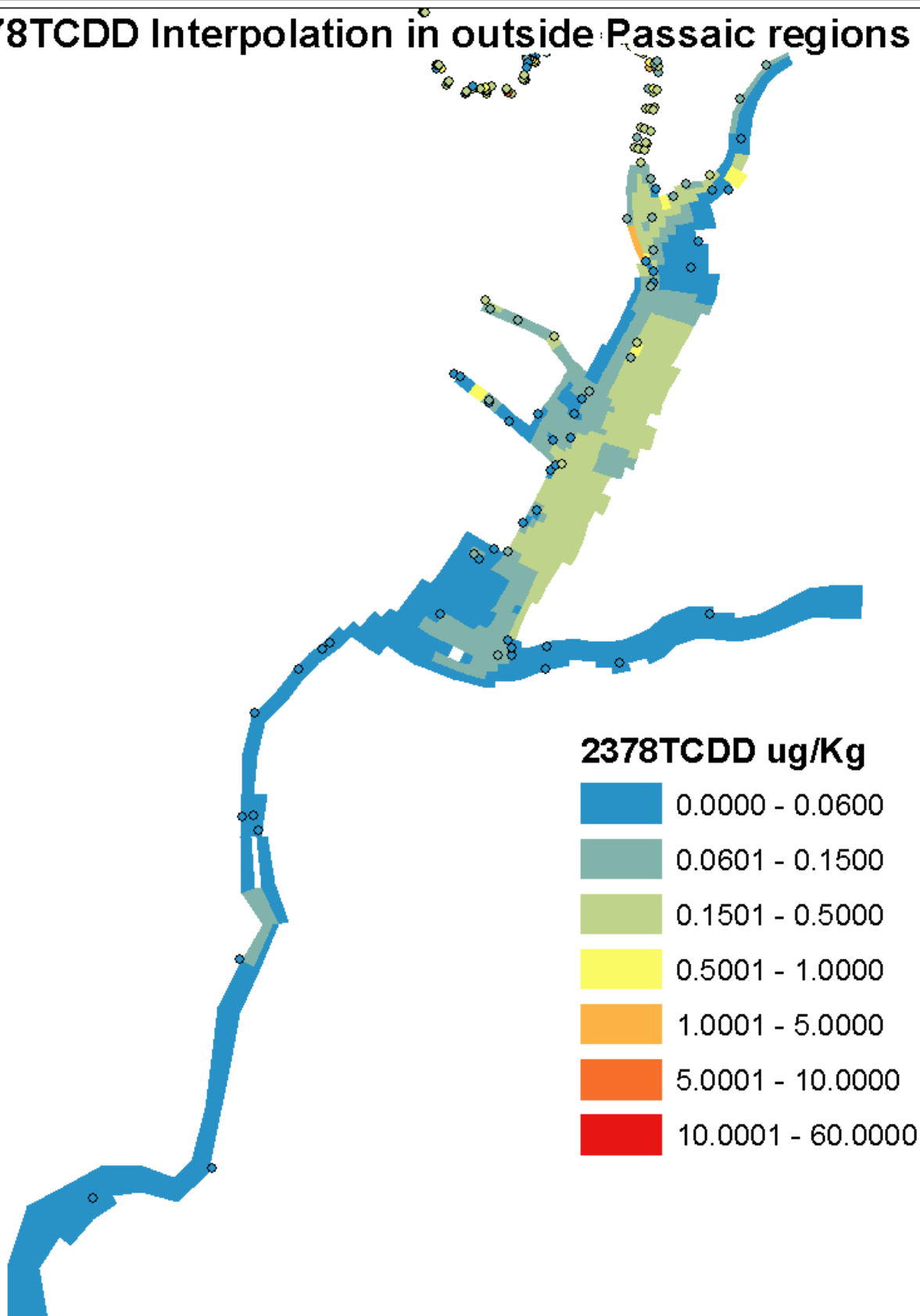
Newark Bay regions



Map of Newark Bay, Arthur Kill and Kill Van Kull Regions

Figure 3-13

2378TCDD Interpolation in outside Passaic regions



Map of 2,3,7,8-TCDD Initial Conditions for the Top Six Inches of the Newark Bay, the Arthur Kill and the Kill Van Kull.

Lower Eight Miles of the Lower Passaic River

Figure 3-14

2014

Layer1 2378TCDD including RM10.9 Data



Map of 2,3,7,8-TCDD Initial Conditions for the Top Six Inches Throughout the Model Domain.

Lower Eight Miles of the Lower Passaic River

Figure 3-15

2014

Sediment Datasets

- Data used for ICs
- A 1990 Surficial Sediment Investigation
- B EPA EMAP 90-92
- C 1991 Core Sediment Investigation
- D NOAA NS&T Hudson-Raritan Phase I, 1991
- E 1992 Core Sediment Investigation
- F 1993 Core Sediment Investigation - 01 (March)
- G 1993 Core Sediment Investigation - 02 (July)
- H 1993 USEPA Surficial Sediment Program
- I NOAA NS&T Hudson-Raritan Phase II, 1993
- J REMAP, 1993
- K 1994 Surficial Sediment Investigation
- L REMAP, 1994
- M 1995 RI Sampling Program
- N 1995 Sediment Grab Sampling Program
- O 1995 USACE Minish Park Investigation
- P 1996 Newark Bay Reach A Sediment Sampling Program
- Q 1997 Newark Bay Reach B,C,D Sampling Program
- S 1998 Newark Bay Elizabeth Channel Sampling Program
- T REMAP, 1998
- U 1999 Late Summer/Early Fall ESP Sampling Program
- X 1999 Prelim Toxicity Identification Eval
- Y 1999/2000 Minish Park Monitoring Program
- a 2000 Spring ESP Sampling Program
- b 2000 Toxicity Identification Evaluation
- c 2005 MPI - Newark Bay Phase I Oversight
- ▲ 2005 Newark Bay RIWP Phase I Sediment Investigation
- d 2005 USEPA-MPI High Res Sediment Core
- e 2006 HRSA RI Sampling Program
- g 1999-2006 Honeywell Intl Sampling
- i 2007 USEPA-MPI-EMBM Sediment Samples
- j 2007 USEPA-MPI Dundee High Res Core
- k 2007 Newark Bay Phase II TSI Sediment Samples
- 2008 CPG Low Resolution Sediment Coring
- m 2009 CPG Benthic Sediment Study
- o 2009 USEPA-MPI Benthic Oversight
- p 2010 CPG Benthic Sediment Sampling
- q 2010 USEPA-CDM Benthic Oversight
- 2011 CPG River Mile 10.9 Data
- r 2012 CDM Smith Background Benthic Sediment
- s 2012 CDM Smith Low Res Coring Supplemental
- t 2012 CPG Background Benthic Sediment
- ▼ 2012 CPG Low Res Coring Supplemental
- u 2012 CPG River Mile 10.9 Data

Water Column Datasets

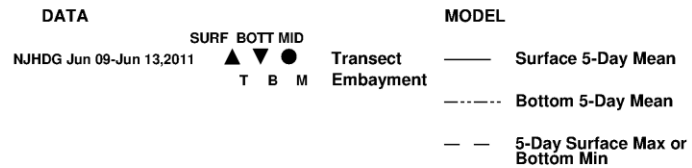
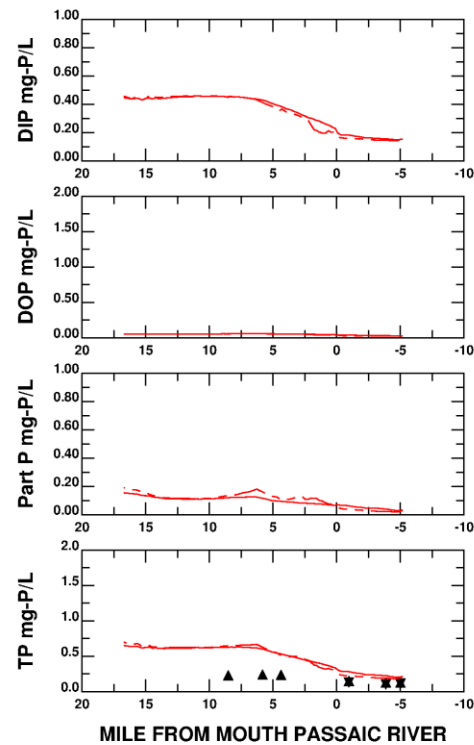
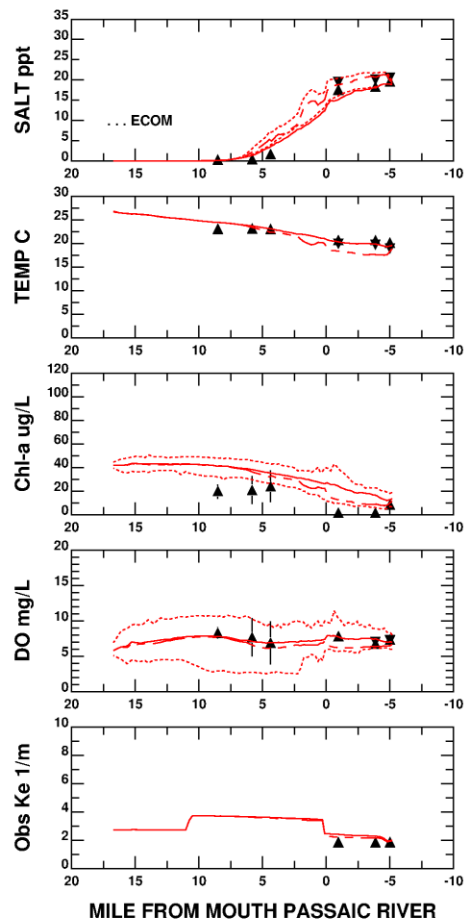
- ▲ 1993-1997 USACE - DMDAT
- B 1995-96 Passaic Study RI/FS Sed Mobility
- C 1997 Outfall Sampling Program
- D 1998-2001 CARP Database
- E 1999 Newark Bay Reach A Monitoring
- F 1999 Newark Bay Reach ABCD Baseline Sampling
- G 1999 USACE Drift Removal Monitoring
- H 1999-2006 Honeywell Intl Sampling
- I 2000 Toxicity Identification Evaluation
- J 2005 Hydrodynamic Mooring
- K 2005 MPI SPMD Deployment
- L 2005 USEPA-MPI High Flow Water Column
- M 2005 USEPA-MPI Large Volume Study
- N 2005 USEPA-MPI Small Volume Water Column
- O 2005 USEPA-MPI Water Column Above RM 8.5
- P 2007 USEPA-MPI-EMBM Water Column Sample
- Q 2009 CPG LPR Water Column Monitoring DEC
- R 2010 CPG LPR-NB PWCM Field Measurements
- S 2010 CPG LPR-NB PWCM Sample Dataset
- T 2010 USEPA LBG-CDM PWCM Oversight
- U 2011 CDM Smith CWCM Sampling Data
- V 2011 CPG CWCM Sampling Data
- W 2012 CDM Smith CWCM Sampling - Round 2
- X 2012 CDM Smith CWCM Sampling - Round 3
- Y 2012 CDM Smith CWCM Sampling - Round 4
- Z 2012 CDM Smith CWCM Sampling - Round 5
- a 2012 CDM Smith CWCM Sampling Round - 6
- b 2012 CPG CWCM Sampling - Low Flow
- c 2012 CPG CWCM Sampling - Round 2
- d 2012 CPG CWCM Sampling - Round 3
- e 2012 CPG CWCM Sampling - Round 4

Legend for Sediment and Water Column Datasets Compared to Model Results

Figure 4-1

Lower Eight Miles of the Lower Passaic River

2014



PASSAIC RIVER AND NEWARK BAY
 RED=model:Collapsed Grid 1011

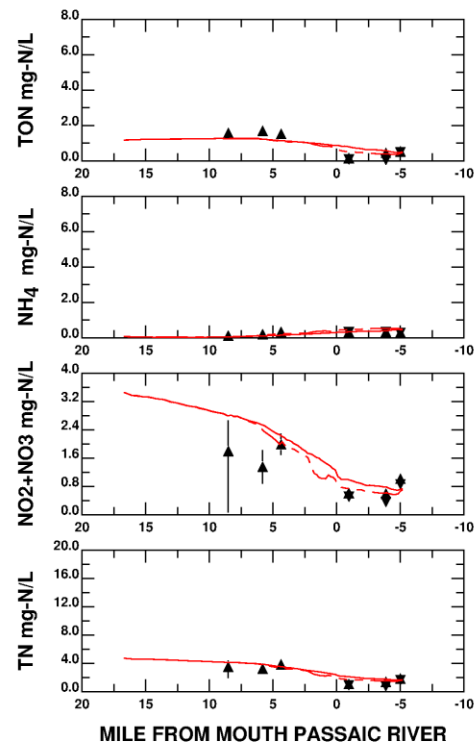
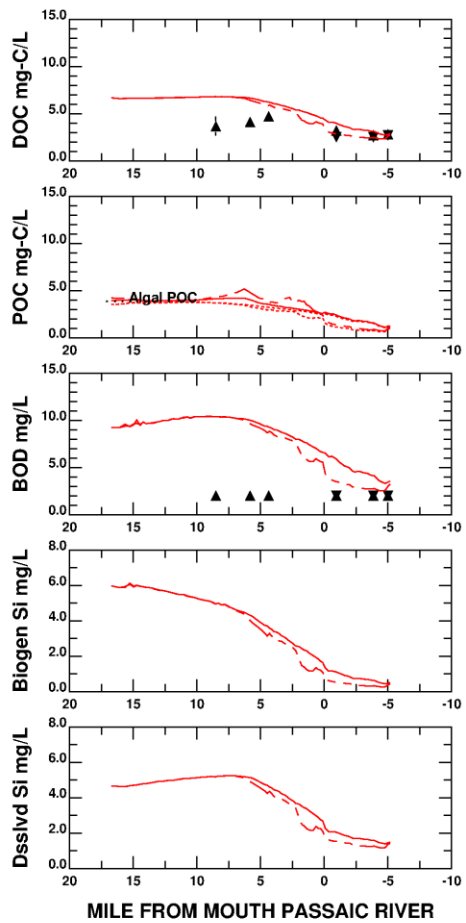
DATE: 1/28/2014 TIME: 14:46:57

Transect Comparison of Carbon Model Compared to NJHDG Data (June 2011, page 1)

Figure 4-2

Lower Eight Miles of the Lower Passaic River

2014



PASSAIC RIVER AND NEWARK BAY
 RED=model:Collapsed Grid 1011

DATE: 1/28/2014 TIME: 14:46:57

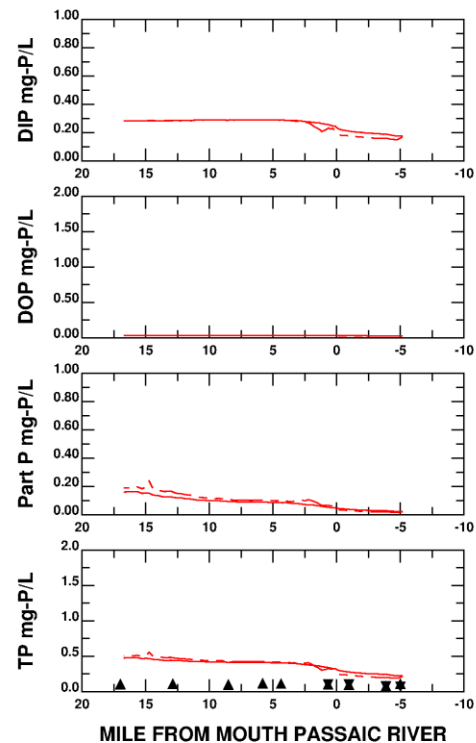
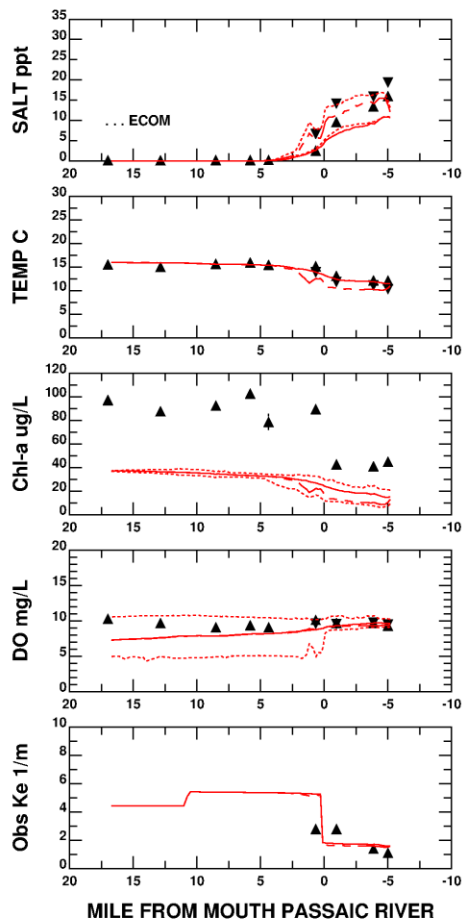
DATA	SURF	BOTT	MID		MODEL
NJHDG Jun 09-Jun 13,2011	▲	▼	●	Transect	— Surface 5-Day Mean
	T	B	M	Embayment	- - - Bottom 5-Day Mean
					- - - 5-Day Surface Max or Bottom Min

Transect Comparison of Carbon Model Compared to NJHDG Data (June 2011, page 2)

Figure 4-3

Lower Eight Miles of the Lower Passaic River

2014



DATA
 NJHDG May 02-May 03,2007 ▲ ▼ ● Transect
 T B M Embayment

MODEL
 ——— Surface 5-Day Mean
 - - - - Bottom 5-Day Mean
 - - - 5-Day Surface Max or Bottom Min

PASSAIC RIVER AND NEWARK BAY
 RED=model:Collapsed Grid 0607

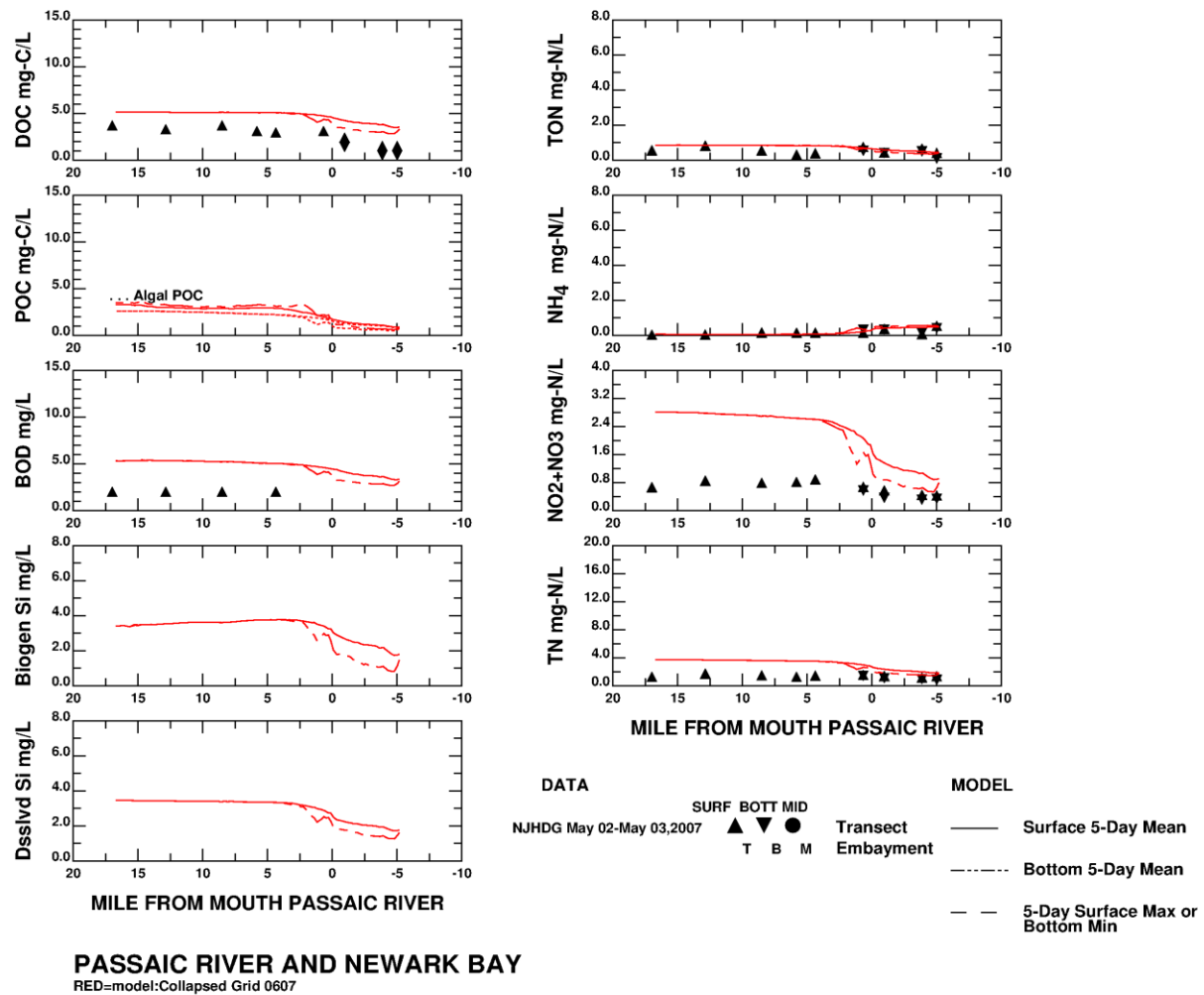
DATE: 1/28/2014 TIME: 14: 3:41

Transect Comparison of Carbon Model Compared to NJHDG Data (May 2007, page 1)

Figure 4-4

Lower Eight Miles of the Lower Passaic River

2014



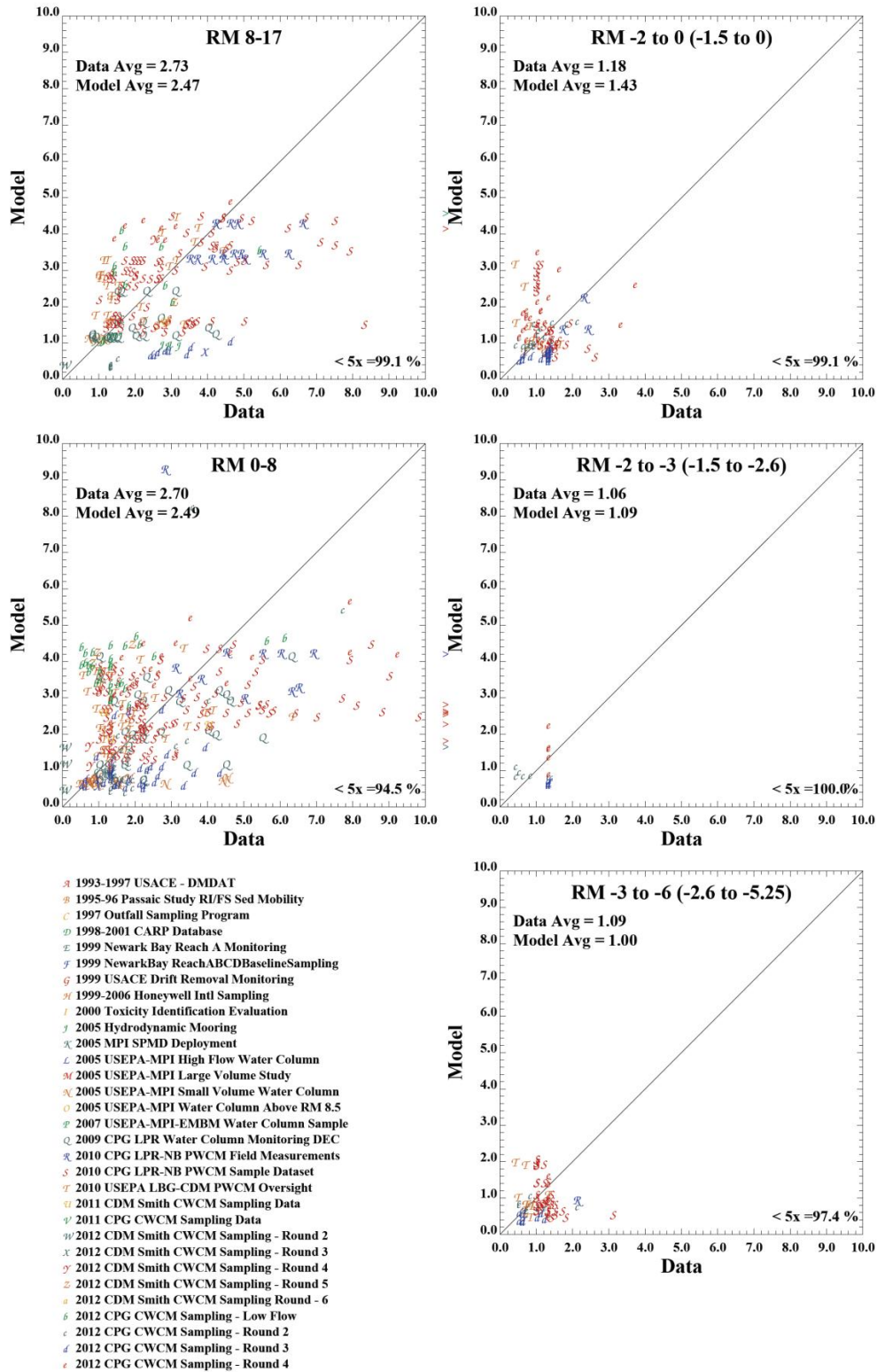
Transect Comparison of Carbon Model Compared to NJHDG Data (May 2007, page 2)

Figure 4-5

Lower Eight Miles of the Lower Passaic River

2014

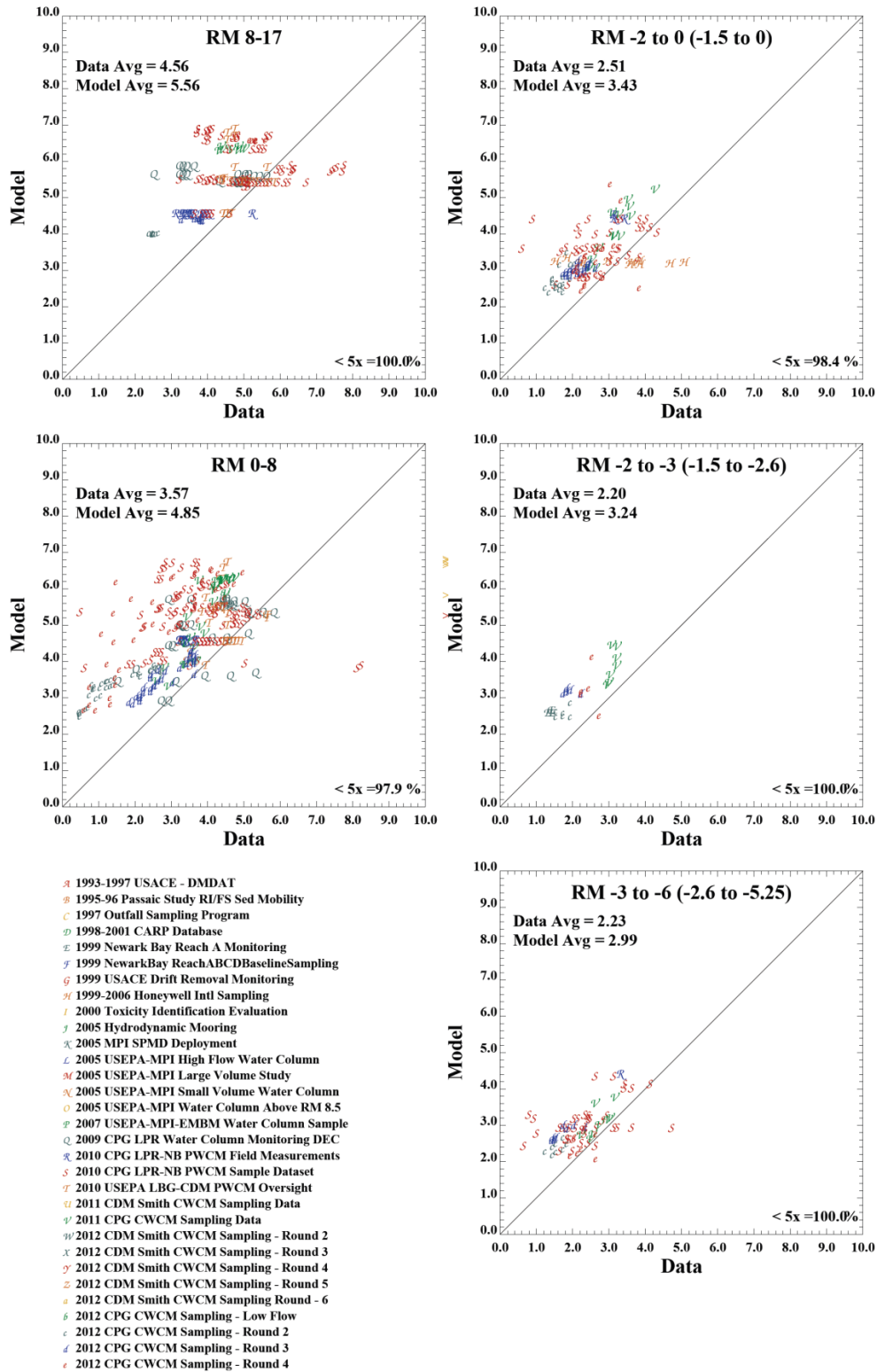
All Layers POC (mg/L)



Water Column POC X-Y Scatter Plot

Figure 4-6

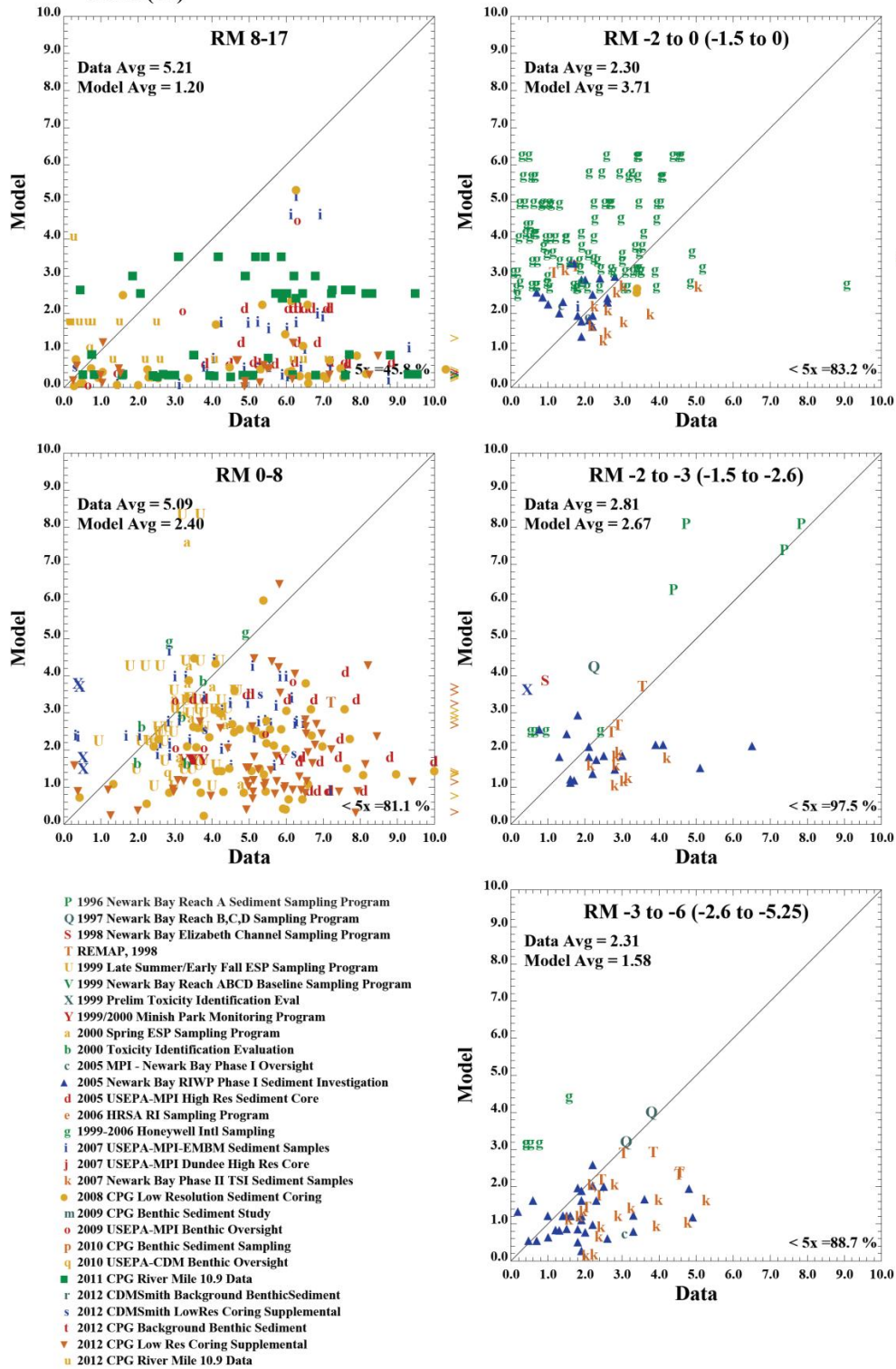
All Layers DOC (mg/L)



Water Column DOC X-Y Scatter Plot

Figure 4-7

**Top 15cm Average Conc.
FOC (%)**



Sediment FOC X-Y Scatter Plot

Figure 4-8

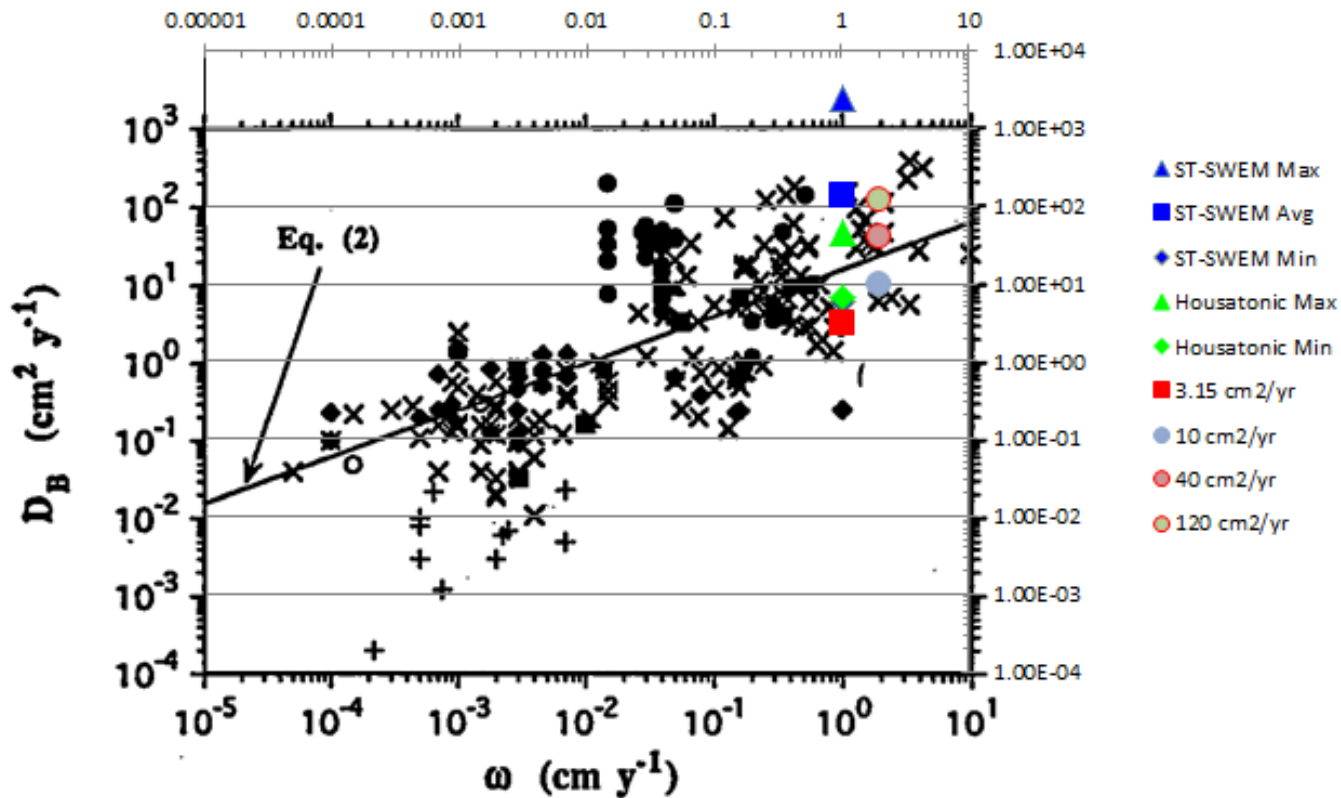


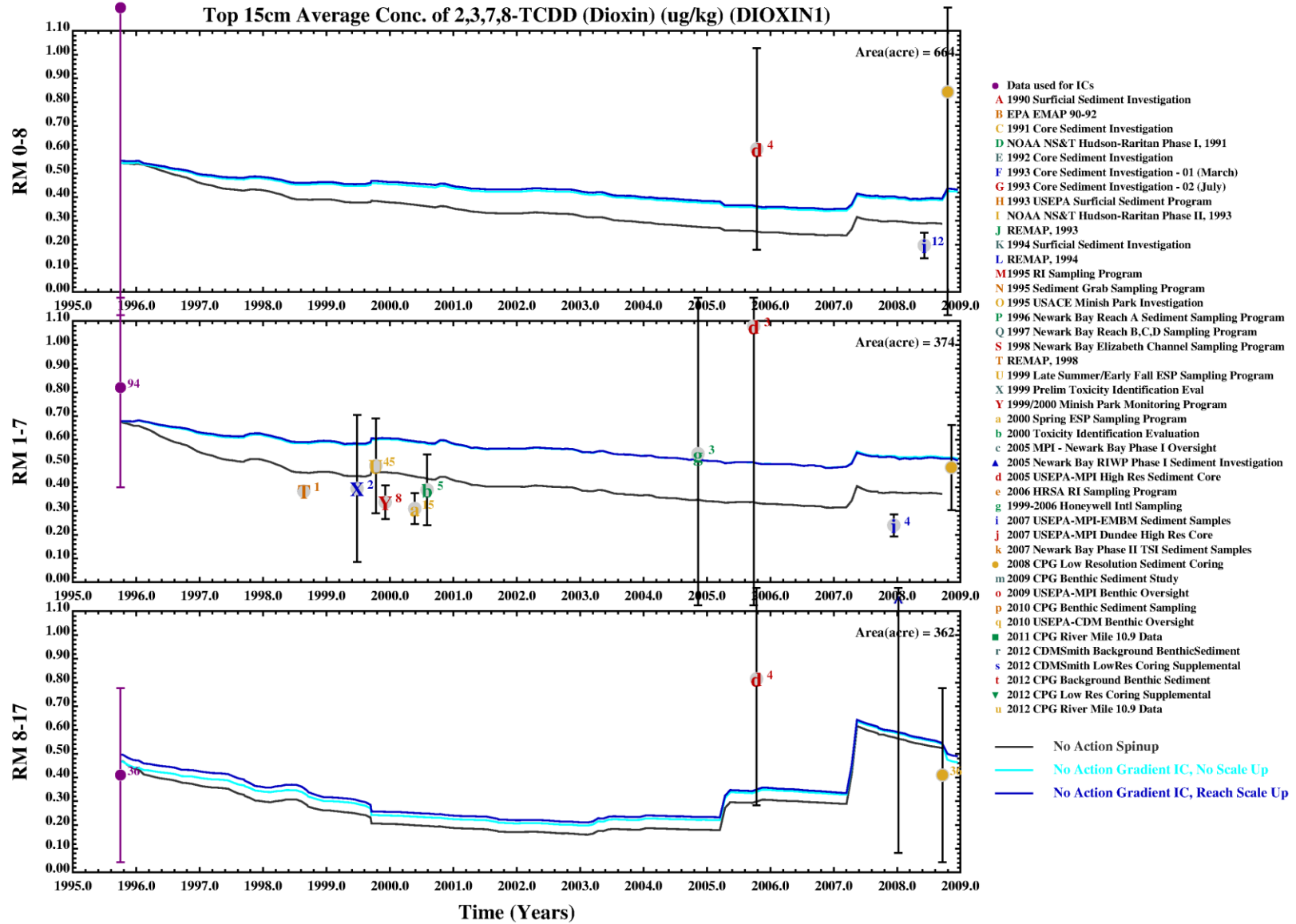
FIG. 1. Plot of mixing coefficient values, D_B , against corresponding burial velocities, ω , cited in the data sources listed in Table 1. The solid line is the best power-law fit given by Eqn. 2 of the text. The different symbols indicate the identity of the tracer used to calculate the corresponding D_B , i.e., \blacklozenge for ^{137}Cs and $^{239,240}\text{Pu}$, \circ for ^{32}Si , \bullet for ^{234}Th and ^{228}Th , \times for ^{210}Pb , $+$ for tektites and ash, \blacktriangle for ^7Be , and \blacksquare for miscellaneous tracers and techniques. (Note that ω in this figure is in units of cm y^{-1} , while it is in units of cm ky^{-1} in Table 1.)

Sediment Particle Mixing Rates From Other Studies (Adapted from Boudreau, 1994)

Figure 4-9

Lower Eight Miles of the Lower Passaic River

2014

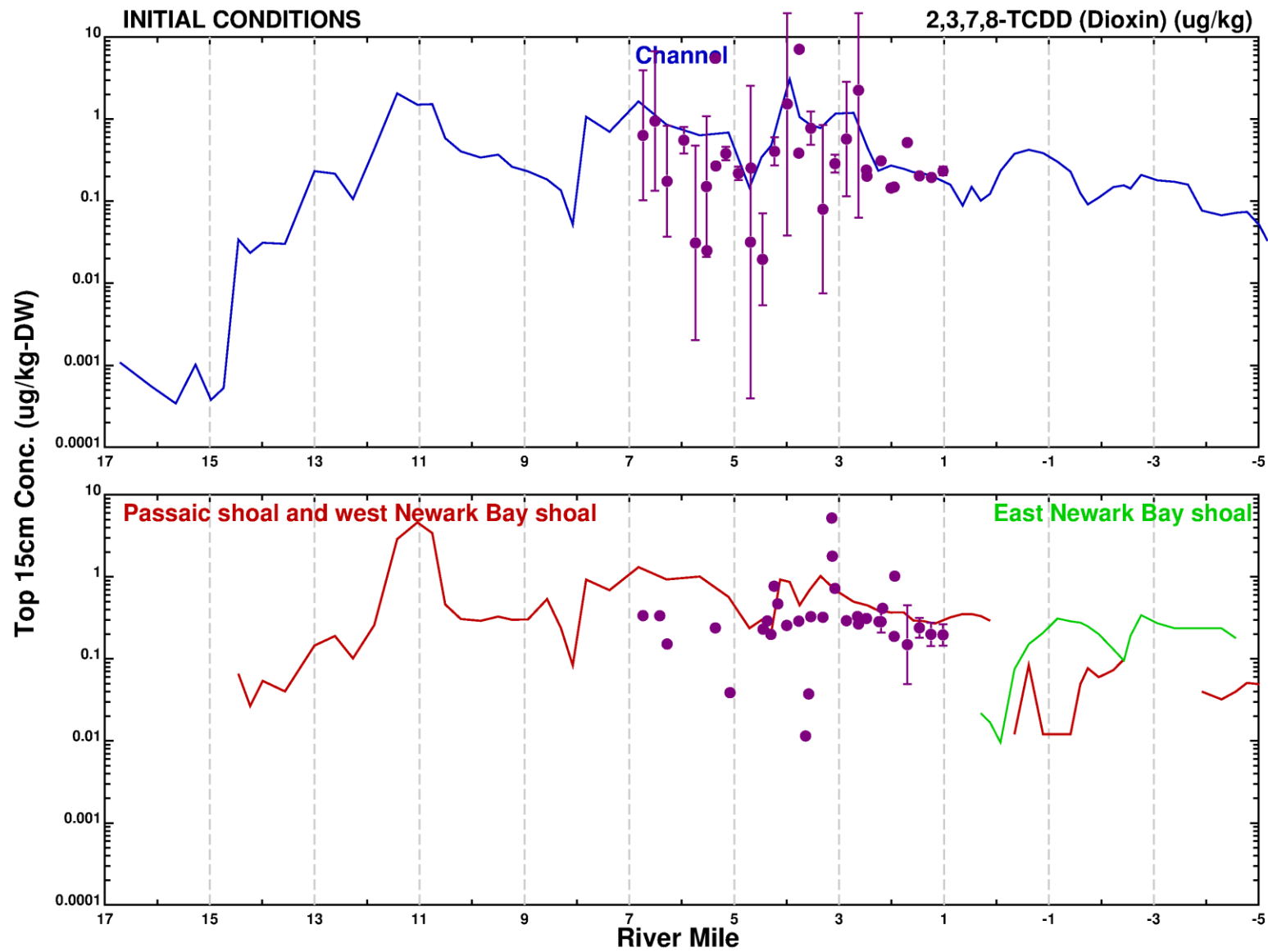


Initial Model Runs to Develop the Starting Point for the Calibration.

Lower Eight Miles of the Lower Passaic River

Figure 4-10

2014

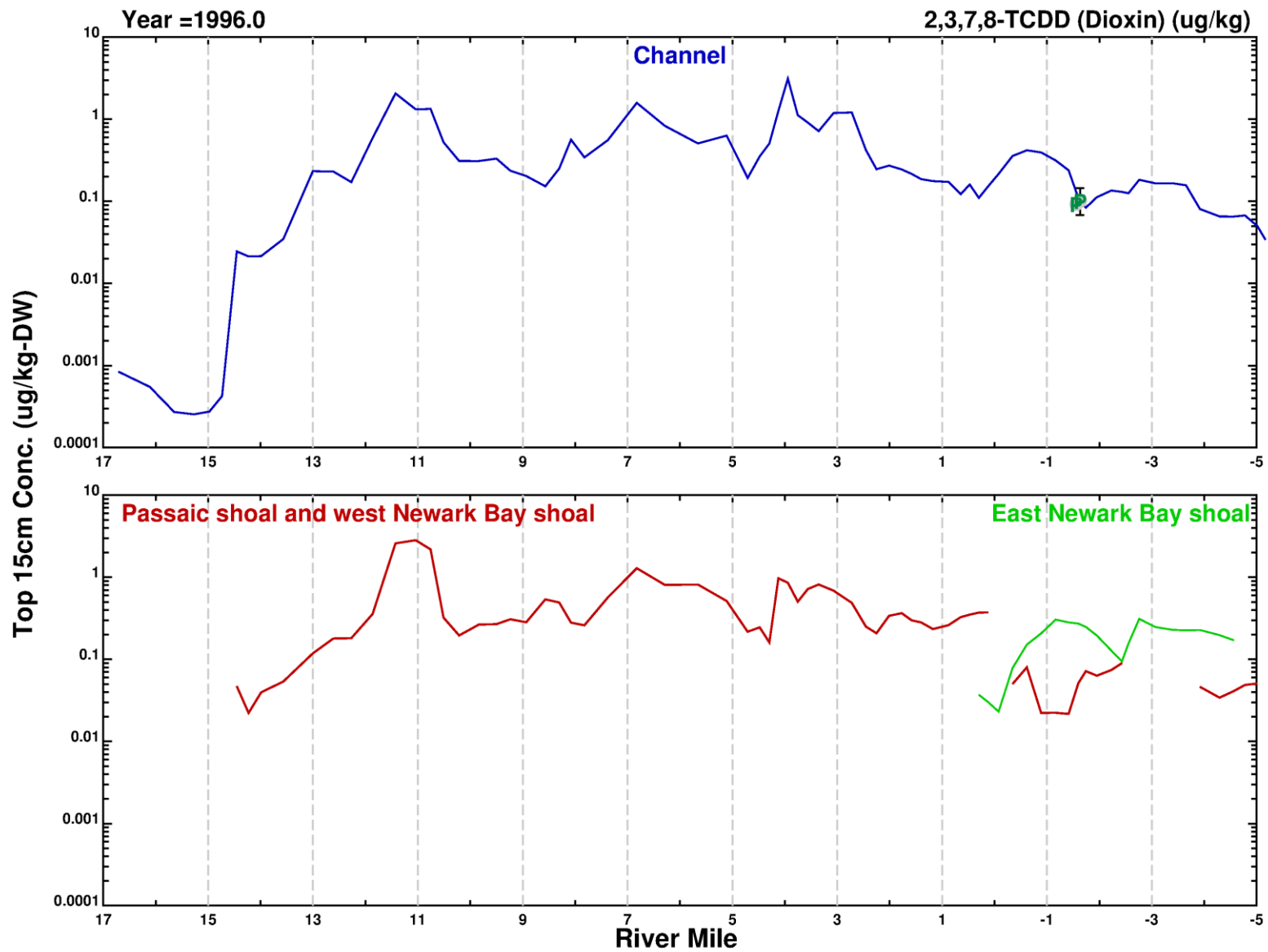


2,3,7,8-TCDD Surface Sediment Transect Plots (1995, Initial Conditions)

Figure 4-11

Lower Eight Miles of the Lower Passaic River

2014

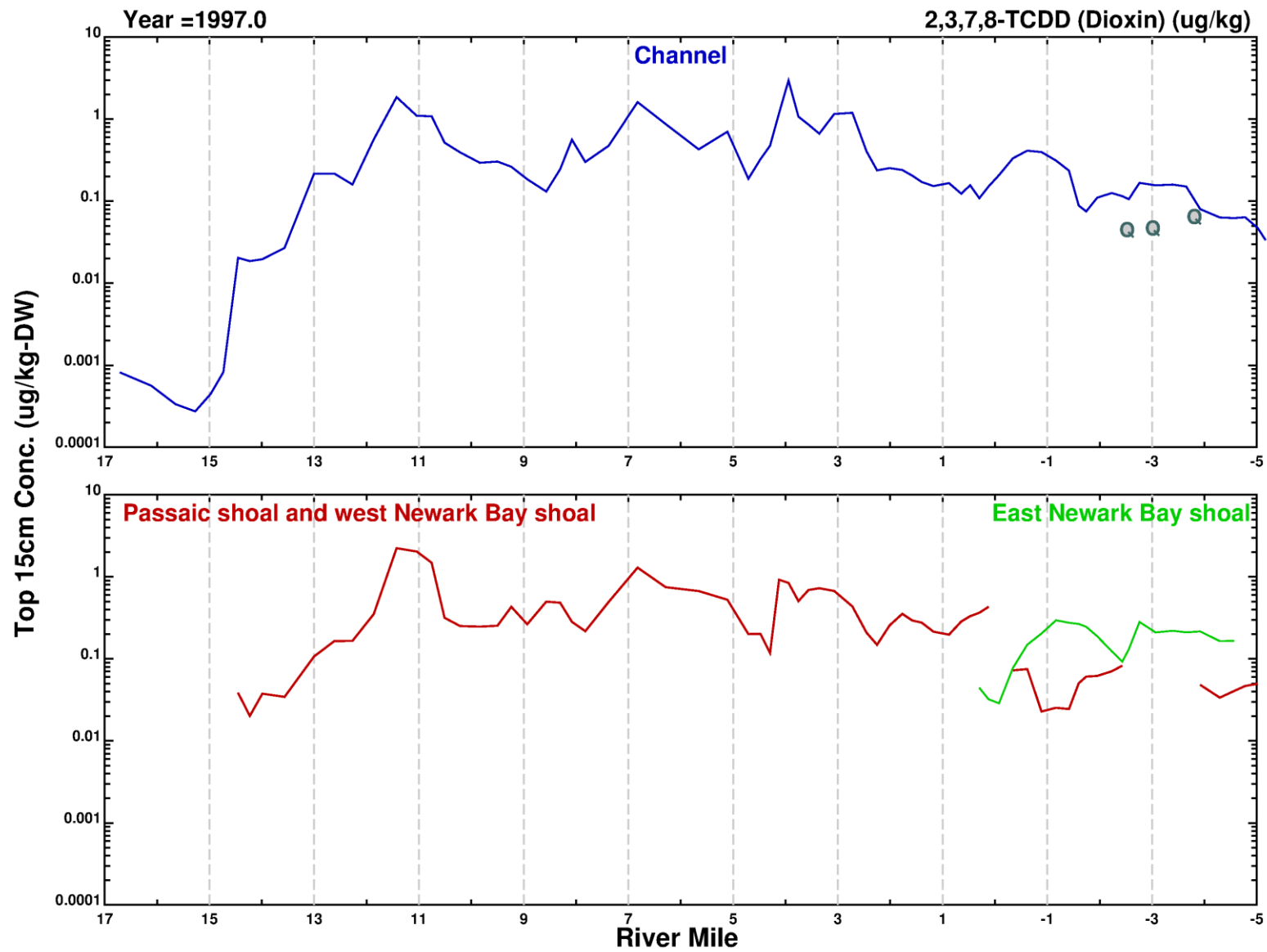


2,3,7,8-TCDD Surface Sediment Transect Plots (1996)

Lower Eight Miles of the Lower Passaic River

Figure 4-12

2014

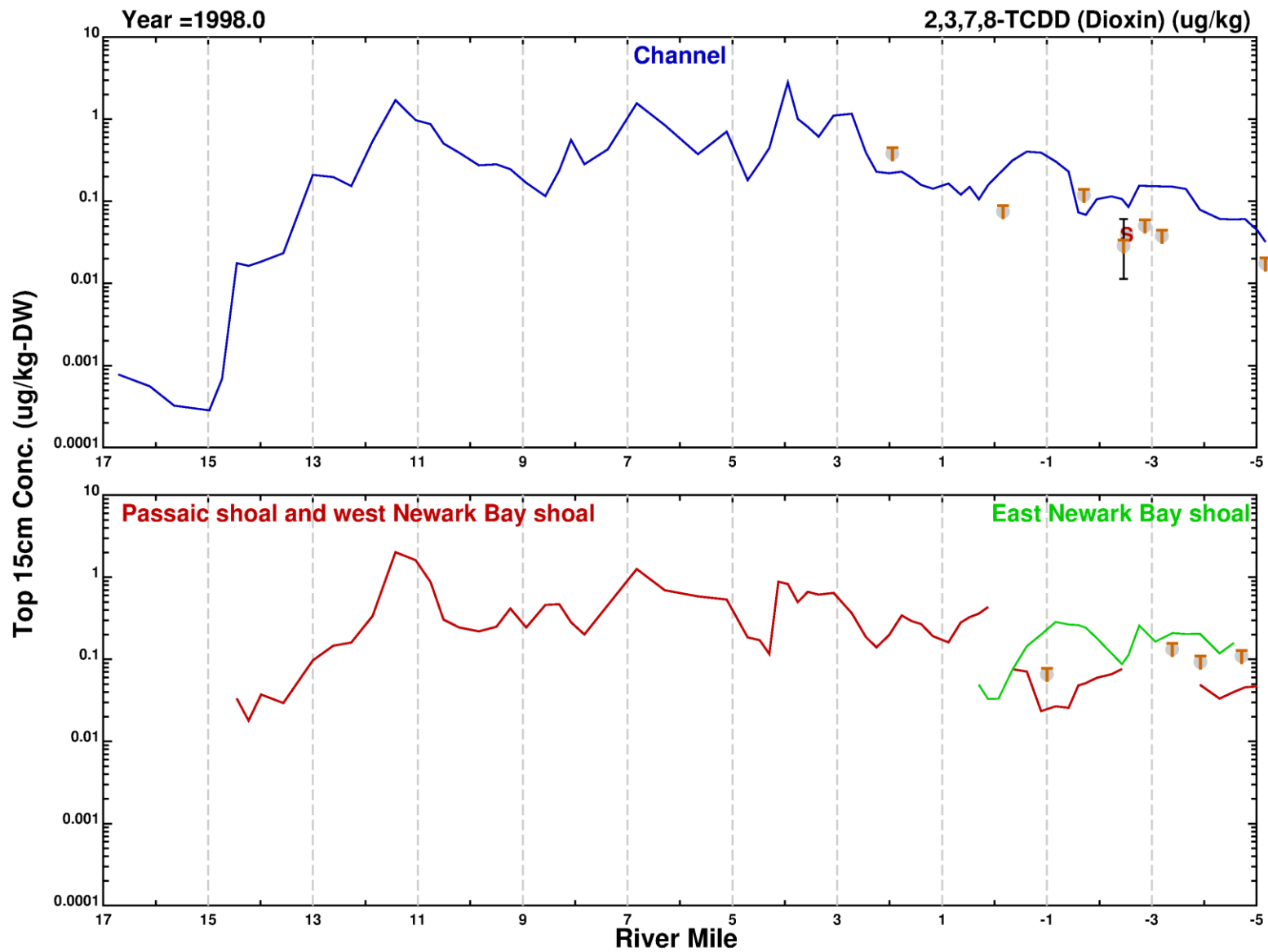


2,3,7,8-TCDD Surface Sediment Transect Plots (1997)

Lower Eight Miles of the Lower Passaic River

Figure 4-13

2014

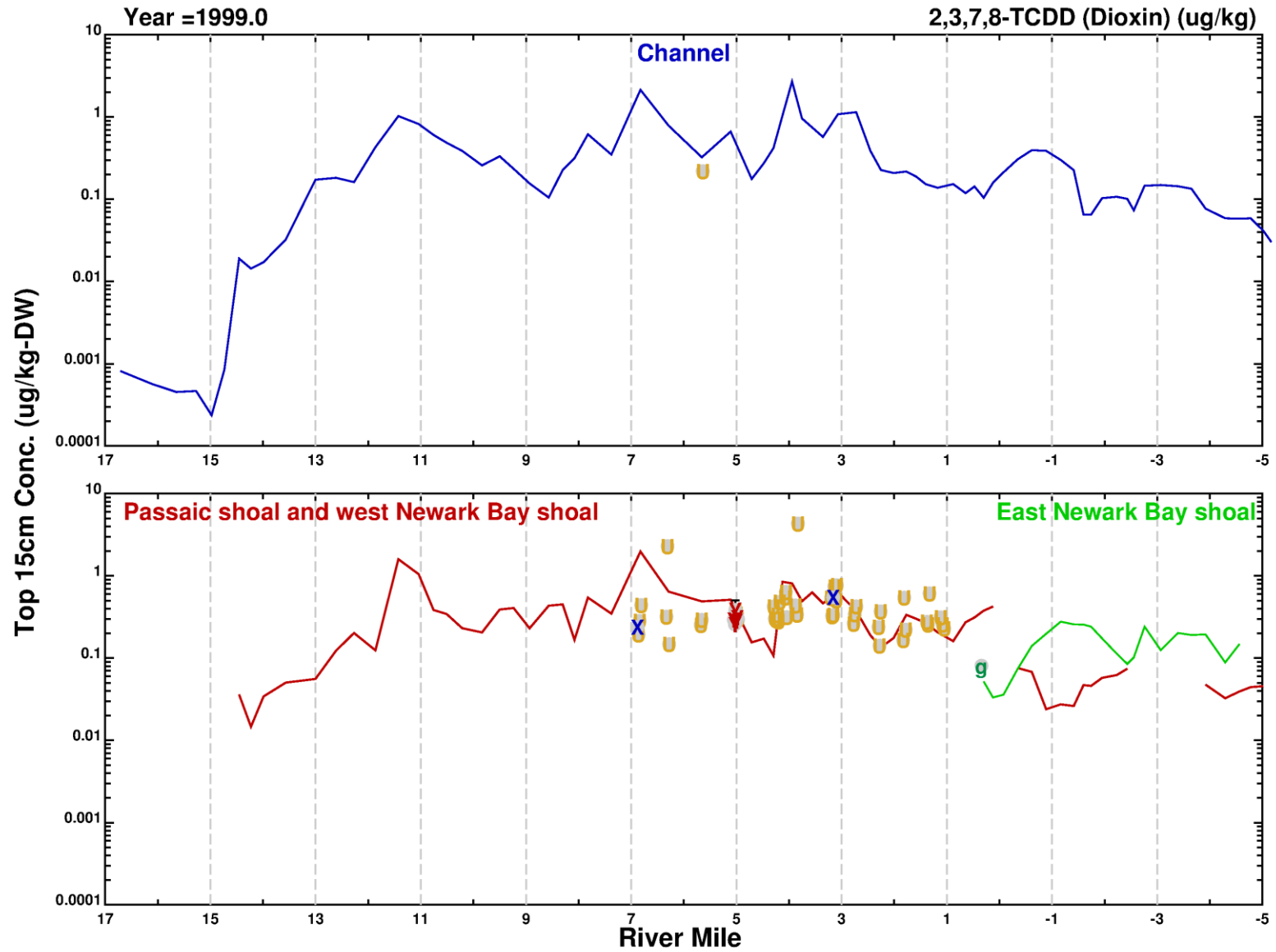


2,3,7,8-TCDD Surface Sediment Transect Plots (1998)

Lower Eight Miles of the Lower Passaic River

Figure 4-14

2014

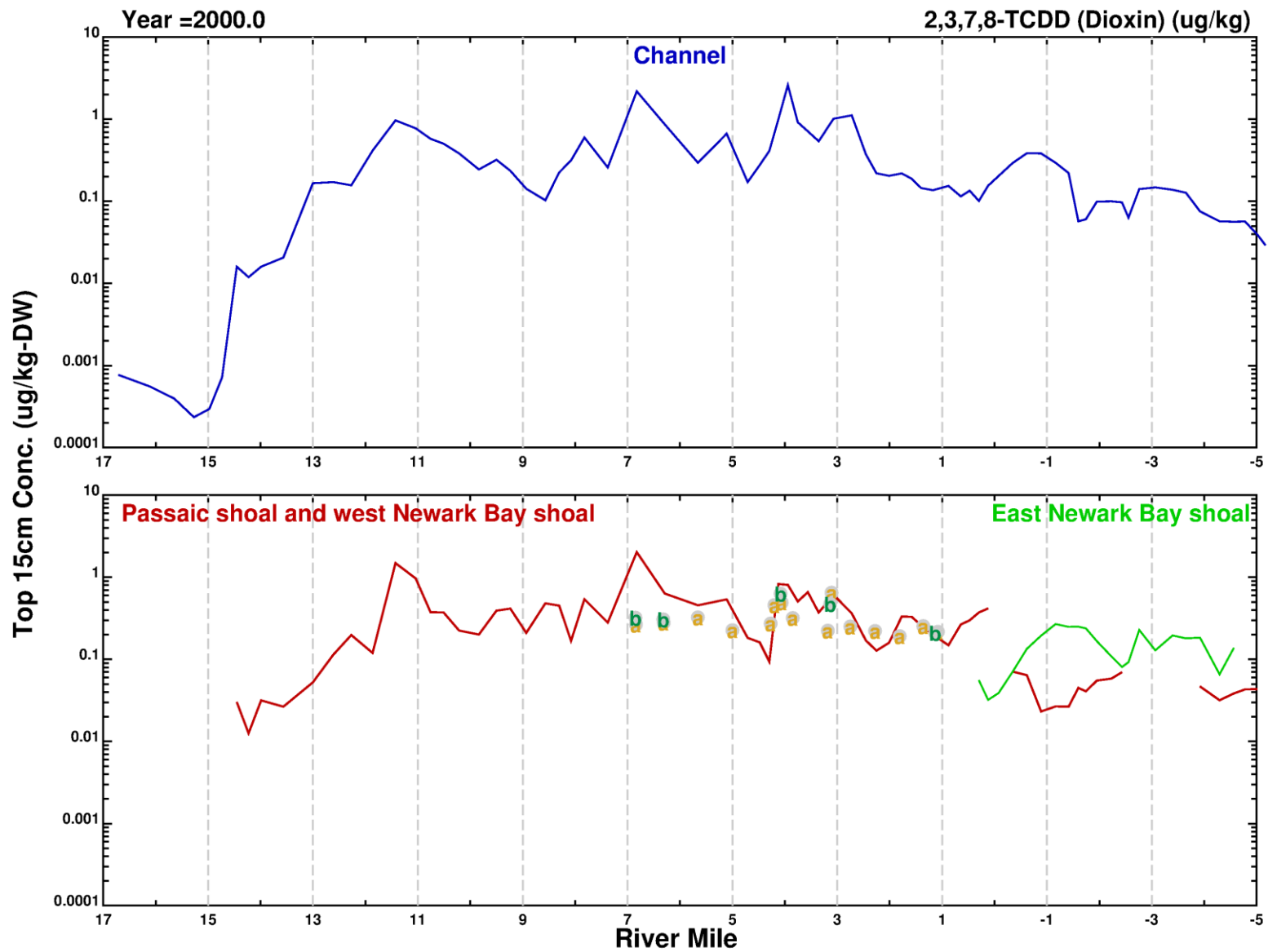


2,3,7,8-TCDD Surface Sediment Transect Plots (1999)

Lower Eight Miles of the Lower Passaic River

Figure 4-15

2014

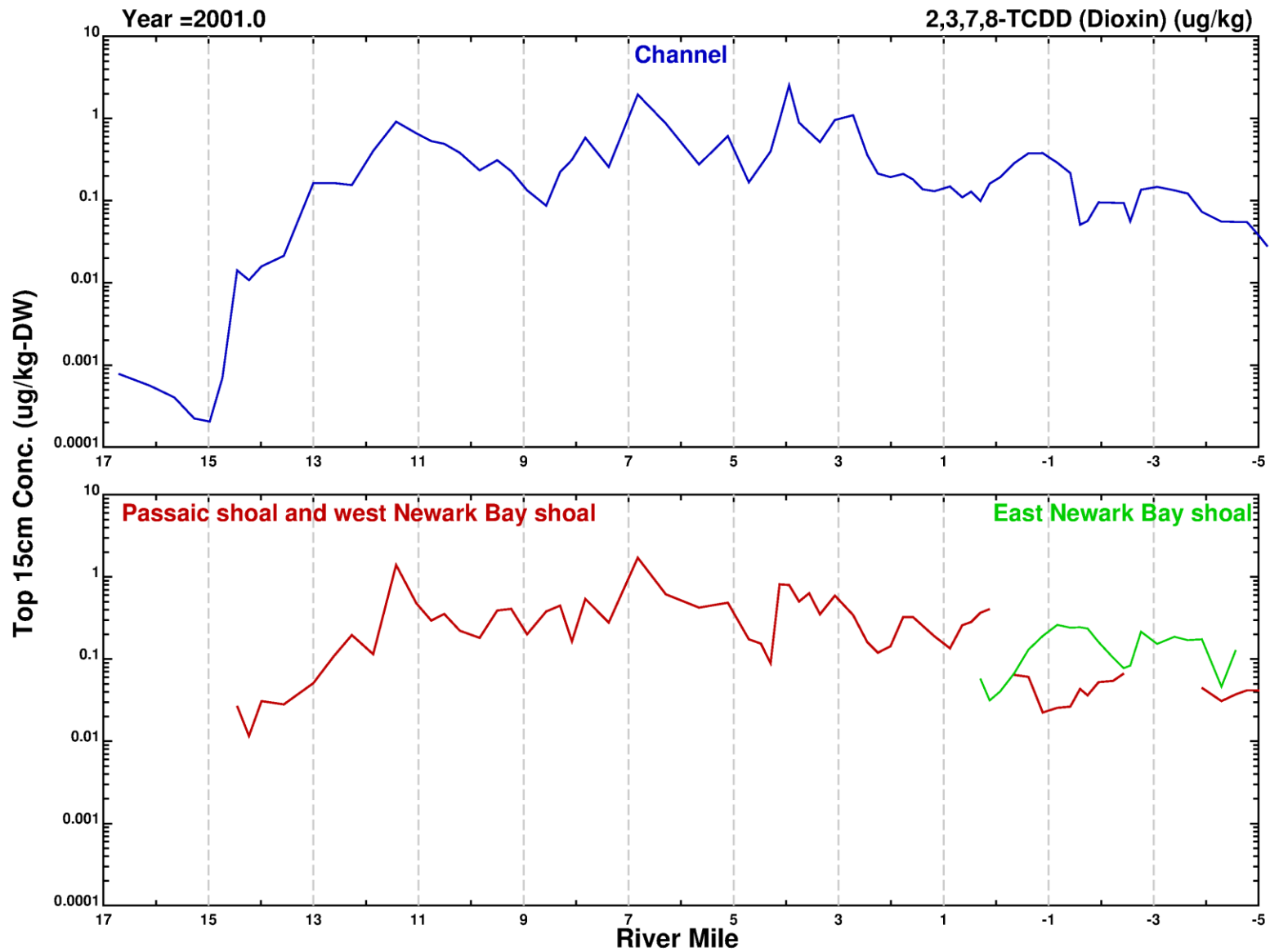


2,3,7,8-TCDD Surface Sediment Transect Plots (2000)

Lower Eight Miles of the Lower Passaic River

Figure 4-16

2014

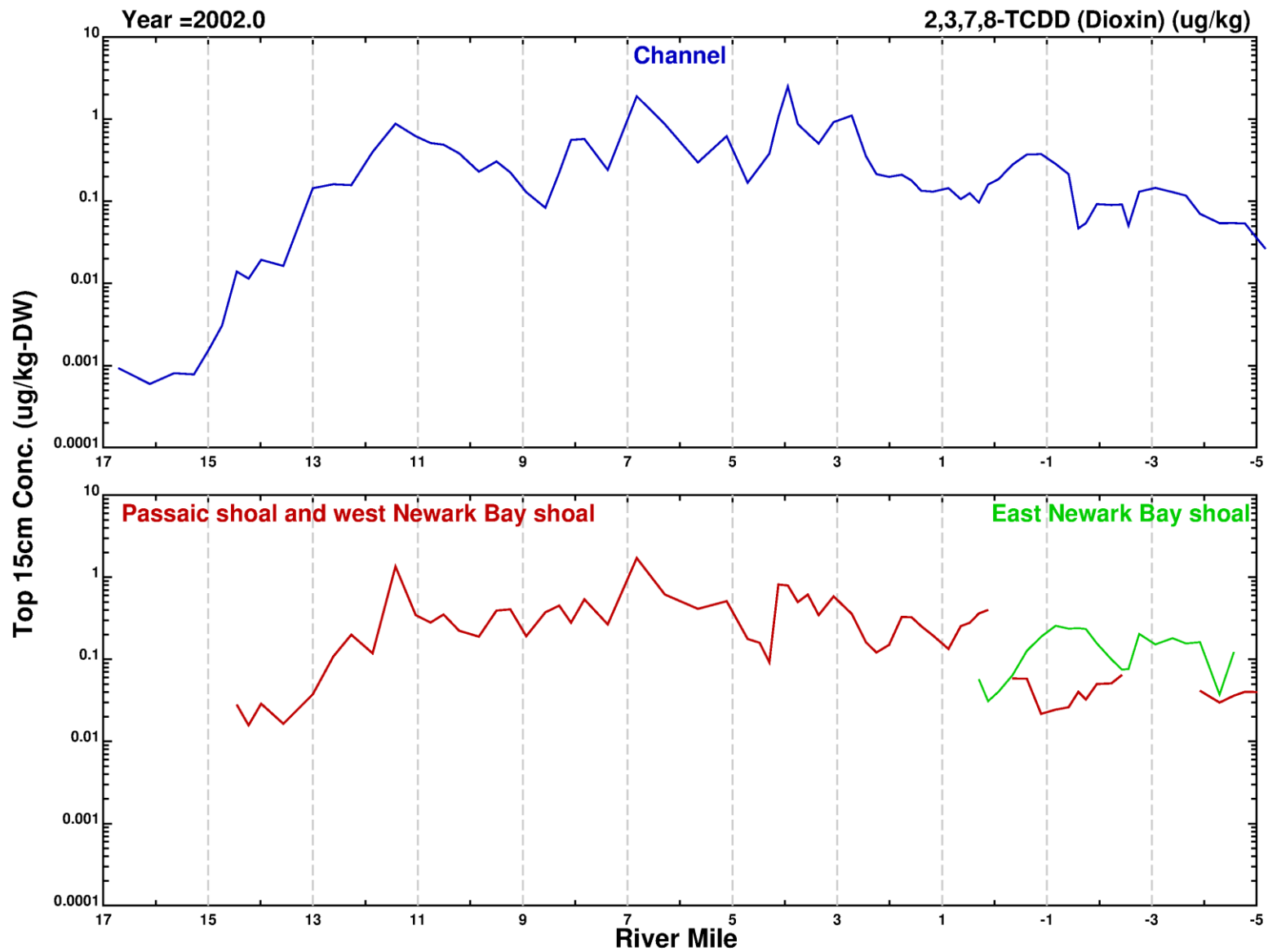


2,3,7,8-TCDD Surface Sediment Transect Plots (2001)

Lower Eight Miles of the Lower Passaic River

Figure 4-17

2014

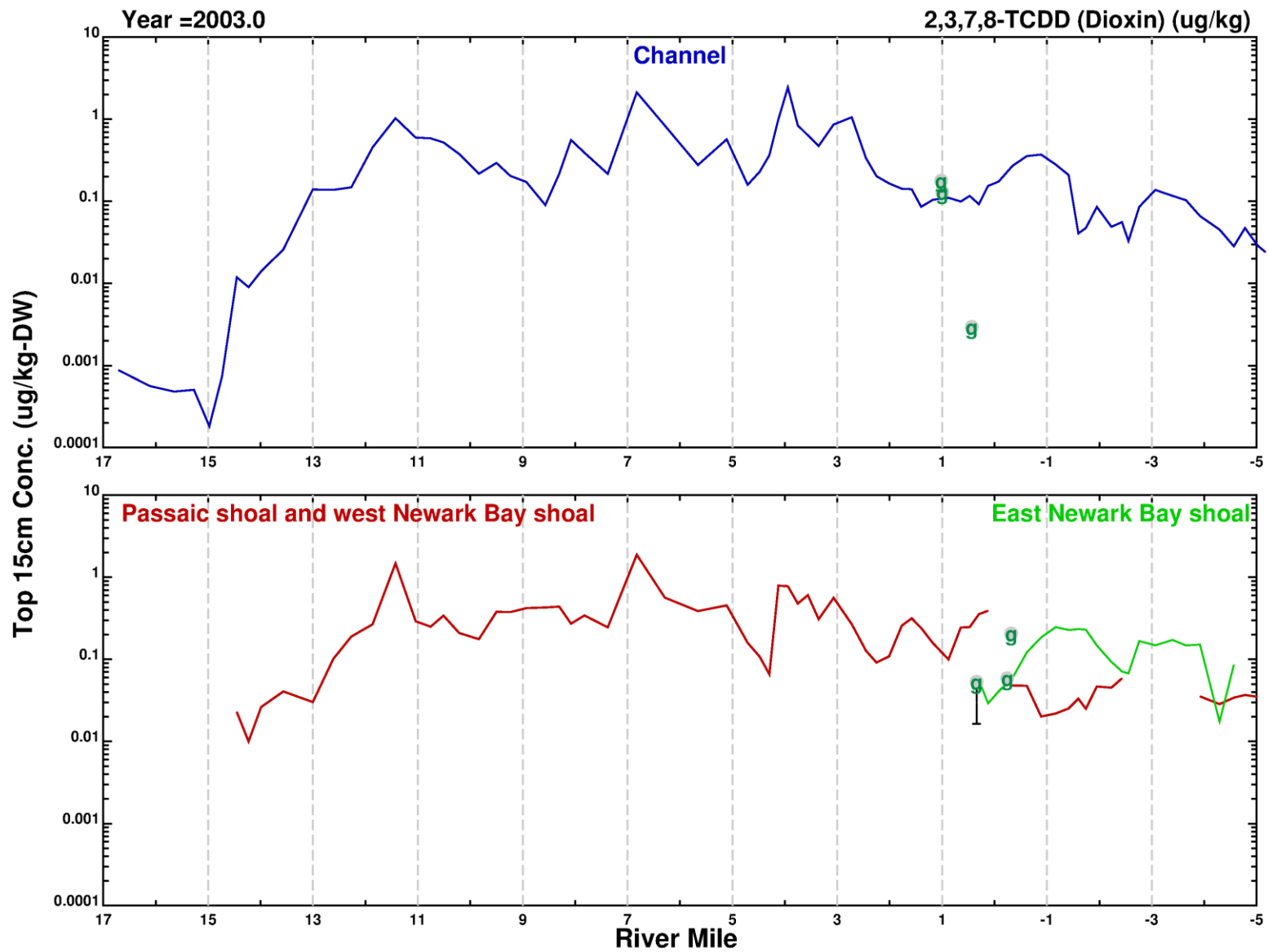


2,3,7,8-TCDD Surface Sediment Transect Plots (2002)

Lower Eight Miles of the Lower Passaic River

Figure 4-18

2014

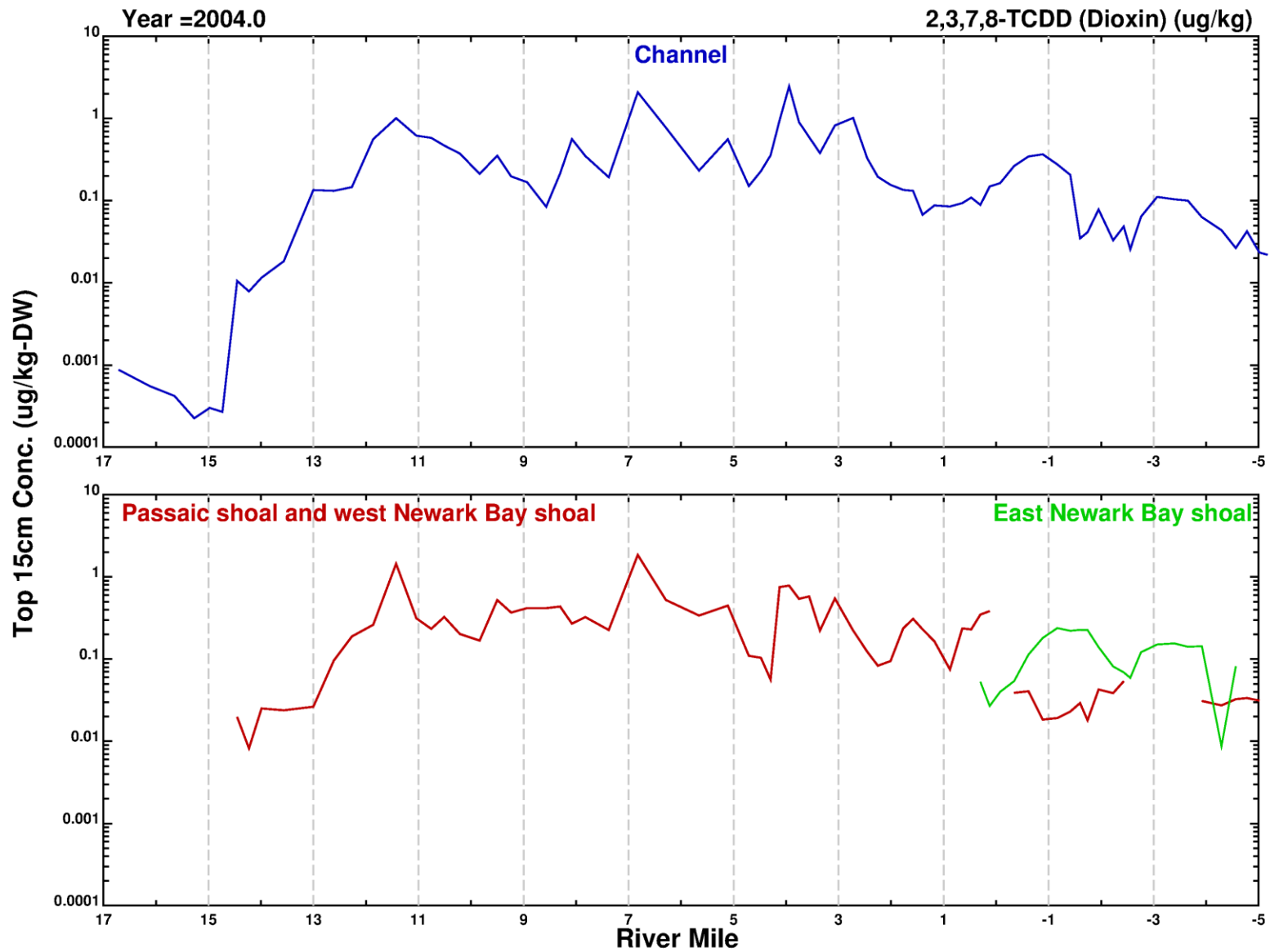


2,3,7,8-TCDD Surface Sediment Transect Plots (2003)

Lower Eight Miles of the Lower Passaic River

Figure 4-19

2014

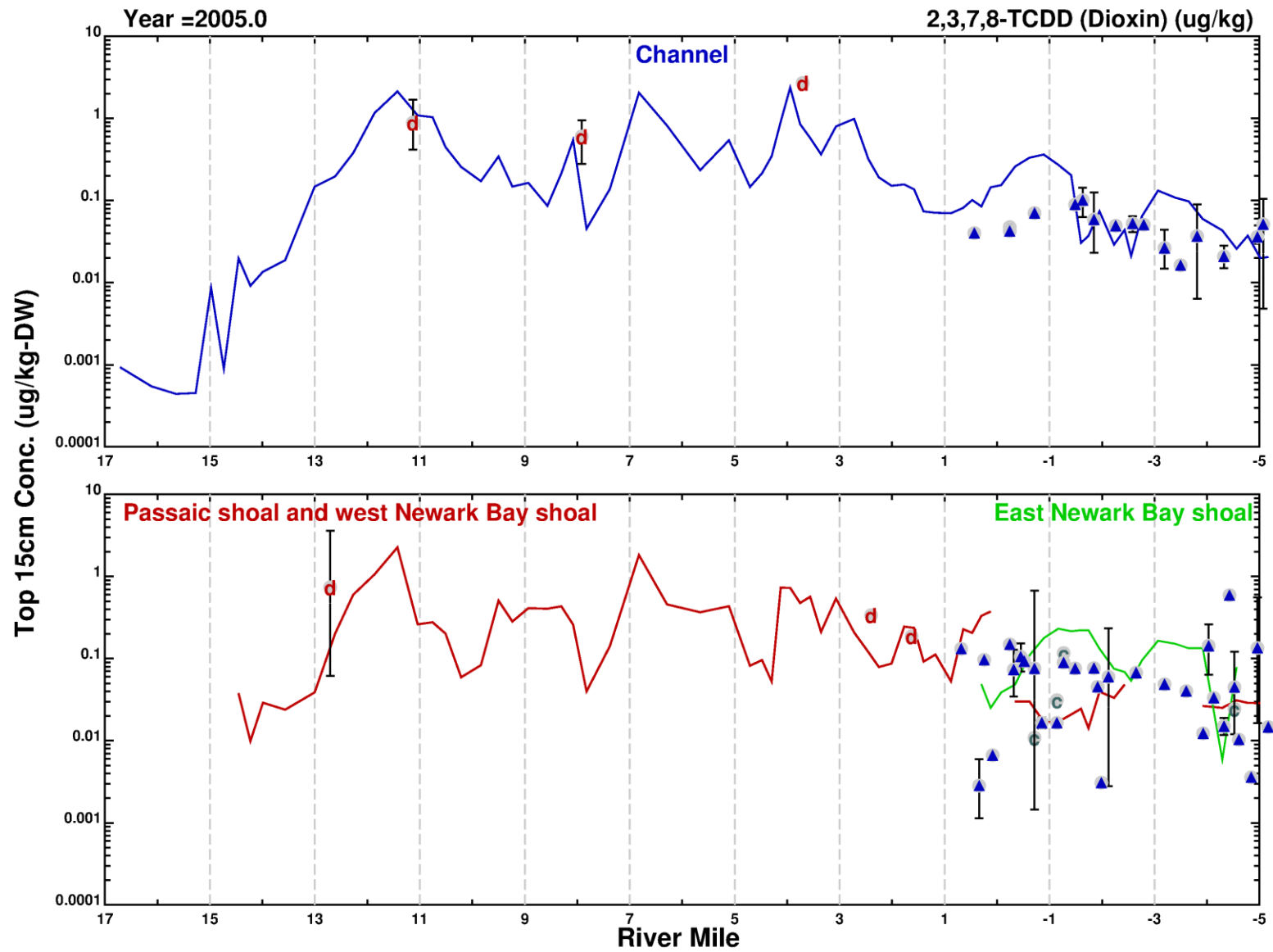


2,3,7,8-TCDD Surface Sediment Transect Plots (2004)

Lower Eight Miles of the Lower Passaic River

Figure 4-20

2014

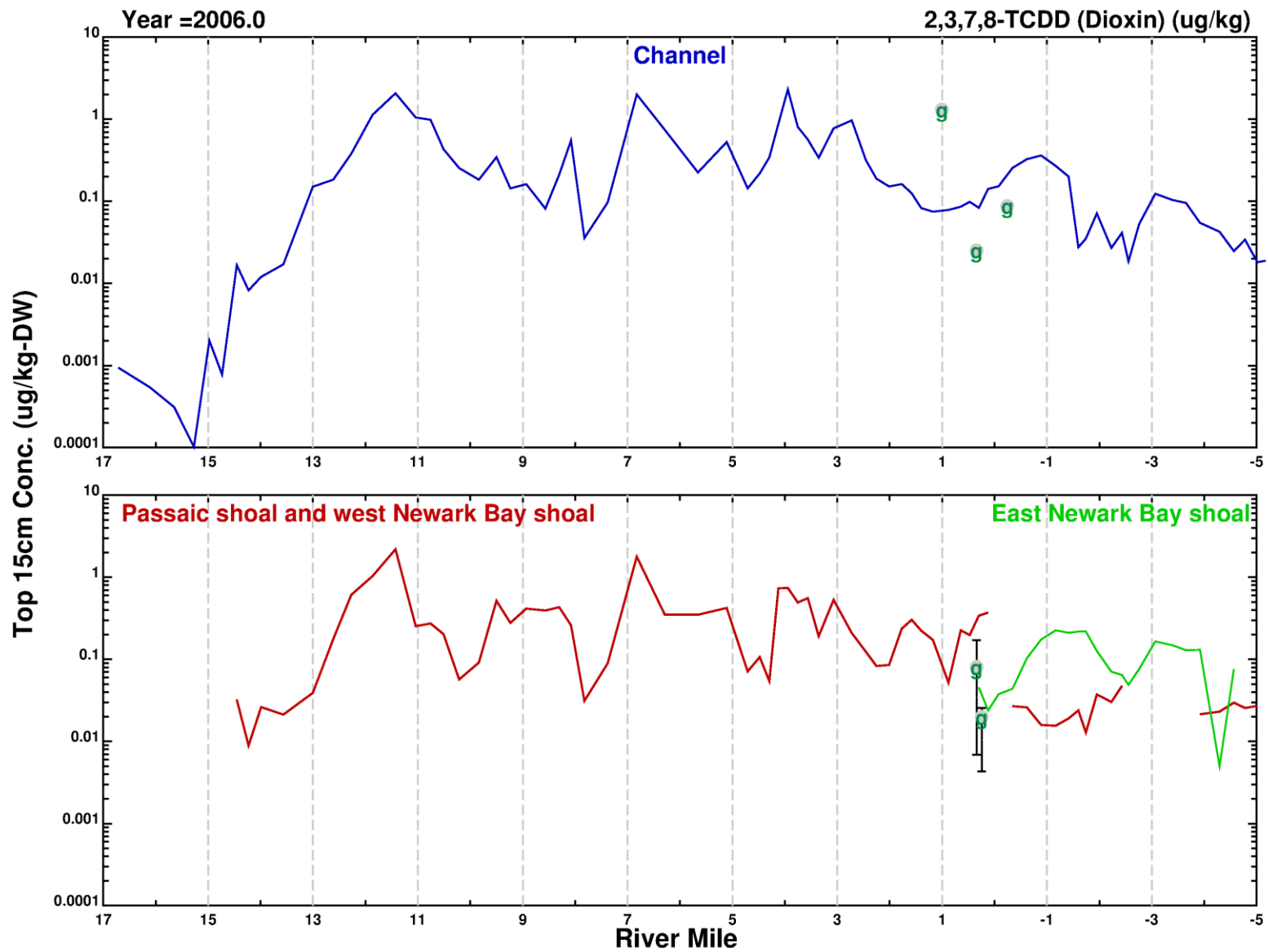


2,3,7,8-TCDD Surface Sediment Transect Plots (2005)

Figure 4-21

Lower Eight Miles of the Lower Passaic River

2014

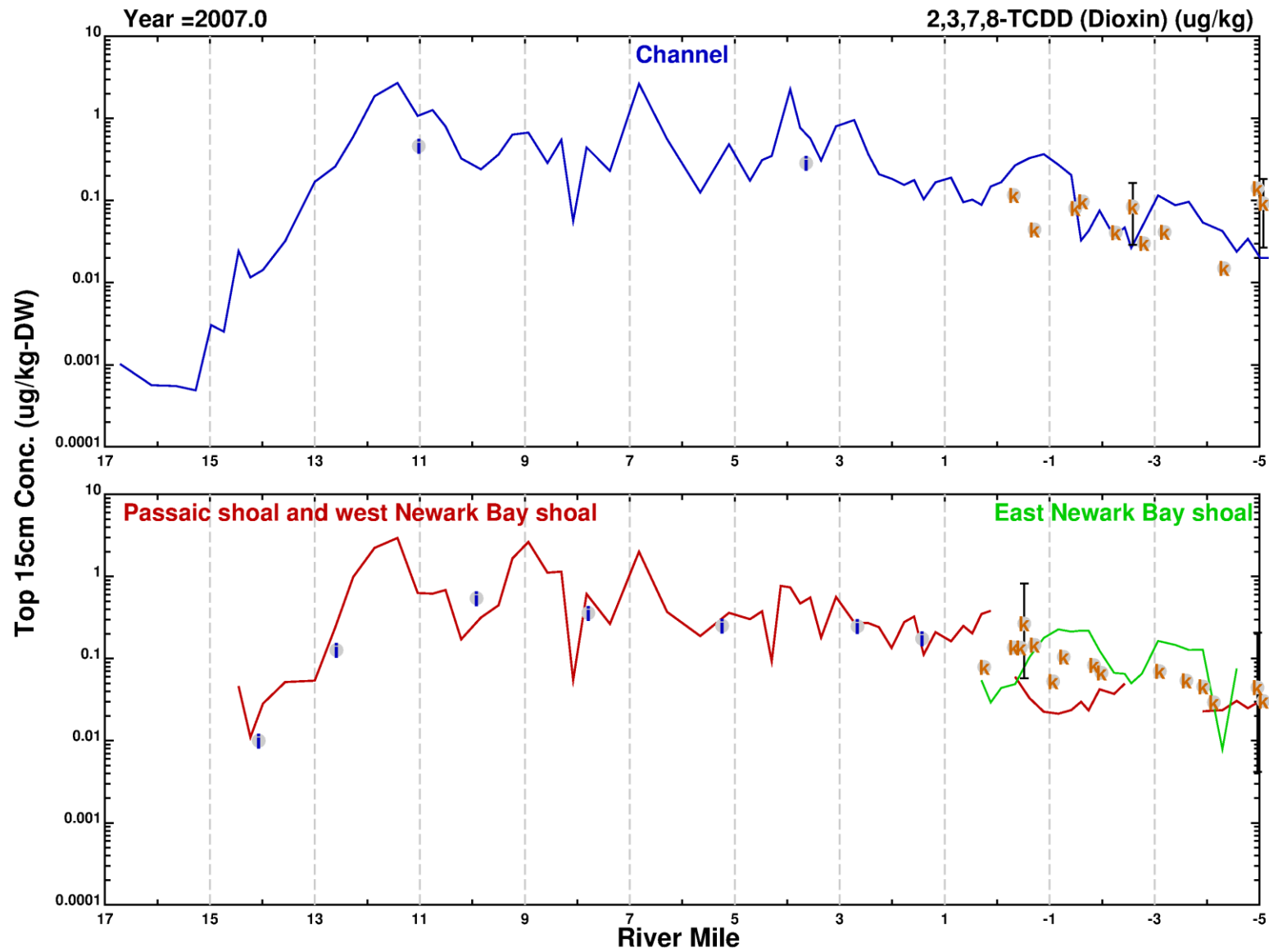


2,3,7,8-TCDD Surface Sediment Transect Plots (2006)

Figure 4-22

Lower Eight Miles of the Lower Passaic River

2014

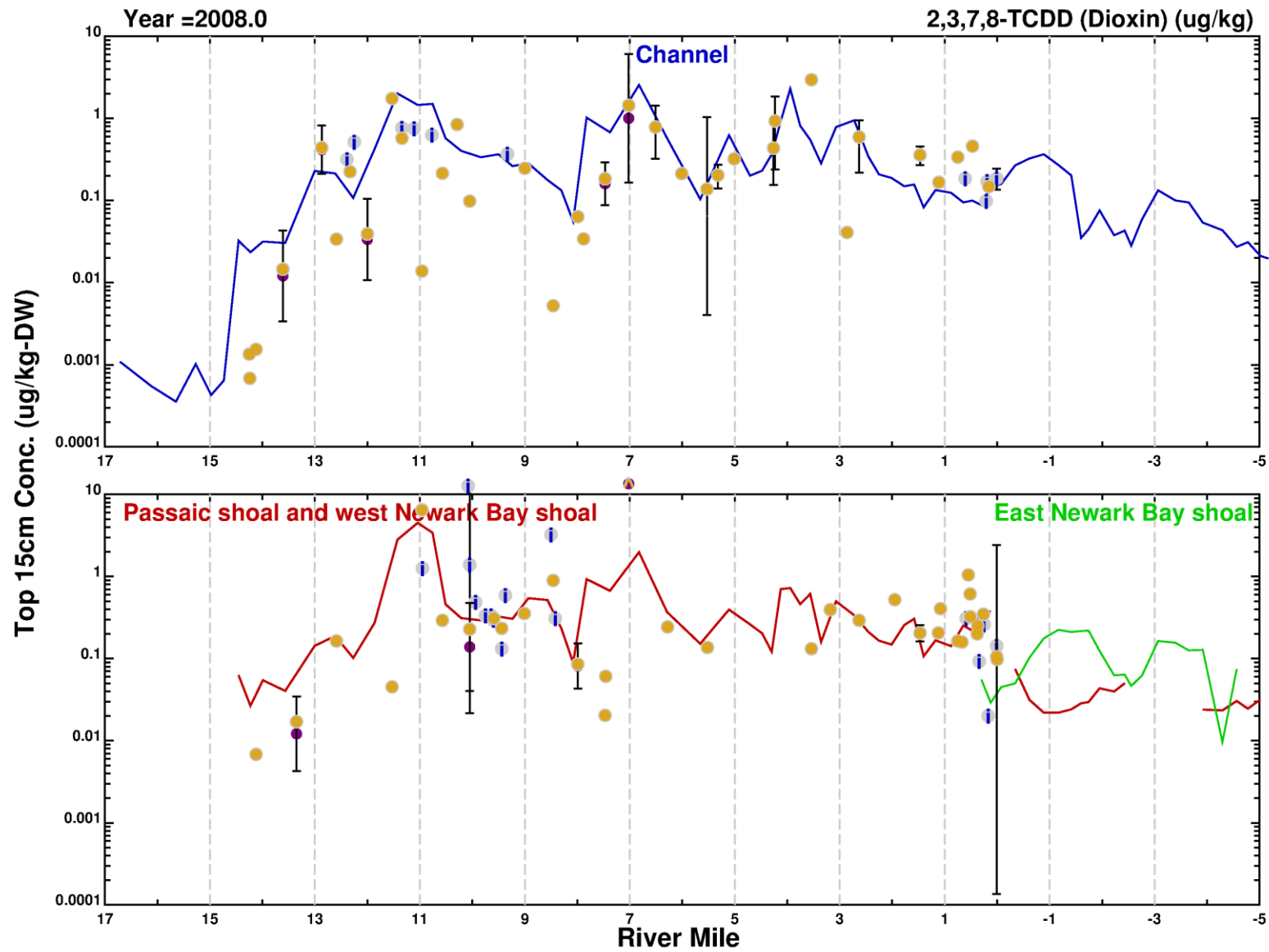


2,3,7,8-TCDD Surface Sediment Transect Plots (2007)

Lower Eight Miles of the Lower Passaic River

Figure 4-23

2014

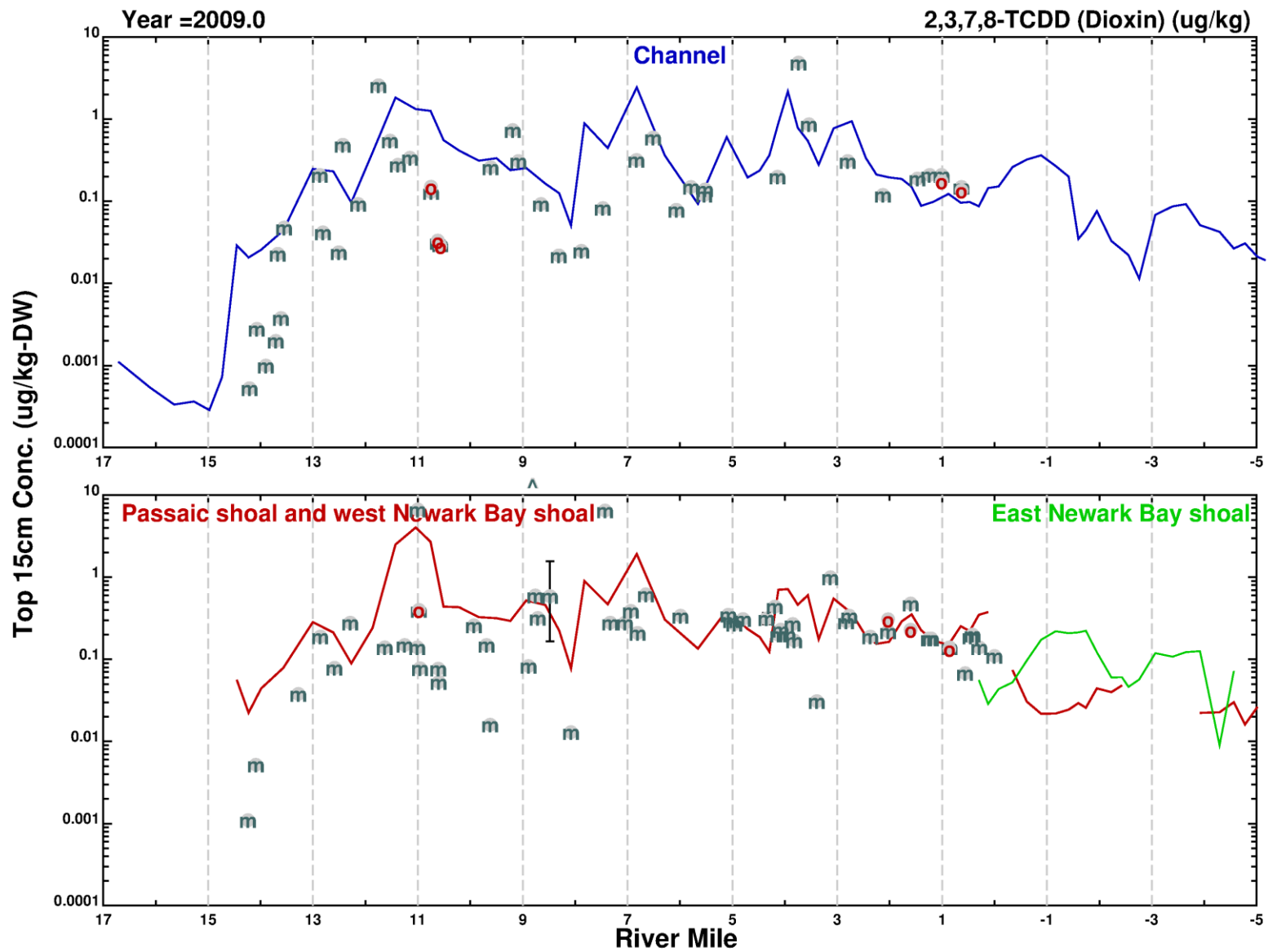


2,3,7,8-TCDD Surface Sediment Transect Plots (2008)

Figure 4-24

Lower Eight Miles of the Lower Passaic River

2014

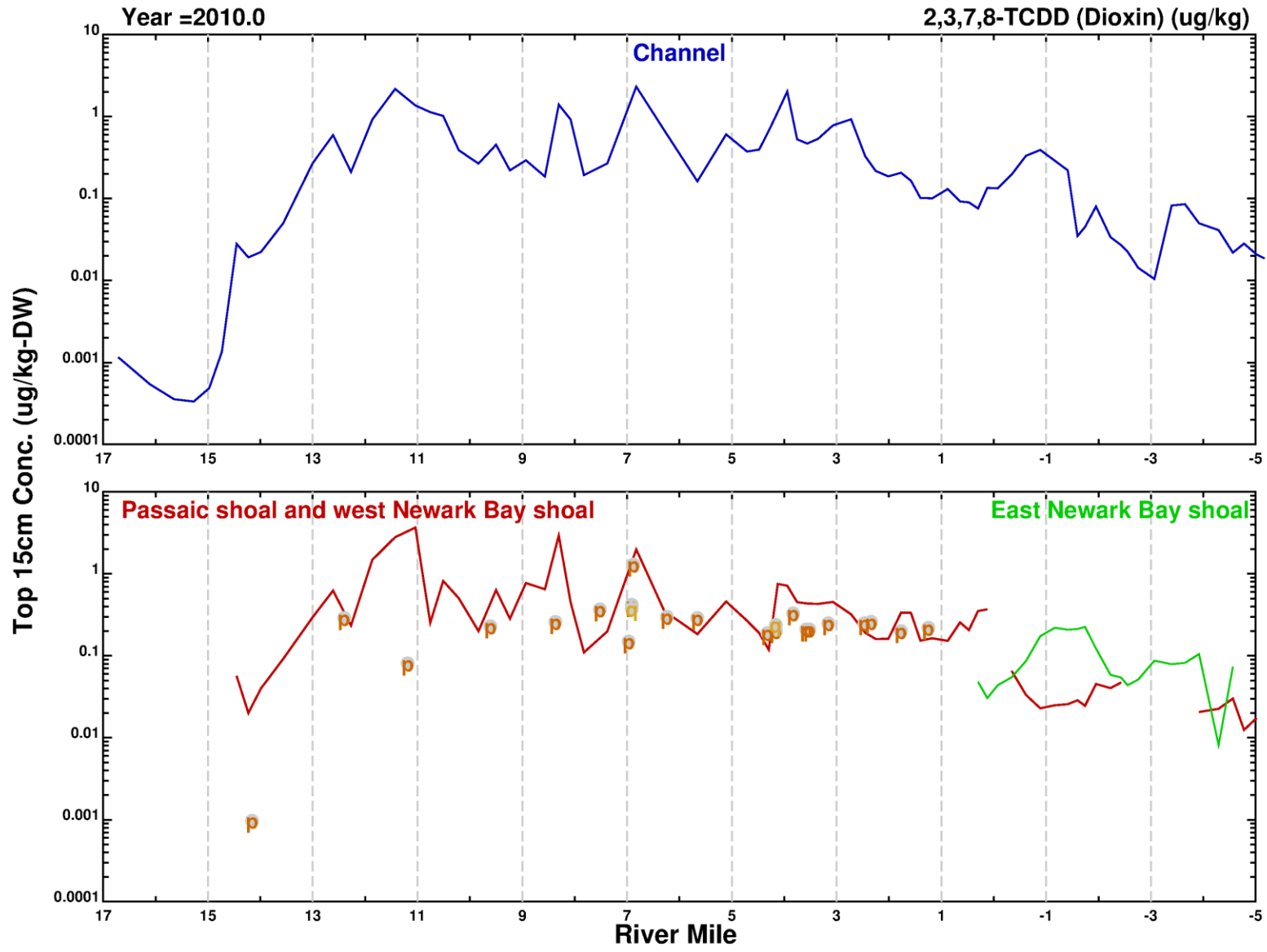


2,3,7,8-TCDD Surface Sediment Transect Plots (2009)

Figure 4-25

Lower Eight Miles of the Lower Passaic River

2014

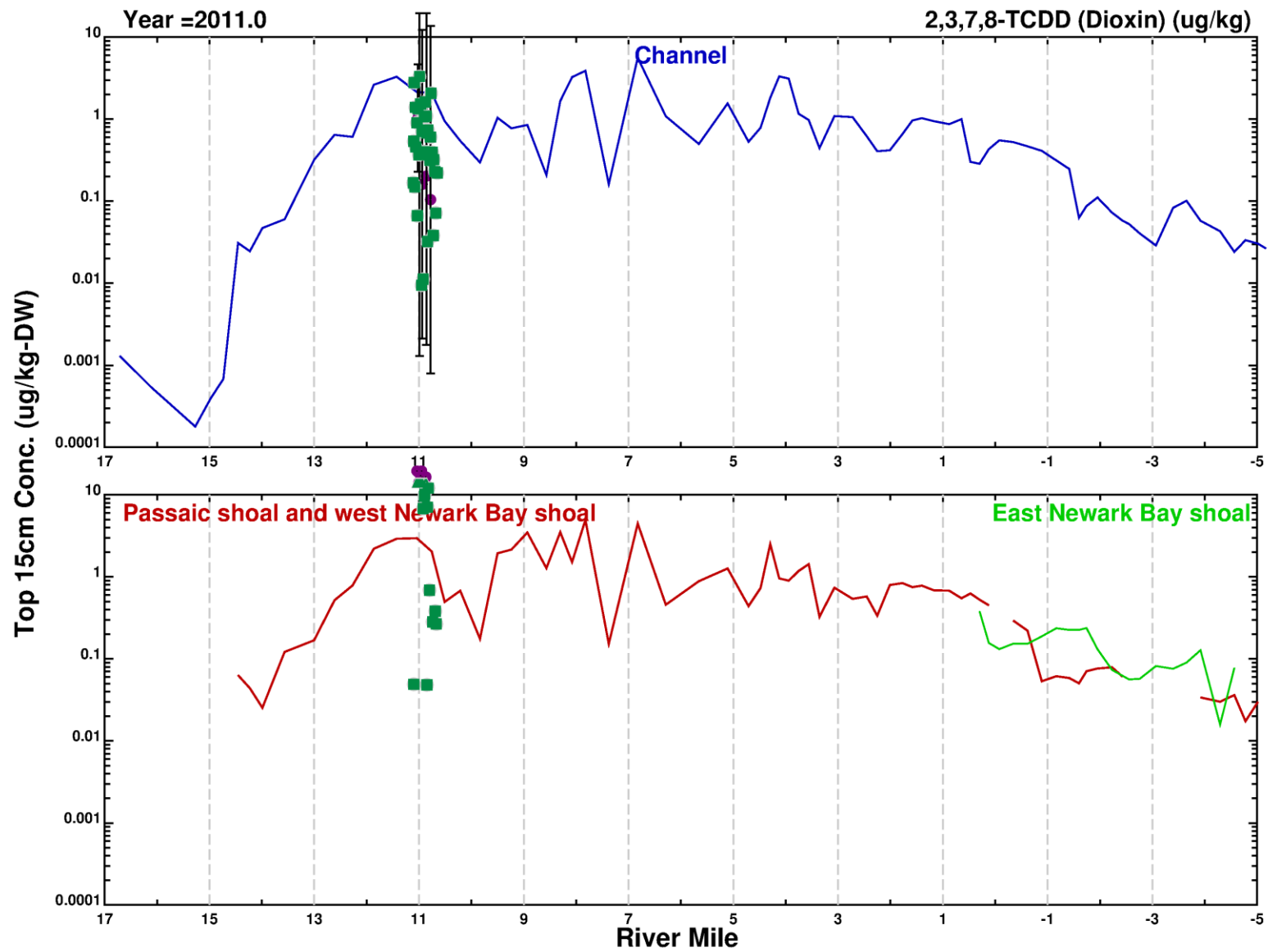


2,3,7,8-TCDD Surface Sediment Transect Plots (2010)

Lower Eight Miles of the Lower Passaic River

Figure 4-26

2014

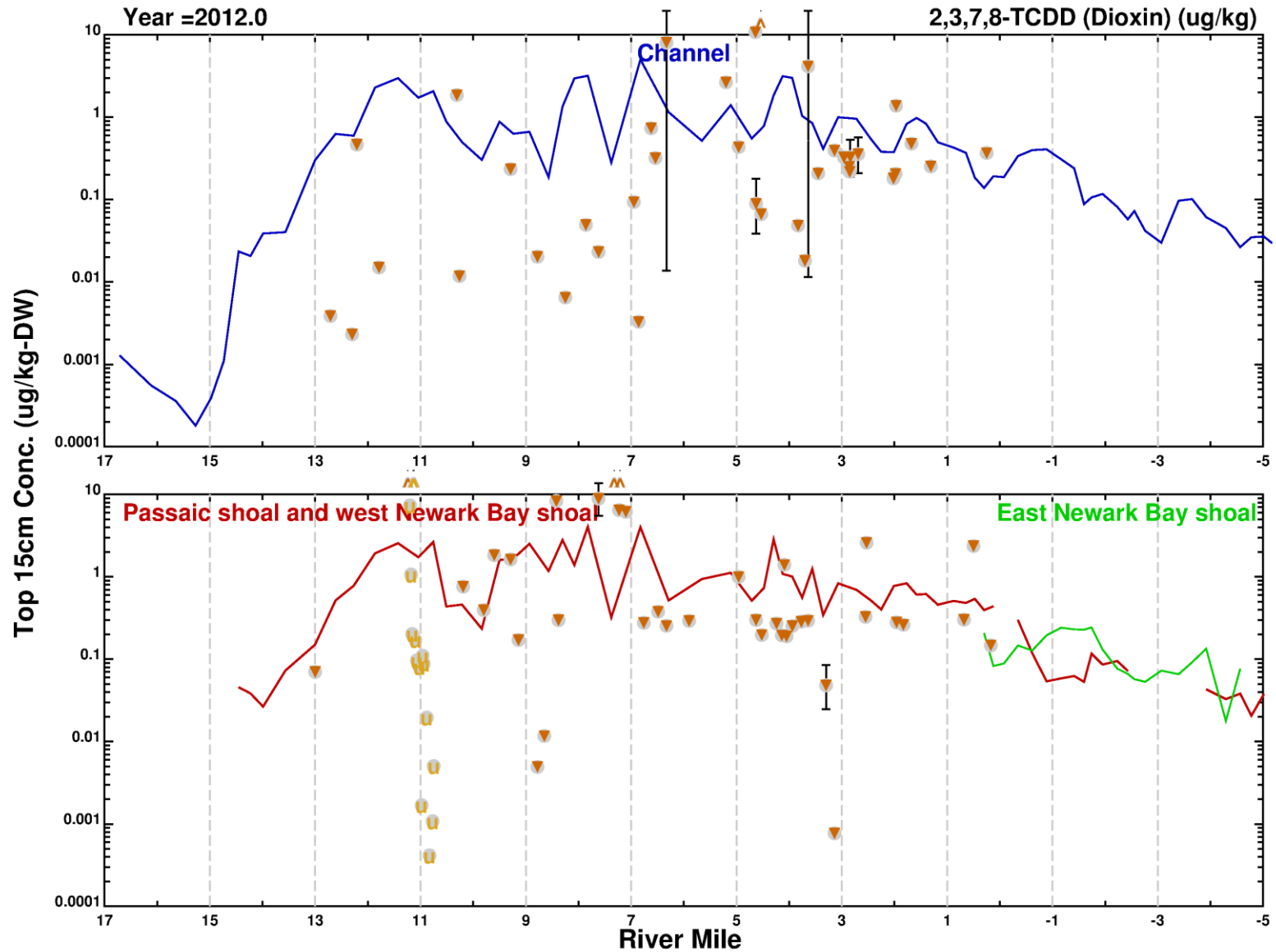


2,3,7,8-TCDD Surface Sediment Transect Plots (2011)

Figure 4-27

Lower Eight Miles of the Lower Passaic River

2014

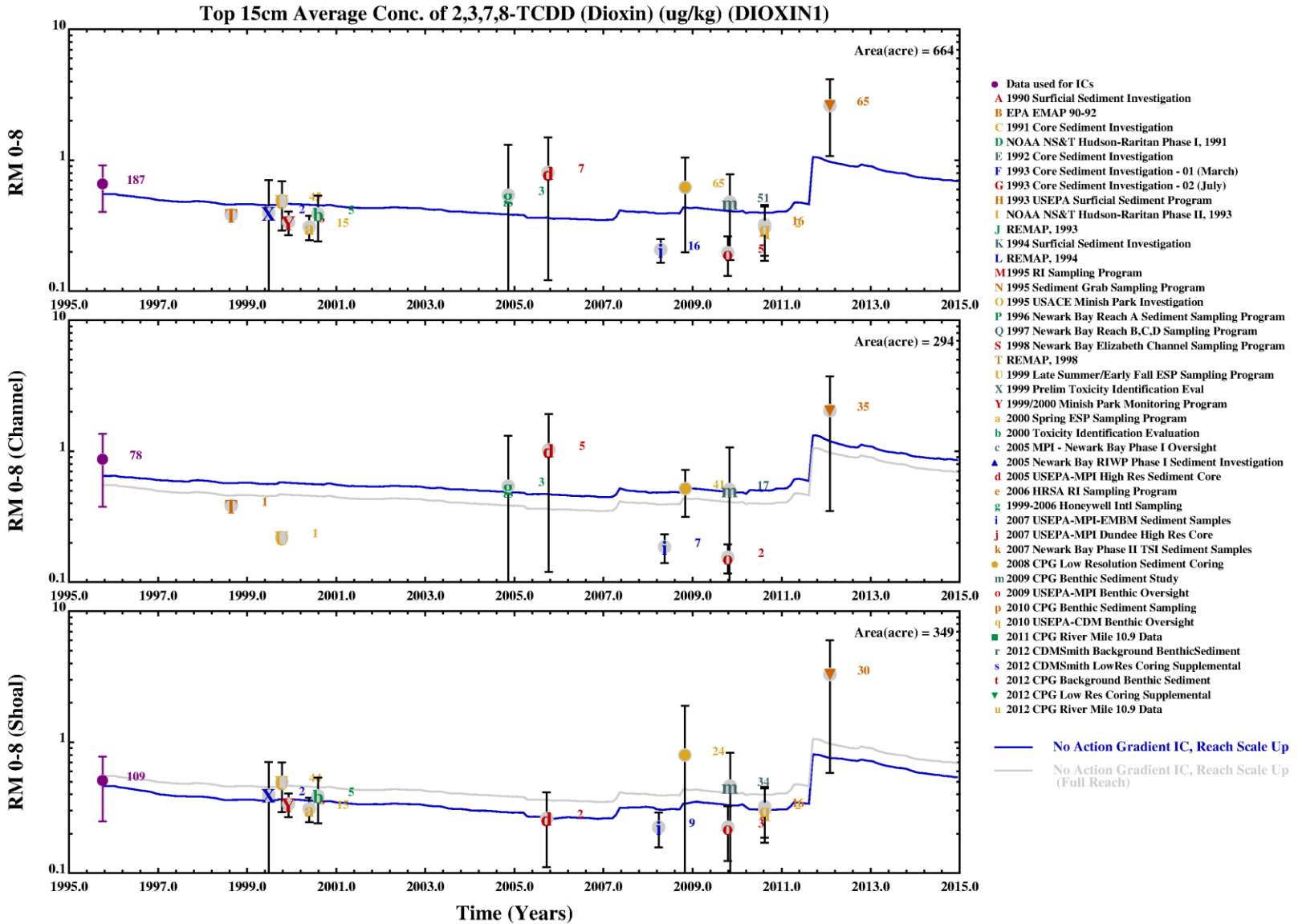


2,3,7,8-TCDD Surface Sediment Transect Plots (2012)

Figure 4-28

Lower Eight Miles of the Lower Passaic River

2014

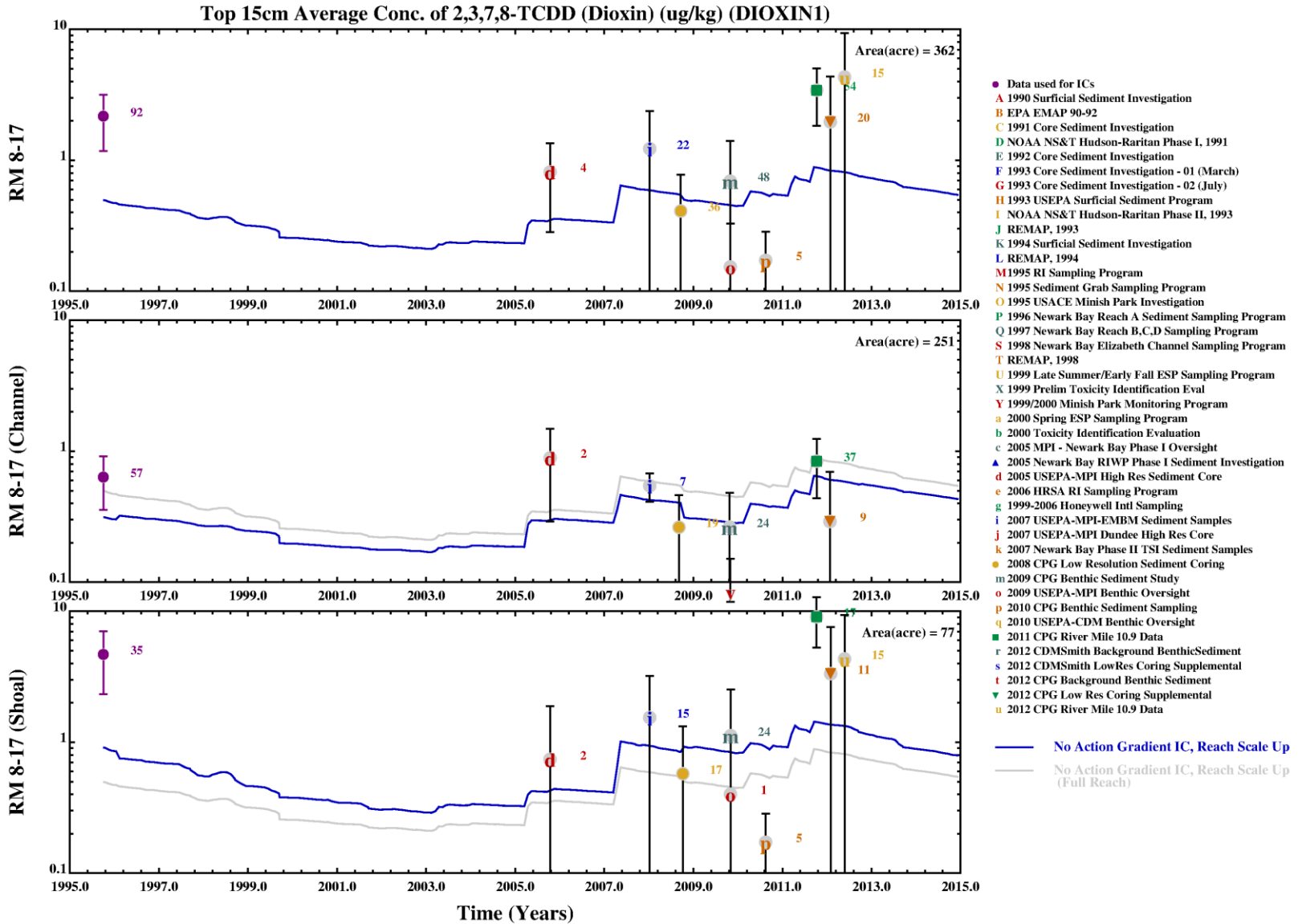


2,3,7,8-TCDD Reach and Sub-reach Sediment Calibration (RM0 to 8.3)

Figure 4-29

Lower Eight Miles of the Lower Passaic River

2014

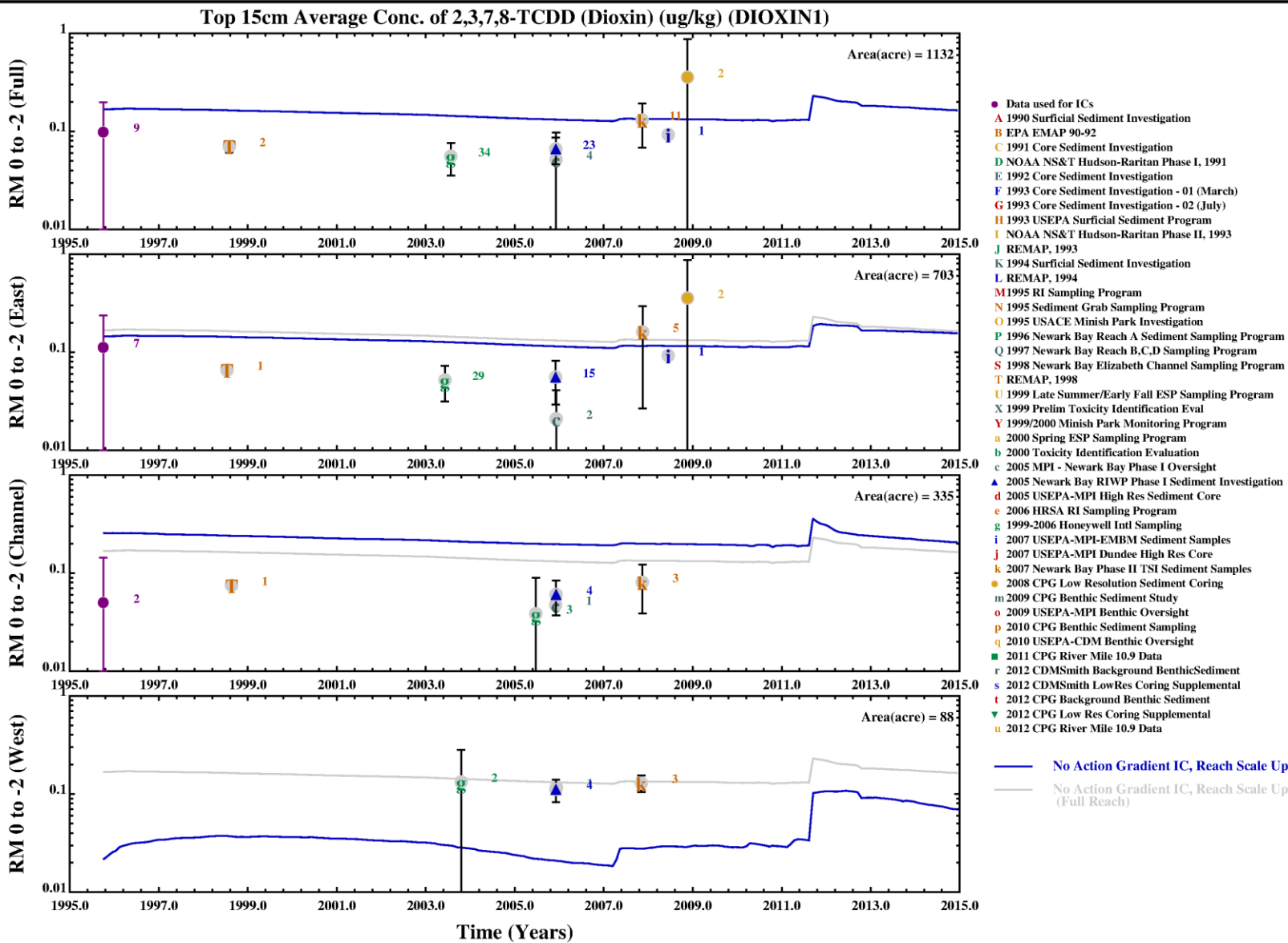


2,3,7,8-TCDD Reach and Sub-reach Sediment Calibration (RM8.3 to 17)

Figure 4-30

Lower Eight Miles of the Lower Passaic River

2014

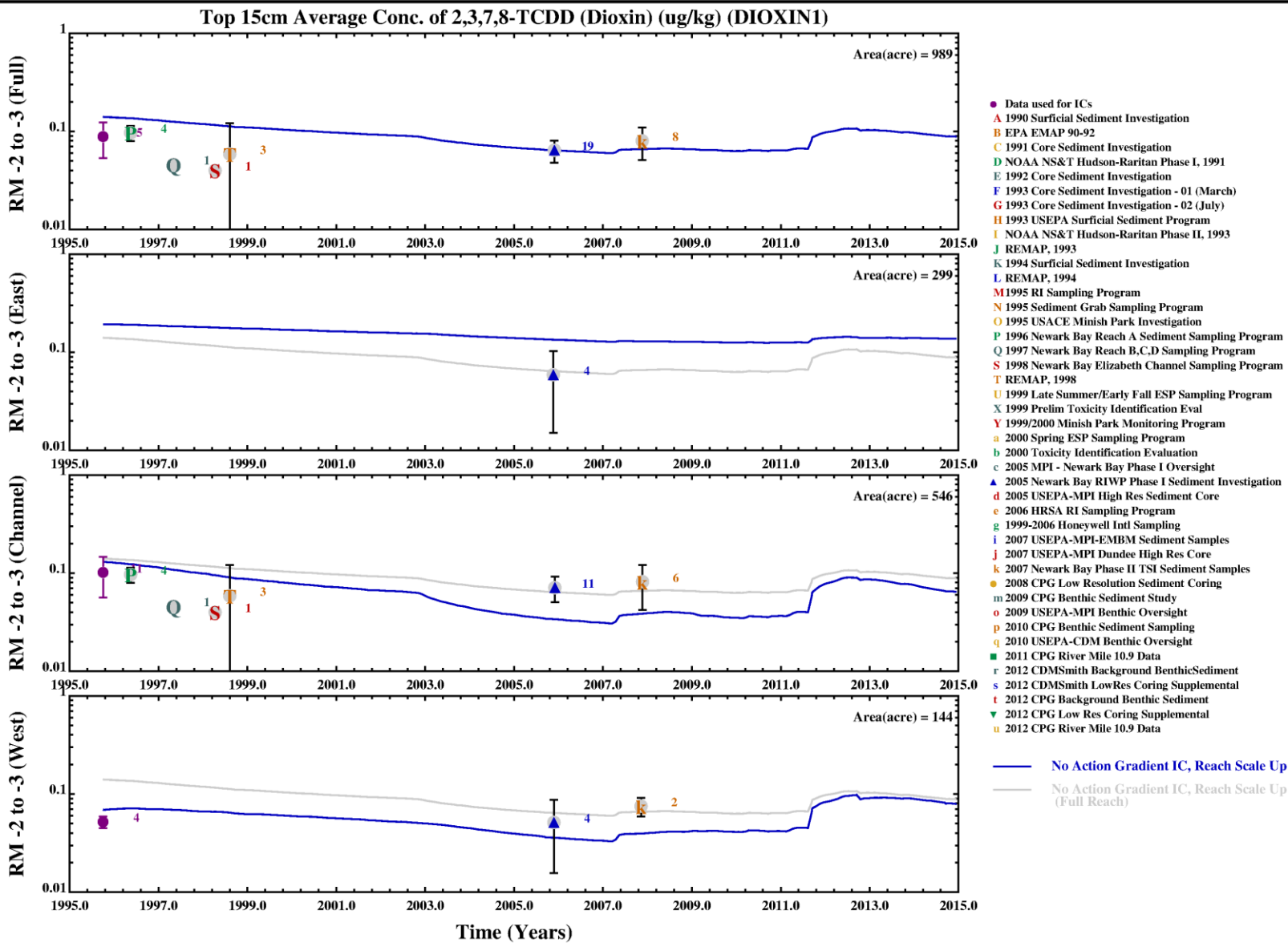


2,3,7,8-TCDD Reach and Sub-reach Sediment Calibration (RM0 to -1.5)

Lower Eight Miles of the Lower Passaic River

Figure 4-31

2014

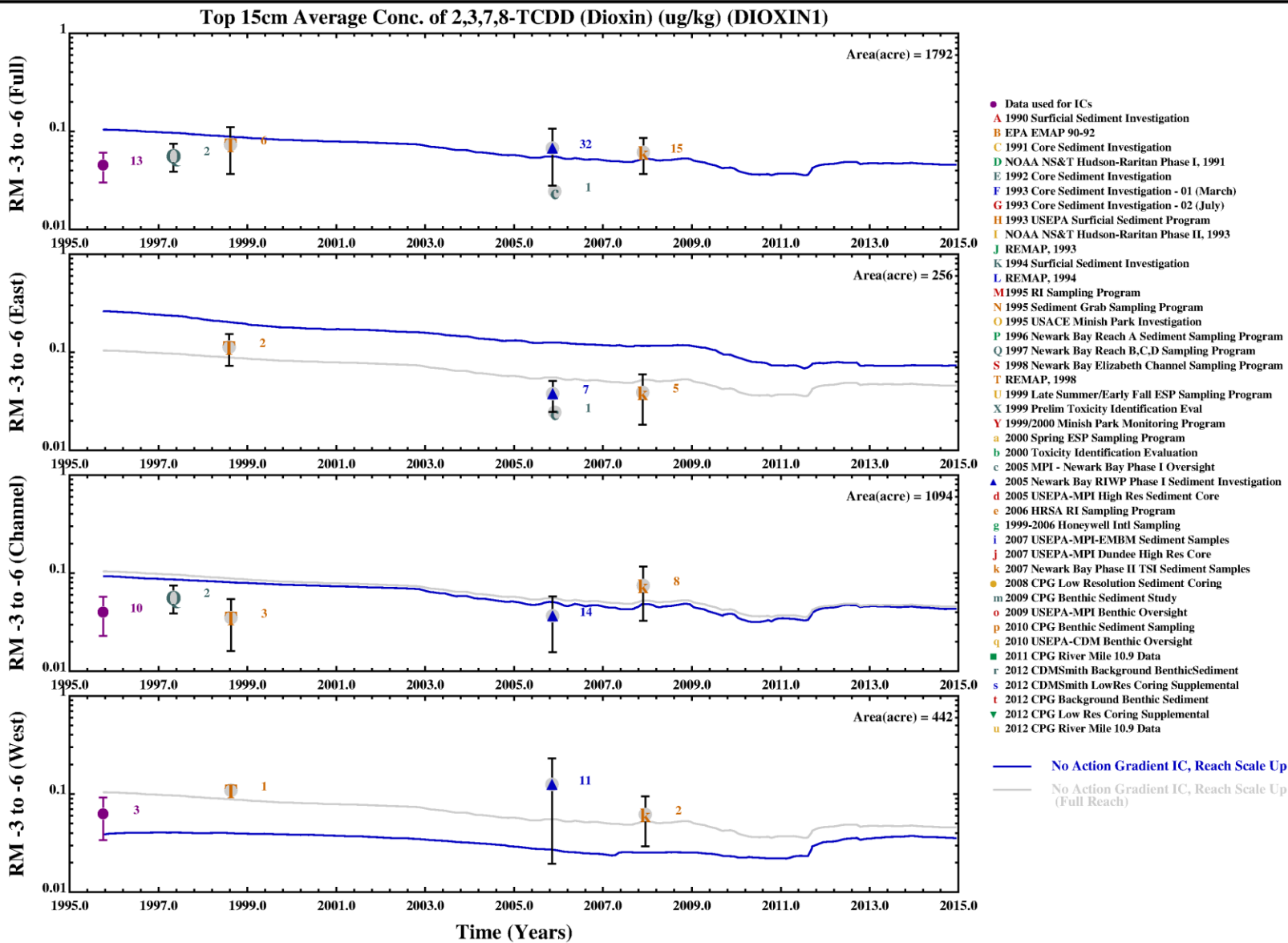


2,3,7,8-TCDD Reach and Sub-reach Sediment Calibration (RM-1.5 to -2.6)

Figure 4-32

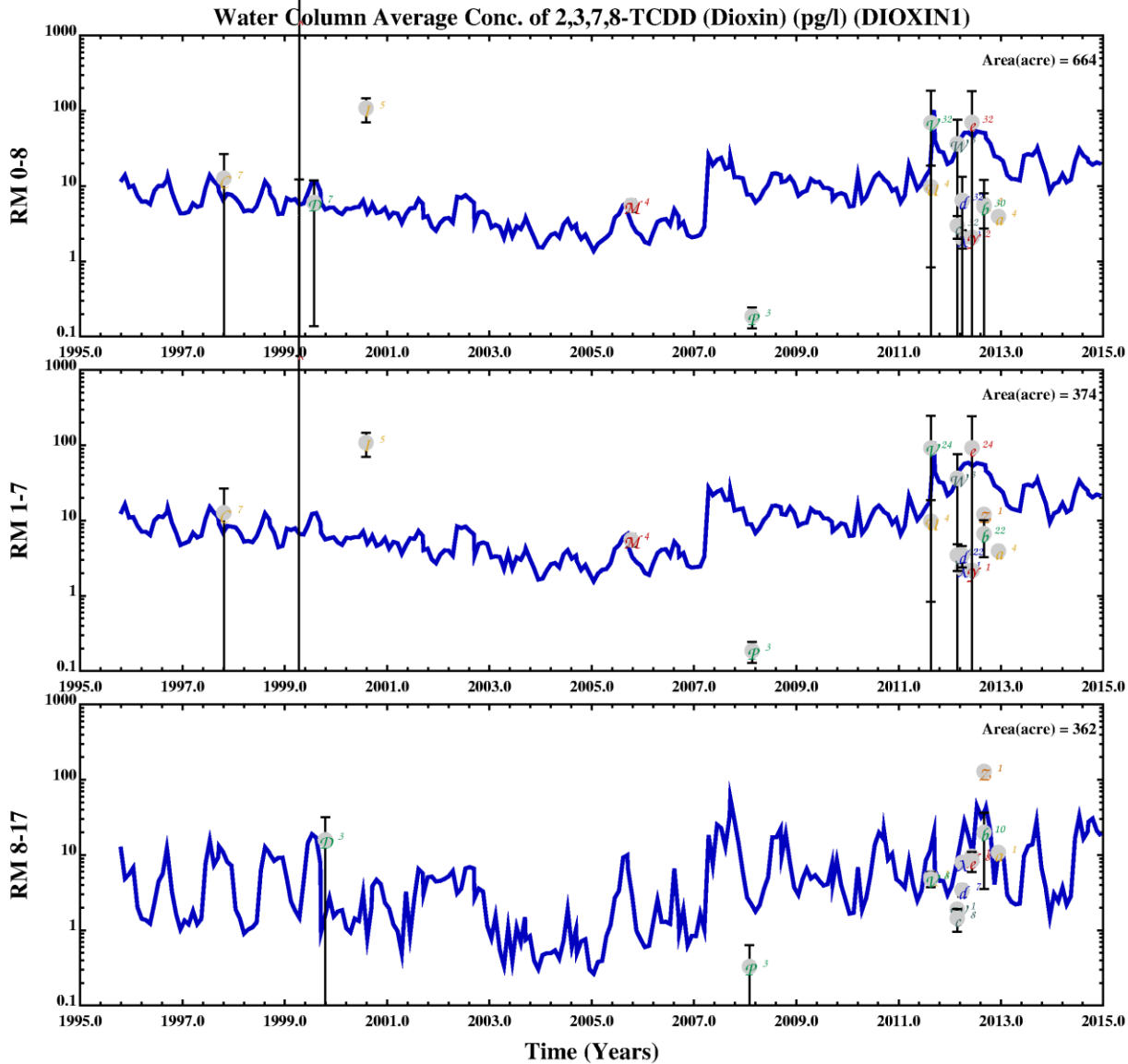
Lower Eight Miles of the Lower Passaic River

2014



2,3,7,8-TCDD Reach and Sub-reach Sediment Calibration (RM-2.6 to -5.25)

Figure 4-33



- 1993-1997 USACE - DMDAT
- 1995-96 Passaic Study RI/FS Sed Mobility
- 1997 Outfall Sampling Program
- 1998-2001 CARP Database
- 1999 Newark Bay Reach A Monitoring
- 1999 Newark Bay Reach ABCD Baseline Sampling
- 1999 USACE Drift Removal Monitoring
- 1999-2006 Honeywell Intl Sampling
- 2000 Toxicity Identification Evaluation
- 2005 Hydrodynamic Mooring
- 2005 MPI SPMD Deployment
- 2005 USEPA-MPI High Flow Water Column
- 2005 USEPA-MPI Large Volume Study
- 2005 USEPA-MPI Small Volume Water Column
- 2005 USEPA-MPI Water Column Above RM 8.5
- 2007 USEPA-MPI-EMBM Water Column Sample
- 2009 CPG LPR Water Column Monitoring DEC
- 2010 CPG LPR-NB PWCM Field Measurements
- 2010 CPG LPR-NB PWCM Sample Dataset
- 2010 USEPA LBG-CDM PWCM Oversight
- 2011 CDM Smith CWCM Sampling Data
- 2011 CPG CWCM Sampling Data
- 2012 CDM Smith CWCM Sampling - Round 2
- 2012 CDM Smith CWCM Sampling - Round 3
- 2012 CDM Smith CWCM Sampling - Round 4
- 2012 CDM Smith CWCM Sampling - Round 5
- 2012 CDM Smith CWCM Sampling - Round - 6
- 2012 CPG CWCM Sampling - Low Flow
- 2012 CPG CWCM Sampling - Round 2
- 2012 CPG CWCM Sampling - Round 3
- 2012 CPG CWCM Sampling - Round 4

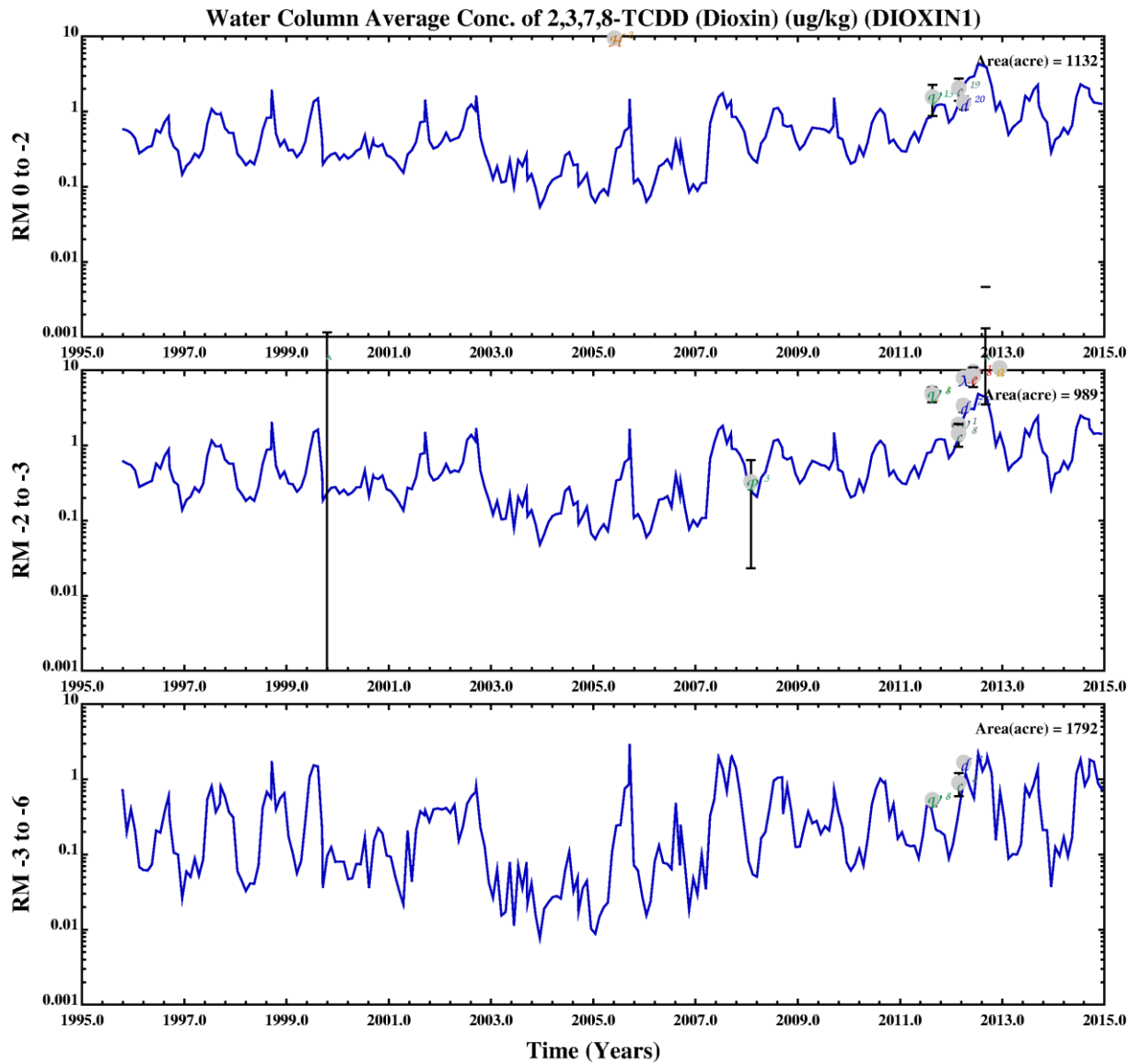
— No Action Gradient IC, Reach Scale Up

2,3,7,8-TCDD Reach Water Column Calibration LPR

Figure 4-34

Lower Eight Miles of the Lower Passaic River

2014



- A 1993-1997 USACE - DMDAT
- B 1995-96 Passaic Study RIFS Sed Mobility
- C 1997 Outfall Sampling Program
- D 1998-2001 CARP Database
- E 1999 Newark Bay Reach A Monitoring
- F 1999 Newark Bay Reach ABCD Baseline Sampling
- G 1999 USACE Drift Removal Monitoring
- H 1999-2006 Honeywell Intl Sampling
- I 2000 Toxicity Identification Evaluation
- J 2005 Hydrodynamic Mooring
- K 2005 MPI SPMD Deployment
- L 2005 USEPA-MPI High Flow Water Column
- M 2005 USEPA-MPI Large Volume Study
- N 2005 USEPA-MPI Small Volume Water Column
- O 2005 USEPA-MPI Water Column Above RM 8.5
- P 2007 USEPA-MPI-EMBM Water Column Sample
- Q 2009 CPG LPR Water Column Monitoring DEC
- R 2010 CPG LPR-NB PWCM Field Measurements
- S 2010 CPG LPR-NB PWCM Sample Dataset
- T 2010 USEPA LBG-CDM PWCM Oversight
- U 2011 CDM Smith CWCM Sampling Data
- V 2011 CPG CWCM Sampling Data
- W 2012 CDM Smith CWCM Sampling - Round 2
- X 2012 CDM Smith CWCM Sampling - Round 3
- Y 2012 CDM Smith CWCM Sampling - Round 4
- Z 2012 CDM Smith CWCM Sampling - Round 5
- a 2012 CDM Smith CWCM Sampling Round - 6
- b 2012 CPG CWCM Sampling - Low Flow
- c 2012 CPG CWCM Sampling - Round 2
- d 2012 CPG CWCM Sampling - Round 3
- e 2012 CPG CWCM Sampling - Round 4

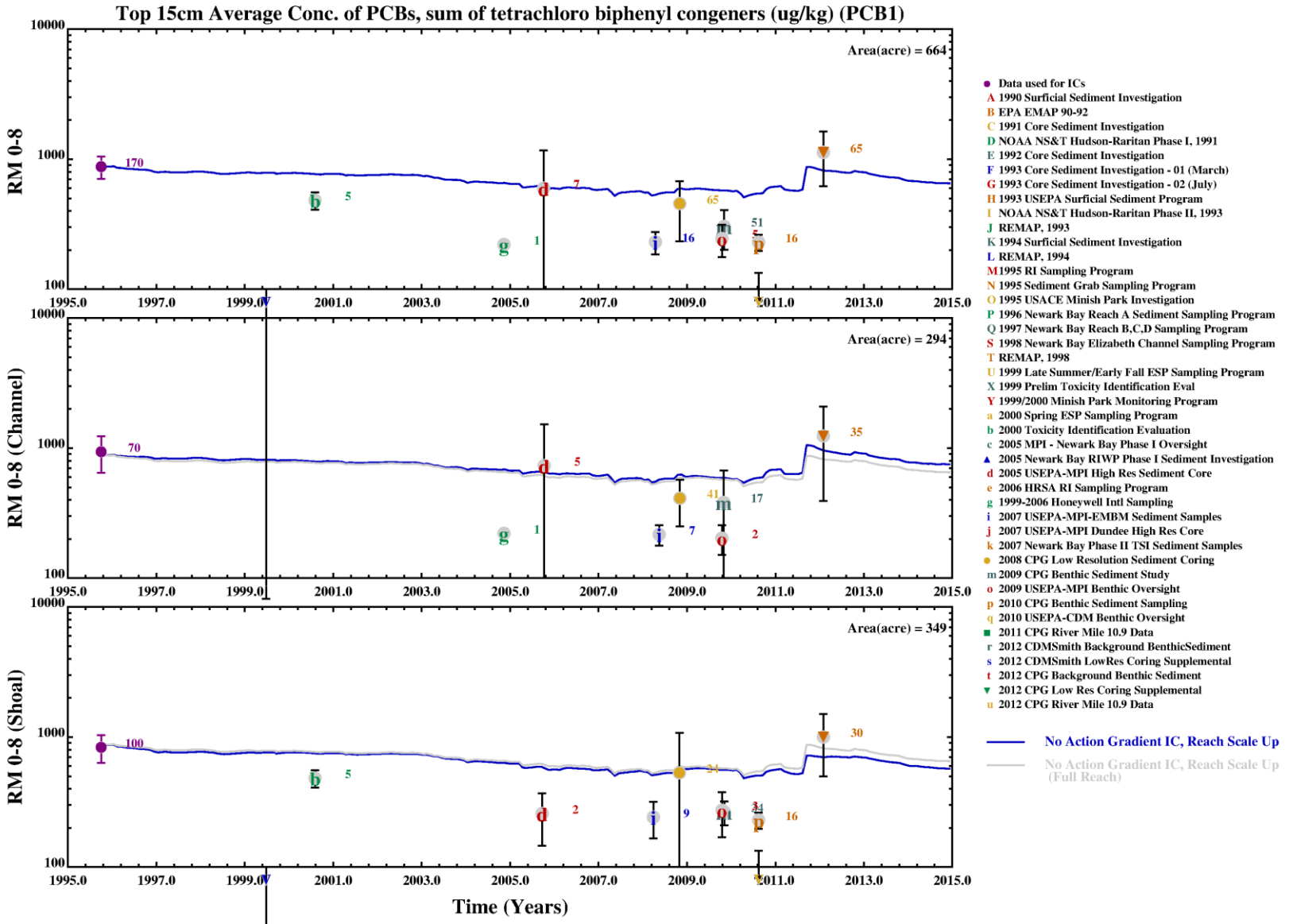
— No Action Gradient IC, Reach Scale Up

2,3,7,8-TCDD Reach Water Column Calibration Newark Bay

Figure 4-35

Lower Eight Miles of the Lower Passaic River

2014

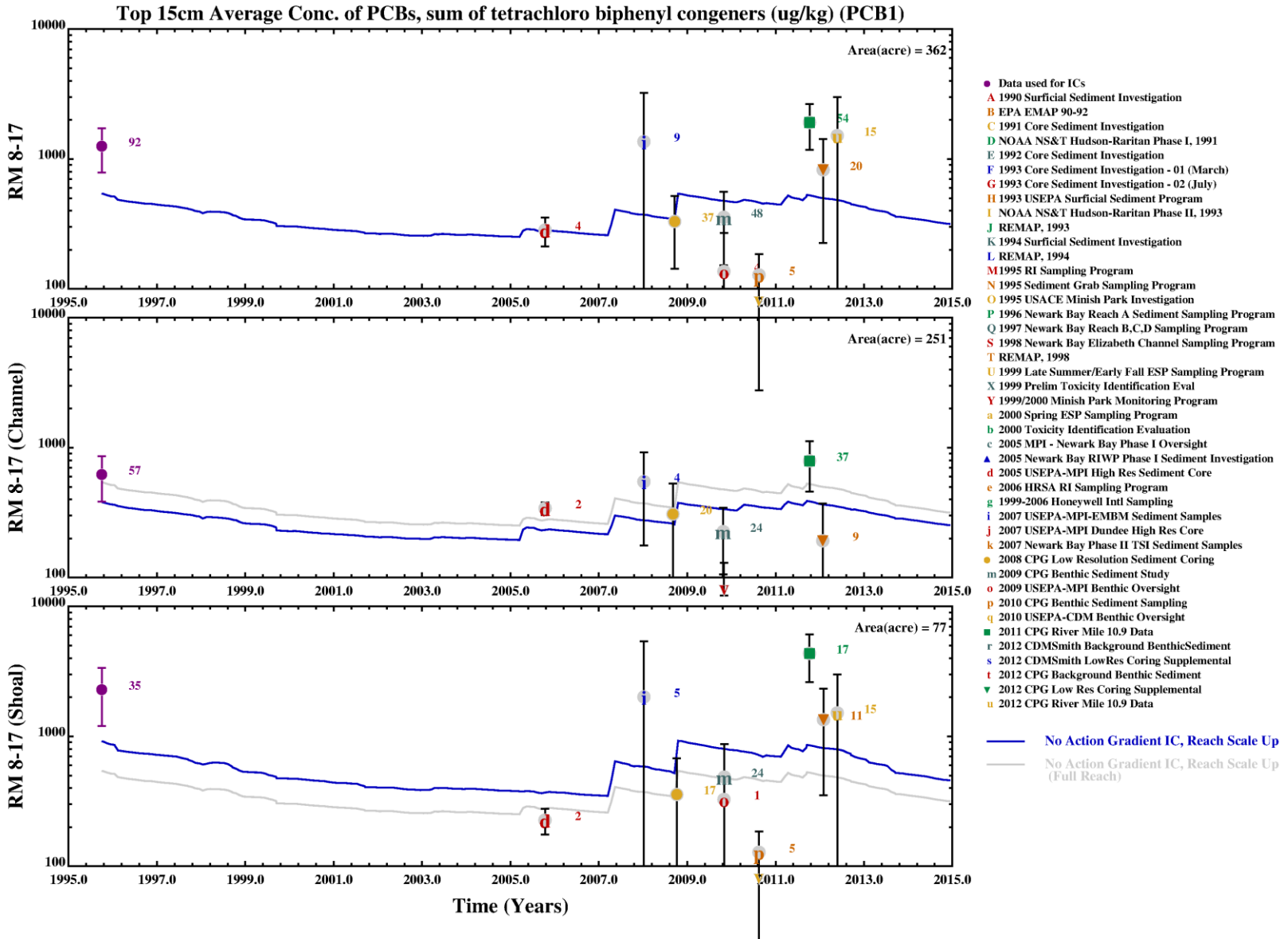


Tetrachlorobiphenyl Reach and Sub-reach Sediment Calibration (RM0 to 8.3)

Figure 4-36

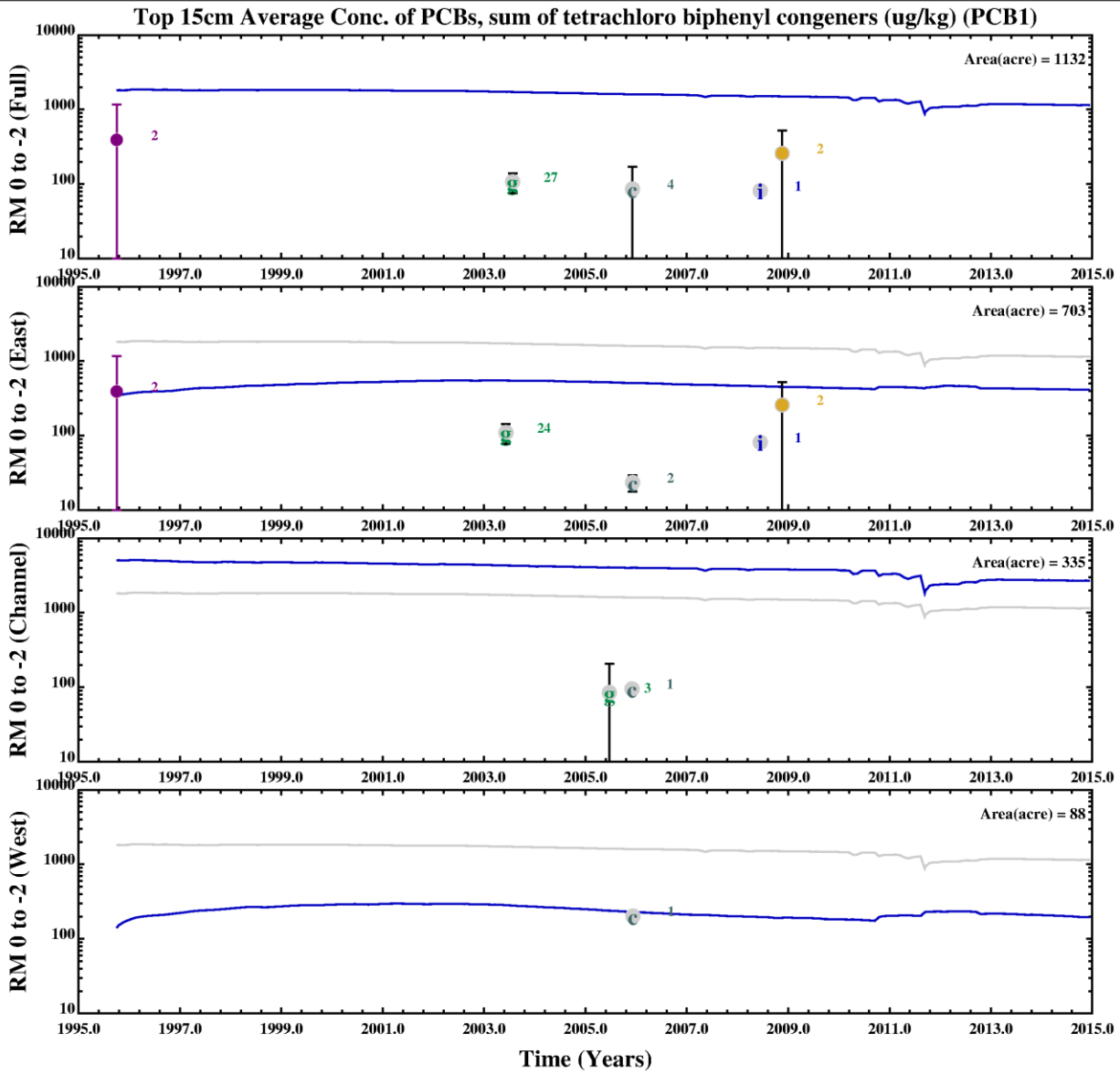
Lower Eight Miles of the Lower Passaic River

2014



Tetrachlorobiphenyl Reach and Sub-reach Sediment Calibration (RM8.3 to 17)

Figure 4-37



- Data used for ICs
- A 1990 Surficial Sediment Investigation
- B EPA EMAP 90-92
- C 1991 Core Sediment Investigation
- D NOAA NS&T Hudson-Raritan Phase I, 1991
- E 1992 Core Sediment Investigation
- F 1993 Core Sediment Investigation - 01 (March)
- G 1993 Core Sediment Investigation - 02 (July)
- H 1993 USEPA Surficial Sediment Program
- I NOAA NS&T Hudson-Raritan Phase II, 1993
- J REMAP, 1993
- K 1994 Surficial Sediment Investigation
- L REMAP, 1994
- M 1995 RI Sampling Program
- N 1995 Sediment Grab Sampling Program
- O 1995 USACE Minish Park Investigation
- P 1996 Newark Bay Reach A Sediment Sampling Program
- Q 1997 Newark Bay Reach B,C,D Sampling Program
- S 1998 Newark Bay Elizabeth Channel Sampling Program
- T REMAP, 1998
- U 1999 Late Summer/Early Fall ESP Sampling Program
- X 1999 Prelim Toxicity Identification Eval
- Y 1999/2000 Minish Park Monitoring Program
- a 2000 Spring ESP Sampling Program
- b 2000 Toxicity Identification Evaluation
- c 2005 MPI - Newark Bay Phase I Oversight
- ▲ 2005 Newark Bay RIWP Phase I Sediment Investigation
- d 2005 USEPA-MPI High Res Sediment Core
- e 2006 HRSA RI Sampling Program
- g 1999-2006 Honeywell Intl Sampling
- i 2007 USEPA-MPI-EMBM Sediment Samples
- j 2007 USEPA-MPI Dundee High Res Core
- k 2007 Newark Bay Phase II TSI Sediment Samples
- 2008 CPG Low Resolution Sediment Coring
- m 2009 CPG Benthic Sediment Study
- o 2009 USEPA-MPI Benthic Oversight
- p 2010 CPG Benthic Sediment Sampling
- q 2010 USEPA-CDM Benthic Oversight
- 2011 CPG River Mile 10.9 Data
- r 2012 CDMSmith Background Benthic Sediment
- s 2012 CDMSmith Low Res Coring Supplemental
- t 2012 CPG Background Benthic Sediment
- v 2012 CPG Low Res Coring Supplemental
- u 2012 CPG River Mile 10.9 Data

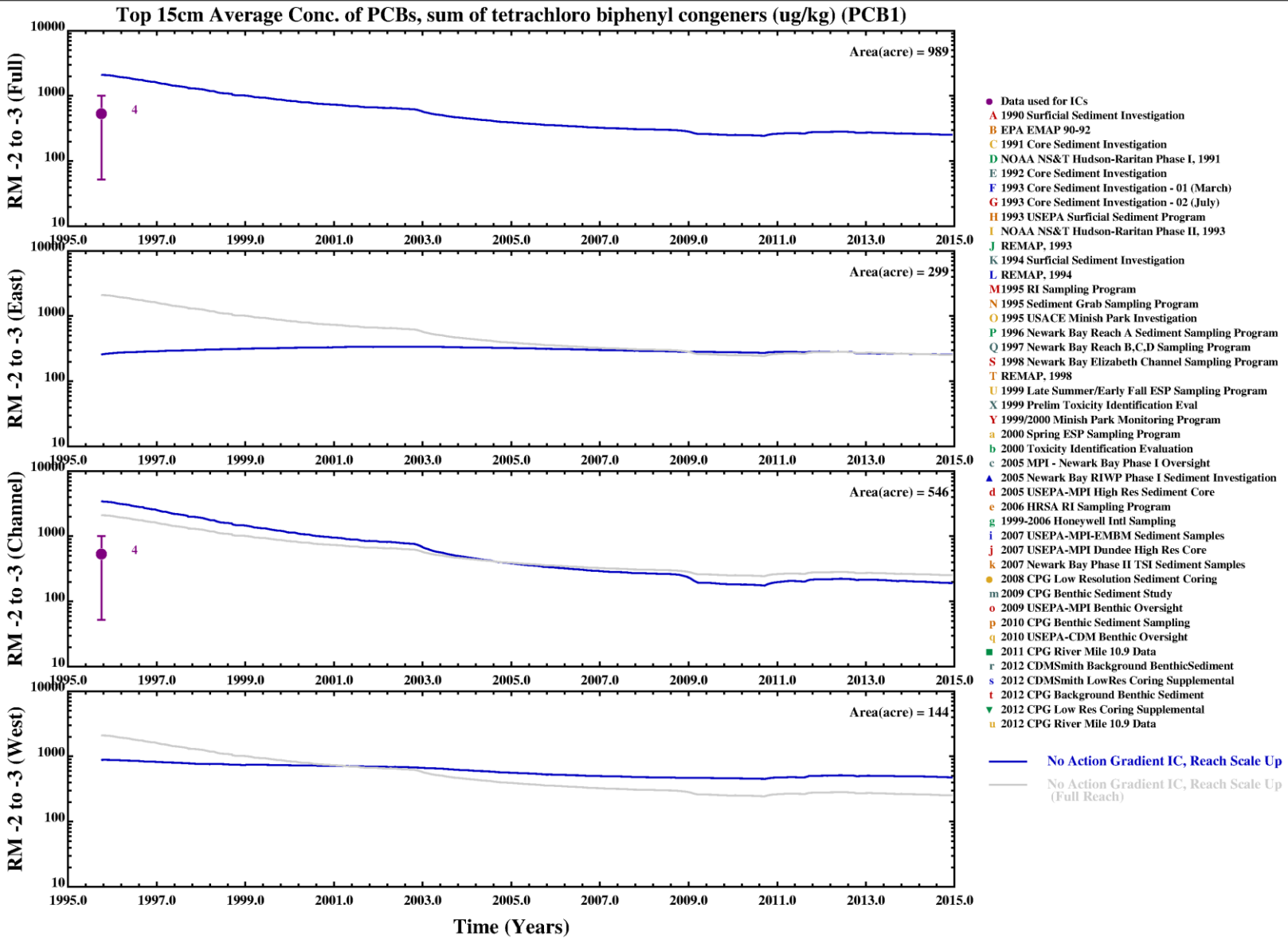
— No Action Gradient IC, Reach Scale Up
 — No Action Gradient IC, Reach Scale Up (Full Reach)

Tetrachlorobiphenyl Reach and Sub-reach Sediment Calibration (RM0 to -1.5)

Figure 4-38

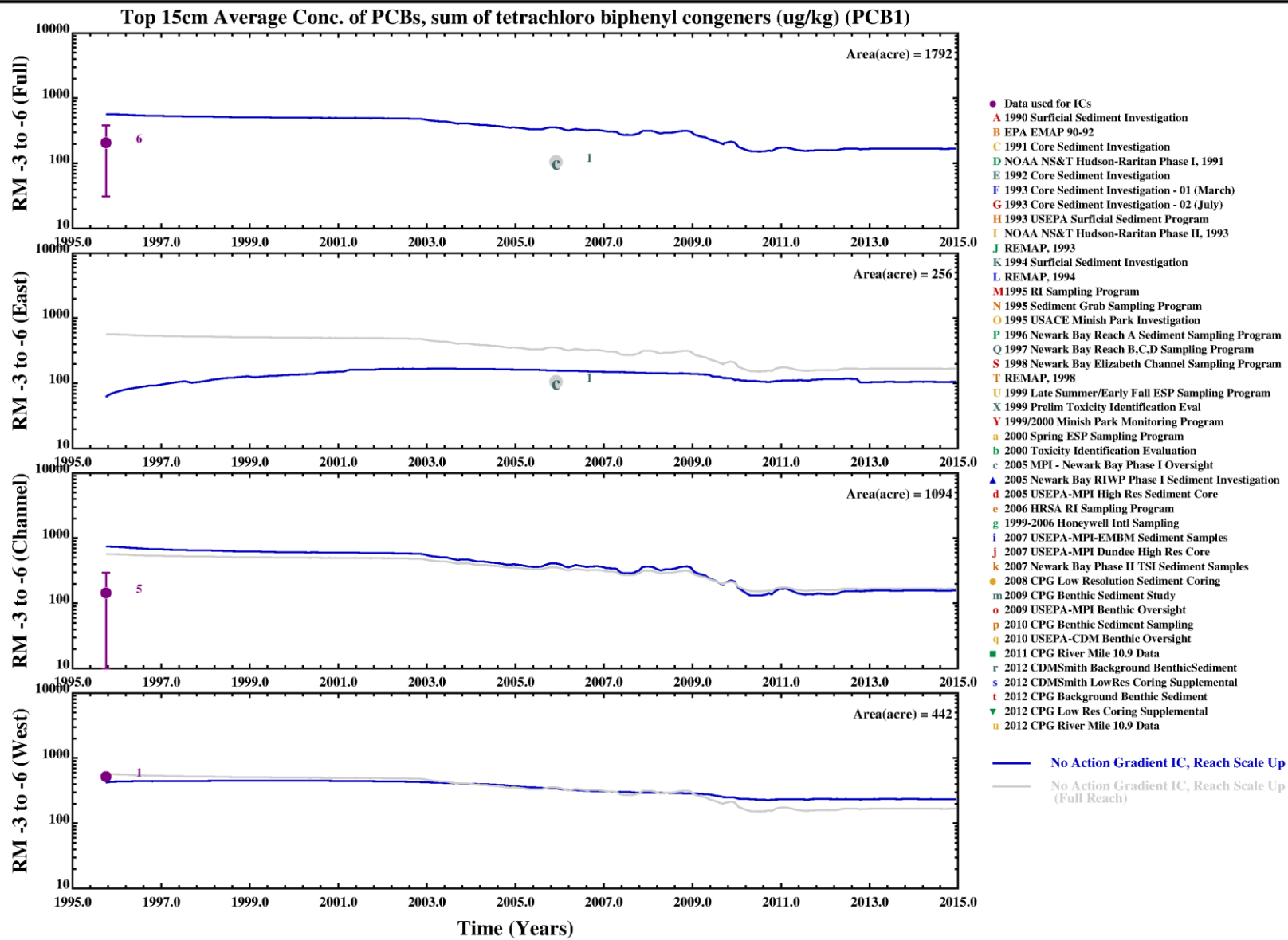
Lower Eight Miles of the Lower Passaic River

2014



Tetrachlorobiphenyl Reach and Sub-reach Sediment Calibration (RM-1.5 to -2.6)

Figure 4-39

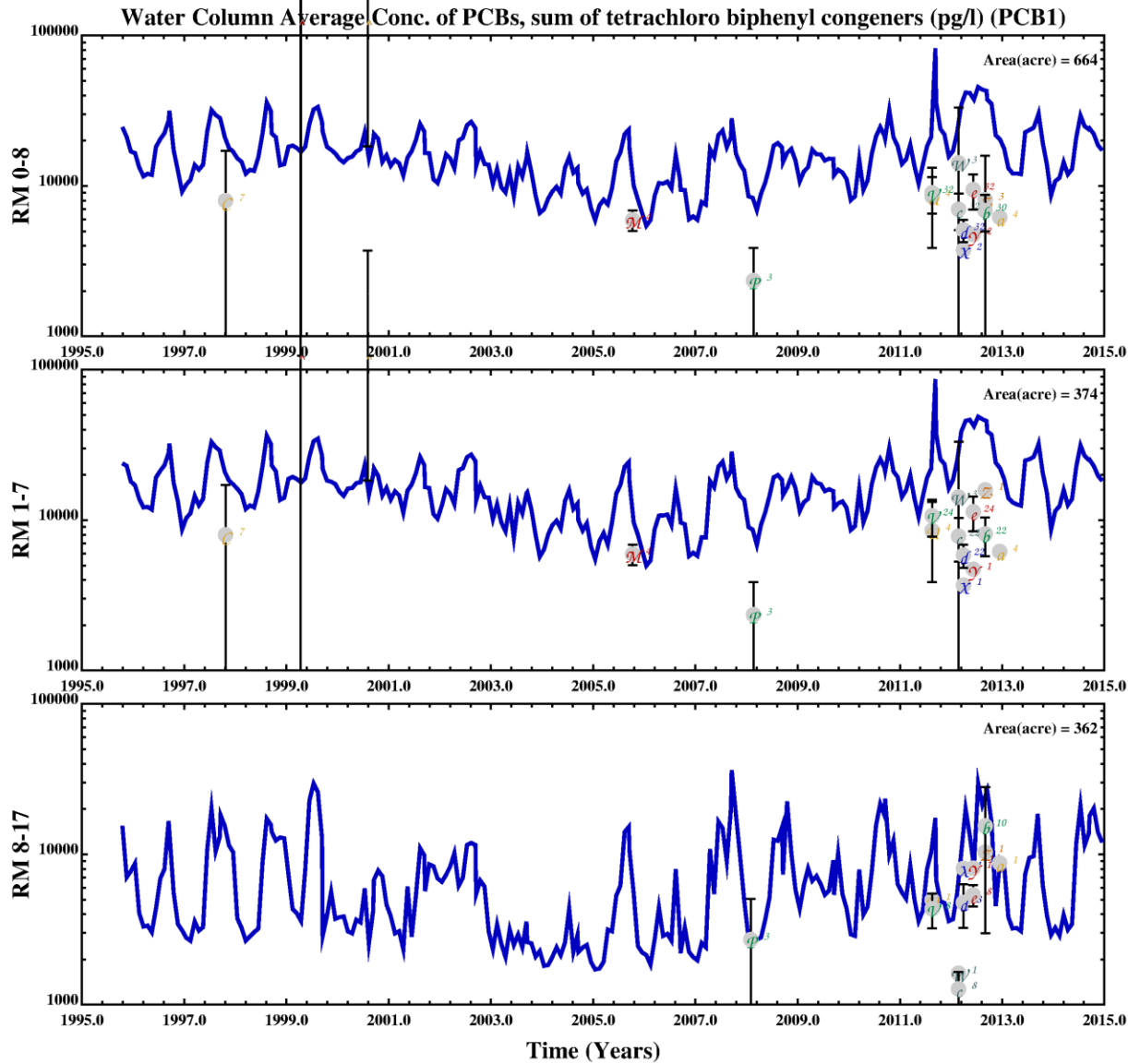


Tetrachlorobiphenyl Reach and Sub-reach Sediment Calibration (RM-2.6 to -5.25)

Lower Eight Miles of the Lower Passaic River

Figure 4-40

2014



- ▲ 1993-1997 USACE - DMDAT
- 1995-96 Passaic Study RI/FS Sed Mobility
- 1997 Outfall Sampling Program
- ◇ 1998-2001 CARP Database
- 1999 Newark Bay Reach A Monitoring
- 1999 Newark Bay Reach ABCD Baseline Sampling
- 1999 USACE Drift Removal Monitoring
- 1999-2006 Honeywell Intl Sampling
- 2000 Toxicity Identification Evaluation
- 2005 Hydrodynamic Mooring
- 2005 MPI SPMD Deployment
- 2005 USEPA-MPI High Flow Water Column
- 2005 USEPA-MPI Large Volume Study
- 2005 USEPA-MPI Small Volume Water Column
- 2005 USEPA-MPI Water Column Above RM 8.5
- 2007 USEPA-MPI-EMBM Water Column Sample
- 2009 CPG LPR Water Column Monitoring DEC
- 2010 CPG LPR-NB PWCM Field Measurements
- 2010 CPG LPR-NB PWCM Sample Dataset
- 2010 USEPA LBG-CDM PWCM Oversight
- 2011 CDM Smith CWCM Sampling Data
- 2011 CPG CWCM Sampling Data
- 2012 CDM Smith CWCM Sampling - Round 2
- 2012 CDM Smith CWCM Sampling - Round 3
- 2012 CDM Smith CWCM Sampling - Round 4
- 2012 CDM Smith CWCM Sampling - Round 5
- 2012 CDM Smith CWCM Sampling Round - 6
- 2012 CPG CWCM Sampling - Low Flow
- 2012 CPG CWCM Sampling - Round 2
- 2012 CPG CWCM Sampling - Round 3
- 2012 CPG CWCM Sampling - Round 4

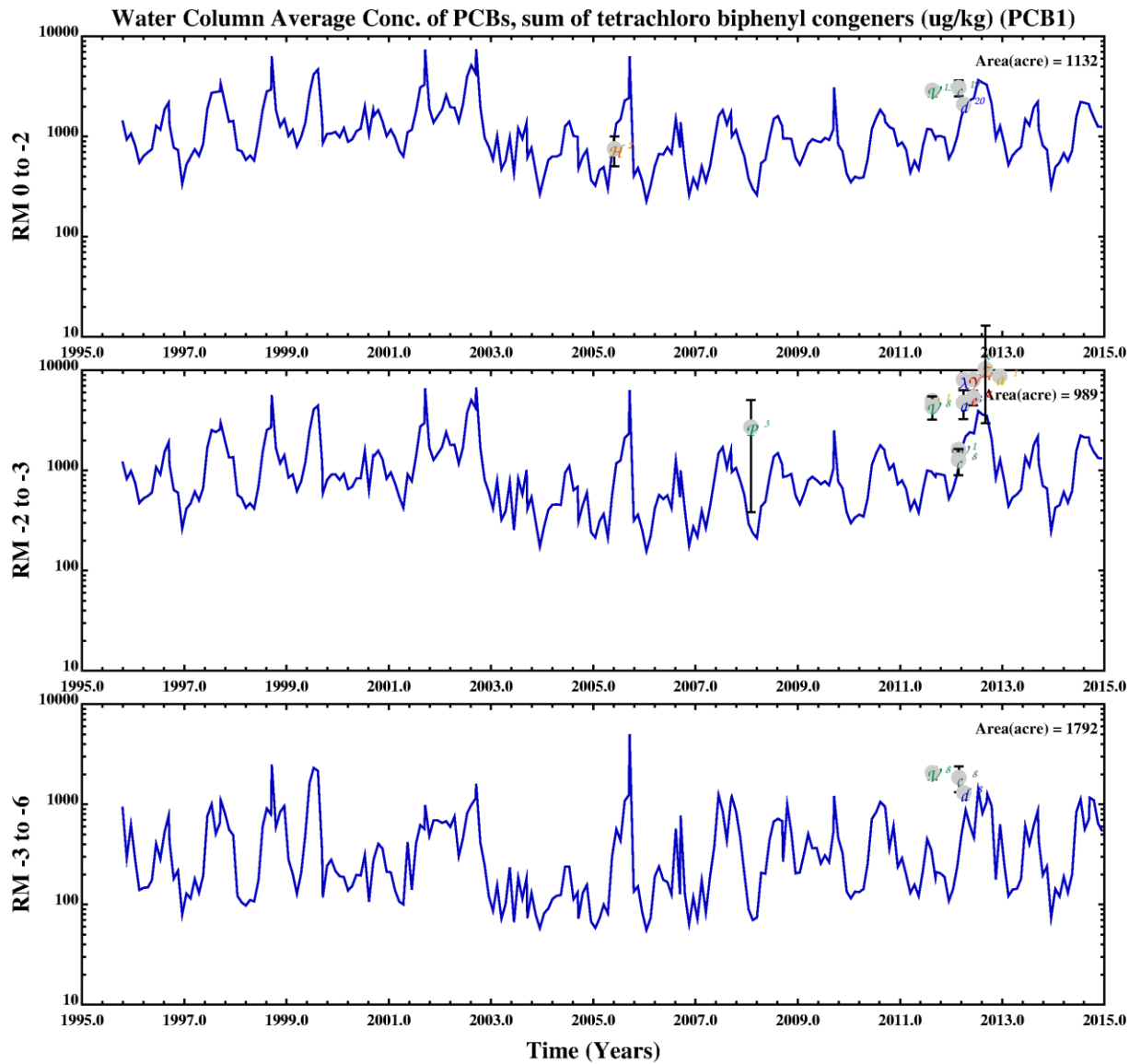
— No Action Gradient IC, Reach Scale Up

Tetrachlorobiphenyl Reach Water Column Calibration LPR

Figure 4-41

Lower Eight Miles of the Lower Passaic River

2014



- A 1993-1997 USACE - DMDAT
- B 1995-96 Passaic Study RIFS Sed Mobility
- C 1997 Outfall Sampling Program
- D 1998-2001 CARP Database
- E 1999 Newark Bay Reach A Monitoring
- F 1999 Newark Bay Reach ABCD Baseline Sampling
- G 1999 USACE Drift Removal Monitoring
- H 1999-2006 Honeywell Intl Sampling
- I 2000 Toxicity Identification Evaluation
- J 2005 Hydrodynamic Mooring
- K 2005 MPI SPMD Deployment
- L 2005 USEPA-MPI High Flow Water Column
- M 2005 USEPA-MPI Large Volume Study
- N 2005 USEPA-MPI Small Volume Water Column
- O 2005 USEPA-MPI Water Column Above RM 8.5
- P 2007 USEPA-MPI-EMBM Water Column Sample
- Q 2009 CPG LPR Water Column Monitoring DEC
- R 2010 CPG LPR-NB PWCM Field Measurements
- S 2010 CPG LPR-NB PWCM Sample Dataset
- T 2010 USEPA LBG-CDM PWCM Oversight
- U 2011 CDM Smith CWCM Sampling Data
- V 2011 CPG CWCM Sampling Data
- W 2012 CDM Smith CWCM Sampling - Round 2
- X 2012 CDM Smith CWCM Sampling - Round 3
- Y 2012 CDM Smith CWCM Sampling - Round 4
- Z 2012 CDM Smith CWCM Sampling - Round 5
- a 2012 CDM Smith CWCM Sampling Round - 6
- b 2012 CPG CWCM Sampling - Low Flow
- c 2012 CPG CWCM Sampling - Round 2
- d 2012 CPG CWCM Sampling - Round 3
- e 2012 CPG CWCM Sampling - Round 4

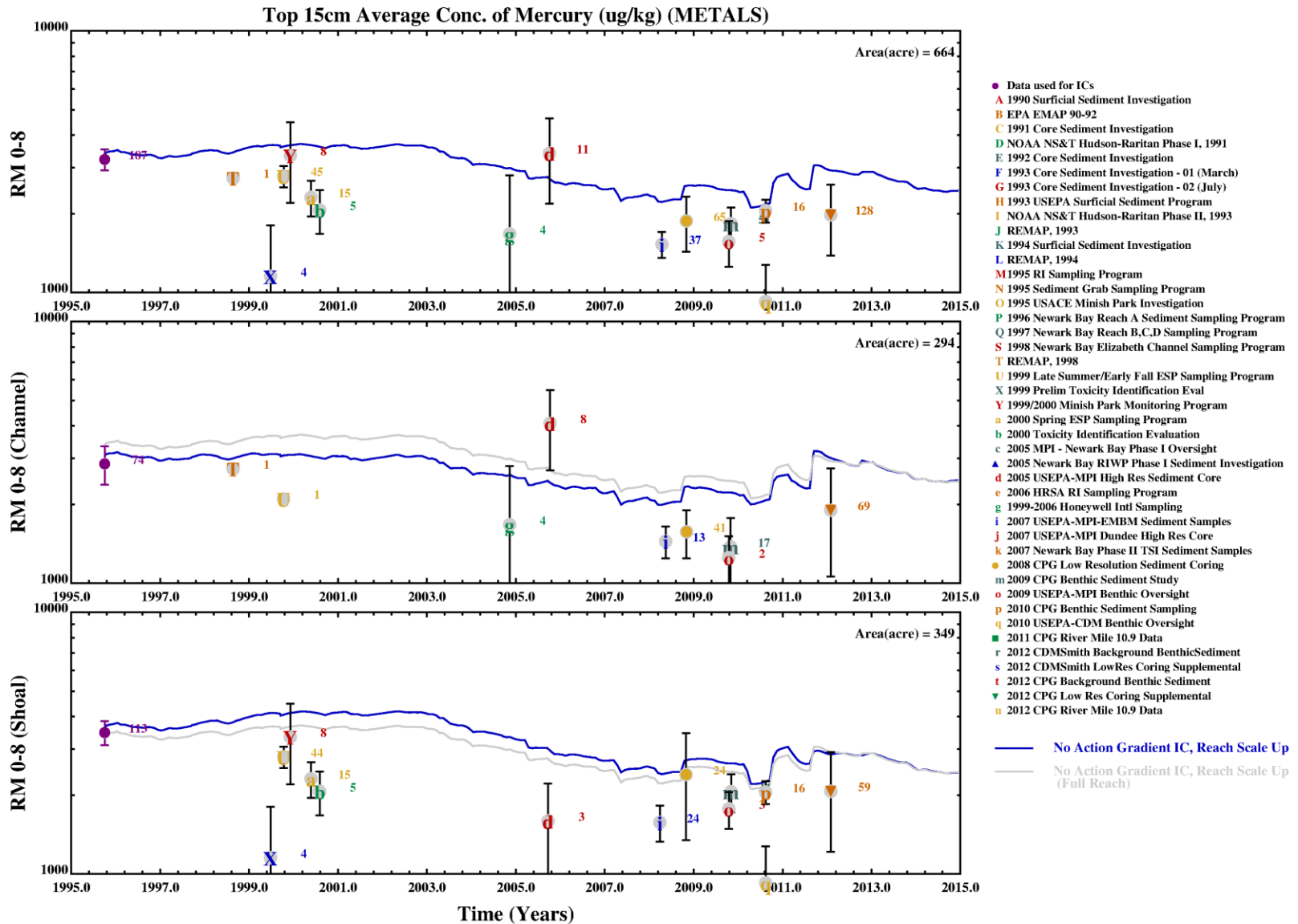
— No Action Gradient IC, Reach Scale Up

Tetrachlorobiphenyl Reach Water Column Calibration Newark Bay

Figure 4-42

Lower Eight Miles of the Lower Passaic River

2014

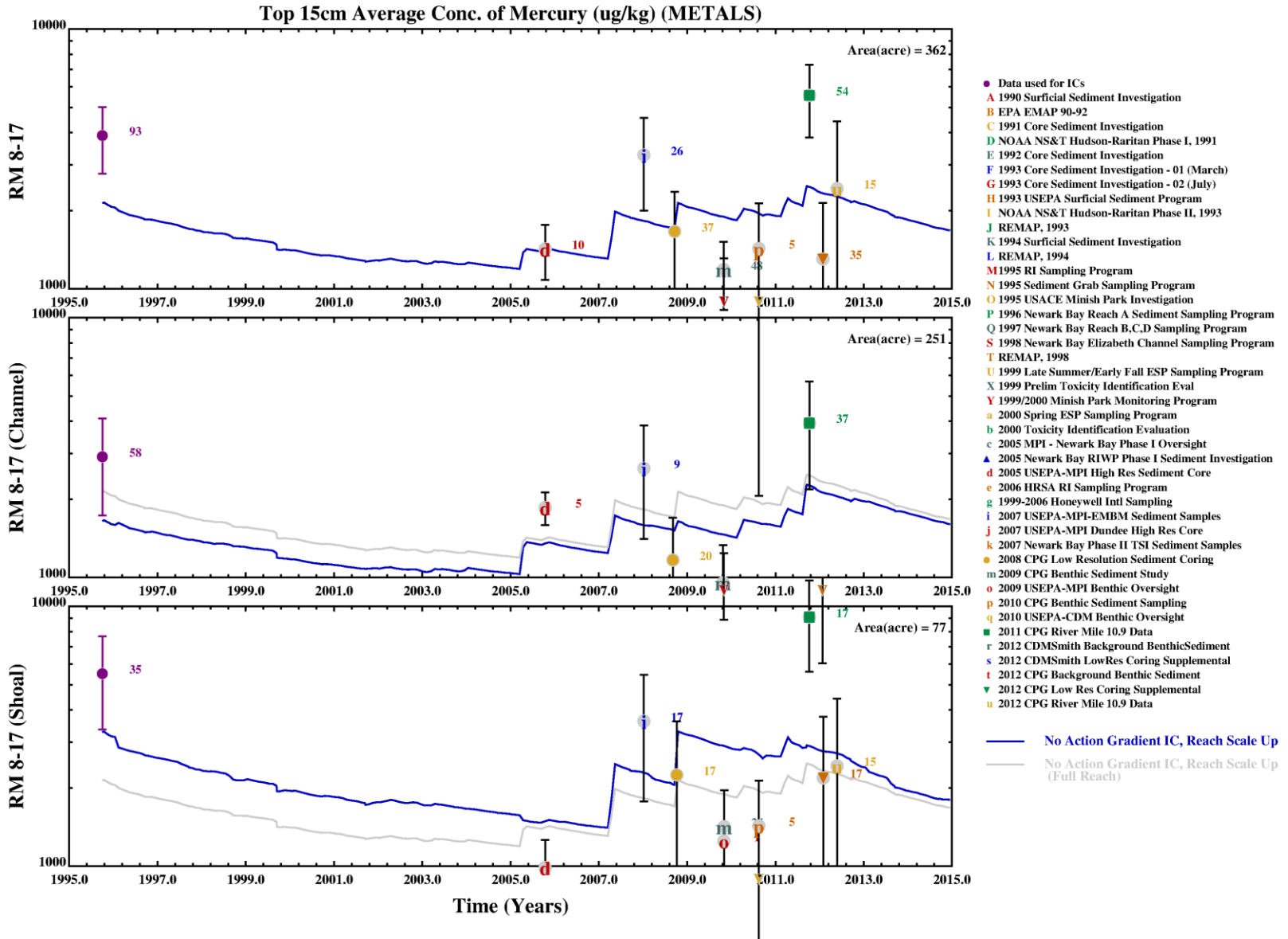


Mercury Reach and Sub-reach Sediment Calibration (RM0 to 8.3)

Lower Eight Miles of the Lower Passaic River

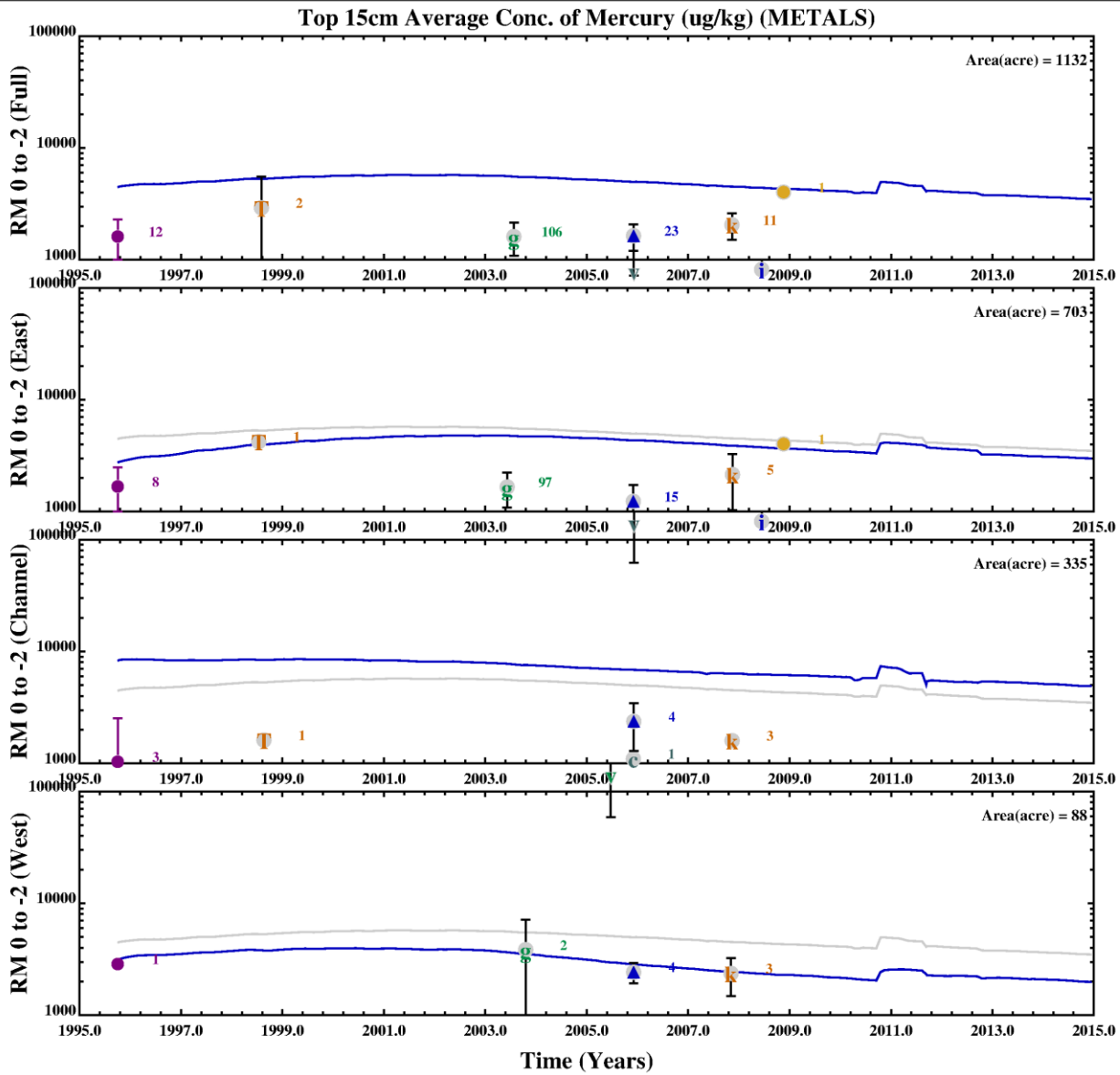
Figure 4-43

2014



Mercury Reach and Sub-reach Sediment Calibration (RM8.3 to 17)

Figure 4-44



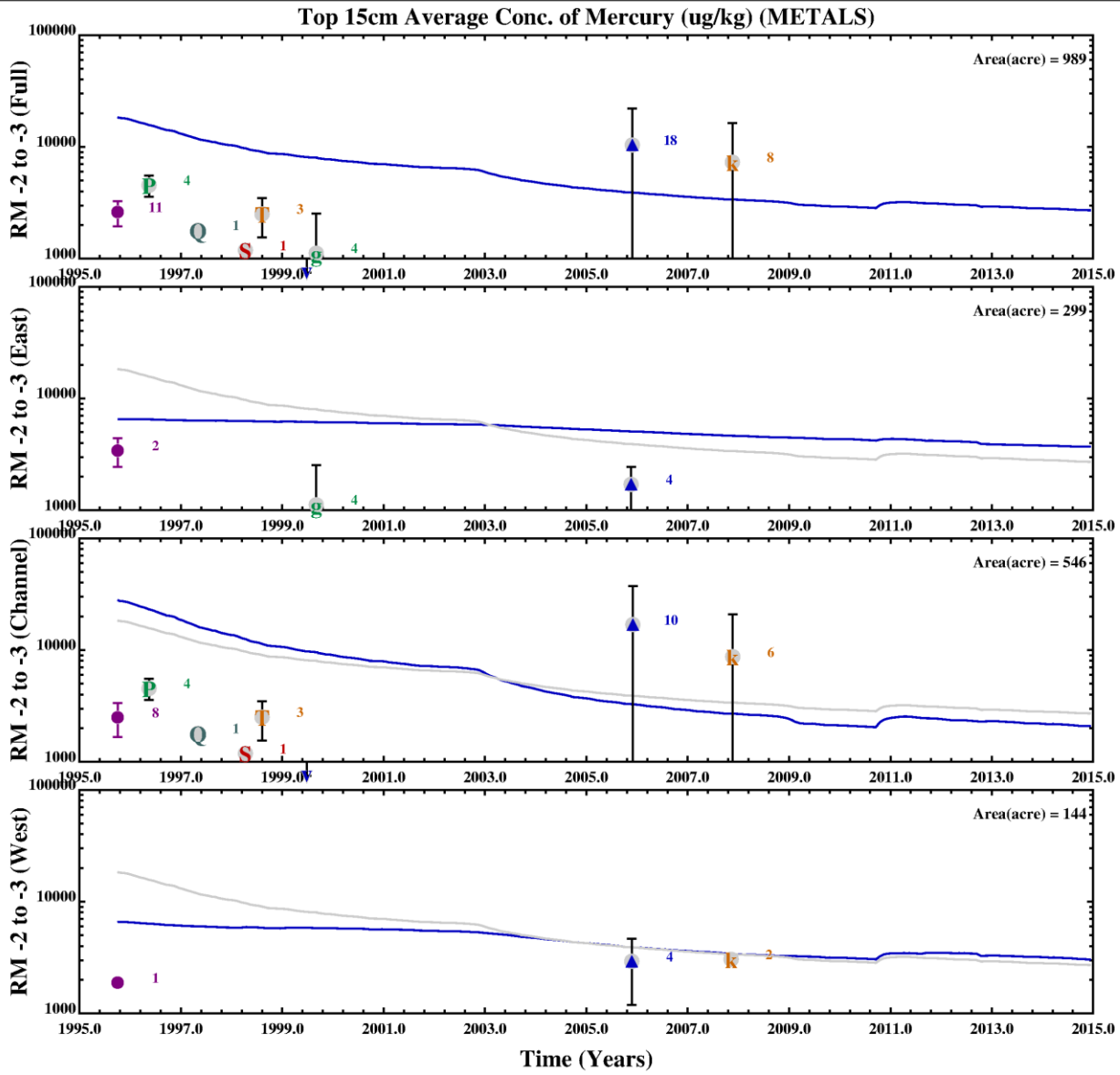
- Data used for ICs
 - A 1990 Surficial Sediment Investigation
 - B EPA EMAP 90-92
 - C 1991 Core Sediment Investigation
 - D NOAA NS&T Hudson-Raritan Phase I, 1991
 - E 1992 Core Sediment Investigation
 - F 1993 Core Sediment Investigation - 01 (March)
 - G 1993 Core Sediment Investigation - 02 (July)
 - H 1993 USEPA Surficial Sediment Program
 - I NOAA NS&T Hudson-Raritan Phase II, 1993
 - J REMAP, 1993
 - K 1994 Surficial Sediment Investigation
 - L REMAP, 1994
 - M 1995 RI Sampling Program
 - N 1995 Sediment Grab Sampling Program
 - O 1995 USACE Minish Park Investigation
 - P 1996 Newark Bay Reach A Sediment Sampling Program
 - Q 1997 Newark Bay Reach B,C,D Sampling Program
 - S 1998 Newark Bay Elizabeth Channel Sampling Program
 - T REMAP, 1998
 - U 1999 Late Summer/Early Fall ESP Sampling Program
 - X 1999 Prelim Toxicity Identification Eval
 - Y 1999/2000 Minish Park Monitoring Program
 - a 2000 Spring ESP Sampling Program
 - b 2000 Toxicity Identification Evaluation
 - c 2005 MPI - Newark Bay Phase I Oversight
 - ▲ 2005 Newark Bay RIWP Phase I Sediment Investigation
 - d 2005 USEPA-MPI High Res Sediment Core
 - e 2006 HRSA RI Sampling Program
 - g 1999-2006 Honeywell Intl Sampling
 - i 2007 USEPA-MPI-EMBM Sediment Samples
 - j 2007 USEPA-MPI Dundee High Res Core
 - k 2007 Newark Bay Phase II TSI Sediment Samples
 - 2008 CPG Low Resolution Sediment Coring
 - m 2009 CPG Benthic Sediment Study
 - o 2009 USEPA-MPI Benthic Oversight
 - p 2010 CPG Benthic Sediment Sampling
 - q 2010 USEPA-CDM Benthic Oversight
 - 2011 CPG River Mile 10.9 Data
 - r 2012 CDMSmith Background Benthic Sediment
 - s 2012 CDMSmith Low Res Coring Supplemental
 - t 2012 CPG Background Benthic Sediment
 - ▼ 2012 CPG Low Res Coring Supplemental
 - u 2012 CPG River Mile 10.9 Data
- No Action Gradient IC, Reach Scale Up
- No Action Gradient IC, Reach Scale Up (Full Reach)

Mercury Reach and Sub-reach Sediment Calibration (RM0 to -1.5)

Figure 4-45

Lower Eight Miles of the Lower Passaic River

2014



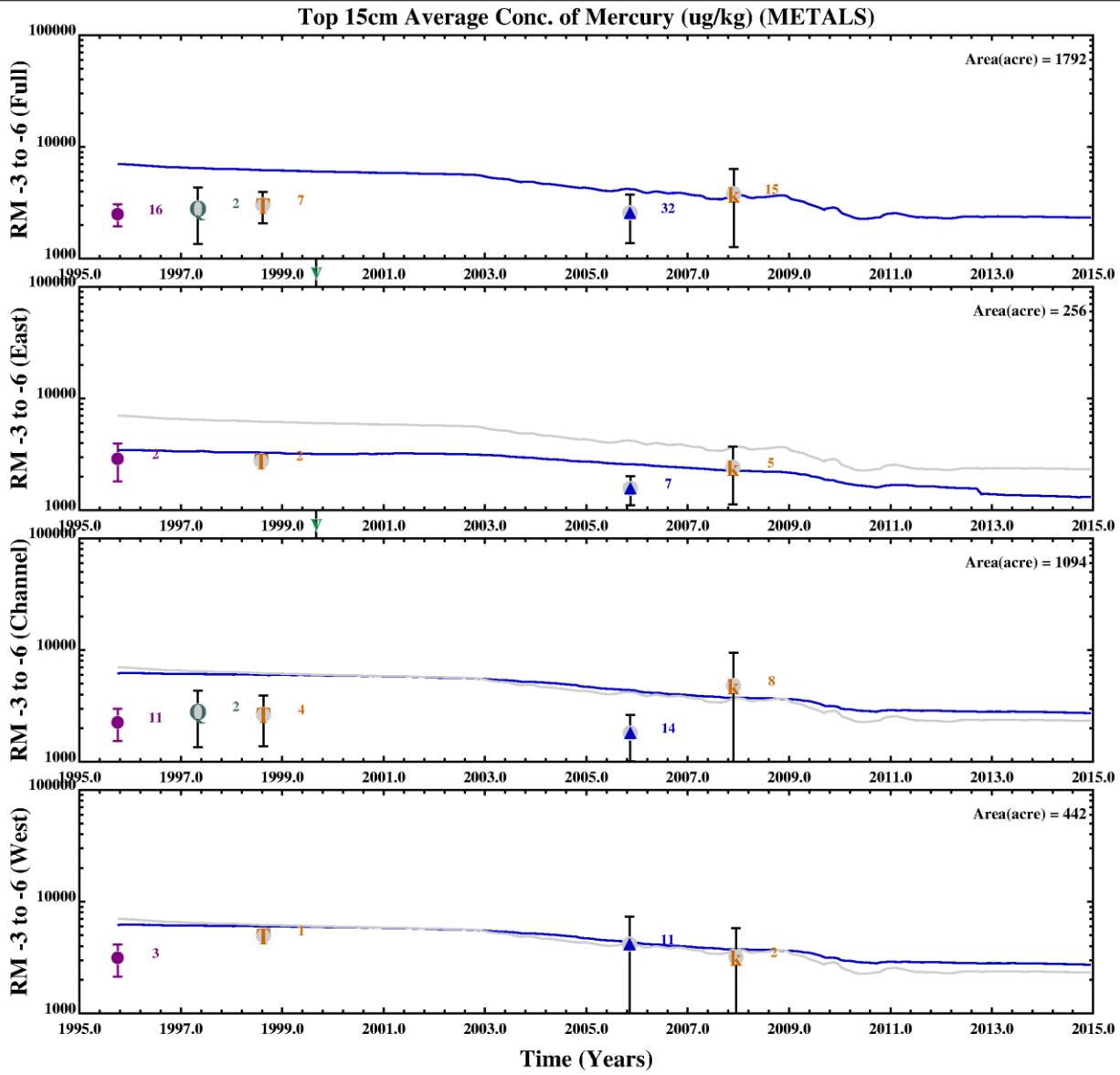
- Data used for ICs
 - A 1990 Surficial Sediment Investigation
 - B EPA EMAP 90-92
 - C 1991 Core Sediment Investigation
 - D NOAA NS&T Hudson-Raritan Phase I, 1991
 - E 1992 Core Sediment Investigation
 - F 1993 Core Sediment Investigation - 01 (March)
 - G 1993 Core Sediment Investigation - 02 (July)
 - H 1993 USEPA Surficial Sediment Program
 - I NOAA NS&T Hudson-Raritan Phase II, 1993
 - J REMAP, 1993
 - K 1994 Surficial Sediment Investigation
 - L REMAP, 1994
 - M 1995 RI Sampling Program
 - N 1995 Sediment Grab Sampling Program
 - O 1995 USACE Minish Park Investigation
 - P 1996 Newark Bay Reach A Sediment Sampling Program
 - Q 1997 Newark Bay Reach B,CD Sampling Program
 - S 1998 Newark Bay Elizabeth Channel Sampling Program
 - T REMAP, 1998
 - U 1999 Late Summer/Early Fall ESP Sampling Program
 - X 1999 Prelim Toxicity Identification Eval
 - Y 1999/2000 Minish Park Monitoring Program
 - a 2000 Spring ESP Sampling Program
 - b 2000 Toxicity Identification Evaluation
 - c 2005 MPI - Newark Bay Phase I Oversight
 - ▲ 2005 Newark Bay RIWP Phase I Sediment Investigation
 - d 2005 USEPA-MPI High Res Sediment Core
 - e 2006 HRSA RI Sampling Program
 - g 1999-2006 Honeywell Intl Sampling
 - i 2007 USEPA-MPI-EMBM Sediment Samples
 - j 2007 USEPA-MPI Dundee High Res Core
 - k 2007 Newark Bay Phase II TSI Sediment Samples
 - 2008 CPG Low Resolution Sediment Coring
 - m 2009 CPG Benthic Sediment Study
 - o 2009 USEPA-MPI Benthic Oversight
 - p 2010 CPG Benthic Sediment Sampling
 - q 2010 USEPA-CDM Benthic Oversight
 - 2011 CPG River Mile 10.9 Data
 - r 2012 CDMSmith Background BenthicSediment
 - s 2012 CDMSmith Low Res Coring Supplemental
 - t 2012 CPG Background Benthic Sediment
 - ▼ 2012 CPG Low Res Coring Supplemental
 - u 2012 CPG River Mile 10.9 Data
- No Action Gradient IC, Reach Scale Up
 — No Action Gradient IC, Reach Scale Up (Full Reach)

Mercury Reach and Sub-reach Sediment Calibration (RM-1.5 to -2.6)

Lower Eight Miles of the Lower Passaic River

Figure 4-46

2014



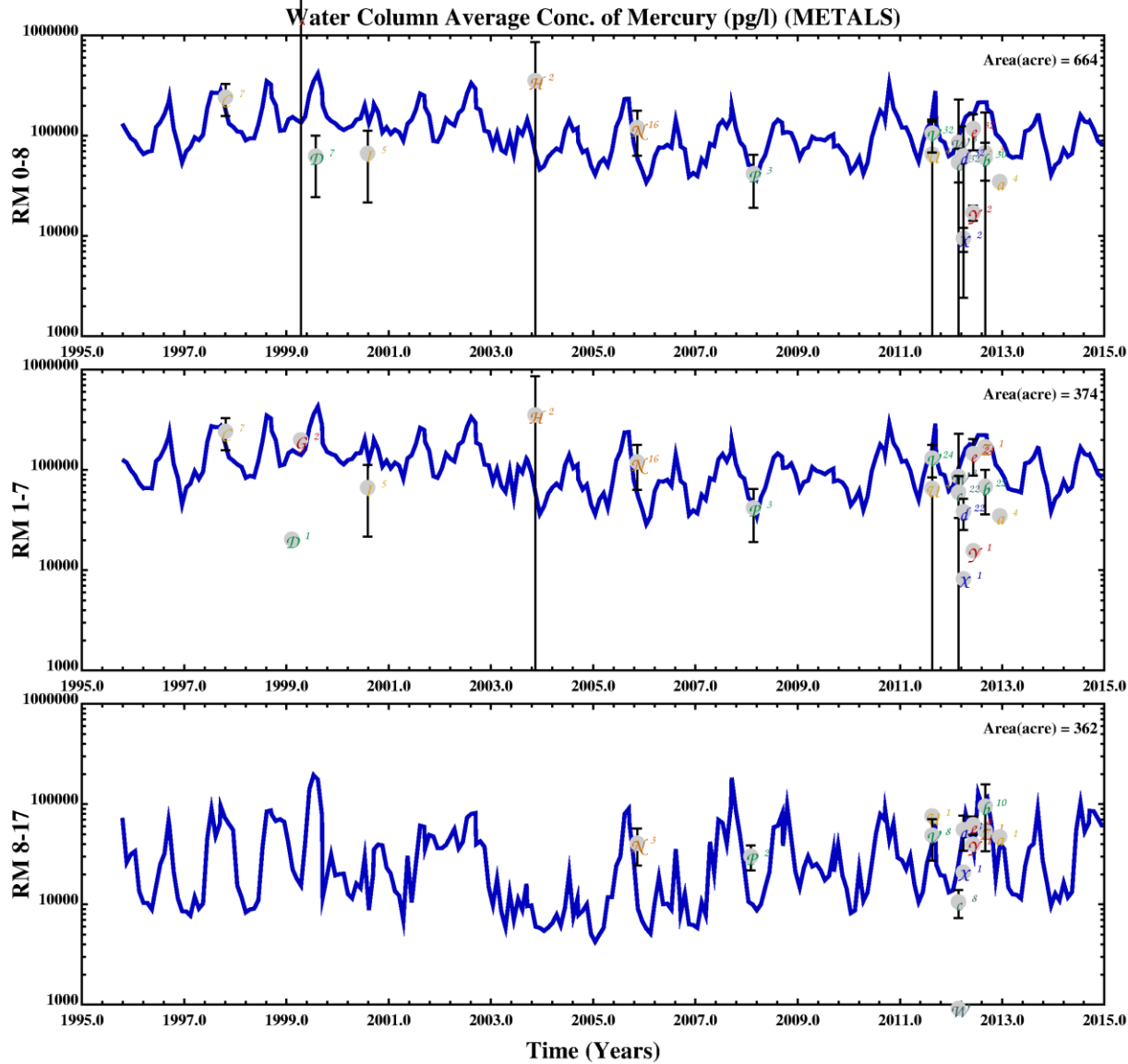
- Data used for ICs
 - A 1990 Surficial Sediment Investigation
 - B EPA EMAP 90-92
 - C 1991 Core Sediment Investigation
 - D NOAA NS&T Hudson-Raritan Phase I, 1991
 - E 1992 Core Sediment Investigation
 - F 1993 Core Sediment Investigation - 01 (March)
 - G 1993 Core Sediment Investigation - 02 (July)
 - H 1993 USEPA Surficial Sediment Program
 - I NOAA NS&T Hudson-Raritan Phase II, 1993
 - J REMAP, 1993
 - K 1994 Surficial Sediment Investigation
 - L REMAP, 1994
 - M 1995 RI Sampling Program
 - N 1995 Sediment Grab Sampling Program
 - O 1995 USACE Minish Park Investigation
 - P 1996 Newark Bay Reach A Sediment Sampling Program
 - Q 1997 Newark Bay Reach B,C,D Sampling Program
 - S 1998 Newark Bay Elizabeth Channel Sampling Program
 - T REMAP, 1998
 - U 1999 Late Summer/Early Fall ESP Sampling Program
 - X 1999 Prelim Toxicity Identification Eval
 - Y 1999/2000 Minish Park Monitoring Program
 - a 2000 Spring ESP Sampling Program
 - b 2000 Toxicity Identification Evaluation
 - c 2005 MPI - Newark Bay Phase I Oversight
 - ▲ 2005 Newark Bay RIWP Phase I Sediment Investigation
 - d 2005 USEPA-MPI High Res Sediment Core
 - e 2006 HRSA RI Sampling Program
 - g 1999-2006 Honeywell Intl Sampling
 - i 2007 USEPA-MPI-EMBM Sediment Samples
 - j 2007 USEPA-MPI Dundee High Res Core
 - k 2007 Newark Bay Phase II TSI Sediment Samples
 - 2008 CPG Low Resolution Sediment Coring
 - m 2009 CPG Benthic Sediment Study
 - o 2009 USEPA-MPI Benthic Oversight
 - p 2010 CPG Benthic Sediment Sampling
 - q 2010 USEPA-CDM Benthic Oversight
 - 2011 CPG River Mile 10.9 Data
 - r 2012 CDMSmith Background BenthicSediment
 - s 2012 CDMSmith Low Res Coring Supplemental
 - t 2012 CPG Background Benthic Sediment
 - ▼ 2012 CPG Low Res Coring Supplemental
 - u 2012 CPG River Mile 10.9 Data
- No Action Gradient IC, Reach Scale Up
- No Action Gradient IC, Reach Scale Up (Full Reach)

Mercury Reach and Sub-reach Sediment Calibration (RM-2.6 to -5.25)

Figure 4-47

Lower Eight Miles of the Lower Passaic River

2014



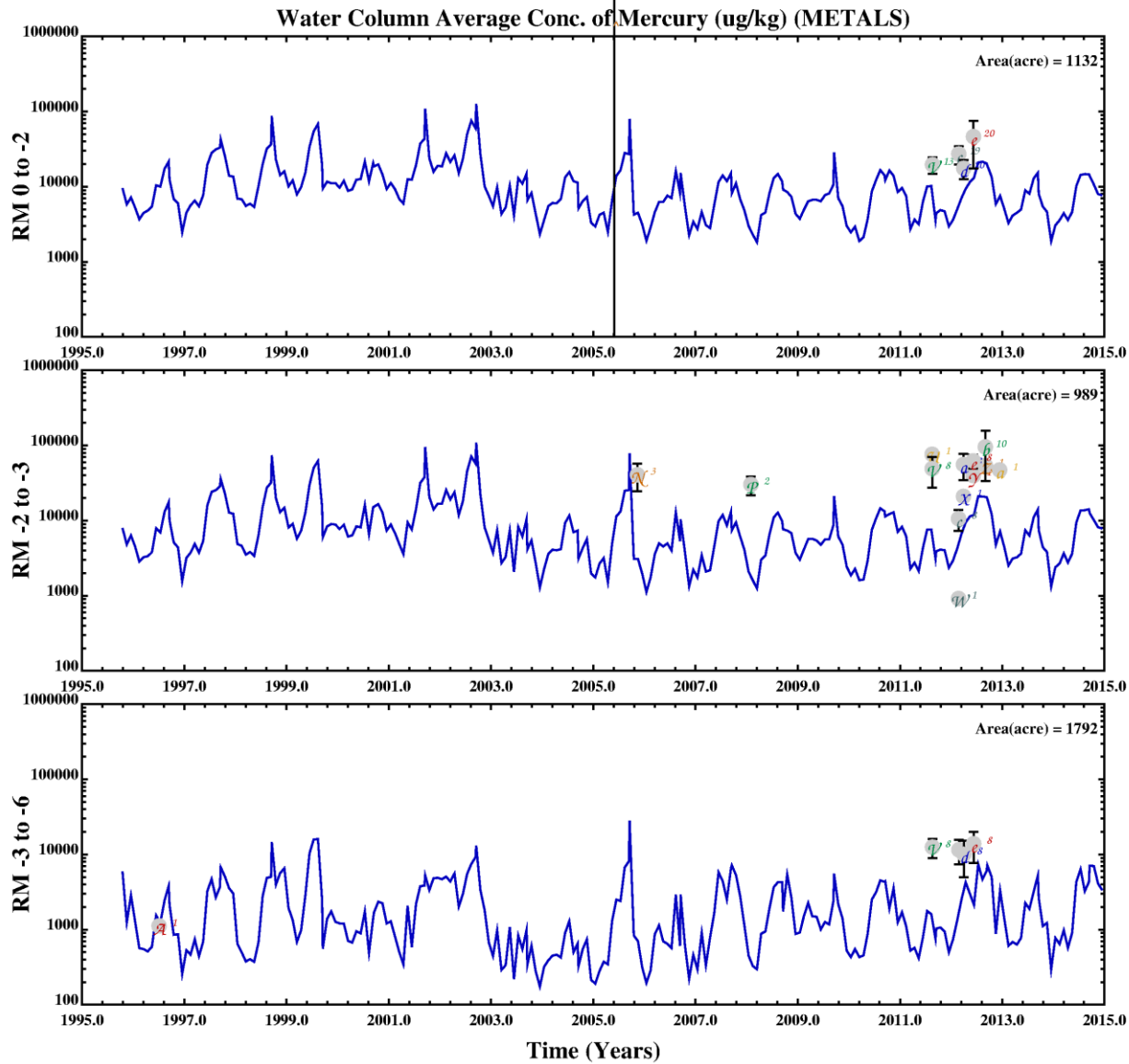
- 1993-1997 USACE - DMDAT
- 1995-96 Passaic Study RI/FIS Sed Mobility
- 1997 Outfall Sampling Program
- 1998-2001 CARP Database
- 1999 Newark Bay Reach A Monitoring
- 1999 NewarkBay ReachABCDBaselineSampling
- 1999 USACE Drift Removal Monitoring
- 1999-2006 Honeywell Intl Sampling
- 2000 Toxicity Identification Evaluation
- 2005 Hydrodynamic Mooring
- 2005 MPI SPMD Deployment
- 2005 USEPA-MPI High Flow Water Column
- 2005 USEPA-MPI Large Volume Study
- 2005 USEPA-MPI Small Volume Water Column
- 2005 USEPA-MPI Water Column Above RM 8.5
- 2007 USEPA-MPI-EMBM Water Column Sample
- 2009 CPG LPR Water Column Monitoring DEC
- 2010 CPG LPR-NB PWCM Field Measurements
- 2010 CPG LPR-NB PWCM Sample Dataset
- 2010 USEPA LBG-CDM PWCM Oversight
- 2011 CDM Smith CWCM Sampling Data
- 2011 CPG CWCM Sampling Data
- 2012 CDM Smith CWCM Sampling - Round 2
- 2012 CDM Smith CWCM Sampling - Round 3
- 2012 CDM Smith CWCM Sampling - Round 4
- 2012 CDM Smith CWCM Sampling - Round 5
- 2012 CDM Smith CWCM Sampling Round - 6
- 2012 CPG CWCM Sampling - Low Flow
- 2012 CPG CWCM Sampling - Round 2
- 2012 CPG CWCM Sampling - Round 3
- 2012 CPG CWCM Sampling - Round 4

Mercury Reach Water Column Calibration LPR

Lower Eight Miles of the Lower Passaic River

Figure 4-48

2014



- Ⓜ 1993-1997 USACE - DMDAT
- Ⓟ 1995-96 Passaic Study RI/FS Sed Mobility
- Ⓒ 1997 Outfall Sampling Program
- Ⓧ 1998-2001 CARP Database
- Ⓢ 1999 Newark Bay Reach A Monitoring
- Ⓝ 1999 Newark Bay Reach ABCD Baseline Sampling
- Ⓓ 1999 USACE Drift Removal Monitoring
- Ⓜ 1999-2006 Honeywell Intl Sampling
- Ⓛ 2000 Toxicity Identification Evaluation
- Ⓜ 2005 Hydrodynamic Mooring
- Ⓧ 2005 MPI SPMD Deployment
- Ⓛ 2005 USEPA-MPI High Flow Water Column
- Ⓜ 2005 USEPA-MPI Large Volume Study
- Ⓧ 2005 USEPA-MPI Small Volume Water Column
- Ⓞ 2005 USEPA-MPI Water Column Above RM 8.5
- Ⓢ 2007 USEPA-MPI-EMBM Water Column Sample
- Ⓚ 2009 CPG LPR Water Column Monitoring DEC
- Ⓧ 2010 CPG LPR-NB PWCM Field Measurements
- Ⓢ 2010 CPG LPR-NB PWCM Sample Dataset
- Ⓢ 2010 USEPA LBG-CDM PWCM Oversight
- Ⓚ 2011 CDM Smith CWCM Sampling Data
- Ⓜ 2011 CPG CWCM Sampling Data
- Ⓜ 2012 CDM Smith CWCM Sampling - Round 2
- Ⓧ 2012 CDM Smith CWCM Sampling - Round 3
- Ⓜ 2012 CDM Smith CWCM Sampling - Round 4
- Ⓢ 2012 CDM Smith CWCM Sampling - Round 5
- Ⓜ 2012 CDM Smith CWCM Sampling Round - 6
- Ⓛ 2012 CPG CWCM Sampling - Low Flow
- Ⓢ 2012 CPG CWCM Sampling - Round 2
- Ⓞ 2012 CPG CWCM Sampling - Round 3
- Ⓢ 2012 CPG CWCM Sampling - Round 4

— No Action Gradient IC, Reach Scale Up

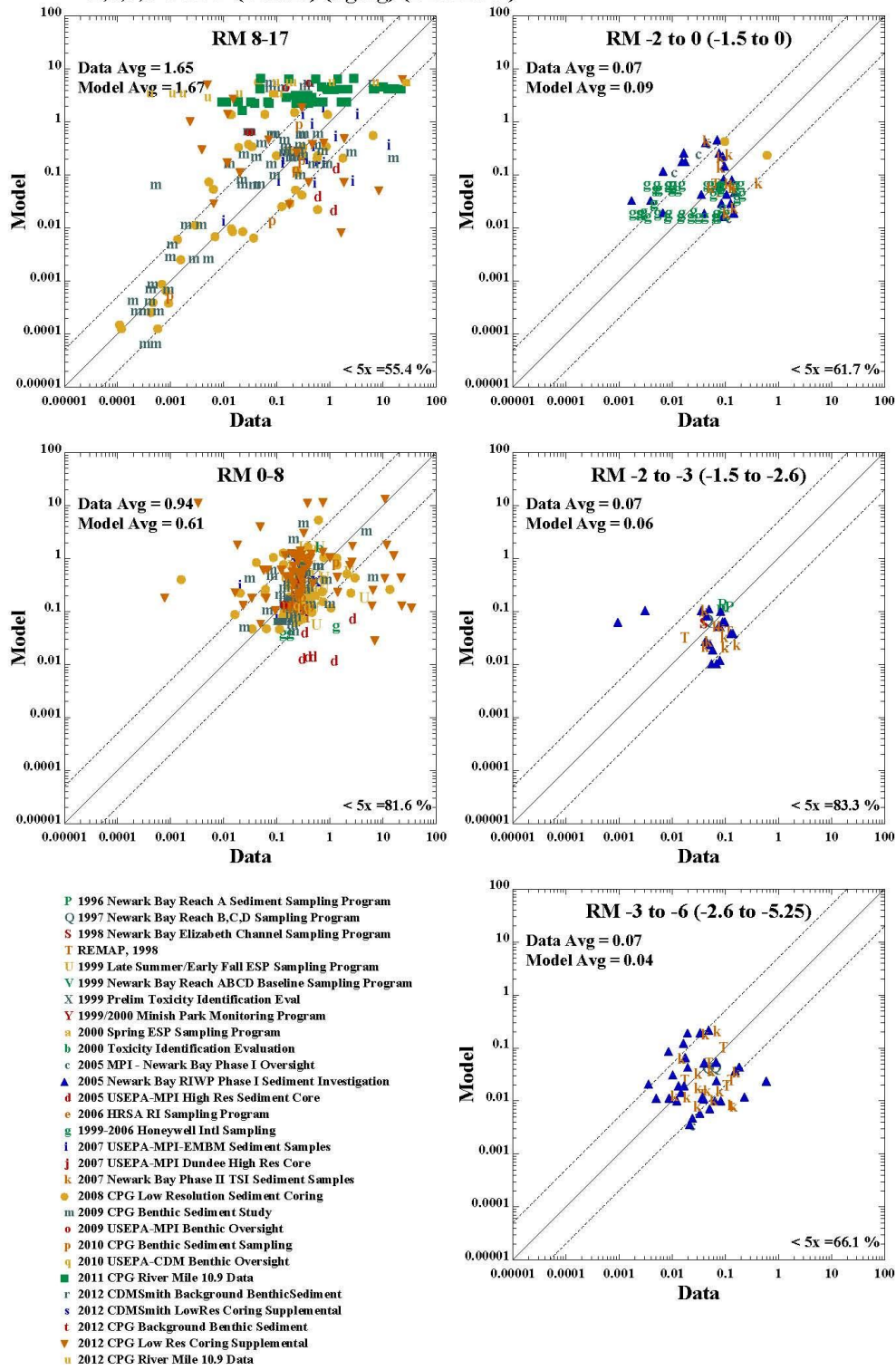
Mercury Reach Water Column Calibration Newark Bay

Figure 4-49

Lower Eight Miles of the Lower Passaic River

2014

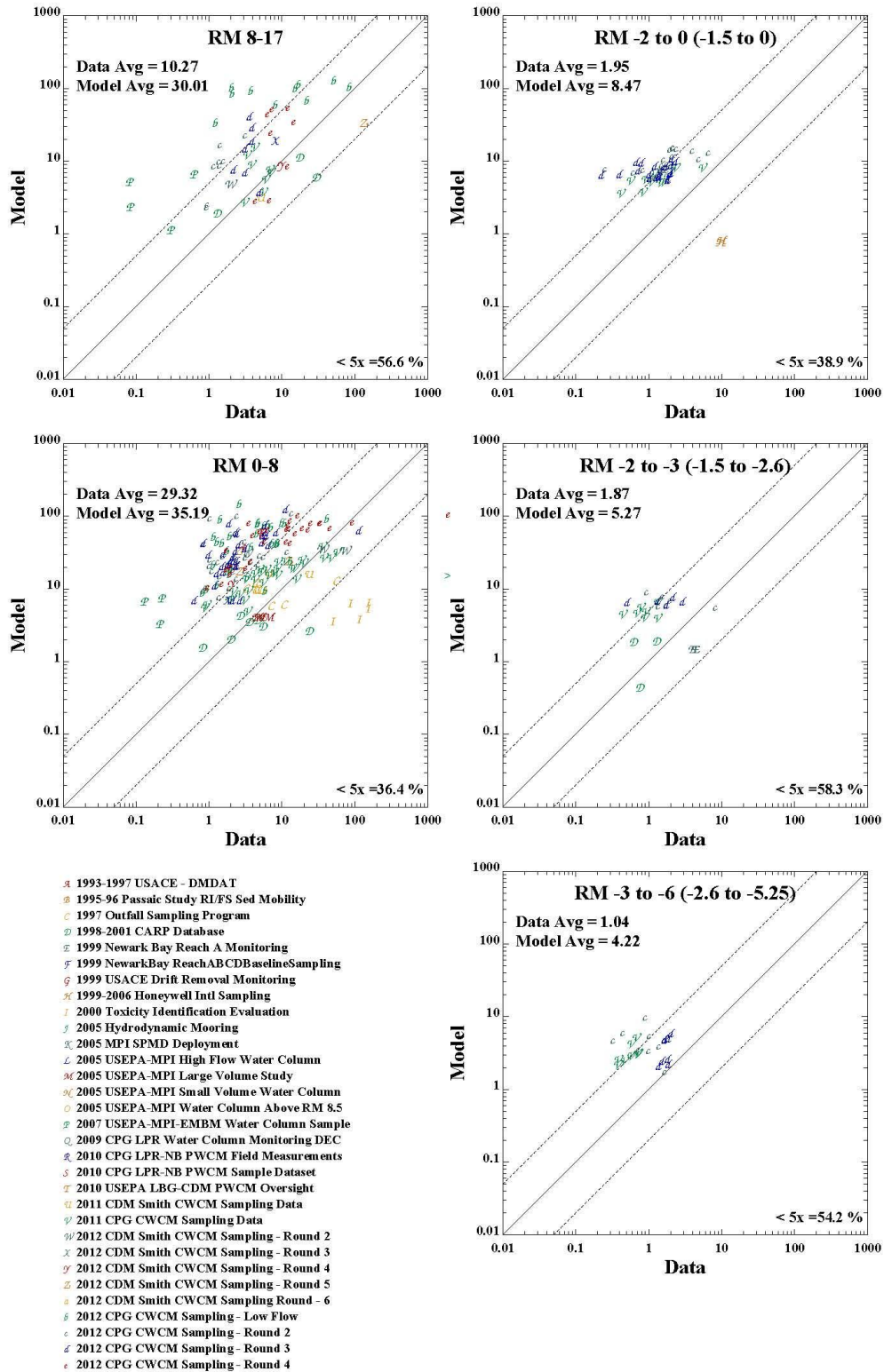
**Top 15cm Average Conc.
2,3,7,8-TCDD (Dioxin) (ug/kg) (DIOXIN1)**



2,3,7,8-TCDD Sediment Data and Model Scatter Plots

Figure 4-50

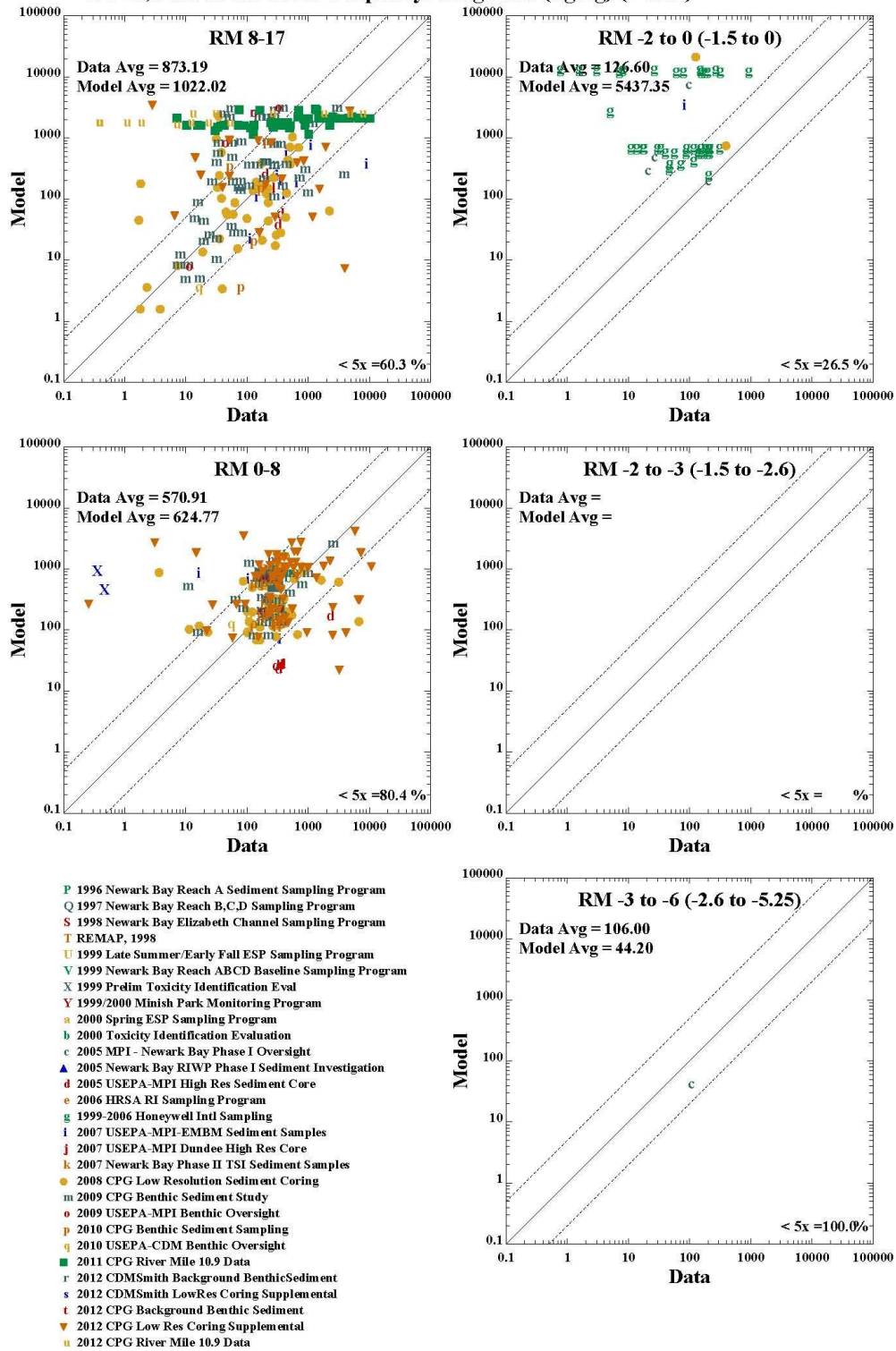
All Layers 2,3,7,8-TCDD (Dioxin) (pg/L) (DIOXIN1)



2,3,7,8-TCDD Water Column Data and Model Scatter Plots

Figure 4-51

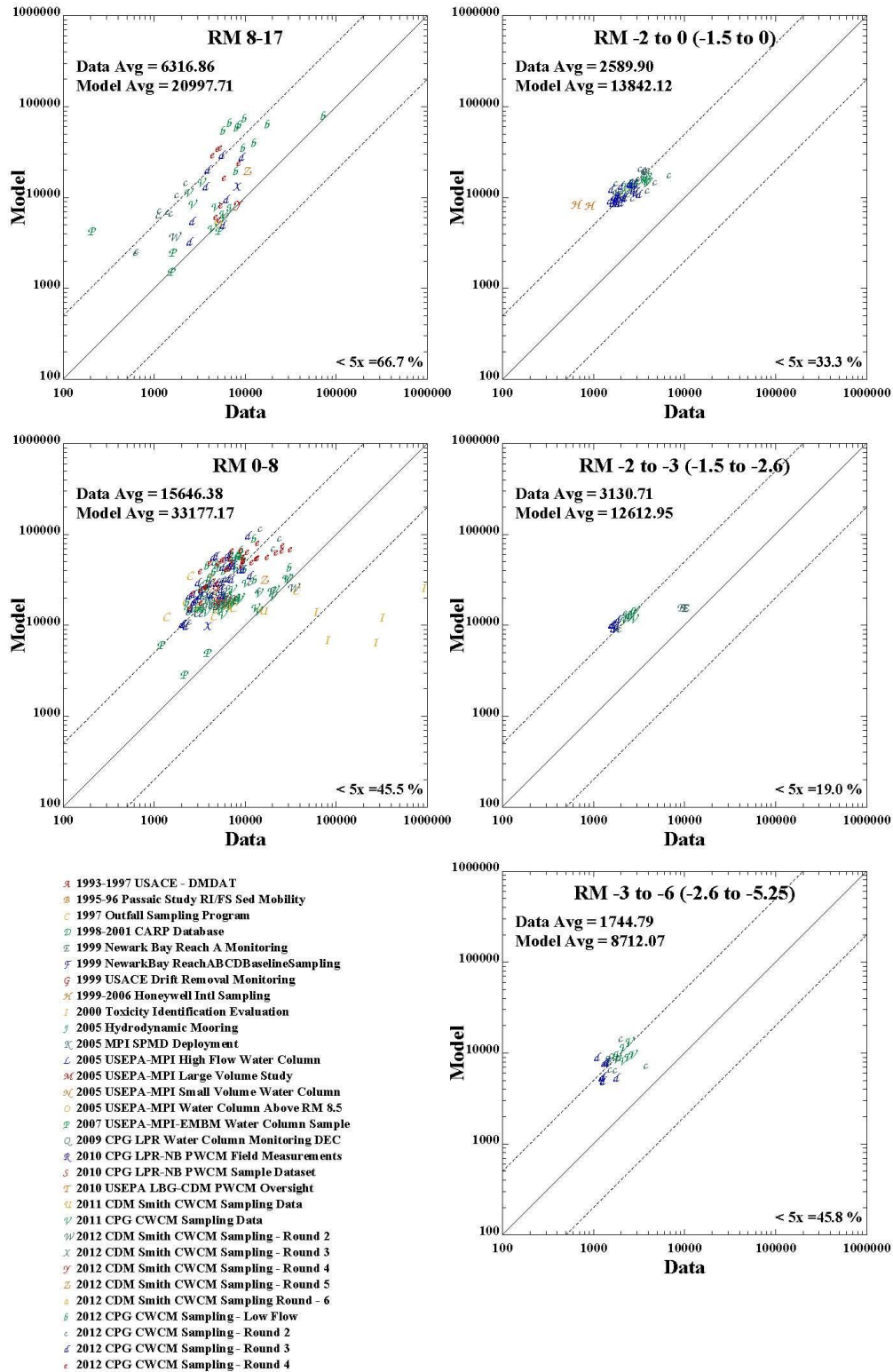
**Top 15cm Average Conc.
PCBs, sum of tetrachloro biphenyl congeners (ug/kg) (PCB1)**



Tetrachlorobiphenyl Sediment Data and Model Scatter Plots

Figure 4-52

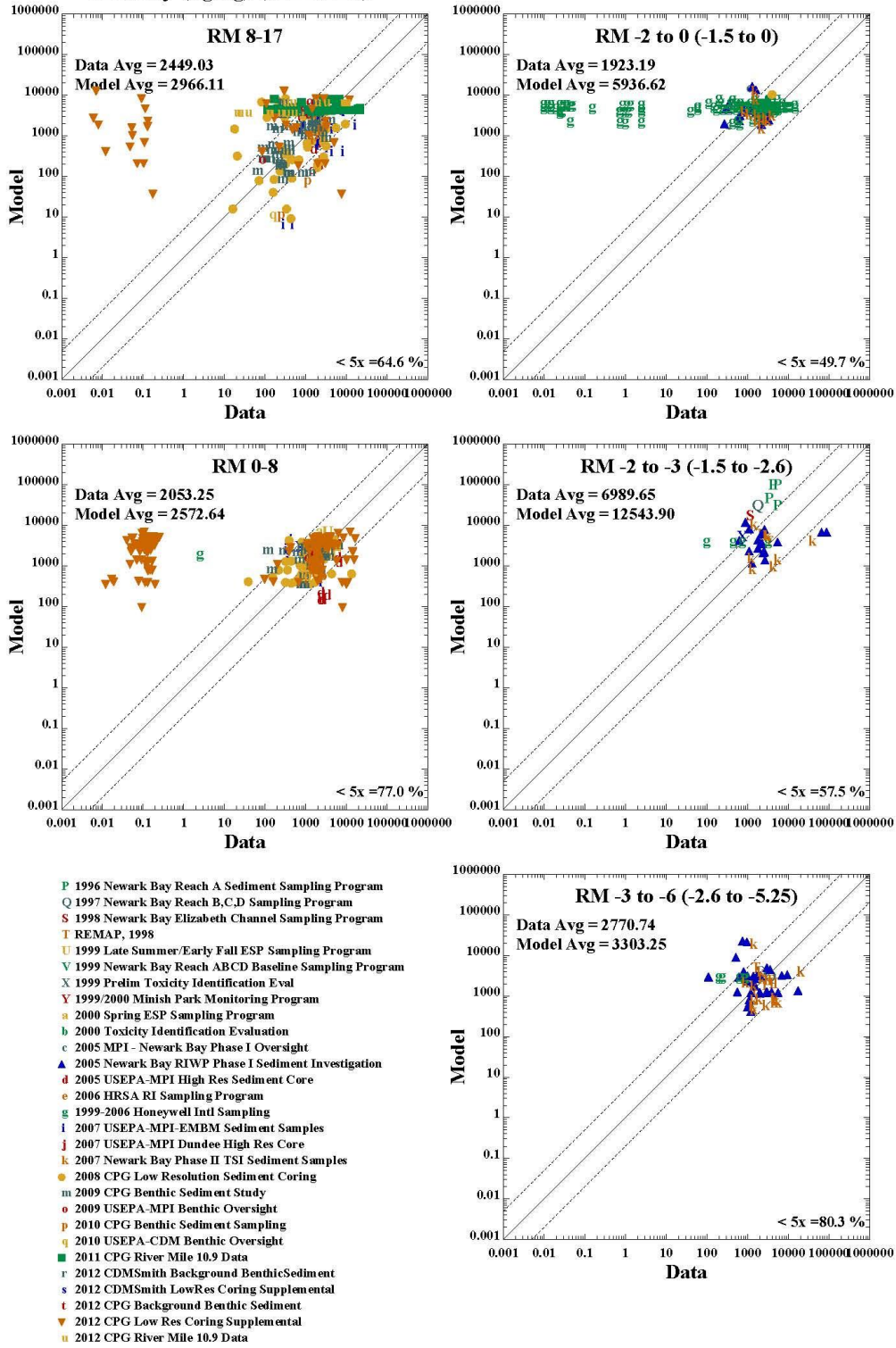
All Layers PCBs, sum of tetrachloro biphenyl congeners (pg/L) (PCB1)



Tetrachlorobiphenyl Water Column Data and Model Scatter Plots

Figure 4-53

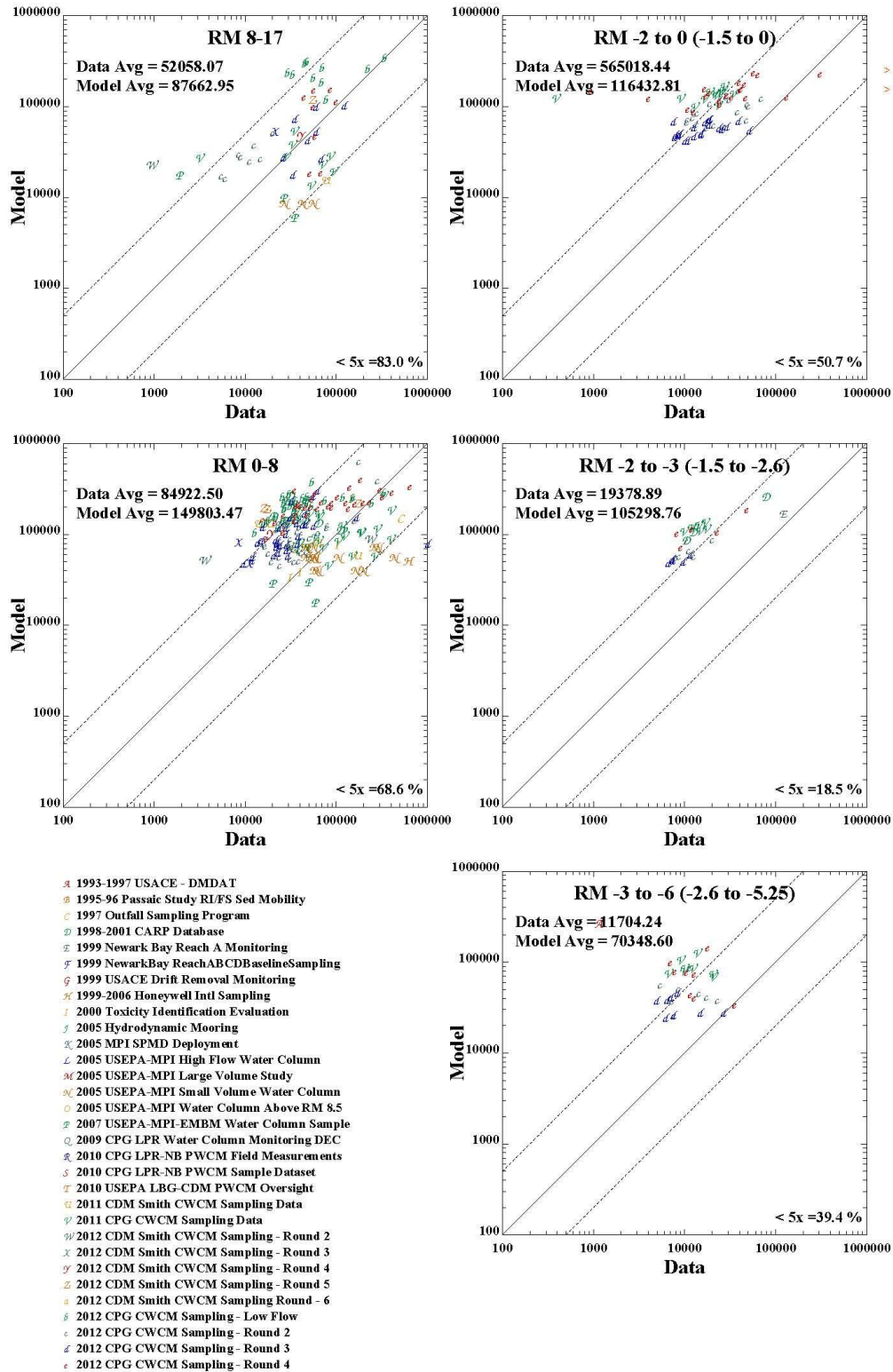
**Top 15cm Average Conc.
Mercury (ug/kg) (METALS)**



Mercury Sediment Data and Model Scatter Plots

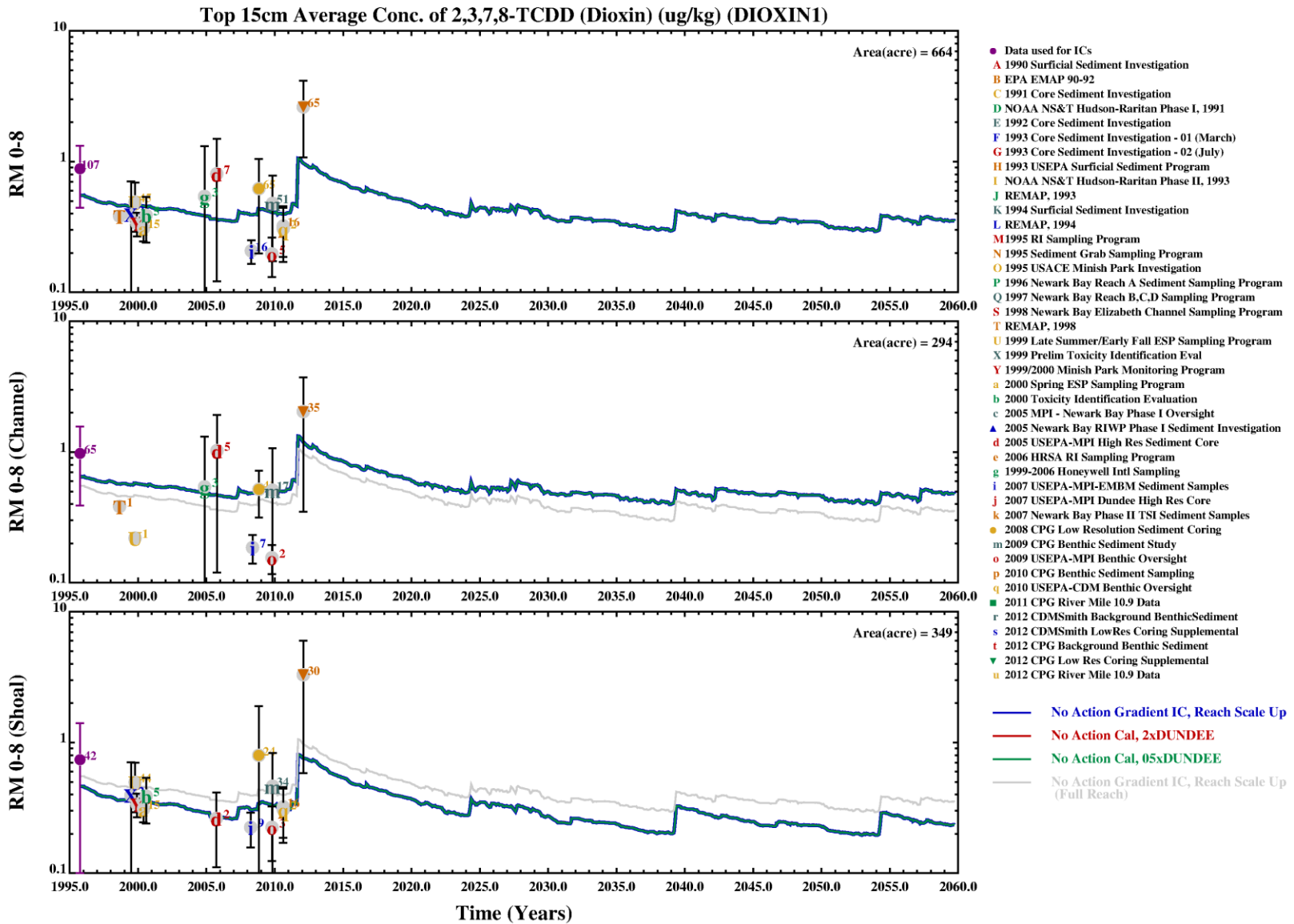
Figure 4-54

All Layers Mercury (pg/L) (METALS)



Mercury Water Column Data and Model Scatter Plots

Figure 4-55

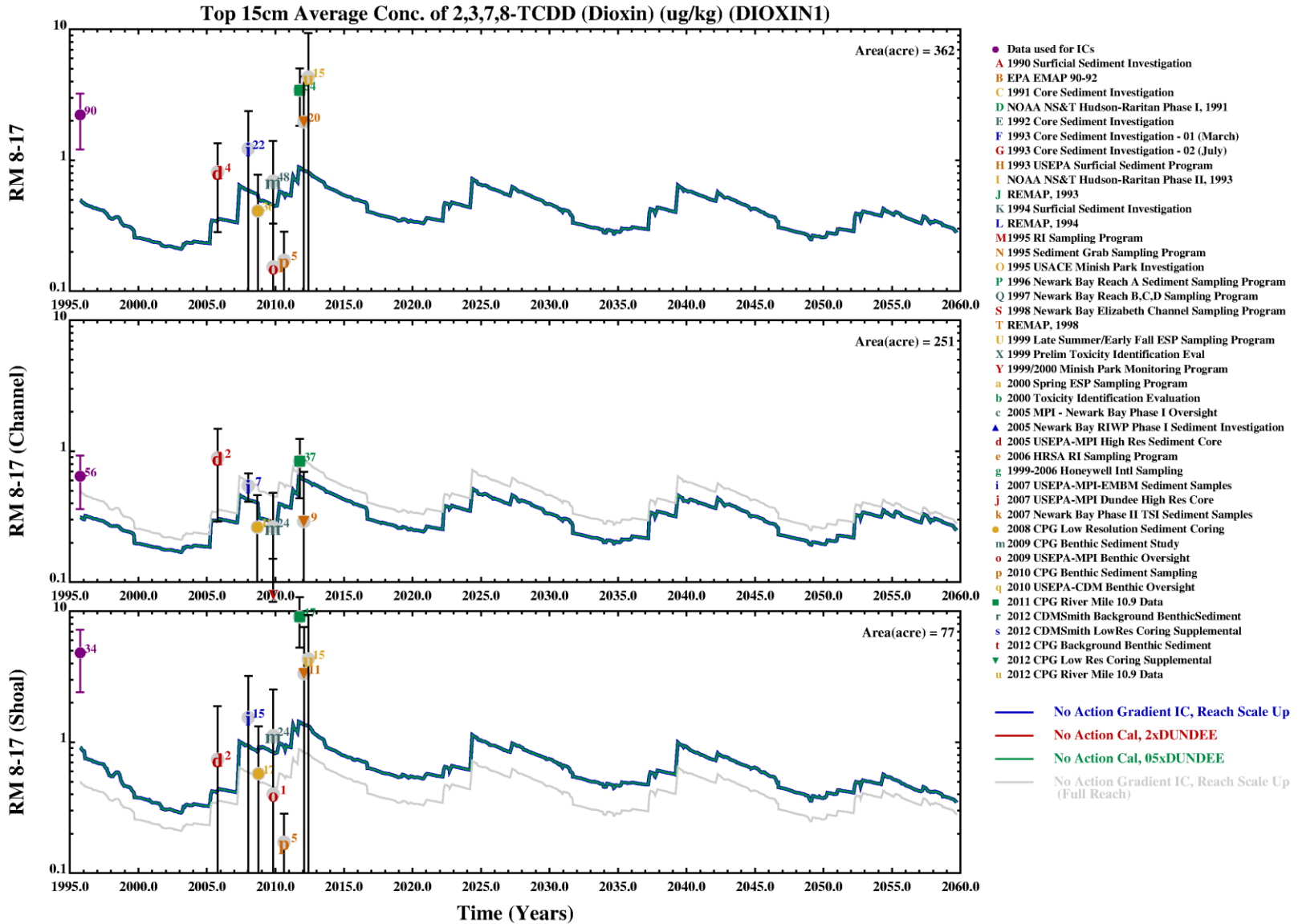


Sediment 2,3,7,8-TCCD Response to Dundee Dam Sensitivity (RM0-8.3)

Lower Eight Miles of the Lower Passaic River

Figure 5-1

2014

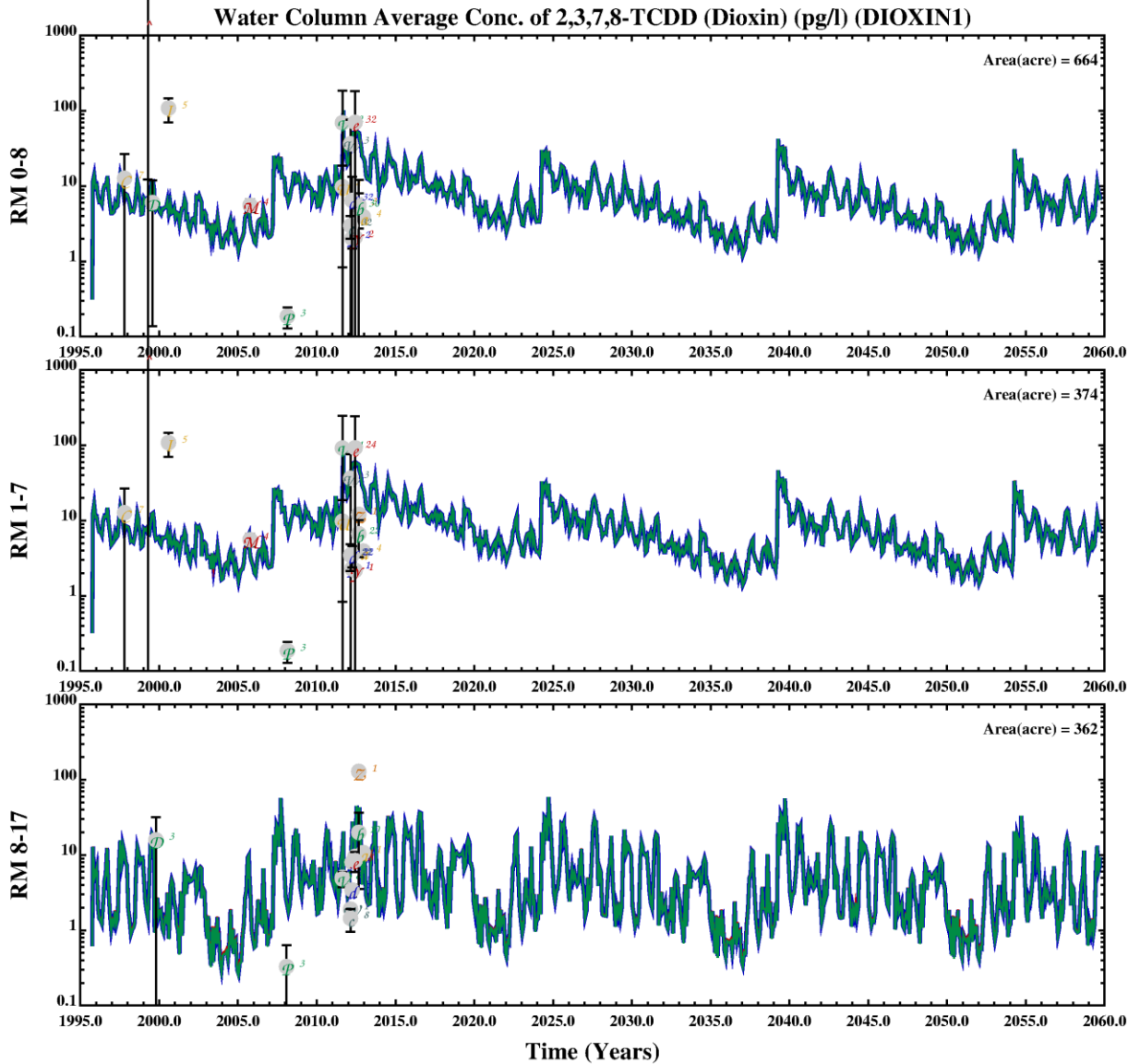


Sediment 2,3,7,8-TCCD Response to Dundee Dam Sensitivity (RM8.3-17)

Lower Eight Miles of the Lower Passaic River

Figure 5-2

2014



- A 1993-1997 USACE - DMDAT
- B 1995-96 Passaic Study RI/FS Sed Mobility
- C 1997 Outfall Sampling Program
- D 1998-2001 CARP Database
- E 1999 Newark Bay Reach A Monitoring
- F 1999 Newark Bay Reach ABCDBaseline Sampling
- G 1999 USACE Drift Removal Monitoring
- H 1999-2006 Honeywell Intl Sampling
- I 2000 Toxicity Identification Evaluation
- J 2005 Hydrodynamic Mooring
- K 2005 MPLSPMD Deployment
- L 2005 USEPA-MPI High Flow Water Column
- M 2005 USEPA-MPI Large Volume Study
- N 2005 USEPA-MPI Small Volume Water Column
- O 2005 USEPA-MPI Water Column Above RM 8.5
- P 2007 USEPA-MPI-EMBM Water Column Sample
- Q 2009 CPG LPR Water Column Monitoring DEC
- R 2010 CPG LPR-NB PWCM Field Measurements
- S 2010 CPG LPR-NB PWCM Sample Dataset
- T 2010 USEPA LBG-CDM PWCM Oversight
- U 2011 CDM Smith CWCM Sampling Data
- V 2011 CPG CWCM Sampling Data
- W 2012 CDM Smith CWCM Sampling - Round 2
- X 2012 CDM Smith CWCM Sampling - Round 3
- Y 2012 CDM Smith CWCM Sampling - Round 4
- Z 2012 CDM Smith CWCM Sampling - Round 5
- a 2012 CDM Smith CWCM Sampling - Round - 6
- b 2012 CPG CWCM Sampling - Low Flow
- c 2012 CPG CWCM Sampling - Round 2
- d 2012 CPG CWCM Sampling - Round 3
- e 2012 CPG CWCM Sampling - Round 4

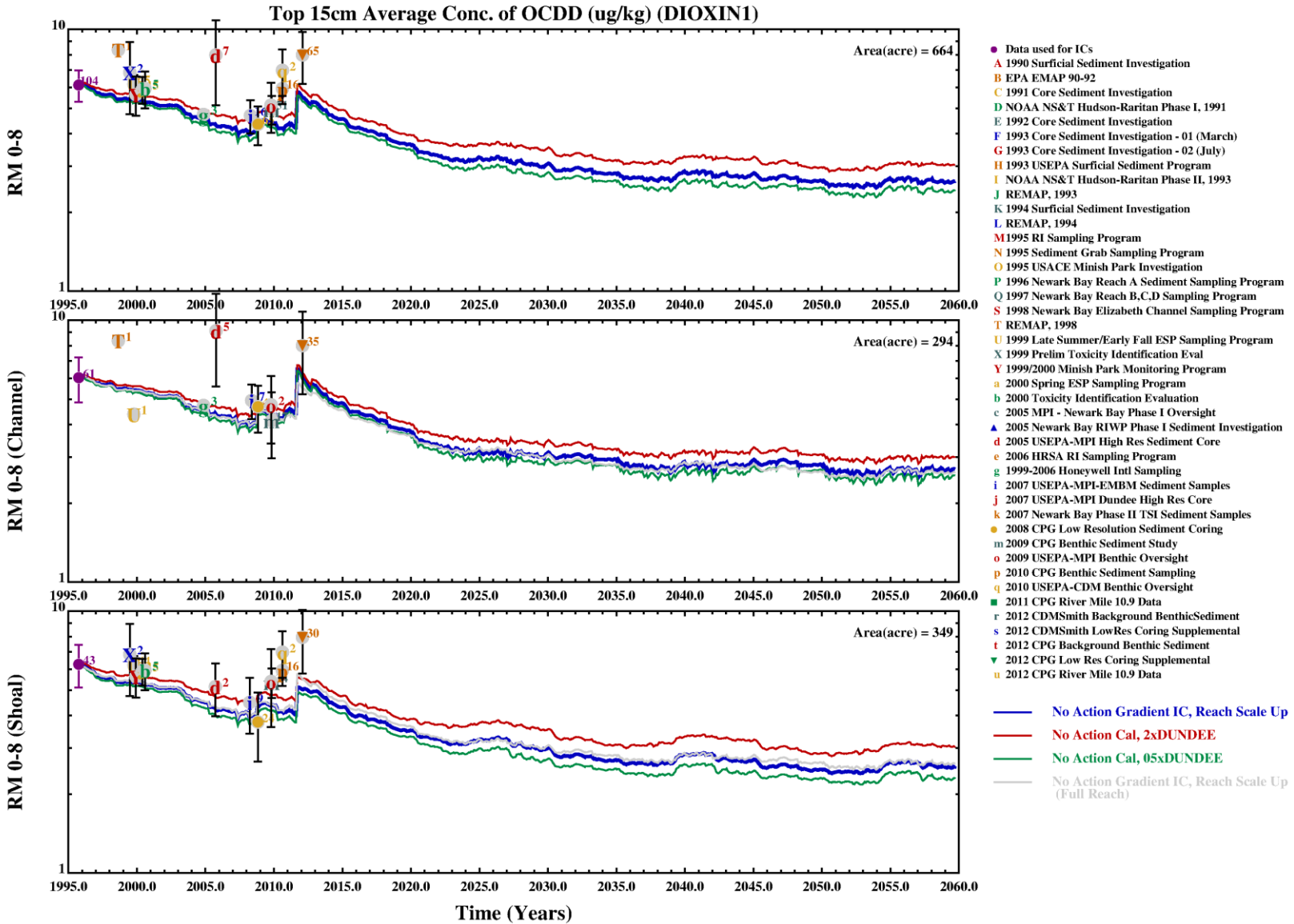
- No Action Gradient IC, Reach Scale Up
- No Action Cal, 2xDUNDEE
- No Action Cal, 05xDUNDEE

Water Column 2,3,7,8-TCDD Response to Dundee Dam Sensitivity

Lower Eight Miles of the Lower Passaic River

Figure 5-3

2014

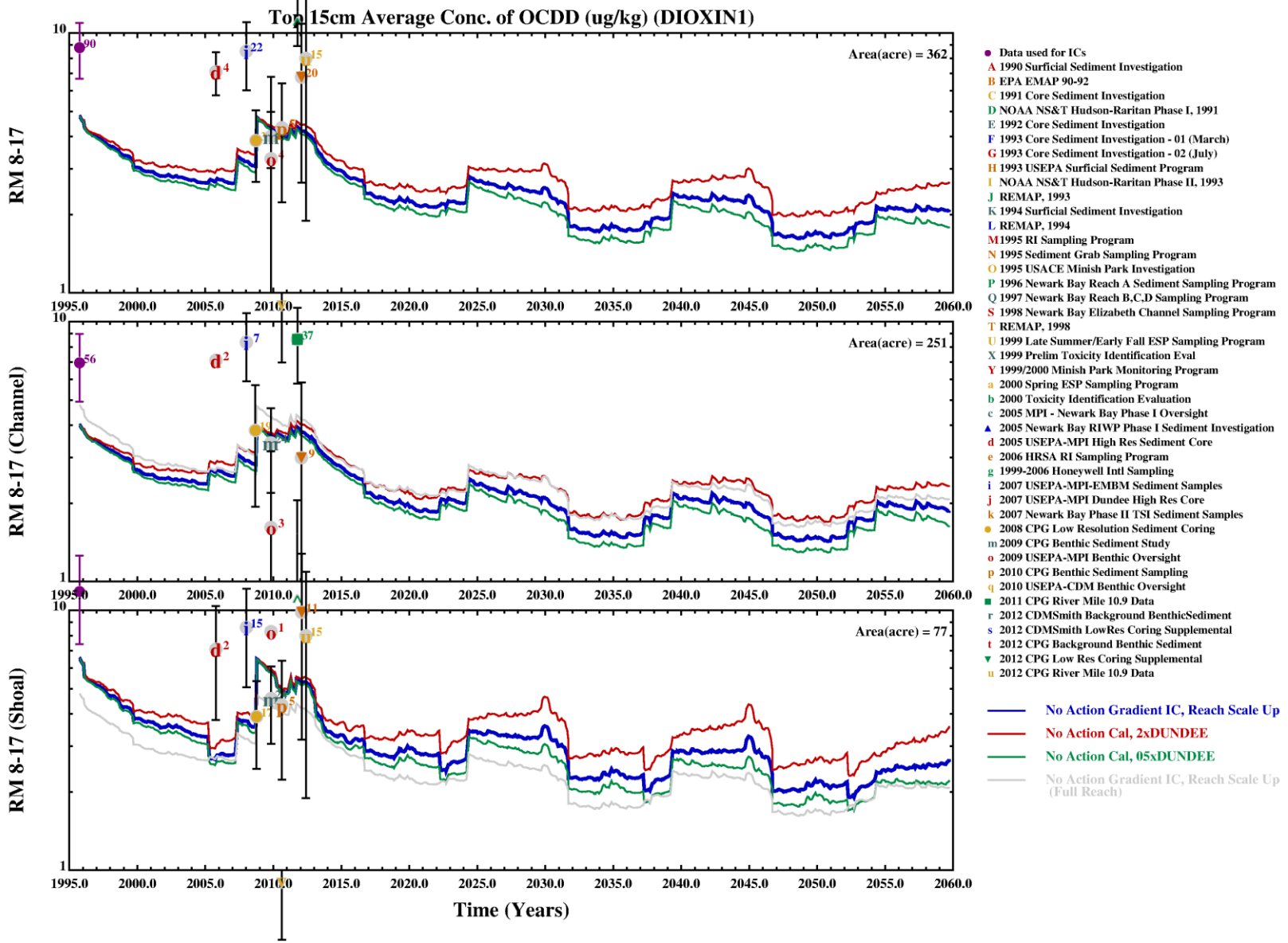


Sediment OCDD Response to Dundee Dam Sensitivity (RM0-8.3)

Lower Eight Miles of the Lower Passaic River

Figure 5-4

2014

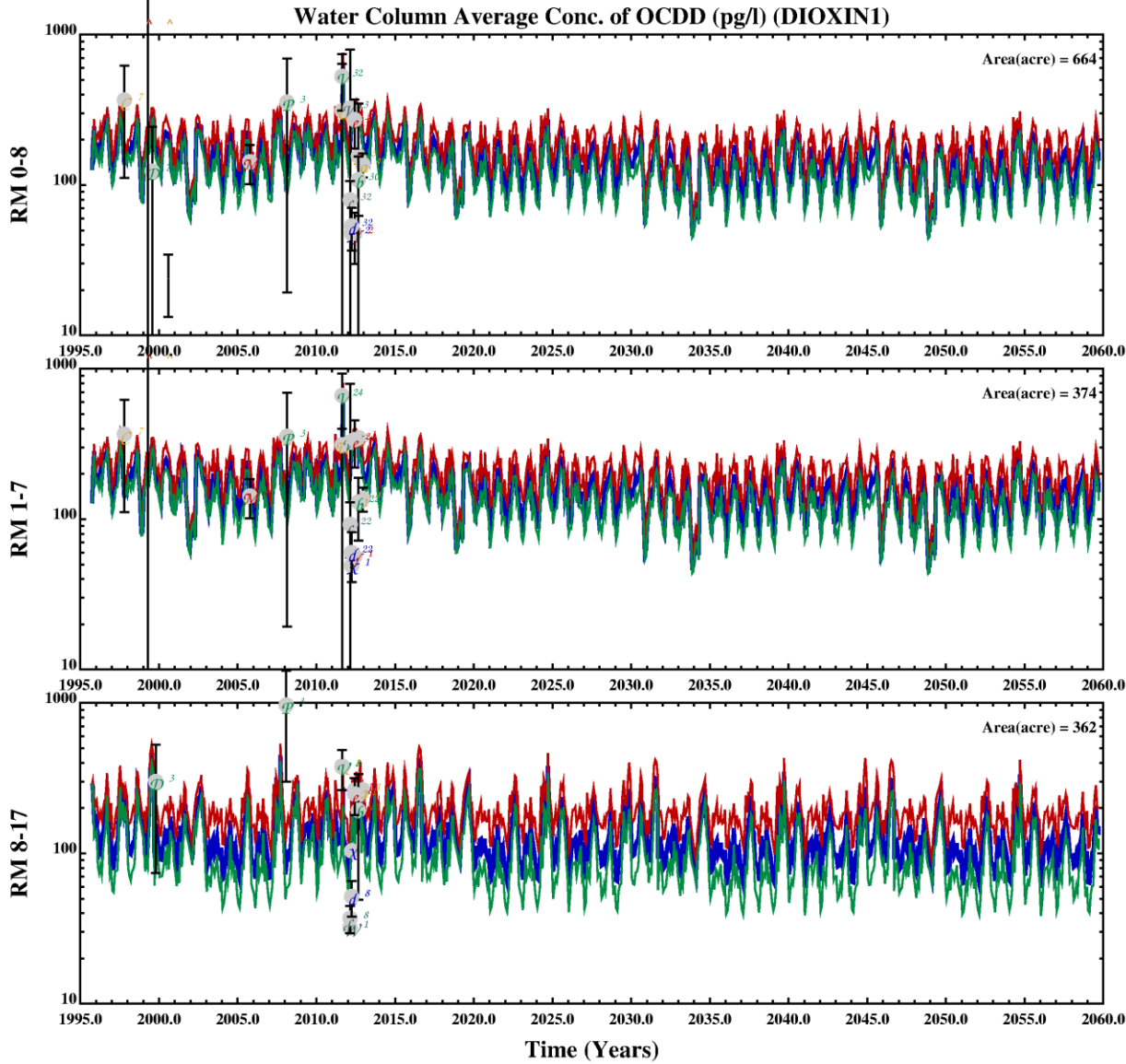


Sediment OCCD Response to Dundee Dam Sensitivity (RM8.3-17)

Lower Eight Miles of the Lower Passaic River

Figure 5-5

2014



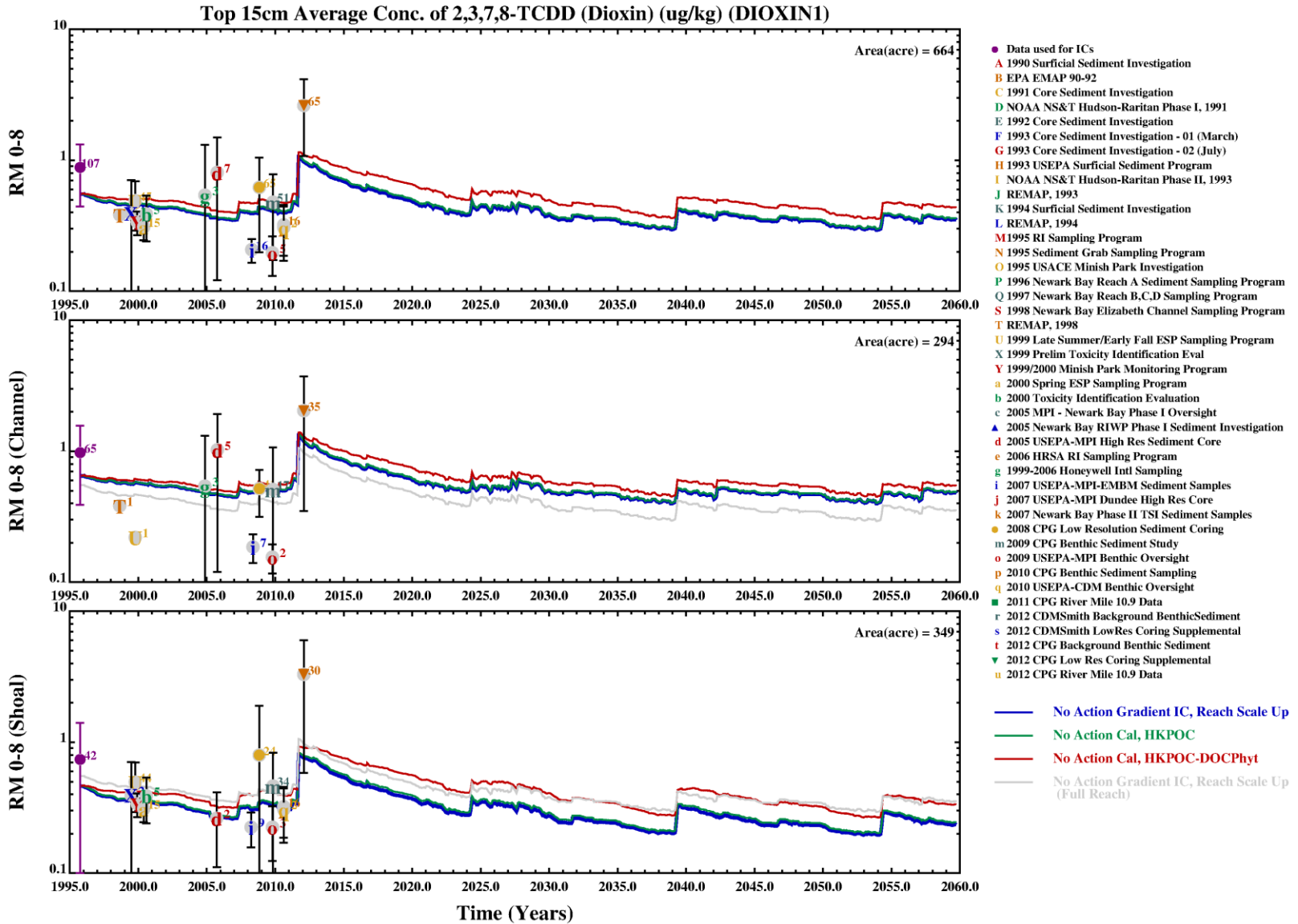
- A 1993-1997 USACE - DMDAT
 - B 1995-96 Passaic Study RI/FS Sed Mobility
 - C 1997 Outfall Sampling Program
 - D 1998-2001 CARP Database
 - E 1999 Newark Bay Reach A Monitoring
 - F 1999 Newark Bay Reach ABCD Baseline Sampling
 - G 1999 USACE Drift Removal Monitoring
 - H 1999-2006 Honeywell Intl Sampling
 - I 2000 Toxicity Identification Evaluation
 - J 2005 Hydrodynamic Mooring
 - K 2005 MPI SPMD Deployment
 - L 2005 USEPA-MPI High Flow Water Column
 - M 2005 USEPA-MPI Large Volume Study
 - N 2005 USEPA-MPI Small Volume Water Column
 - O 2005 USEPA-MPI Water Column Above RM 8.5
 - P 2007 USEPA-MPI-EMBM Water Column Sample
 - Q 2009 CPG LPR Water Column Monitoring DEC
 - R 2010 CPG LPR-NB PWCM Field Measurements
 - S 2010 CPG LPR-NB PWCM Sample Dataset
 - T 2010 USEPA LBG-CDM PWCM Oversight
 - U 2011 CDM Smith CWCM Sampling Data
 - V 2011 CPG CWCM Sampling Data
 - W 2012 CDM Smith CWCM Sampling - Round 2
 - X 2012 CDM Smith CWCM Sampling - Round 3
 - Y 2012 CDM Smith CWCM Sampling - Round 4
 - Z 2012 CDM Smith CWCM Sampling - Round 5
 - 1 2012 CDM Smith CWCM Sampling Round - 6
 - 2 2012 CPG CWCM Sampling - Low Flow
 - 3 2012 CPG CWCM Sampling - Round 2
 - 4 2012 CPG CWCM Sampling - Round 3
 - 5 2012 CPG CWCM Sampling - Round 4
- No Action Gradient IC, Reach Scale Up
- No Action Cal, 2xDUNDEE
- No Action Cal, 05xDUNDEE

Water Column OCCD Response to Dundee Dam Sensitivity

Lower Eight Miles of the Lower Passaic River

Figure 5-6

2014

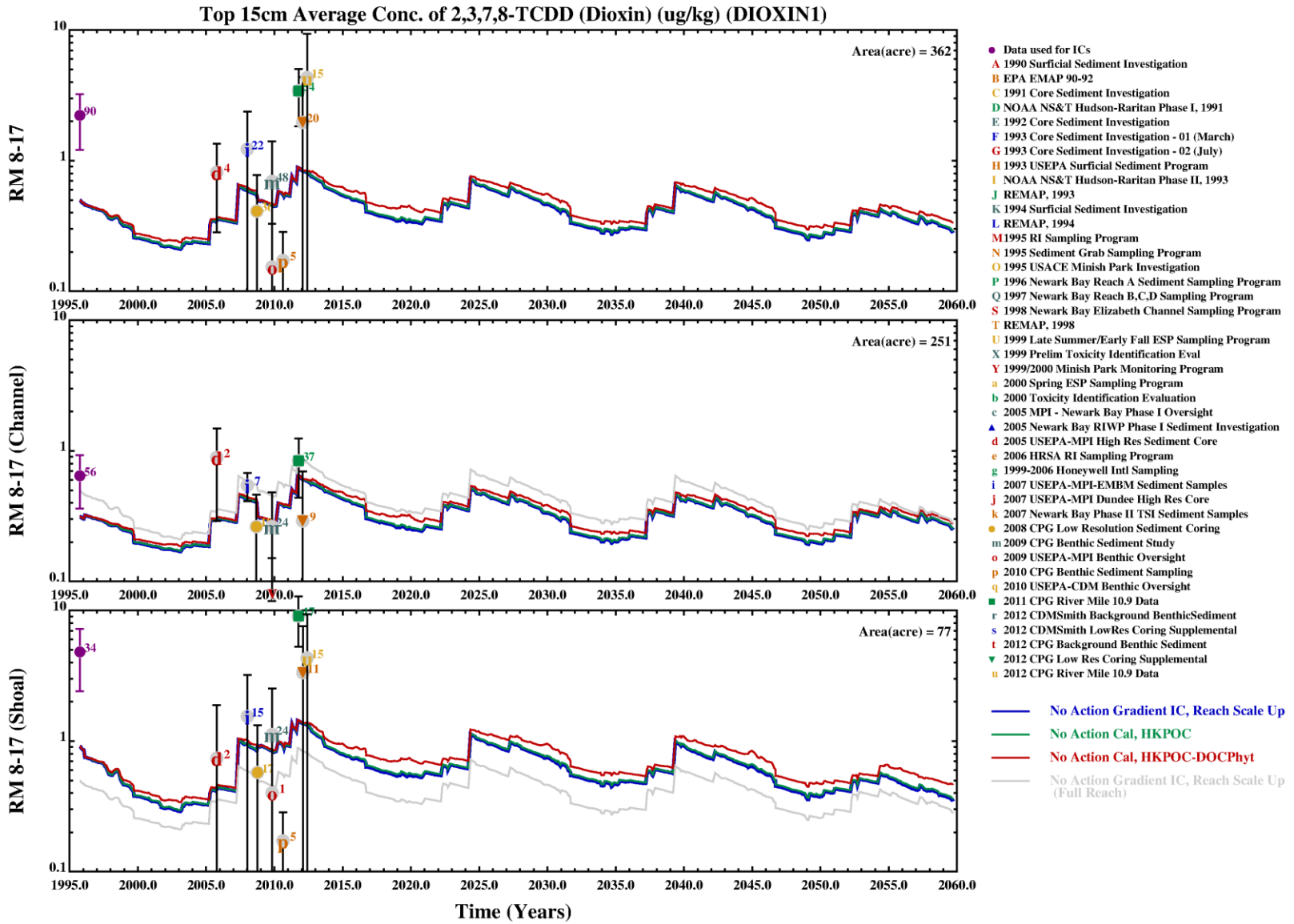


Sediment 2,3,7,8-TCCD Response to Partition Coefficient Sensitivity (RM0-8.3)

Lower Eight Miles of the Lower Passaic River

Figure 5-7

2014

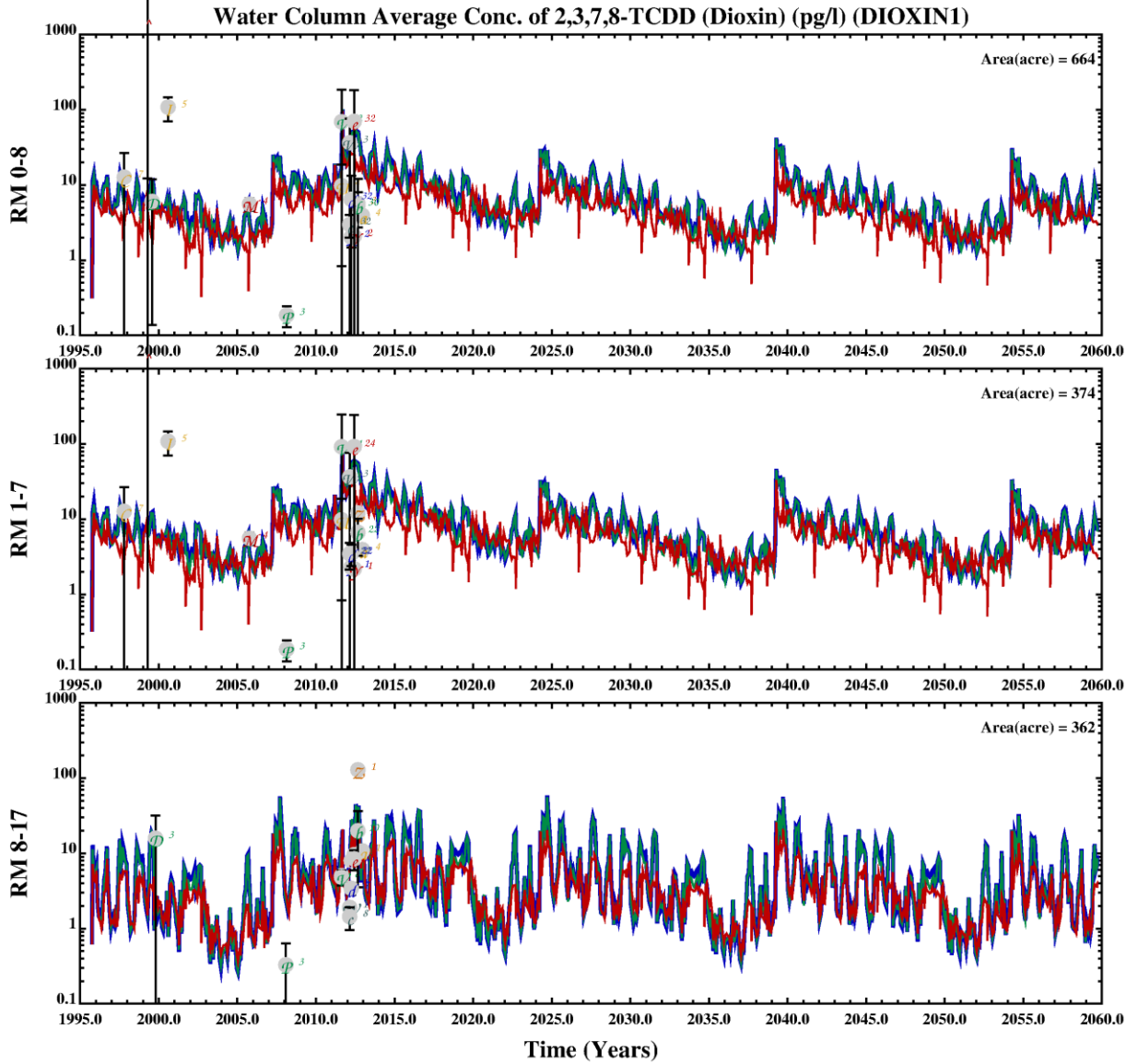


Sediment 2,3,7,8-TCDD Response to Partition Coefficient Sensitivity (RM8.3-17)

Figure 5-8

Lower Eight Miles of the Lower Passaic River

2014

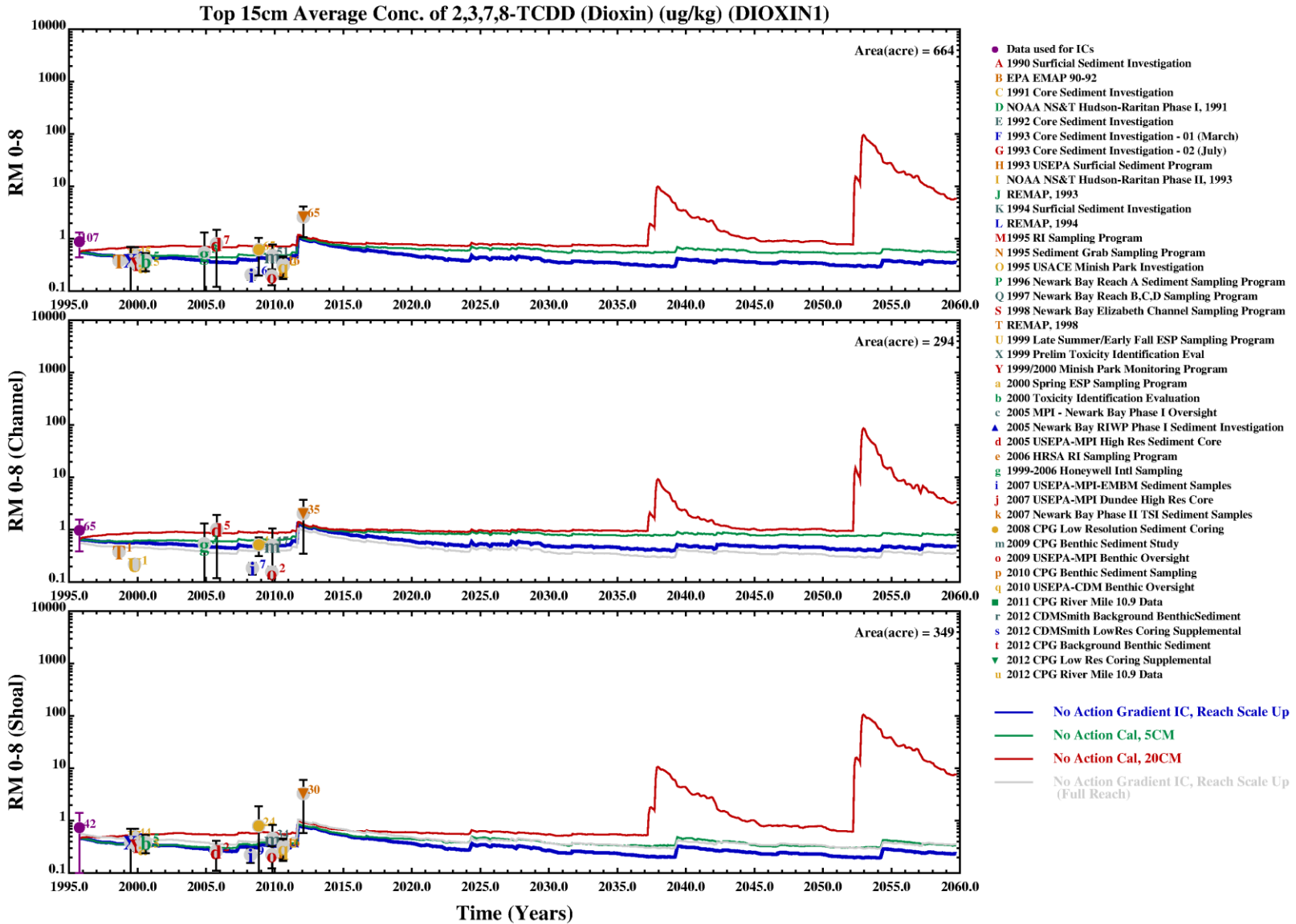


Water Column 2,3,7,8-TCDD Response to Partition Coefficient Sensitivity

Lower Eight Miles of the Lower Passaic River

Figure 5-9

2014

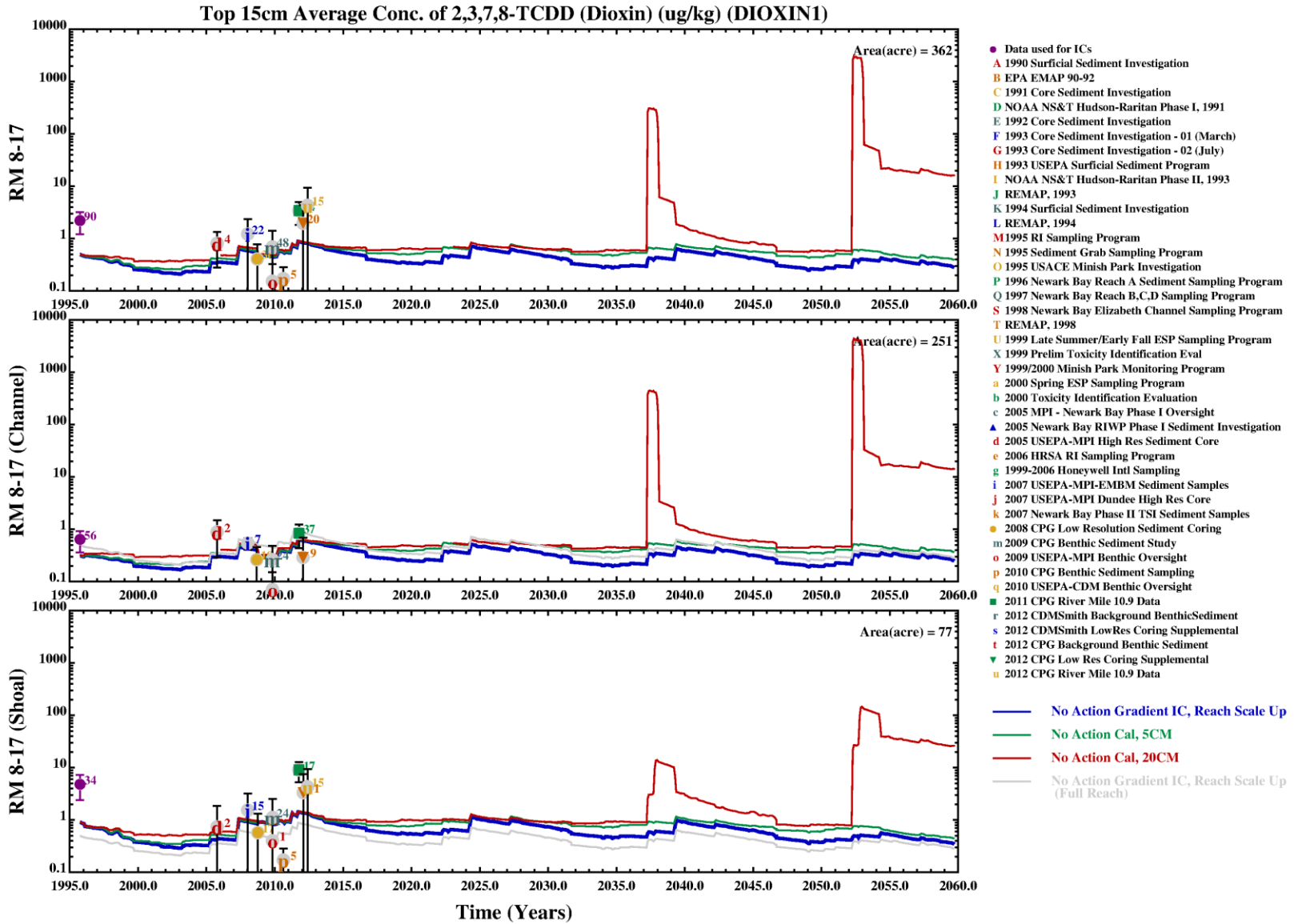


Sediment 2,3,7,8-TCDD Response to Depth of Mixing Sensitivity (RM0-8.3)

Figure 5-10

Lower Eight Miles of the Lower Passaic River

2014

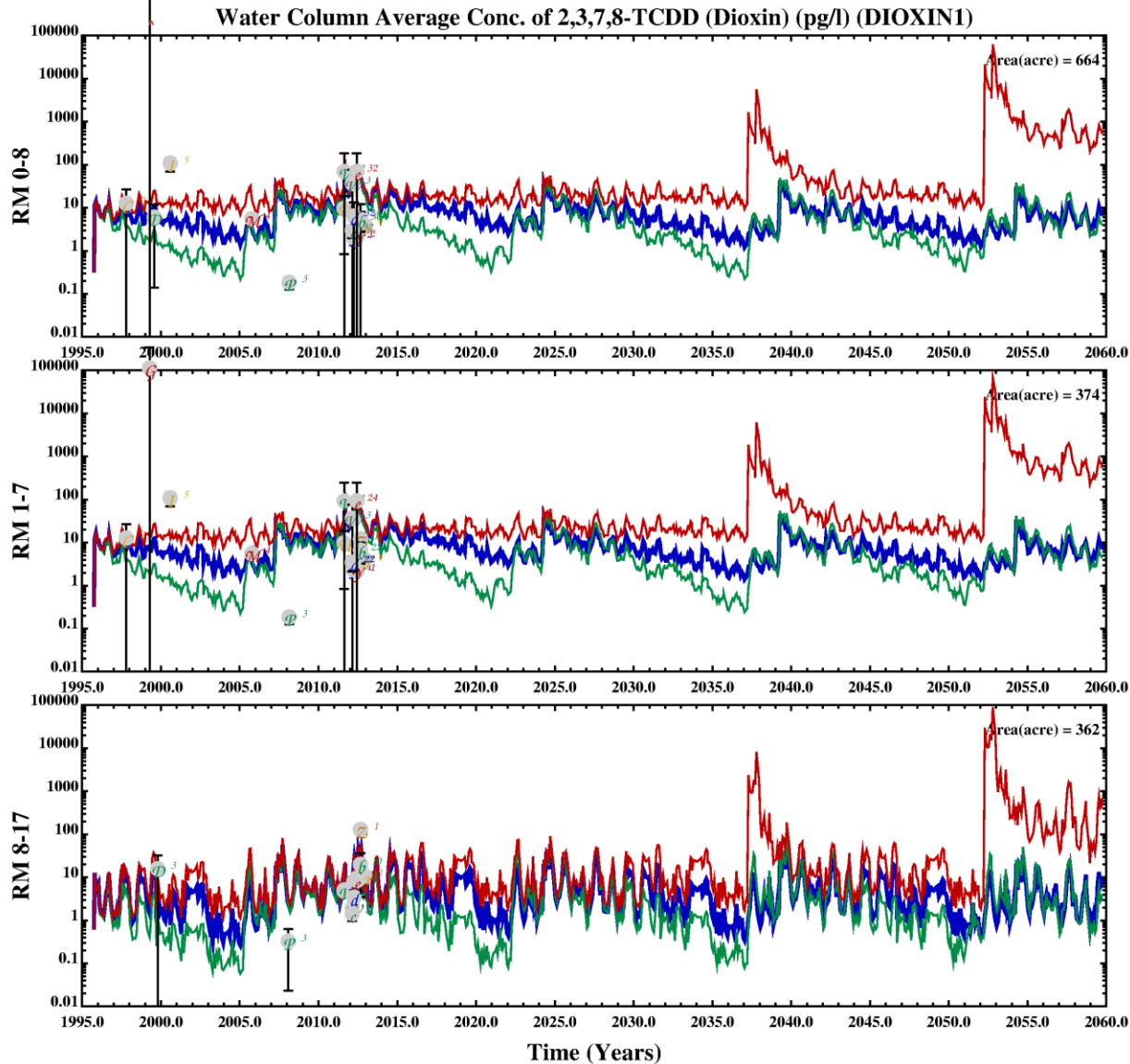


Sediment 2,3,7,8-TCDD Response to Depth of Mixing Sensitivity (RM8.3-17)

Lower Eight Miles of the Lower Passaic River

Figure 5-11

2014



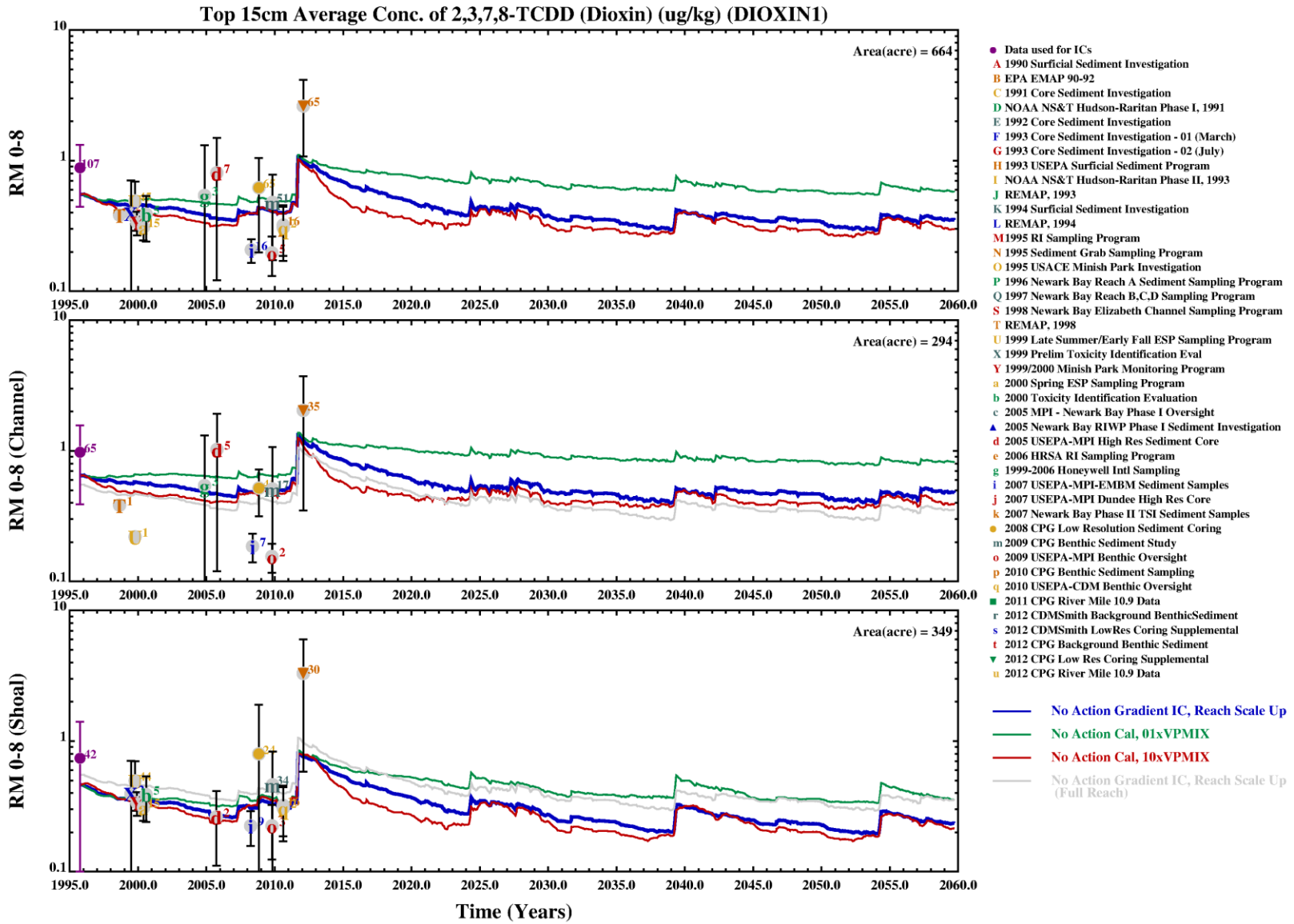
- A 1993-1997 USACE - DMDAT
 - B 1995-96 Passaic Study R/FS Sed Mobility
 - C 1997 Outfall Sampling Program
 - D 1998-2001 CARP Database
 - E 1999 Newark Bay Reach A Monitoring
 - F 1999 Newark Bay Reach ABCDBaseline Sampling
 - G 1999 USACE Drift Removal Monitoring
 - H 1999-2006 Honeywell Intl Sampling
 - I 2000 Toxicity Identification Evaluation
 - J 2005 Hydrodynamic Mooring
 - K 2005 MPI SPMD Deployment
 - L 2005 USEPA-MPI High Flow Water Column
 - M 2005 USEPA-MPI Large Volume Study
 - N 2005 USEPA-MPI Small Volume Water Column
 - O 2005 USEPA-MPI Water Column Above RM 8.5
 - P 2007 USEPA-MPI-EMBM Water Column Sample
 - Q 2009 CPG LPR Water Column Monitoring DEC
 - R 2010 CPG LPR-NB PWCM Field Measurements
 - S 2010 CPG LPR-NB PWCM Sample Dataset
 - T 2010 USEPA LBG-CDM PWCM Oversight
 - U 2011 CDM Smith CWCM Sampling Data
 - V 2011 CPG CWCM Sampling Data
 - W 2012 CDM Smith CWCM Sampling - Round 2
 - X 2012 CDM Smith CWCM Sampling - Round 3
 - Y 2012 CDM Smith CWCM Sampling - Round 4
 - Z 2012 CDM Smith CWCM Sampling - Round 5
 - 1 2012 CDM Smith CWCM Sampling Round - 6
 - 2 2012 CPG CWCM Sampling - Low Flow
 - 3 2012 CPG CWCM Sampling - Round 2
 - 4 2012 CPG CWCM Sampling - Round 3
 - 5 2012 CPG CWCM Sampling - Round 4
- No Action Gradient IC, Reach Scale Up
— No Action Cal, 5CM
— No Action Cal, 20CM

Water Column 2,3,7,8-TCDD Response to Depth of Mixing Sensitivity

Lower Eight Miles of the Lower Passaic River

Figure 5-12

2014

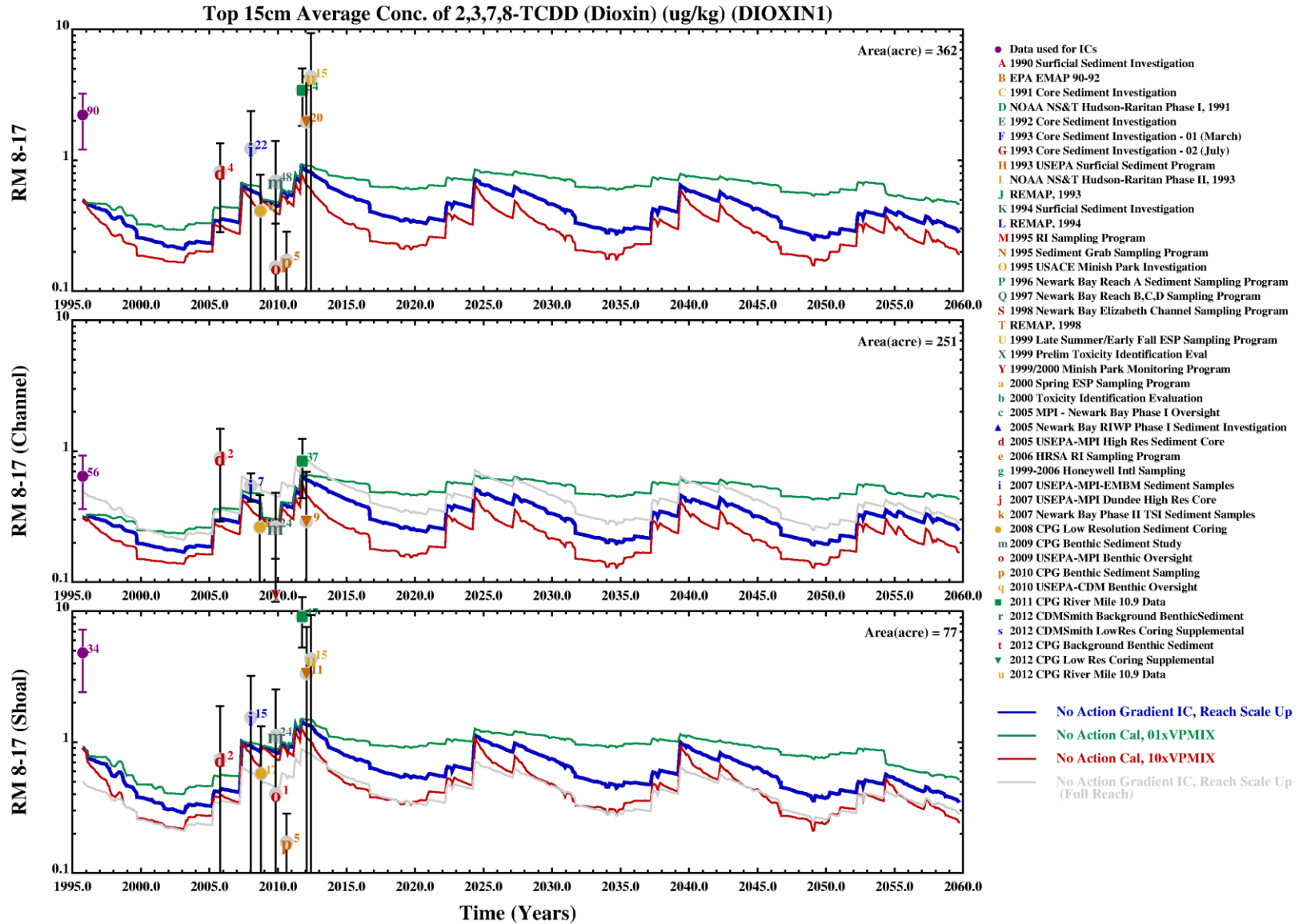


Sediment 2,3,7,8-TCDD Response to Rate of Mixing Sensitivity (RM0-8.3)

Figure 5-13

Lower Eight Miles of the Lower Passaic River

2014

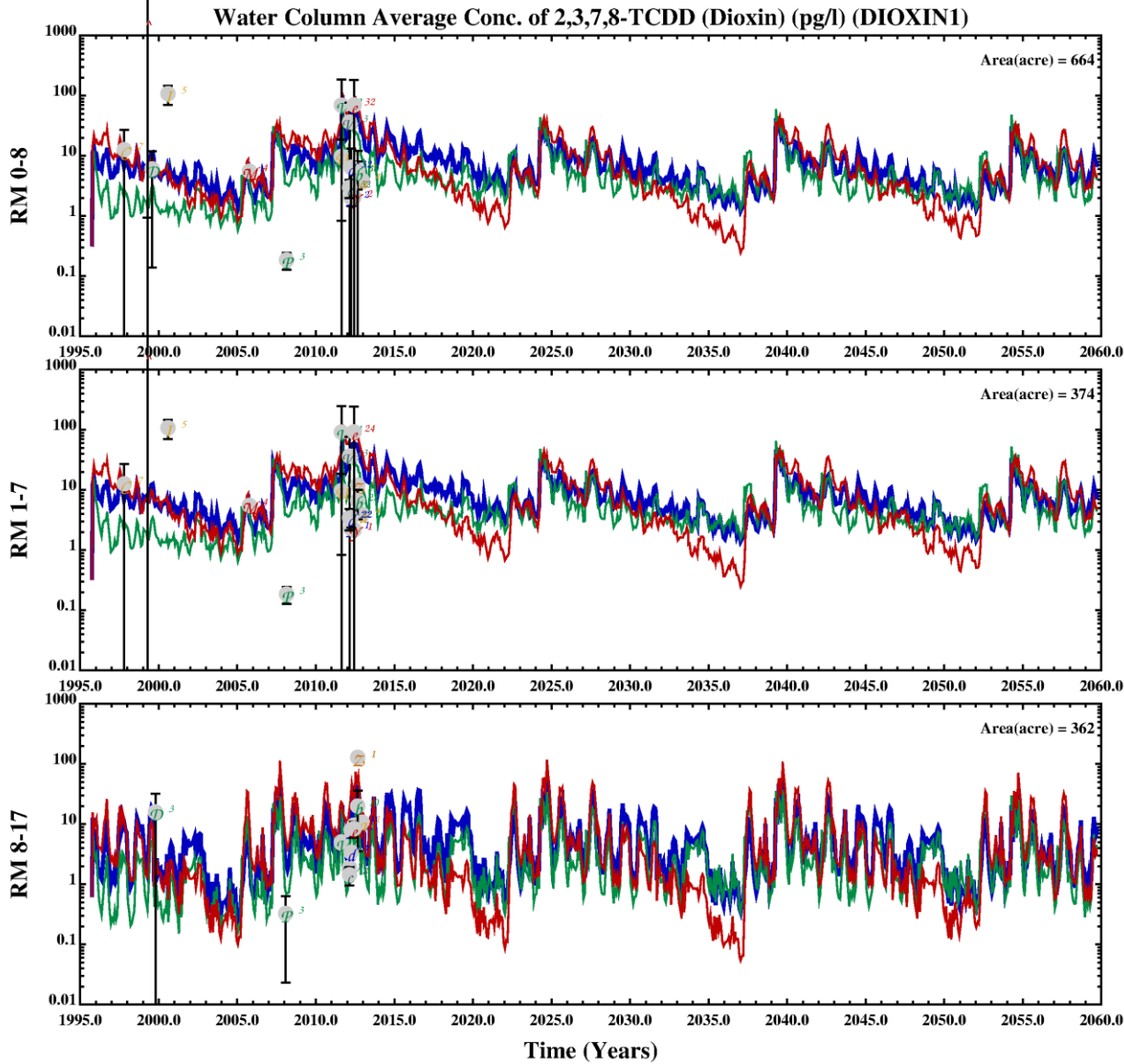


Sediment 2,3,7,8-TCDD Response to Rate of Mixing Sensitivity (RM8.3-17)

Figure 5-14

Lower Eight Miles of the Lower Passaic River

2014



- 1993-1997 USACE - DMDAT
- 1995-96 Passaic Study RI/FS Sed Mobility
- 1997 Outfall Sampling Program
- 1998-2001 CARP Database
- 1999 Newark Bay Reach A Monitoring
- 1999 Newark Bay Reach ABCD Baseline Sampling
- 1999 USACE Drift Removal Monitoring
- 1999-2006 Honeywell Intl Sampling
- 2000 Toxicity Identification Evaluation
- 2005 Hydrodynamic Mooring
- 2005 MPI SPMD Deployment
- 2005 USEPA-MPI High Flow Water Column
- 2005 USEPA-MPI Large Volume Study
- 2005 USEPA-MPI Small Volume Water Column
- 2005 USEPA-MPI Water Column Above RM 8.5
- 2007 USEPA-MPI-EMBM Water Column Sample
- 2009 CPG LPR Water Column Monitoring DEC
- 2010 CPG LPR-NB PWCM Field Measurements
- 2010 CPG LPR-NB PWCM Sample Dataset
- 2010 USEPA LBG-CDM PWCM Oversight
- 2011 CDM Smith CWCM Sampling Data
- 2011 CPG CWCM Sampling Data
- 2012 CDM Smith CWCM Sampling - Round 2
- 2012 CDM Smith CWCM Sampling - Round 3
- 2012 CDM Smith CWCM Sampling - Round 4
- 2012 CDM Smith CWCM Sampling - Round 5
- 2012 CDM Smith CWCM Sampling Round - 6
- 2012 CPG CWCM Sampling - Low Flow
- 2012 CPG CWCM Sampling - Round 2
- 2012 CPG CWCM Sampling - Round 3
- 2012 CPG CWCM Sampling - Round 4

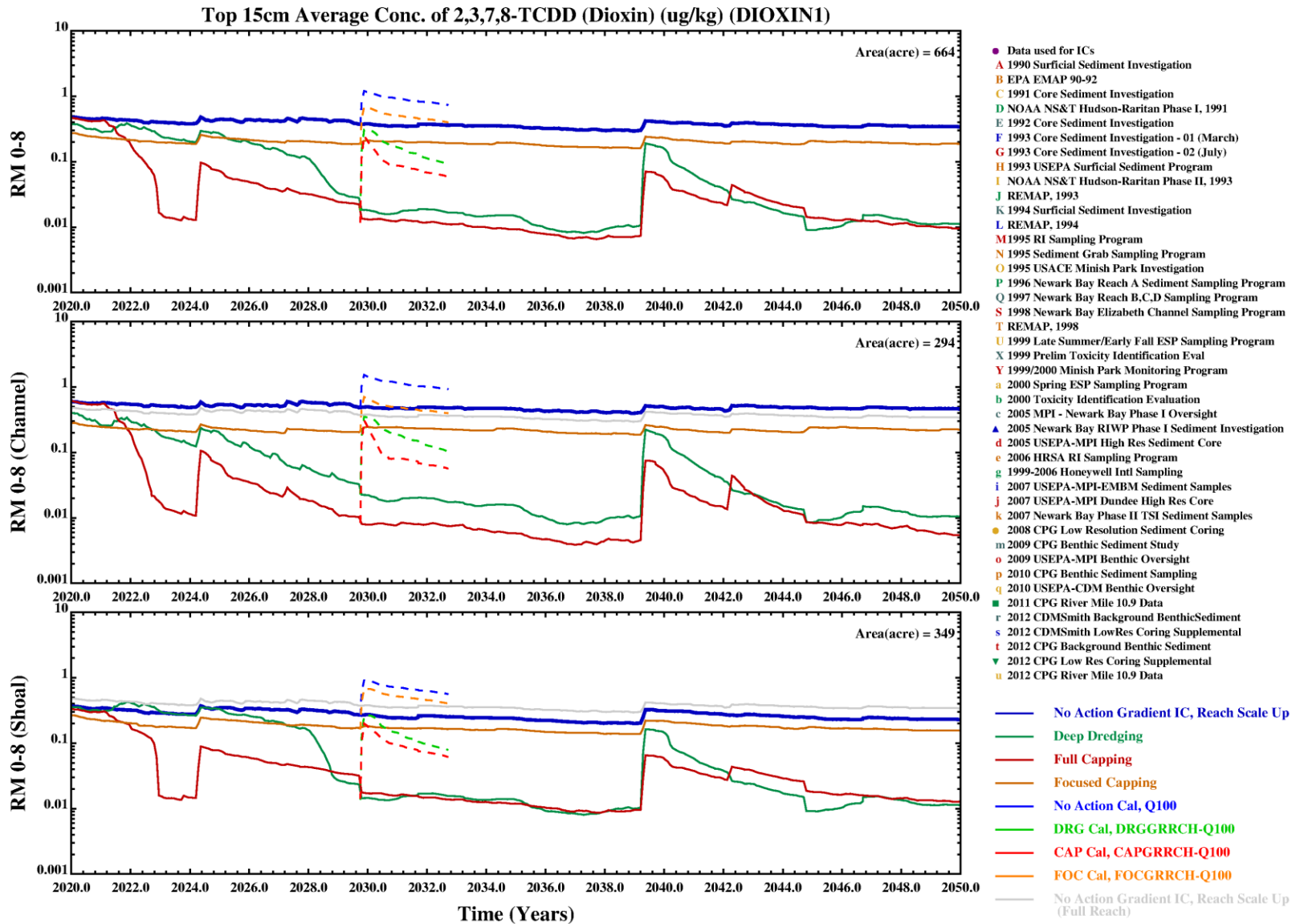
- No Action Gradient IC, Reach Scale Up
- No Action Cal, 01xVPMIX
- No Action Cal, 10xVPMIX

Water Column 2,3,7,8-TCDD Response to Rate of Mixing Sensitivity

Lower Eight Miles of the Lower Passaic River

Figure 5-15

2014

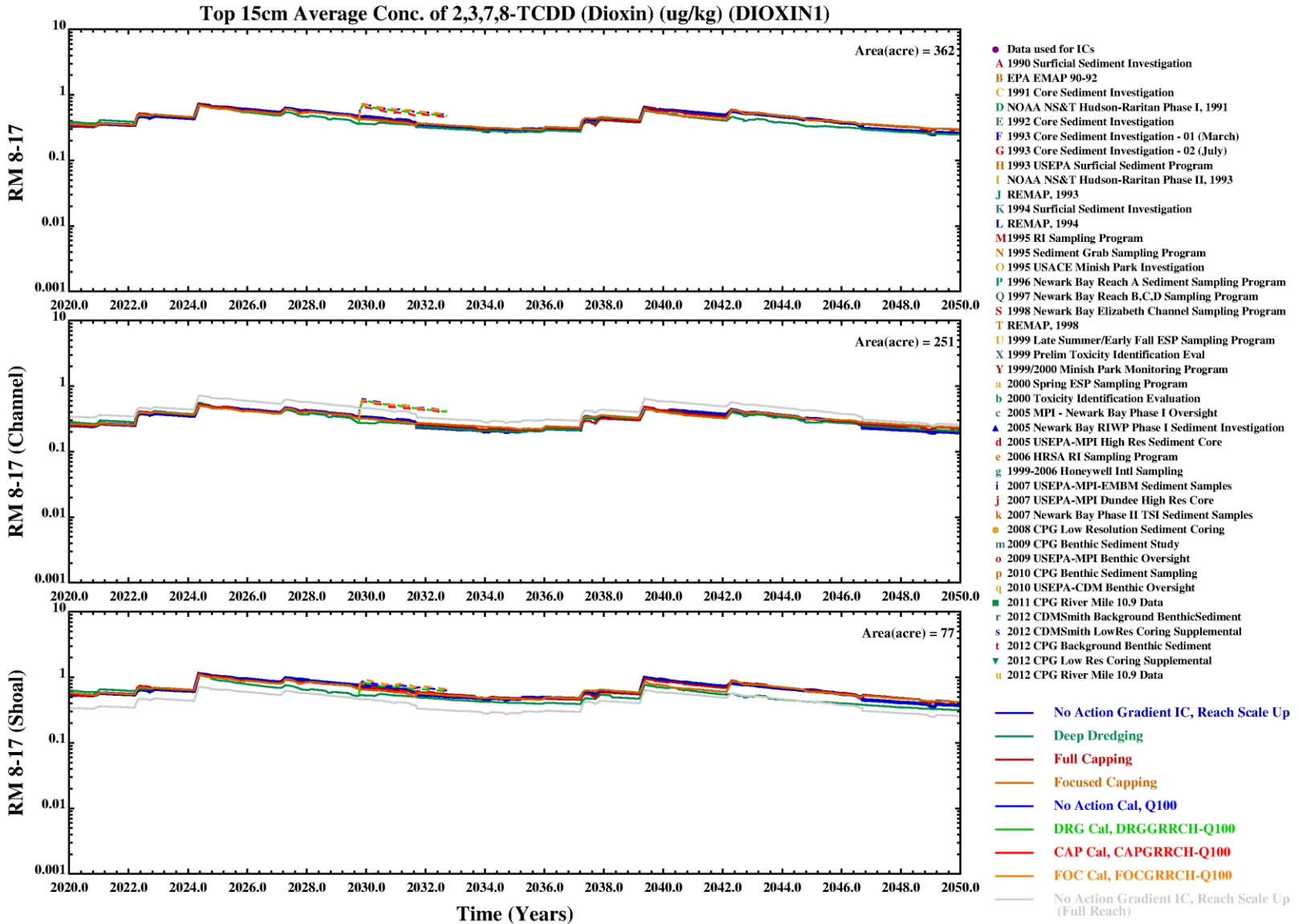


Sediment 2,3,7,8-TCDD Response to One Hundred Year Storm Sensitivity (RM0-8.3)

Figure 5-16

Lower Eight Miles of the Lower Passaic River

2014

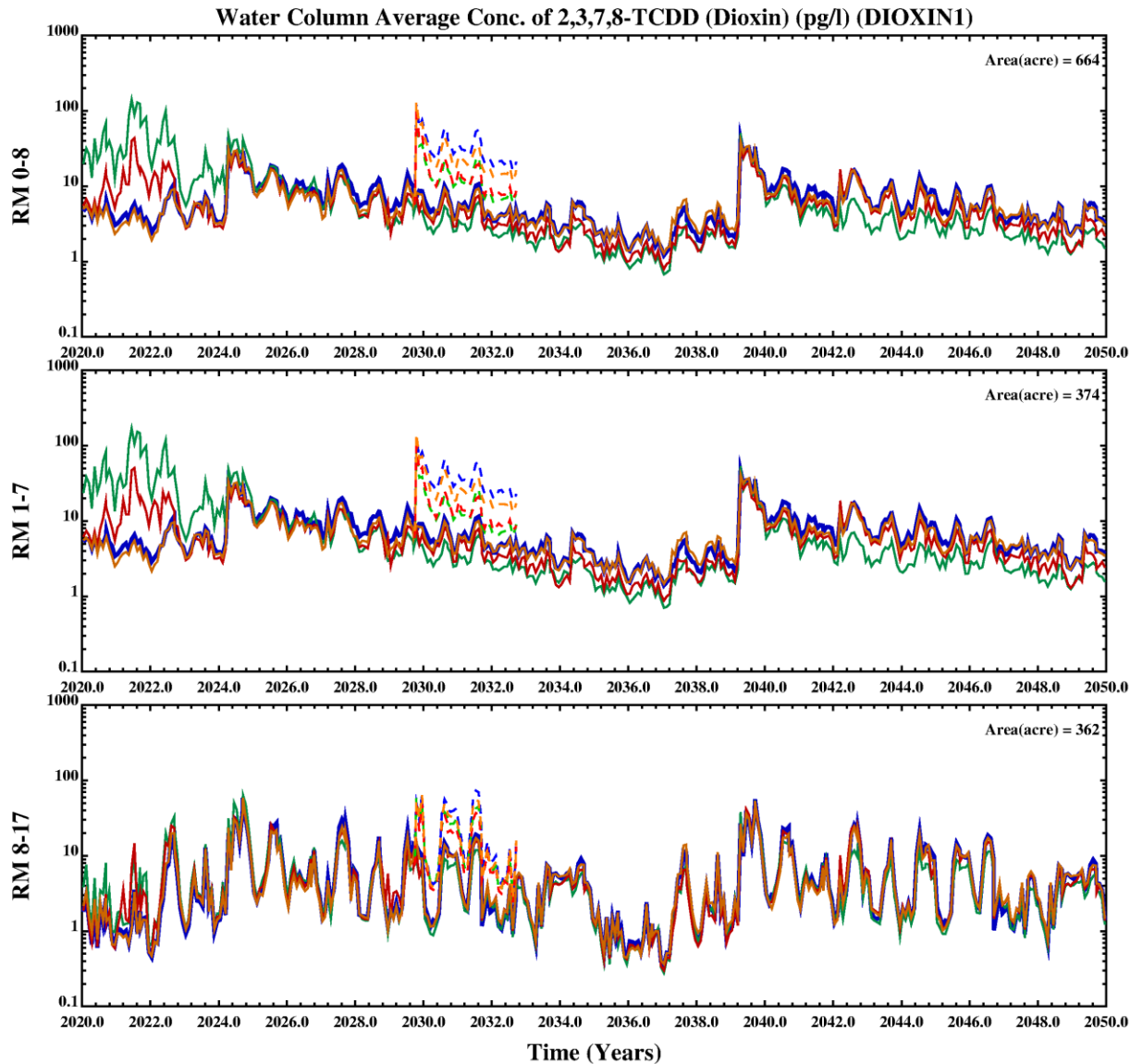


Sediment 2,3,7,8-TCDD Response to One Hundred Year Storm Sensitivity (RM8.3-17)

Figure 5-17

Lower Eight Miles of the Lower Passaic River

2014

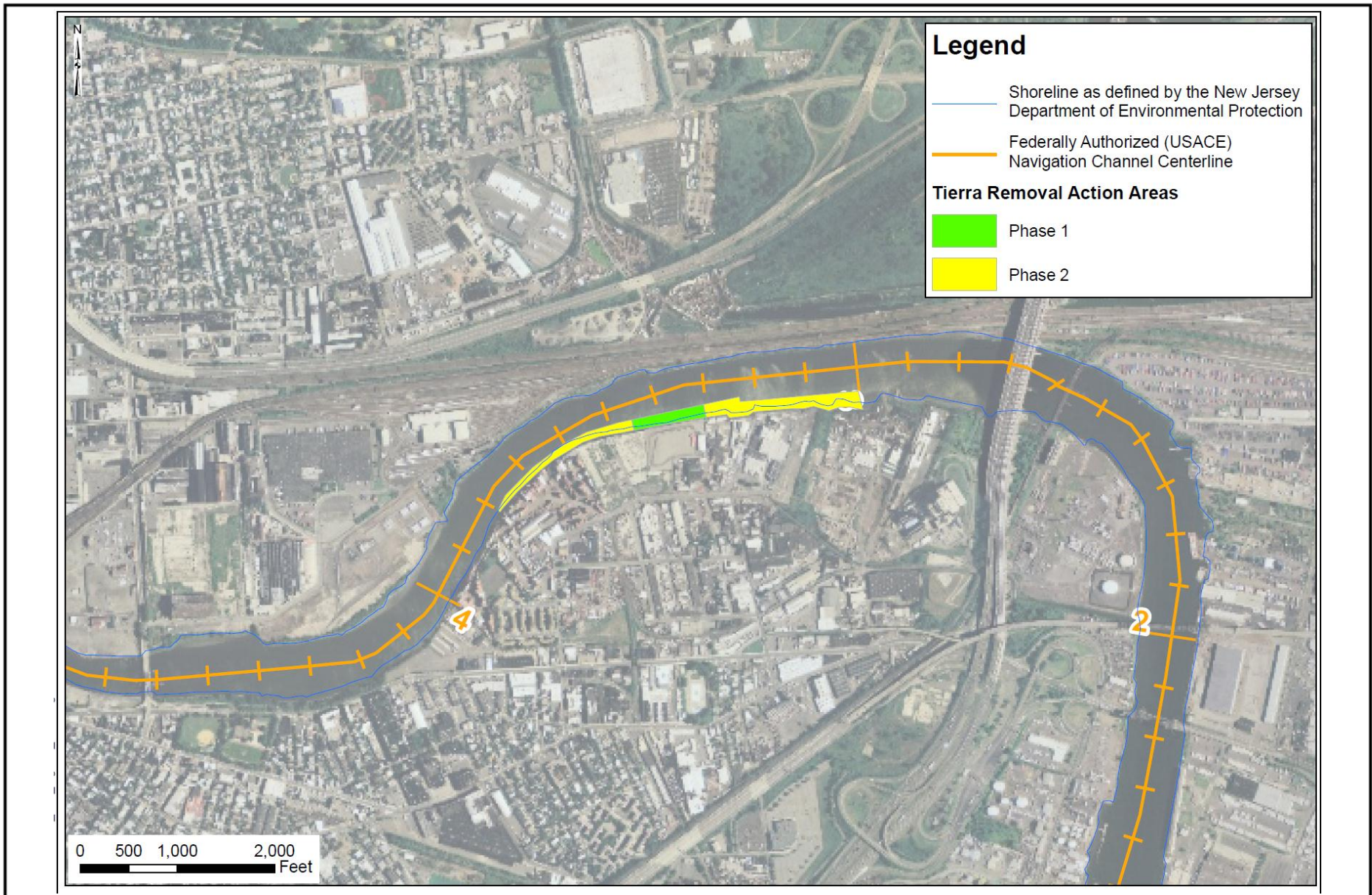


Water Column 2,3,7,8-TCDD Response to One Hundred Year Storm Sensitivity

Figure 5-18

Lower Eight Miles of the Lower Passaic River

2014



Tierra Removal, Phase 1 and Phase 2 Areas

Figure 6-1

Lower Eight Miles of the Lower Passaic River

2014

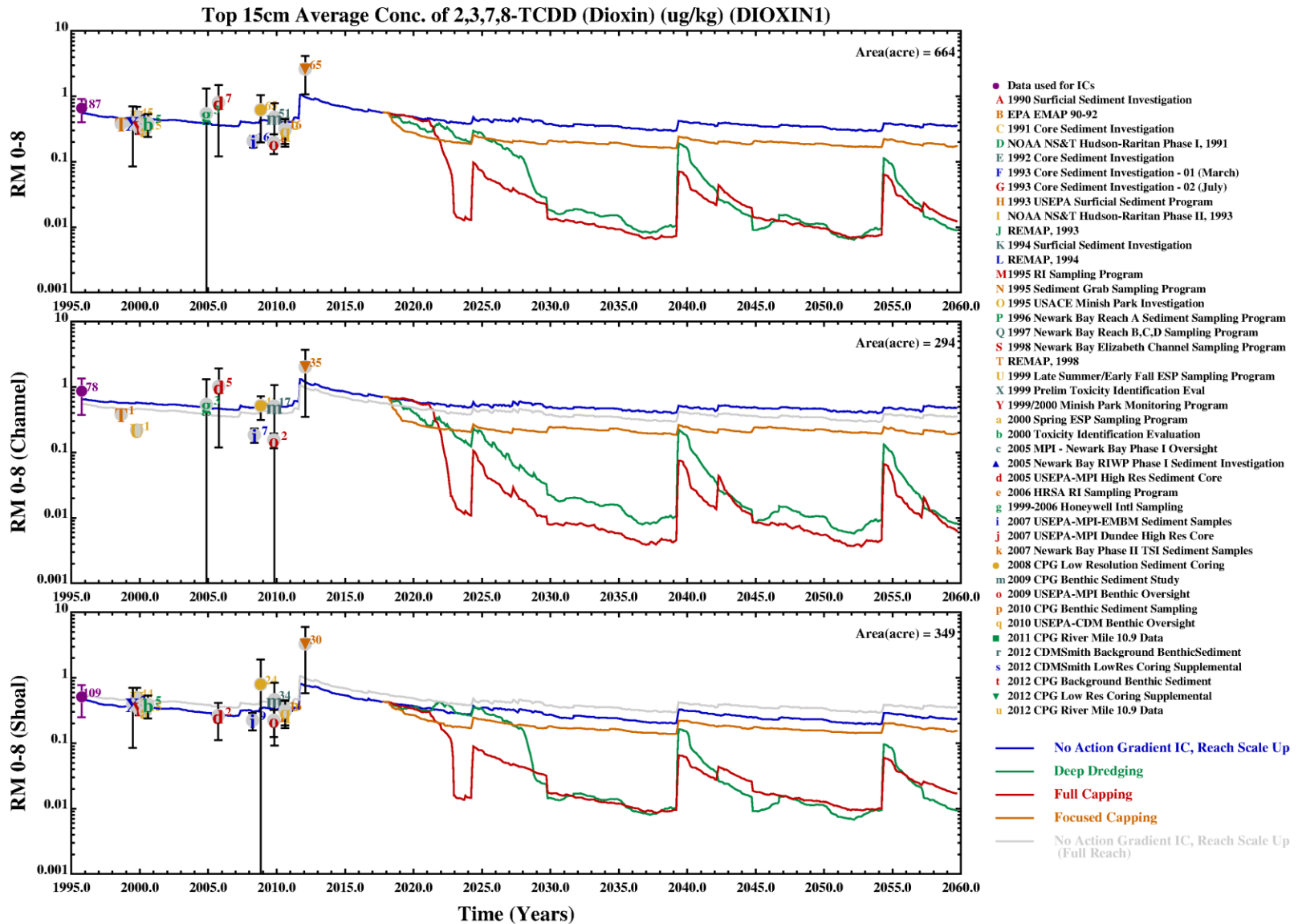


Areas Capped in Alternative 4 - Focused Capping with Dredging for Flooding

Lower Eight Miles of the Lower Passaic River

Figure 6-2

2014

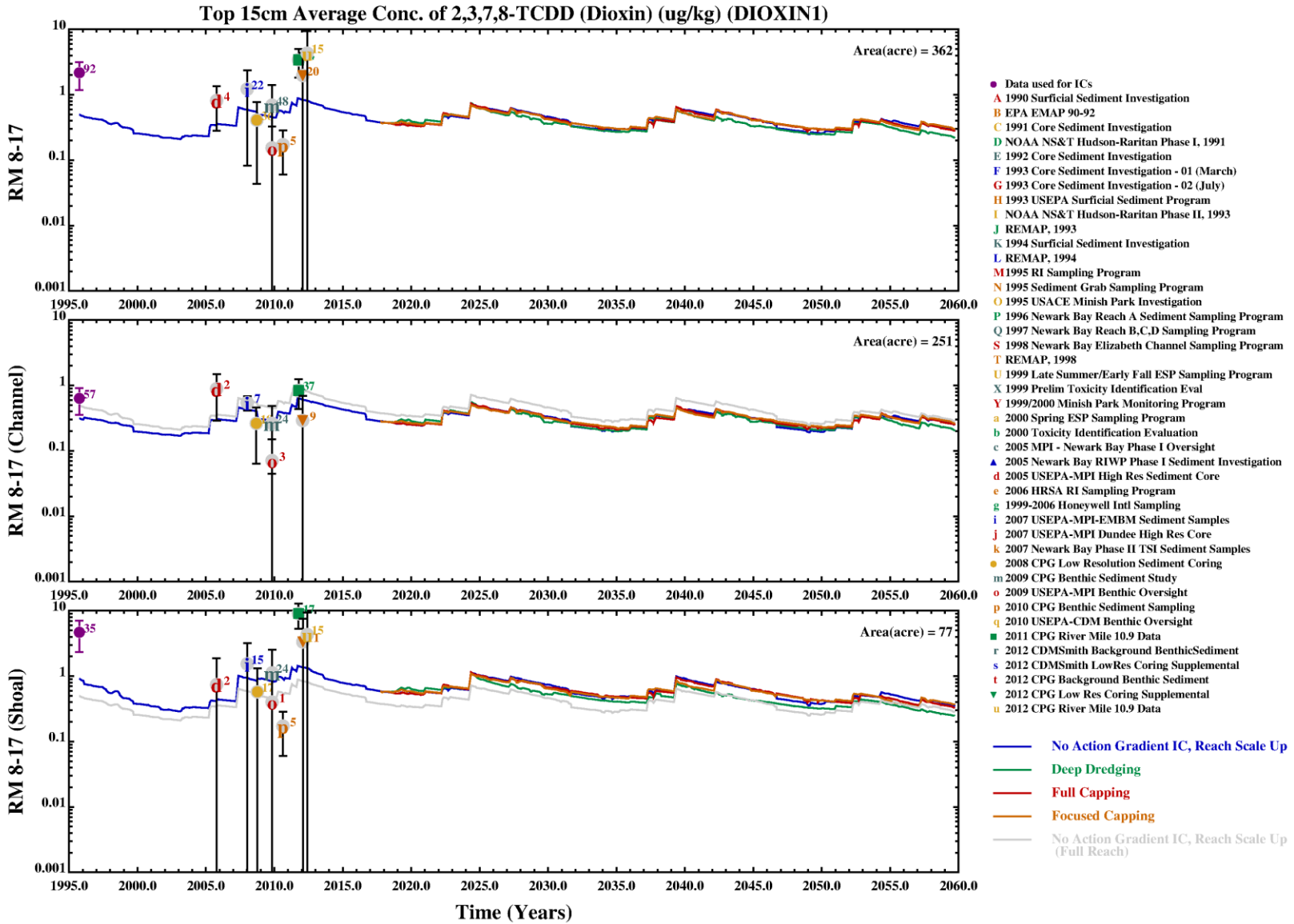


Log Scale Temporal Plots of 2,3,7,8 TCDD Sediment Concentrations for No Action and Three Remedial Alternatives (RM0-8.3)

Lower Eight Miles of the Lower Passaic River

Figure 6-3

2014

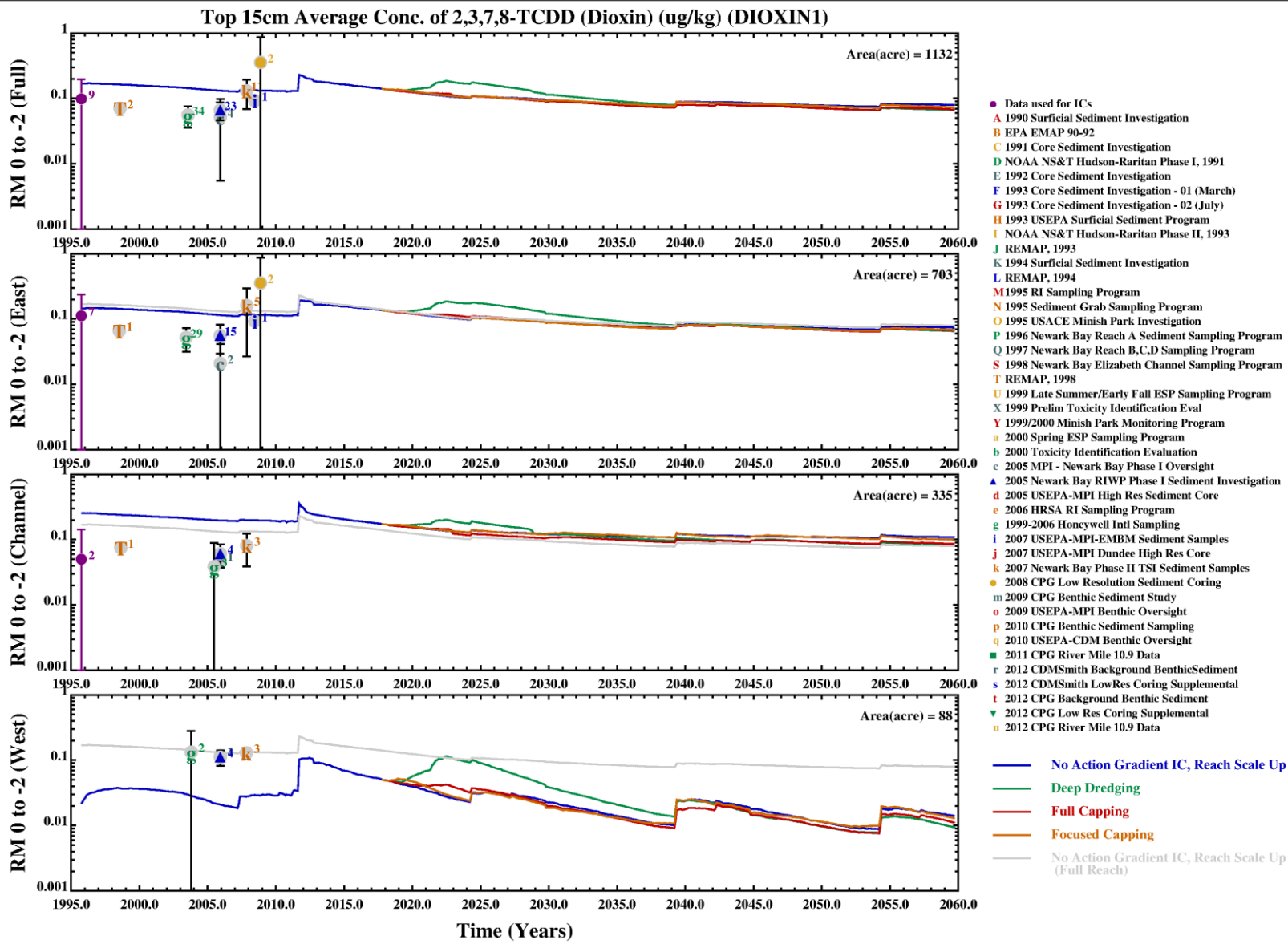


Log Scale Temporal Plots of 2,3,7,8 TCDD Sediment Concentrations for No Action and Three Remedial Alternatives (RM8.3-17)

Lower Eight Miles of the Lower Passaic River

Figure 6-4

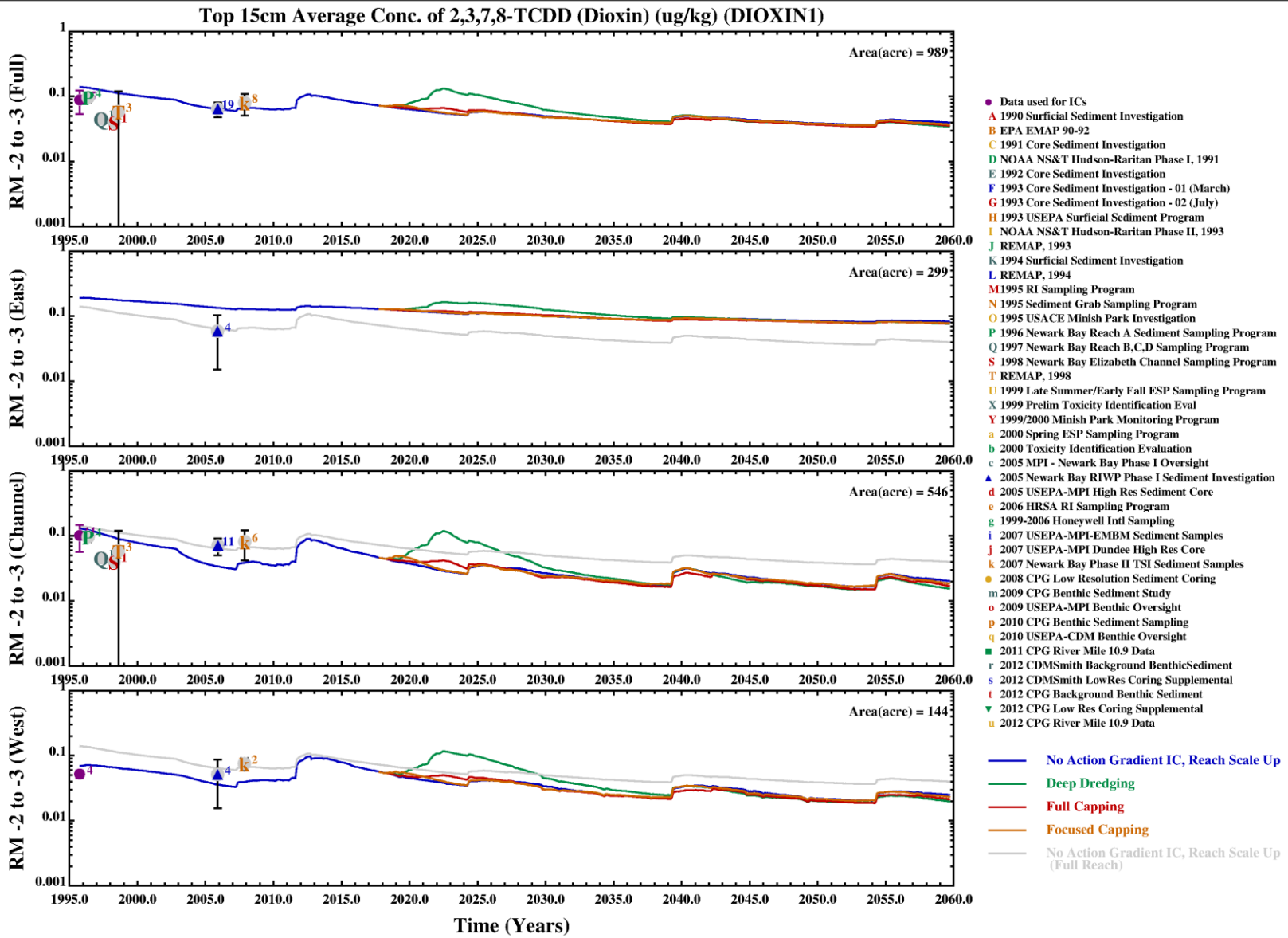
2014



Log Scale Temporal Plots of 2,3,7,8 TCDD Sediment Concentrations for No Action and Three Remedial Alternatives (RM0 to -1.5)
Lower Eight Miles of the Lower Passaic River

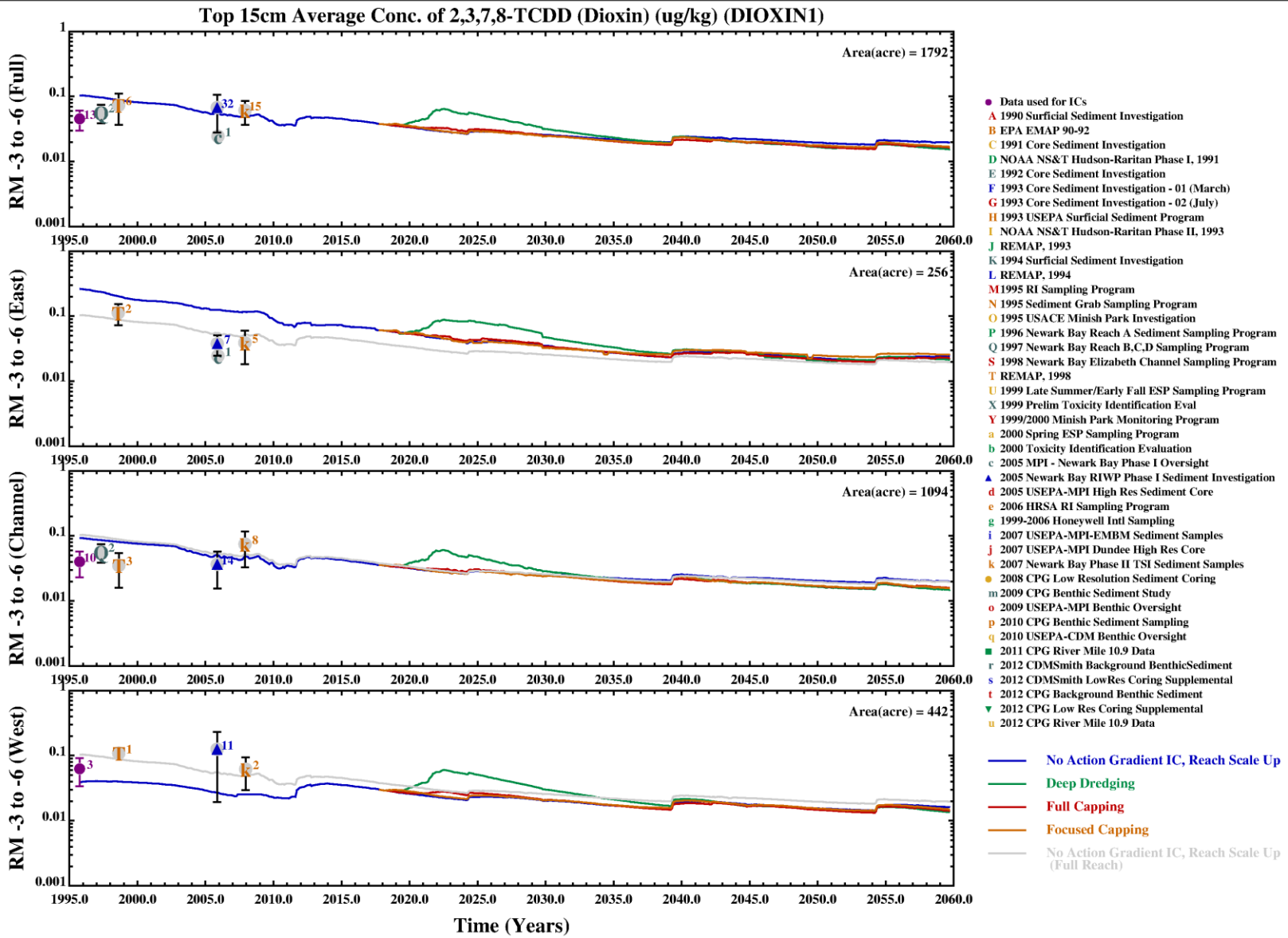
Figure 6-5

2014



Log Scale Temporal Plots of 2,3,7,8 TCDD Sediment Concentrations for No Action and Three Remedial Alternatives (RM-1.5 to -2.6)
 Lower Eight Miles of the Lower Passaic River

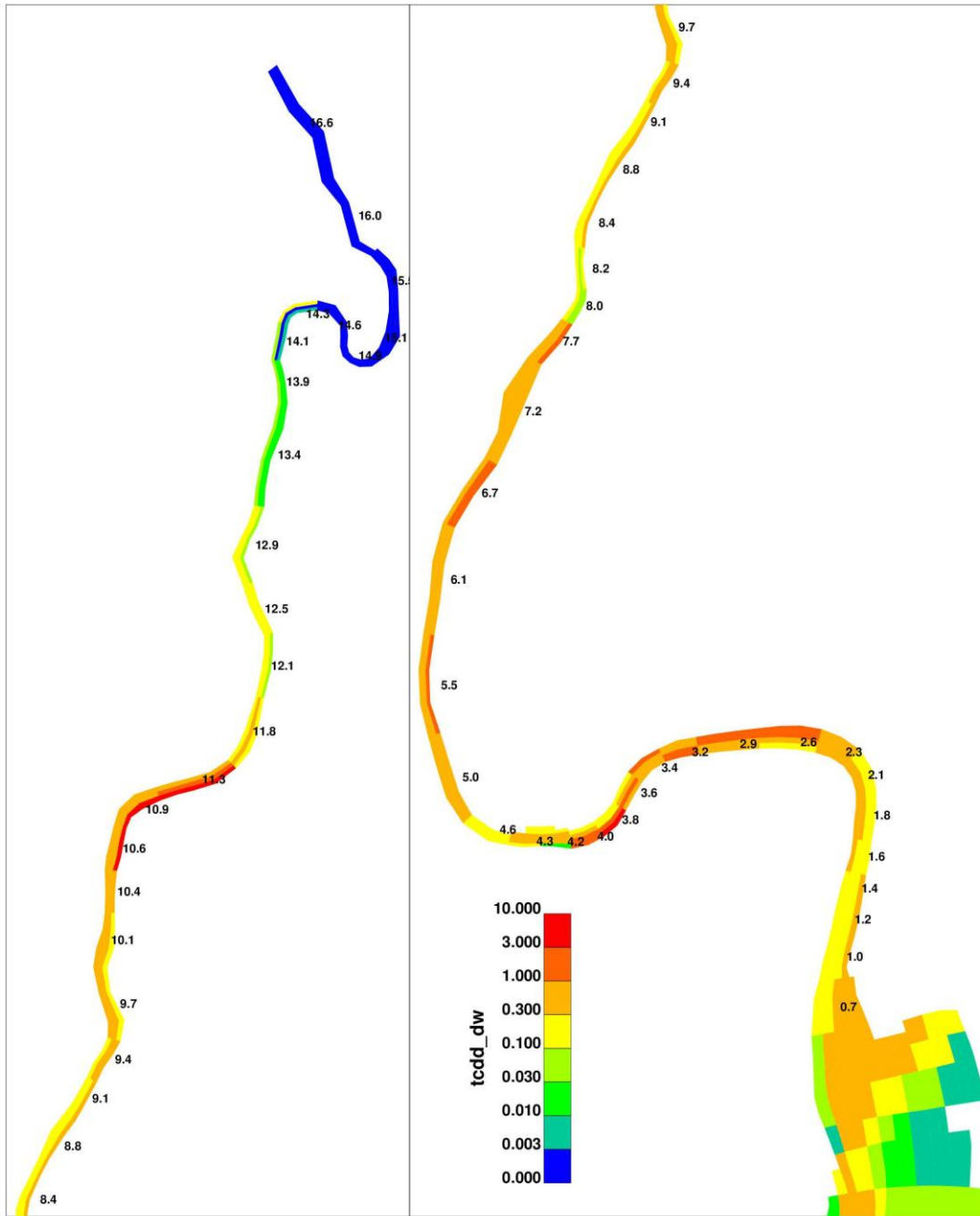
Figure 6-6
 2014



Log Scale Temporal Plots of 2,3,7,8 TCDD Sediment Concentrations for No Action and Three Remedial Alternatives (RM-2.6 to -5.25)
Lower Eight Miles of the Lower Passaic River

Figure 6-7
2014

No Action
Top 15 cm 2,3,7,8-TeCDD (ug/Kg-DW) in yr: 1995.75



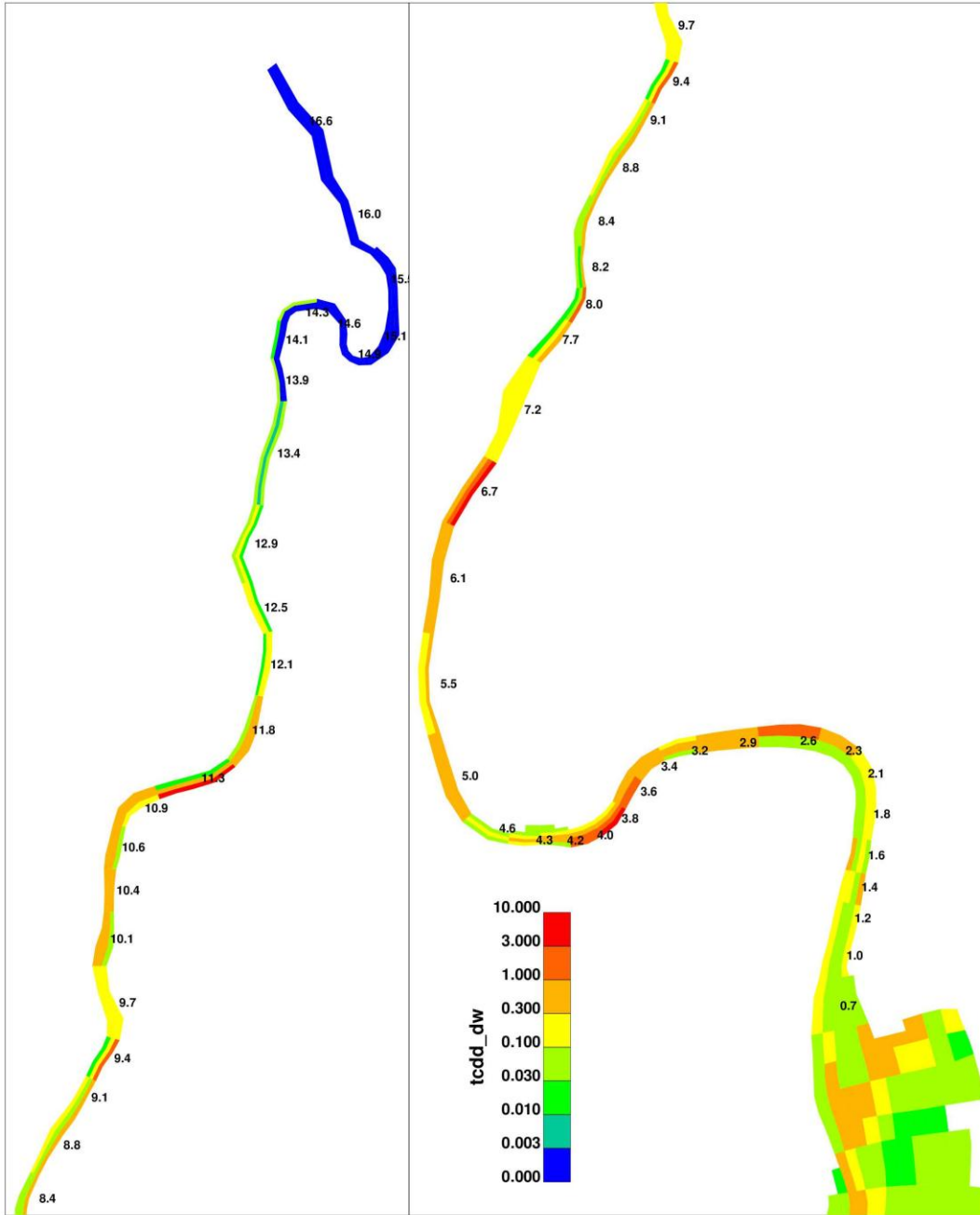
Spatial Distribution of 2,3,7,8 TCDD in October 1995

Figure 6-8

Lower Eight Miles of the Lower Passaic River

2014

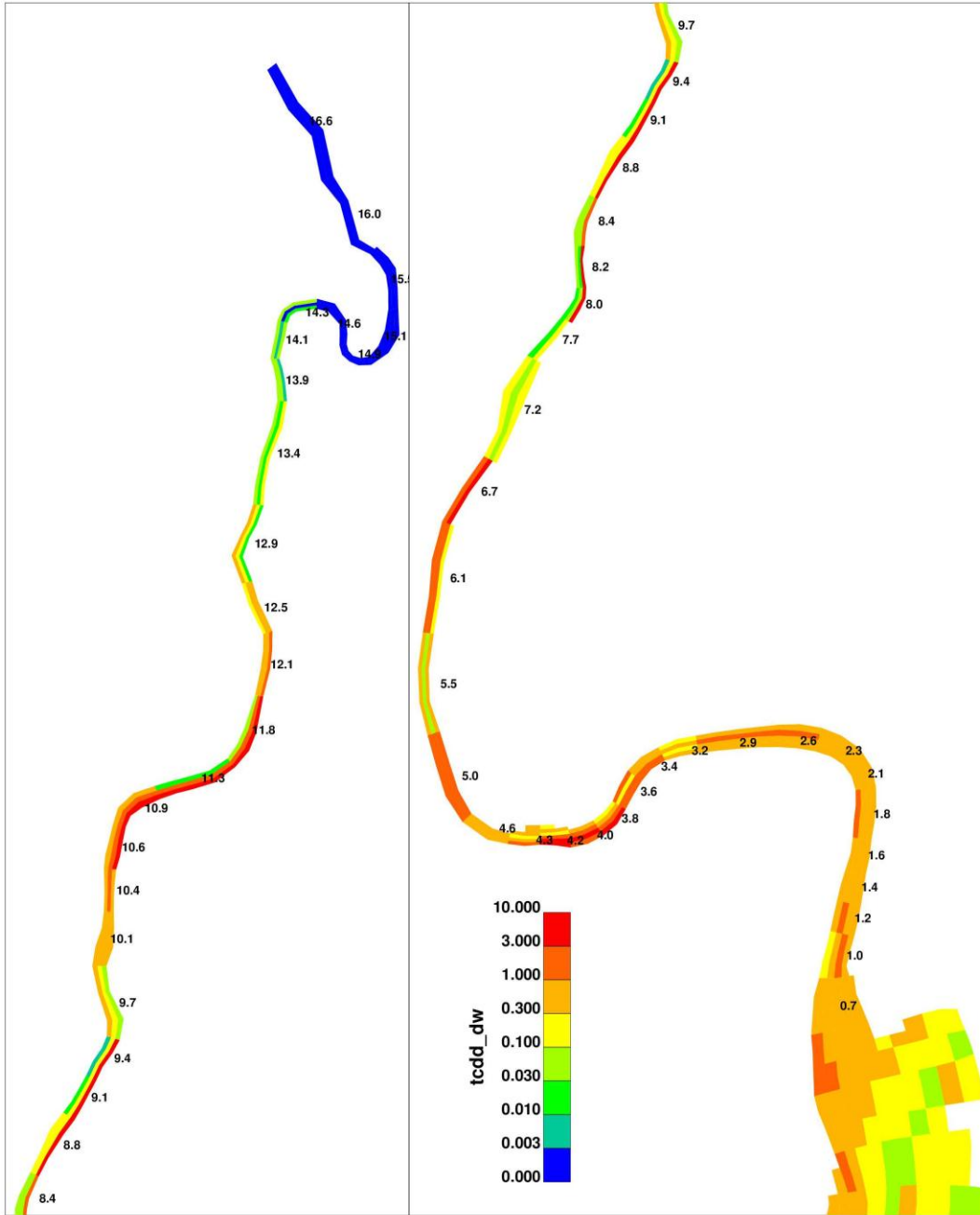
No Action
Top 15 cm 2,3,7,8-TeCDD (ug/Kg-DW) in yr: 2005.04



Spatial Distribution of 2,3,7,8 TCDD in January 2005

Figure 6-9

No Action
Top 15 cm 2,3,7,8-TeCDD (ug/Kg-DW) in yr: 2012.04



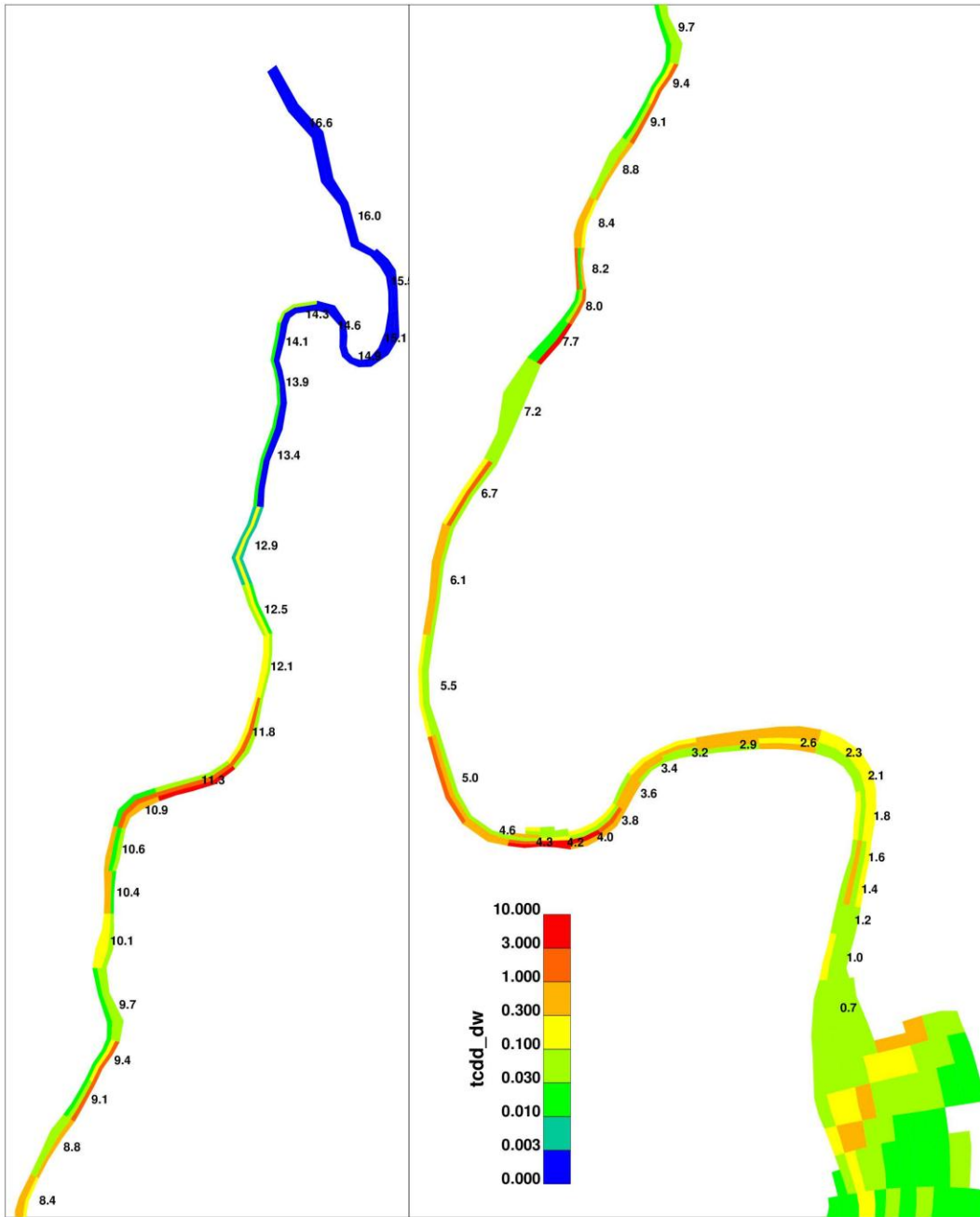
Spatial Distribution of 2,3,7,8 TCDD in January 2012

Figure 6-10

Lower Eight Miles of the Lower Passaic River

2014

No Action
Top 15 cm 2,3,7,8-TeCDD (ug/Kg-DW) in yr: 2059.74



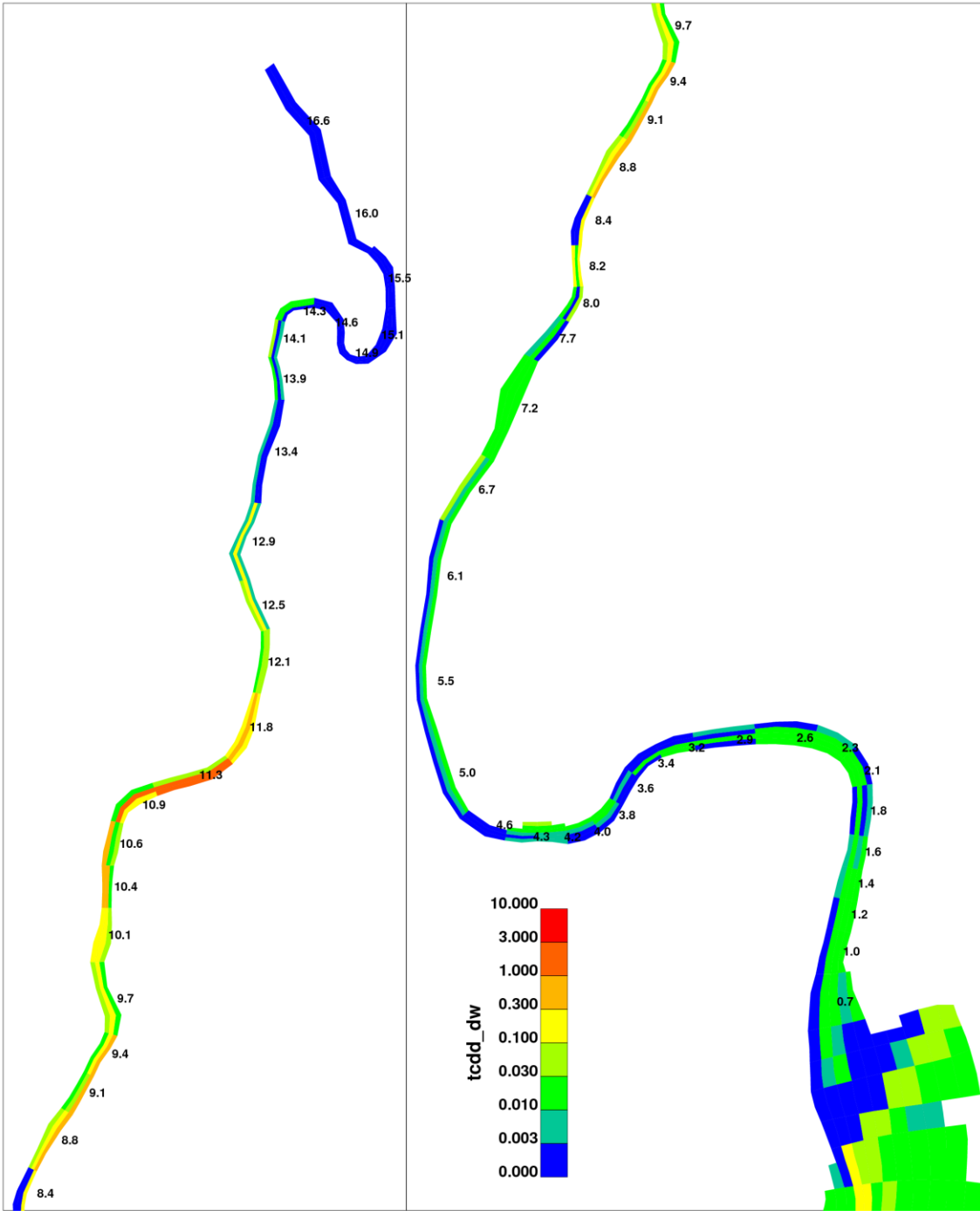
Spatial Distribution of 2,3,7,8 TCDD in January 2059 - No Action Simulation

Lower Eight Miles of the Lower Passaic River

Figure 6-11

2014

Dredging Scenario
Top 15 cm 2,3,7,8-TeCDD (ug/Kg-DW) in yr: 2059.74



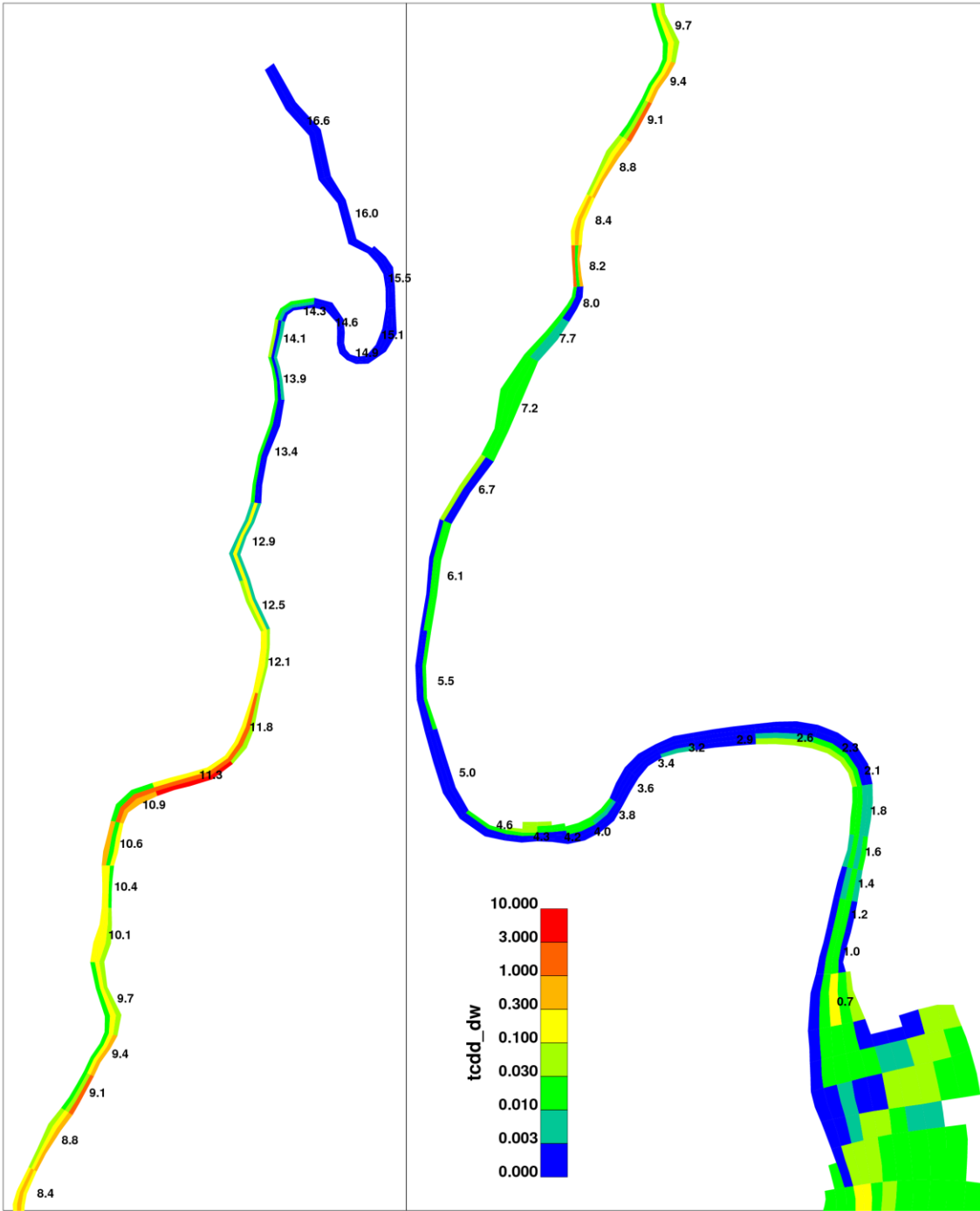
Spatial Distribution of 2,3,7,8 TCDD in January 2059 - Deep Dredging Simulation

Lower Eight Miles of the Lower Passaic River

Figure 6-12

2014

Capping Scenario
Top 15 cm 2,3,7,8-TeCDD (ug/Kg-DW) in yr: 2059.74



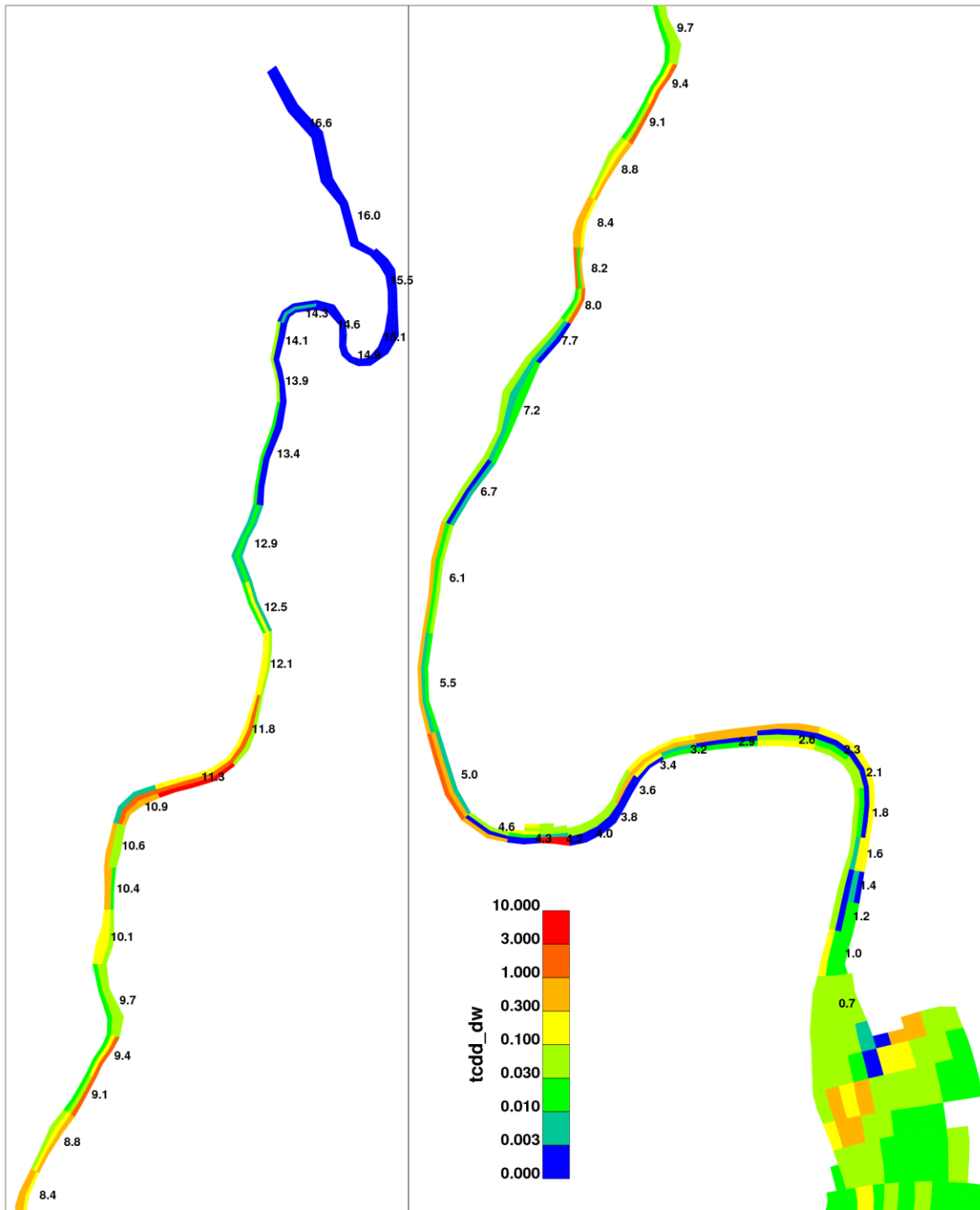
Spatial Distribution of 2,3,7,8 TCDD in January 2059 - Full Capping Simulation

Lower Eight Miles of the Lower Passaic River

Figure 6-13

2014

Focused Capping Scenario
Top 15 cm 2,3,7,8-TeCDD (ug/Kg-DW) in yr: 2059.74

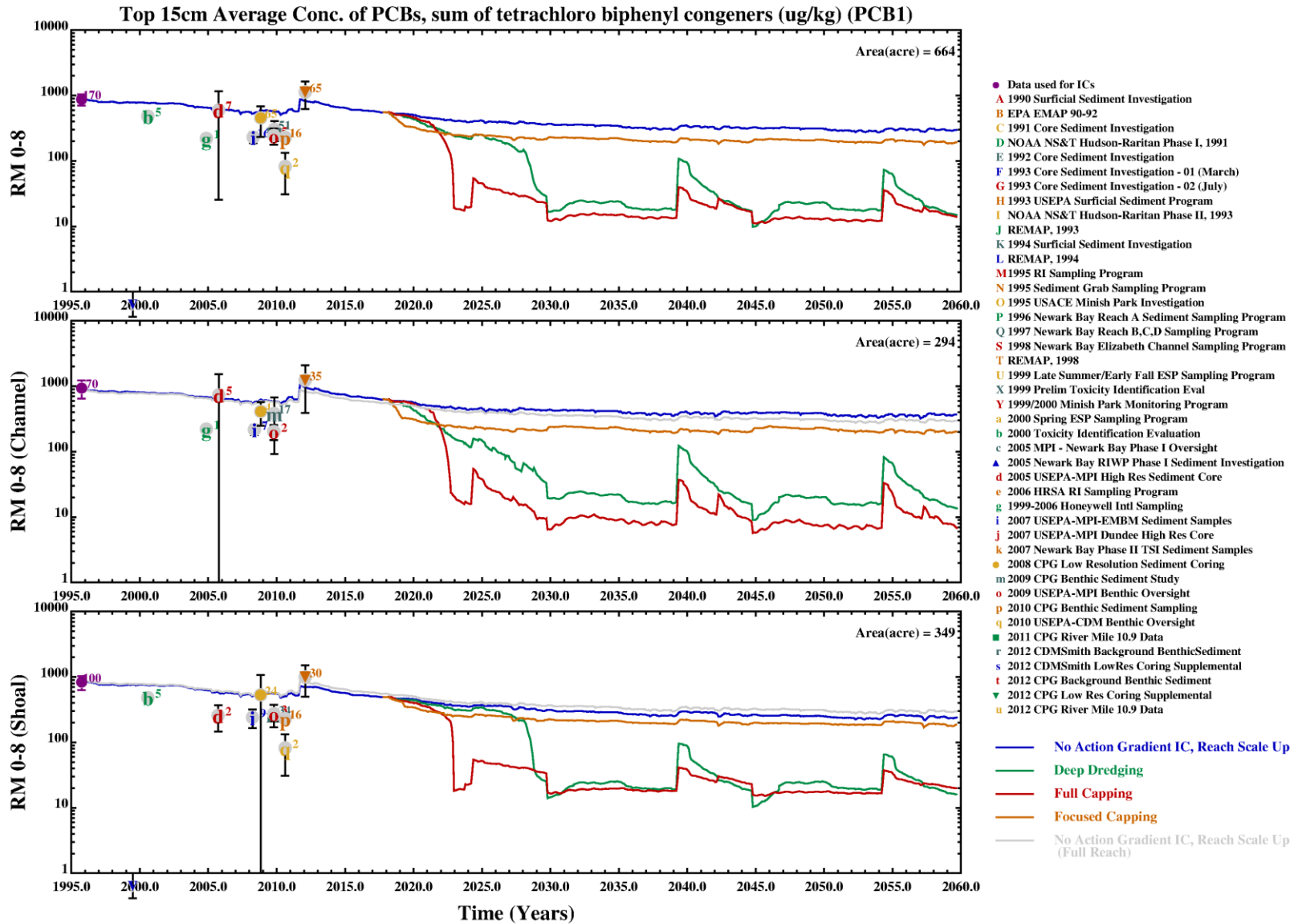


Spatial Distribution of 2,3,7,8 TCDD in January 2059 - Focused Capping Simulation

Lower Eight Miles of the Lower Passaic River

Figure 6-14

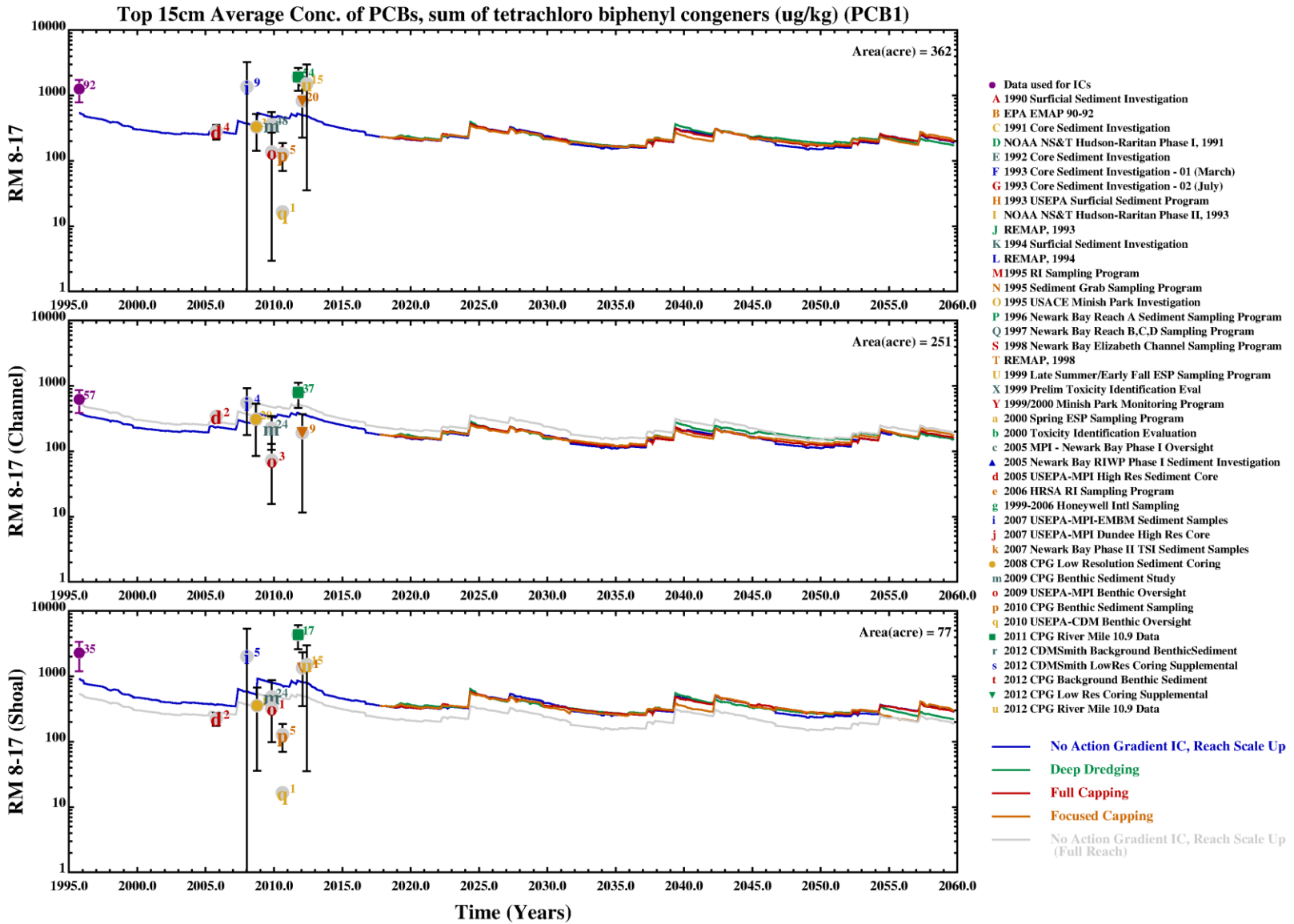
2014



Log Scale Temporal Plots of Tetra-PCB Homolog Group Sediment Concentrations for No Action and Three Remedial Alternatives (RM0-8.3)
Lower Eight Miles of the Lower Passaic River

Figure 6-15

2014

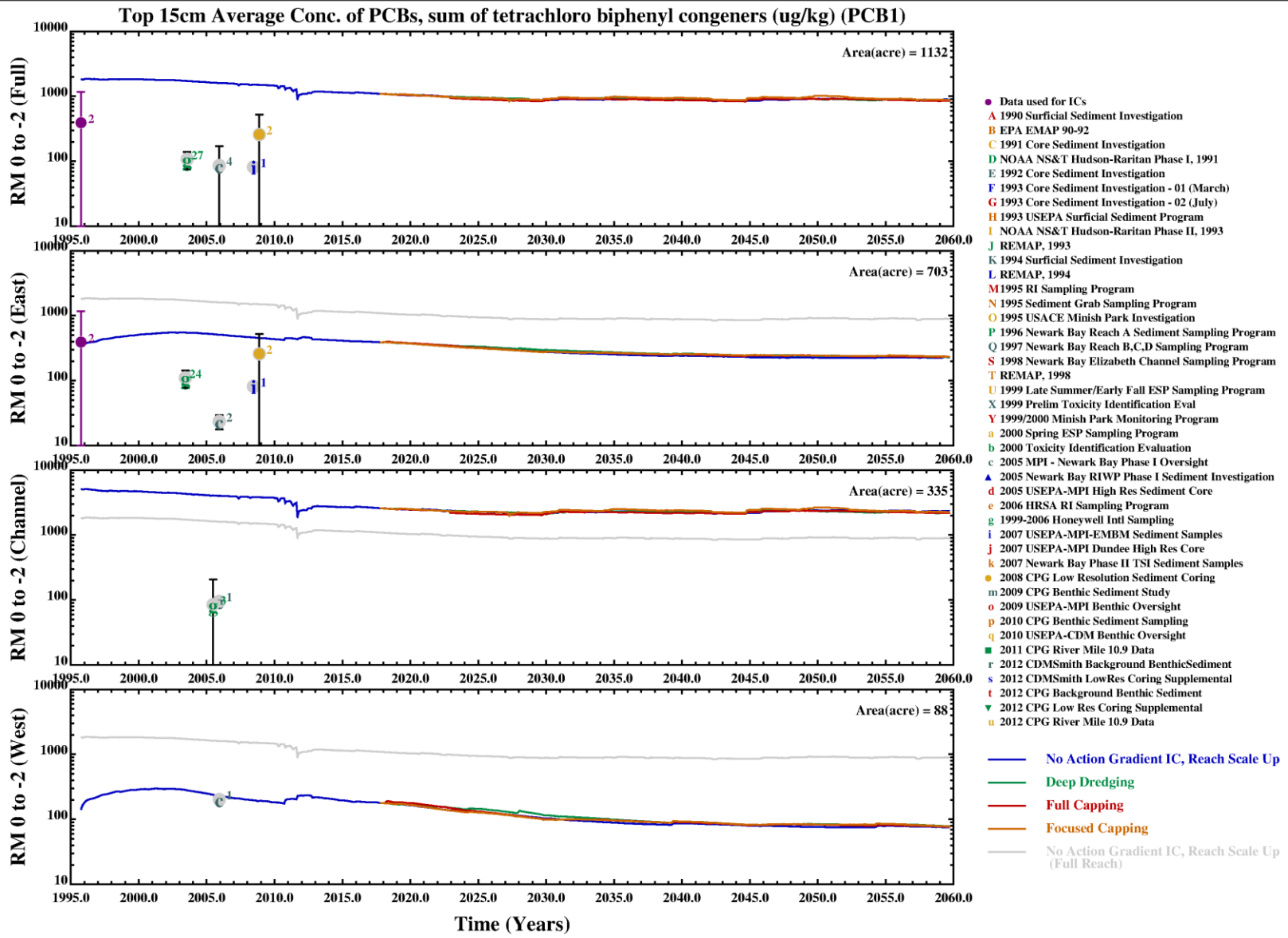


Log Scale Temporal Plots of Tetra-PCB Homolog Group Sediment Concentrations for No Action and Three Remedial Alternatives (RM8.3-17)

Lower Eight Miles of the Lower Passaic River

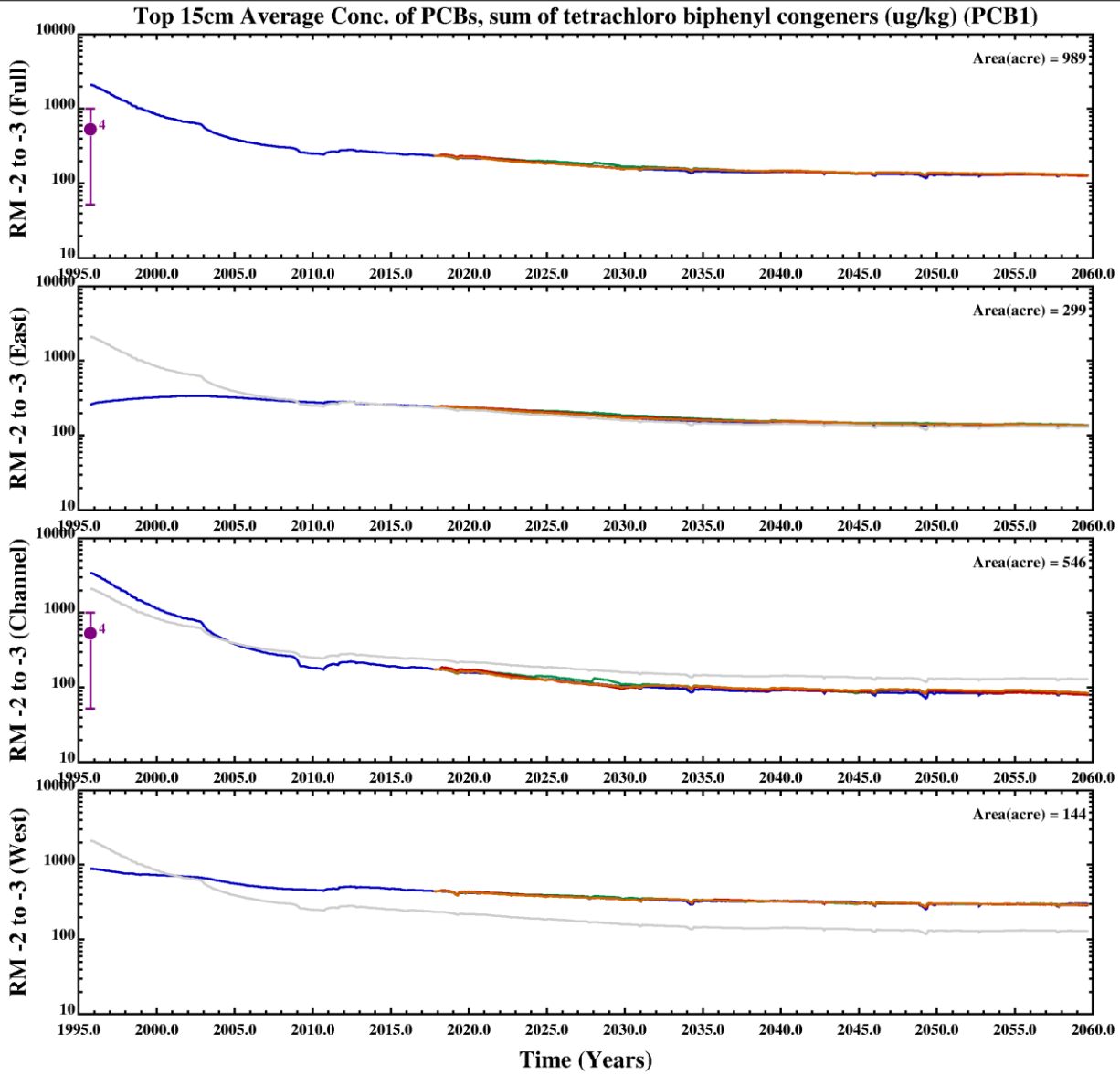
Figure 6-16

2014



Log Scale Temporal Plots of Tetra-PCB Homolog Group Sediment Concentrations for No Action and Three Remedial Alternatives (RM0 to -1.5)
Lower Eight Miles of the Lower Passaic River

Figure 6-17
2014

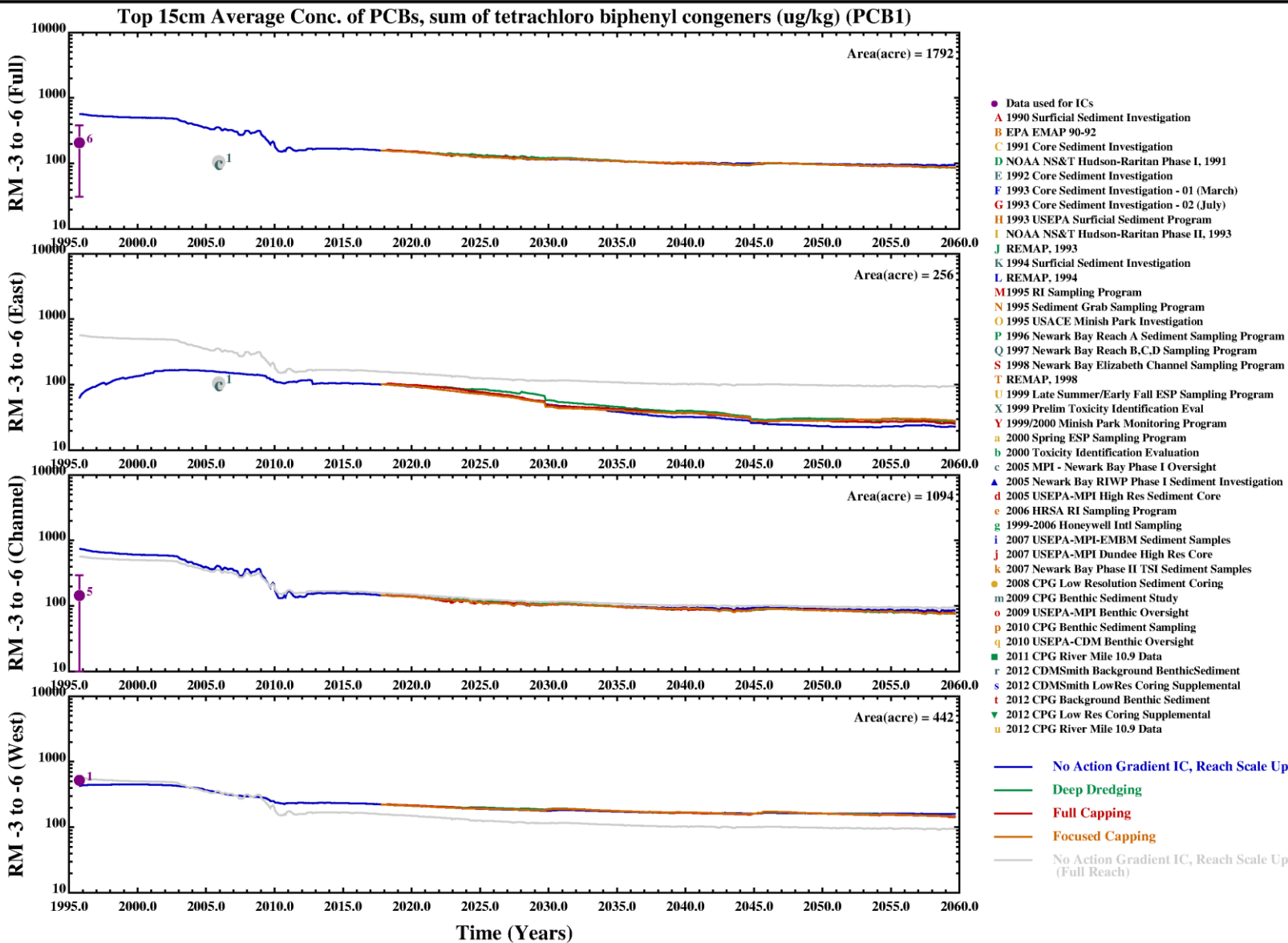


- Data used for ICs
 - A 1990 Surficial Sediment Investigation
 - B EPA EMAP 90-92
 - C 1991 Core Sediment Investigation
 - D NOAA NS&T Hudson-Raritan Phase I, 1991
 - E 1992 Core Sediment Investigation
 - F 1993 Core Sediment Investigation - 01 (March)
 - G 1993 Core Sediment Investigation - 02 (July)
 - H 1993 USEPA Surficial Sediment Program
 - I NOAA NS&T Hudson-Raritan Phase II, 1993
 - J REMAP, 1993
 - K 1994 Surficial Sediment Investigation
 - L REMAP, 1994
 - M 1995 RI Sampling Program
 - N 1995 Sediment Grab Sampling Program
 - O 1995 USACE Minish Park Investigation
 - P 1996 Newark Bay Reach A Sediment Sampling Program
 - Q 1997 Newark Bay Reach B,C,D Sampling Program
 - S 1998 Newark Bay Elizabeth Channel Sampling Program
 - T REMAP, 1998
 - U 1999 Late Summer/Early Fall ESP Sampling Program
 - X 1999 Prelim Toxicity Identification Eval
 - Y 1999/2000 Minish Park Monitoring Program
 - a 2000 Spring ESP Sampling Program
 - b 2000 Toxicity Identification Evaluation
 - c 2005 MPI - Newark Bay Phase I Oversight
 - ▲ 2005 Newark Bay RIWP Phase I Sediment Investigation
 - d 2005 USEPA-MPI High Res Sediment Core
 - e 2006 HRSA RI Sampling Program
 - g 1999-2006 Honeywell Intl Sampling
 - i 2007 USEPA-MPI-EMBM Sediment Samples
 - j 2007 USEPA-MPI Dundee High Res Core
 - k 2007 Newark Bay Phase II TSI Sediment Samples
 - 2008 CPG Low Resolution Sediment Coring
 - m 2009 CPG Benthic Sediment Study
 - o 2009 USEPA-MPI Benthic Oversight
 - p 2010 CPG Benthic Sediment Sampling
 - q 2010 USEPA-CDM Benthic Oversight
 - 2011 CPG River Mile 10.9 Data
 - r 2012 CDMSmith Background Benthic Sediment
 - s 2012 CDMSmith Low Res Coring Supplemental
 - t 2012 CPG Background Benthic Sediment
 - v 2012 CPG Low Res Coring Supplemental
 - u 2012 CPG River Mile 10.9 Data
- No Action Gradient IC, Reach Scale Up
 - Deep Dredging
 - Full Capping
 - Focused Capping
 - No Action Gradient IC, Reach Scale Up (Full Reach)

Log Scale Temporal Plots of Tetra-PCB Homolog Group Sediment Concentrations for No Action and Three Remedial Alternatives (RM-1.5 to -2.6)
Lower Eight Miles of the Lower Passaic River

Figure 6-18

2014



Log Scale Temporal Plots of Tetra-PCB Homolog Group Sediment Concentrations for No Action and Three Remedial Alternatives (RM-2.6 to -5.25)
Lower Eight Miles of the Lower Passaic River

Figure 6-19
2014

No Action
Top 15 cm Tetrachlorobiphenyl (mg/Kg-DW) in yr: 1995.75



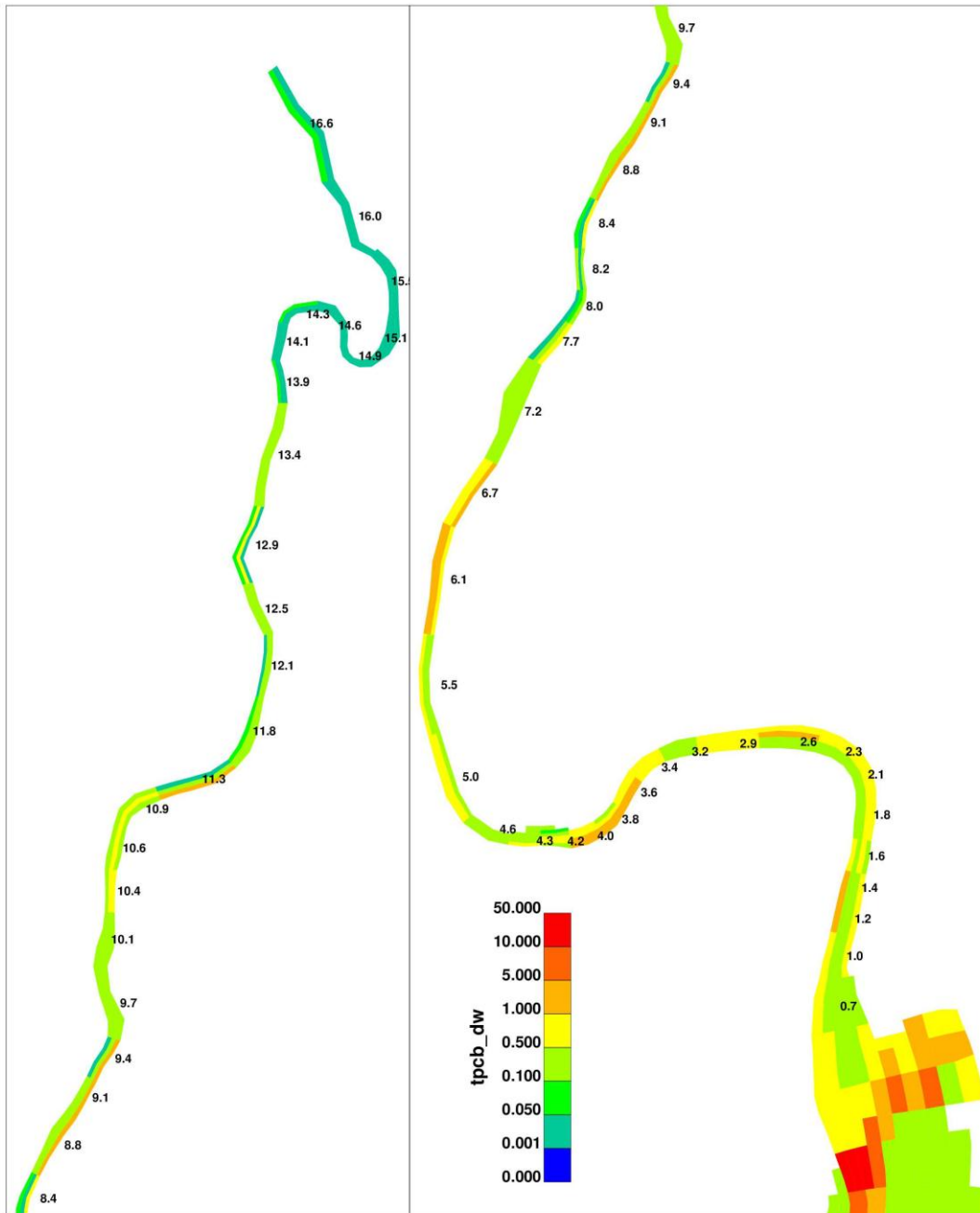
Spatial Distribution of Tetra-PCB Homolog Group in October 1995

Figure 6-20

Lower Eight Miles of the Lower Passaic River

2014

No Action
Top 15 cm Tetrachlorobiphenyl (mg/Kg-DW) in yr: 2005.04



Spatial Distribution of Tetra-PCB Homolog Group in January 2005

Figure 6-21

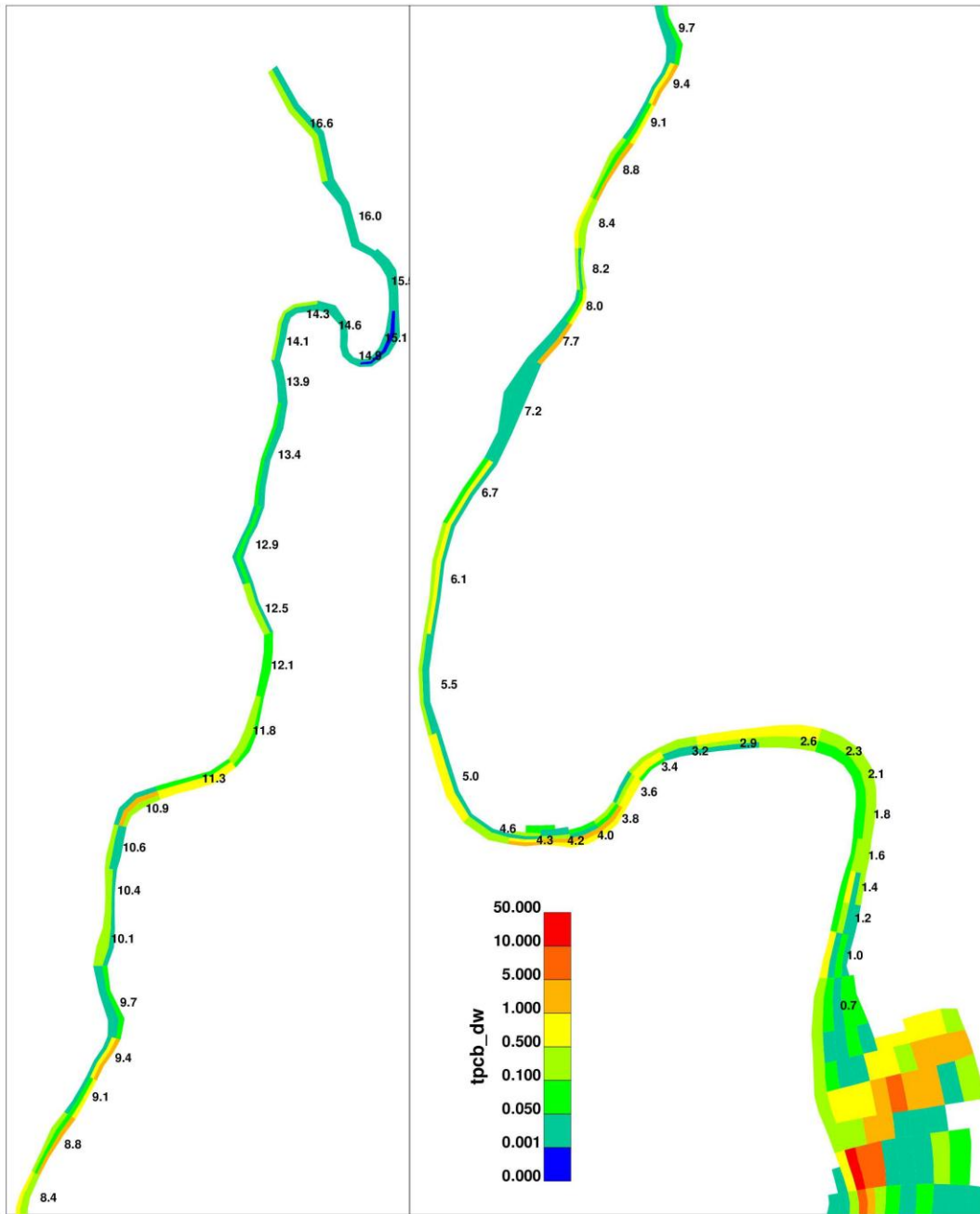
No Action
Top 15 cm Tetrachlorobiphenyl (mg/Kg-DW) in yr: 2012.04



Spatial Distribution of Tetra-PCB Homolog Group in January 2012

Figure 6-22

**No Action
Top 15 cm Tetrachlorobiphenyl (mg/Kg-DW) in yr: 2059.74**



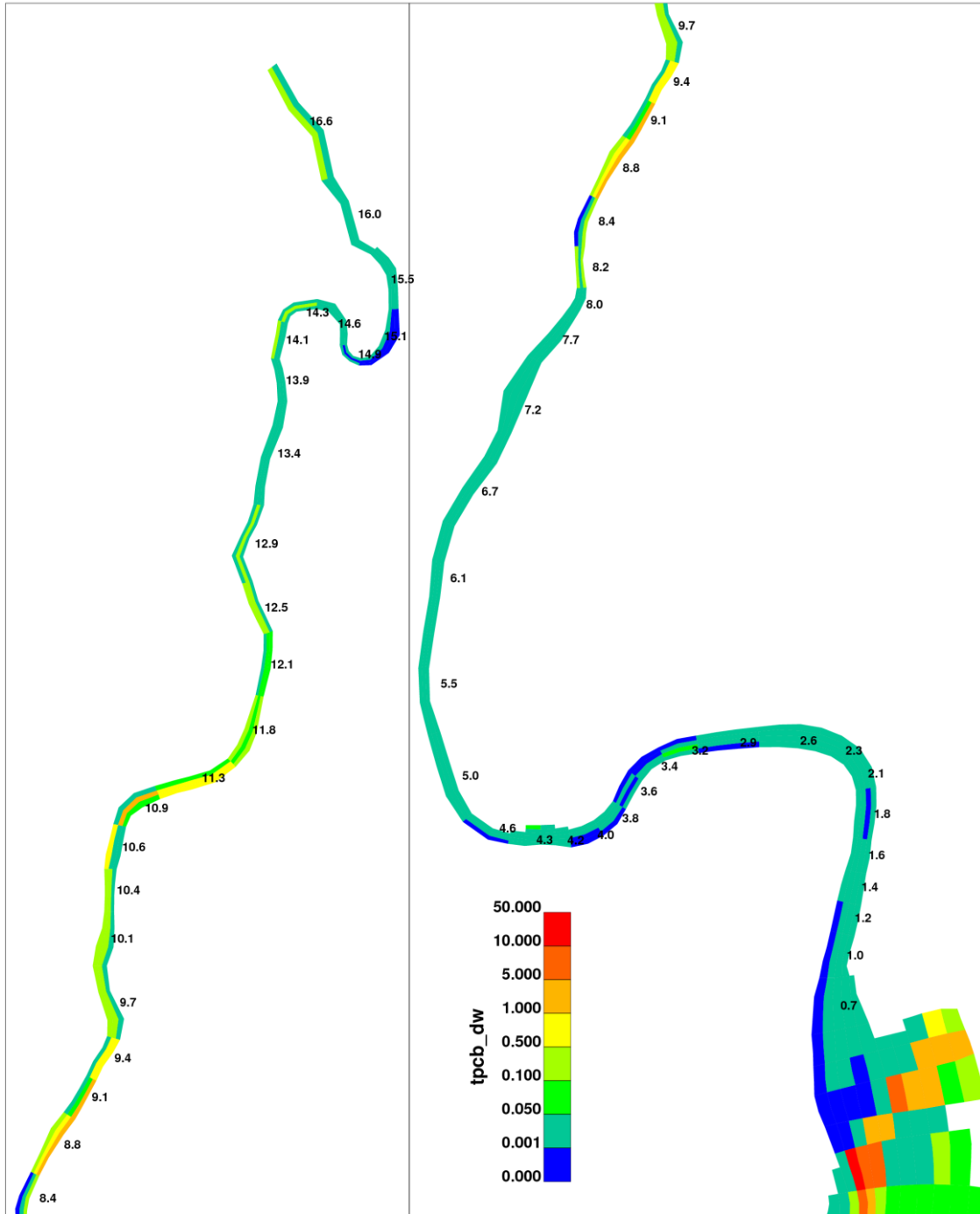
Spatial Distribution of Tetra-PCB Homolog Group in January 2059 - No Action Simulation

Lower Eight Miles of the Lower Passaic River

Figure 6-23

2014

**Dredging
Top 15 cm Tetrachlorobiphenyl (mg/Kg-DW) in yr: 2059.74**



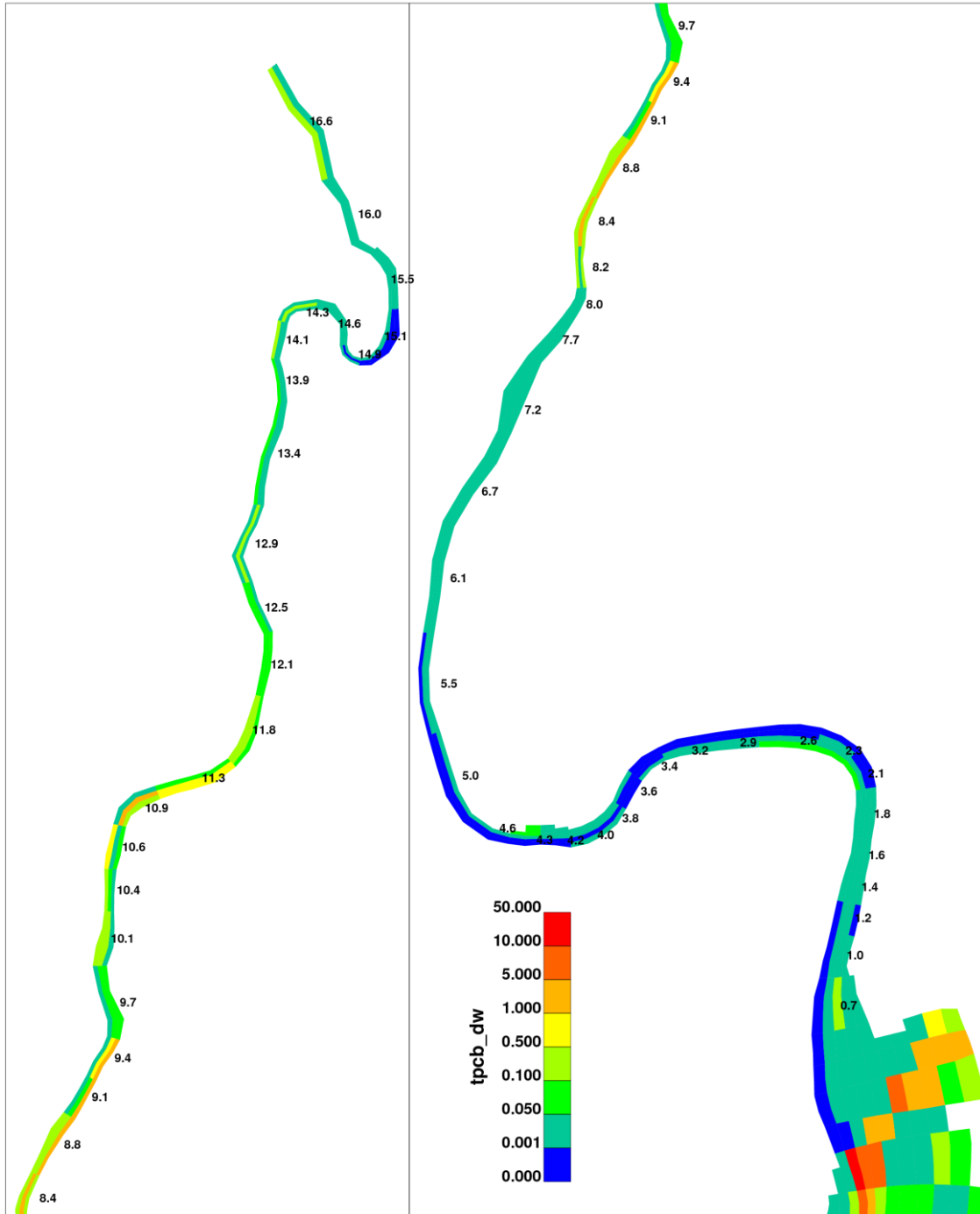
Spatial Distribution of Tetra-PCB Homolog Group in January 2059 -
Deep Dredging Simulation

Lower Eight Miles of the Lower Passaic River

Figure 6-24

2014

**Capping
Top 15 cm Tetrachlorobiphenyl (mg/Kg-DW) in yr: 2059.74**



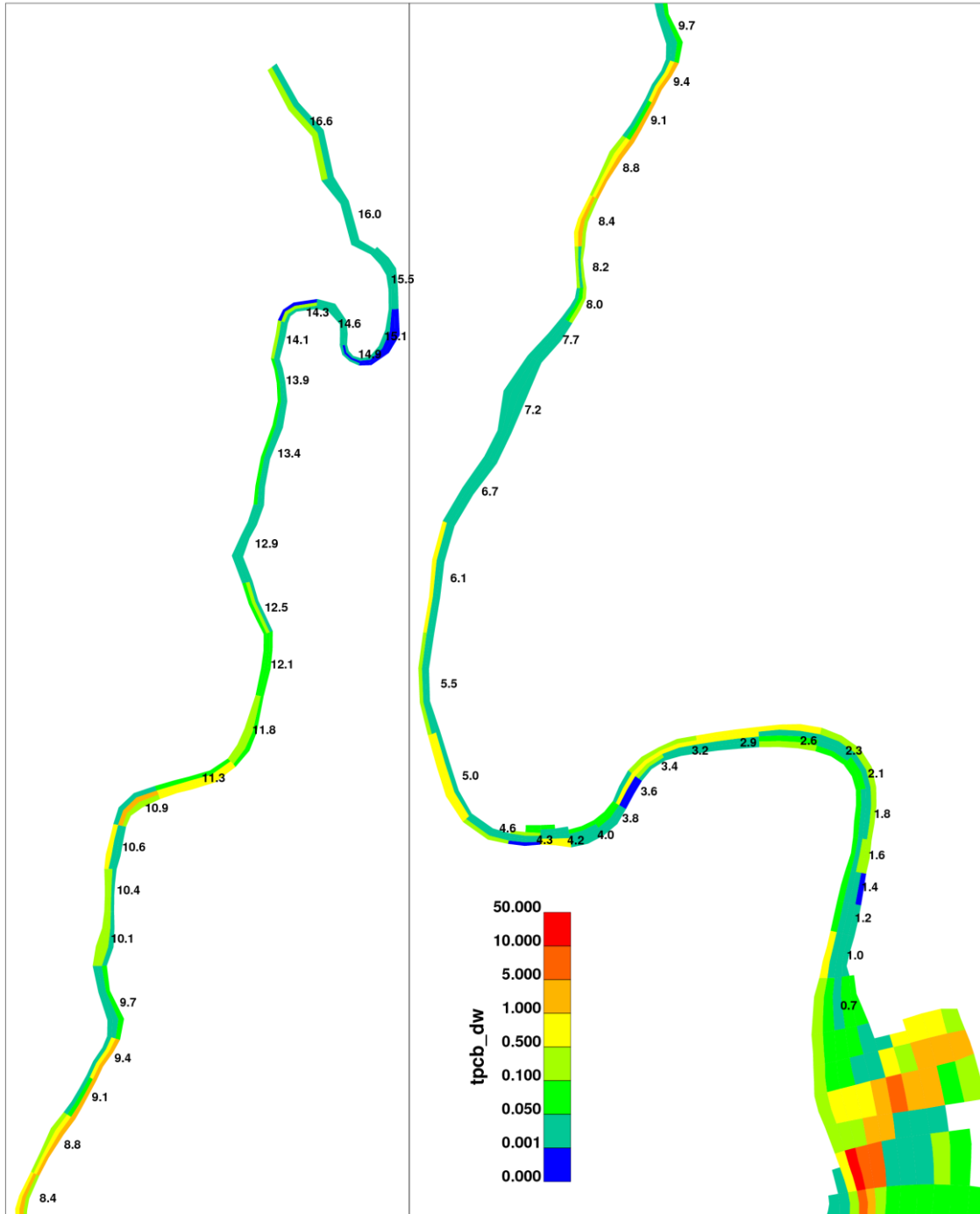
Spatial Distribution of Tetra-PCB Homolog Group in January 2059 - Full Capping Simulation

Lower Eight Miles of the Lower Passaic River

Figure 6-25

2014

Focused Capping
Top 15 cm Tetrachlorobiphenyl (mg/Kg-DW) in yr: 2059.74

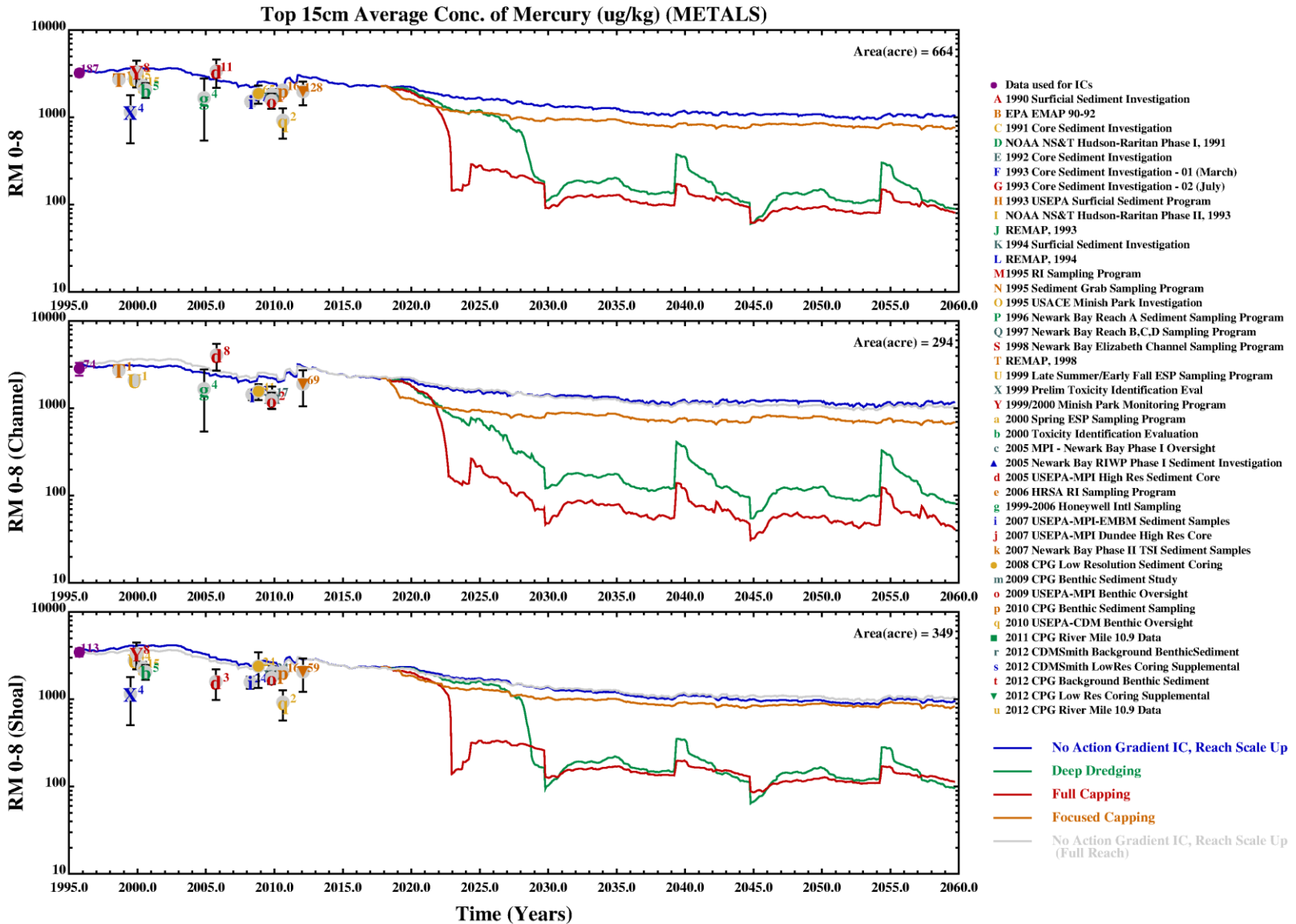


Spatial Distribution of Tetra-PCB Homolog Group in January 2059 -
 Focused Capping Simulation

Lower Eight Miles of the Lower Passaic River

Figure 6-26

2014

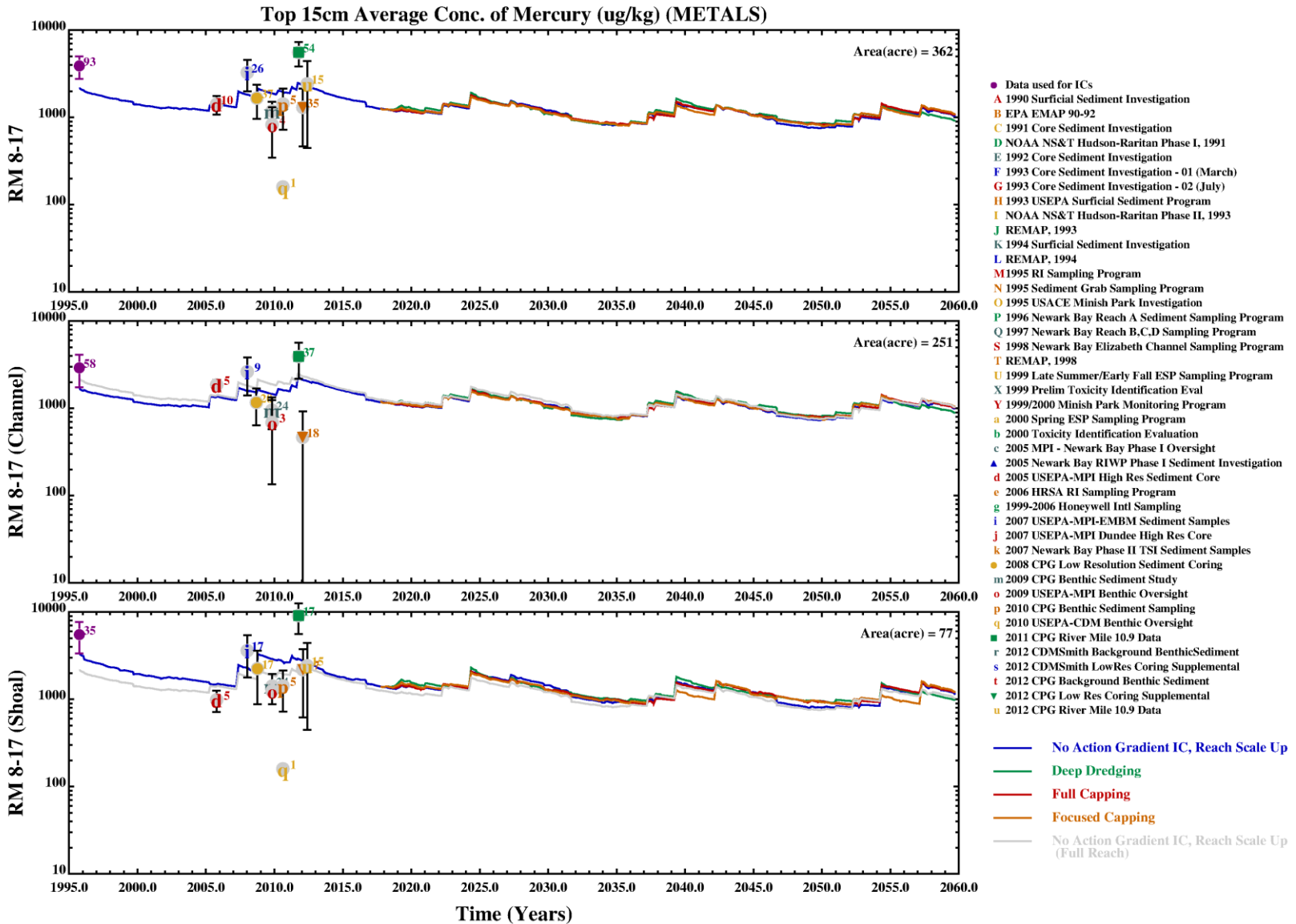


Log Scale Temporal Plots of Total Mercury Sediment Concentrations for No Action and Three Remedial Alternatives (RM0-8.3)

Lower Eight Miles of the Lower Passaic River

Figure 6-27

2014

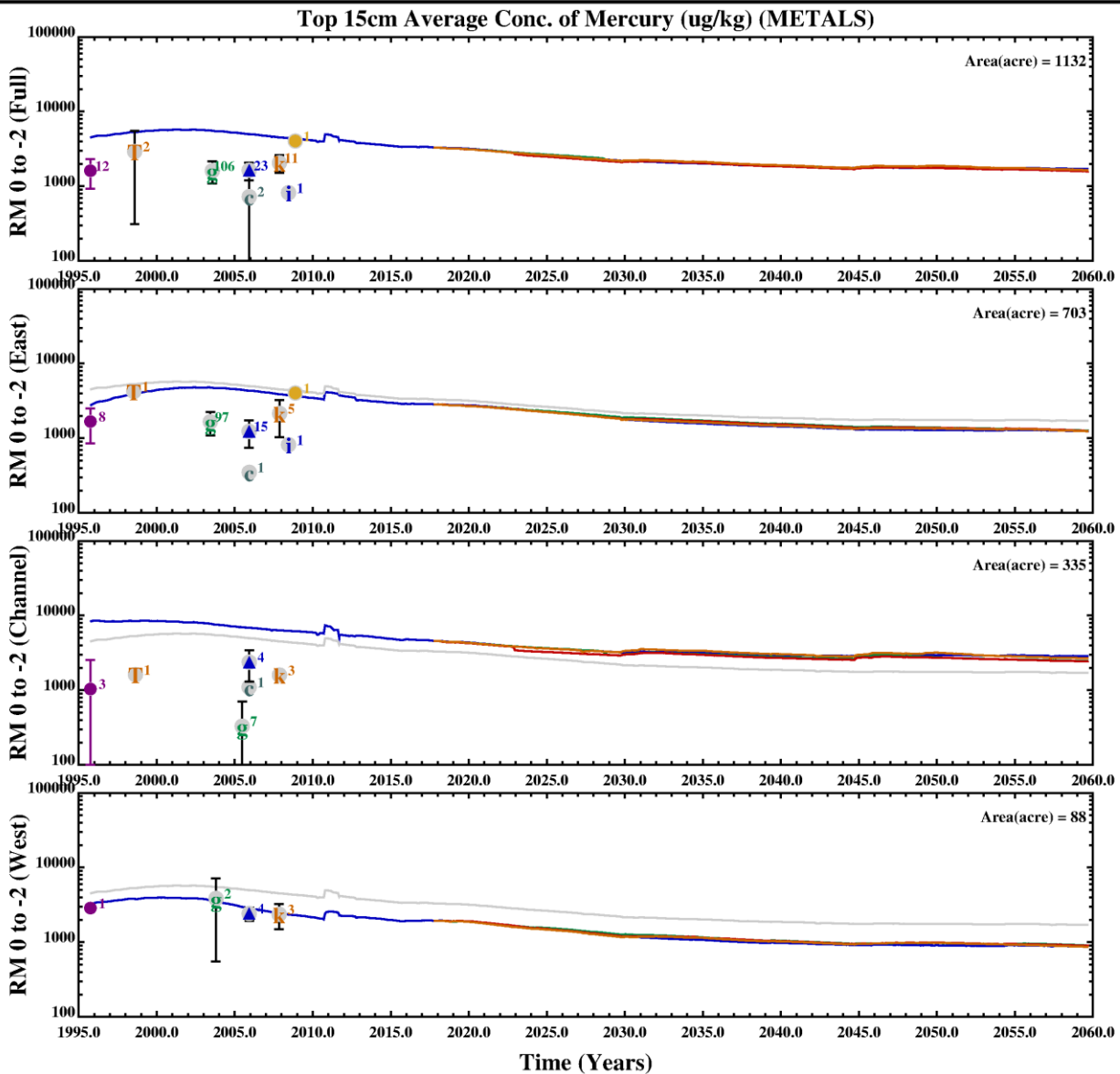


Log Scale Temporal Plots of Total Mercury Sediment Concentrations for No Action and Three Remedial Alternatives (RM8.3-17)

Lower Eight Miles of the Lower Passaic River

Figure 6-28

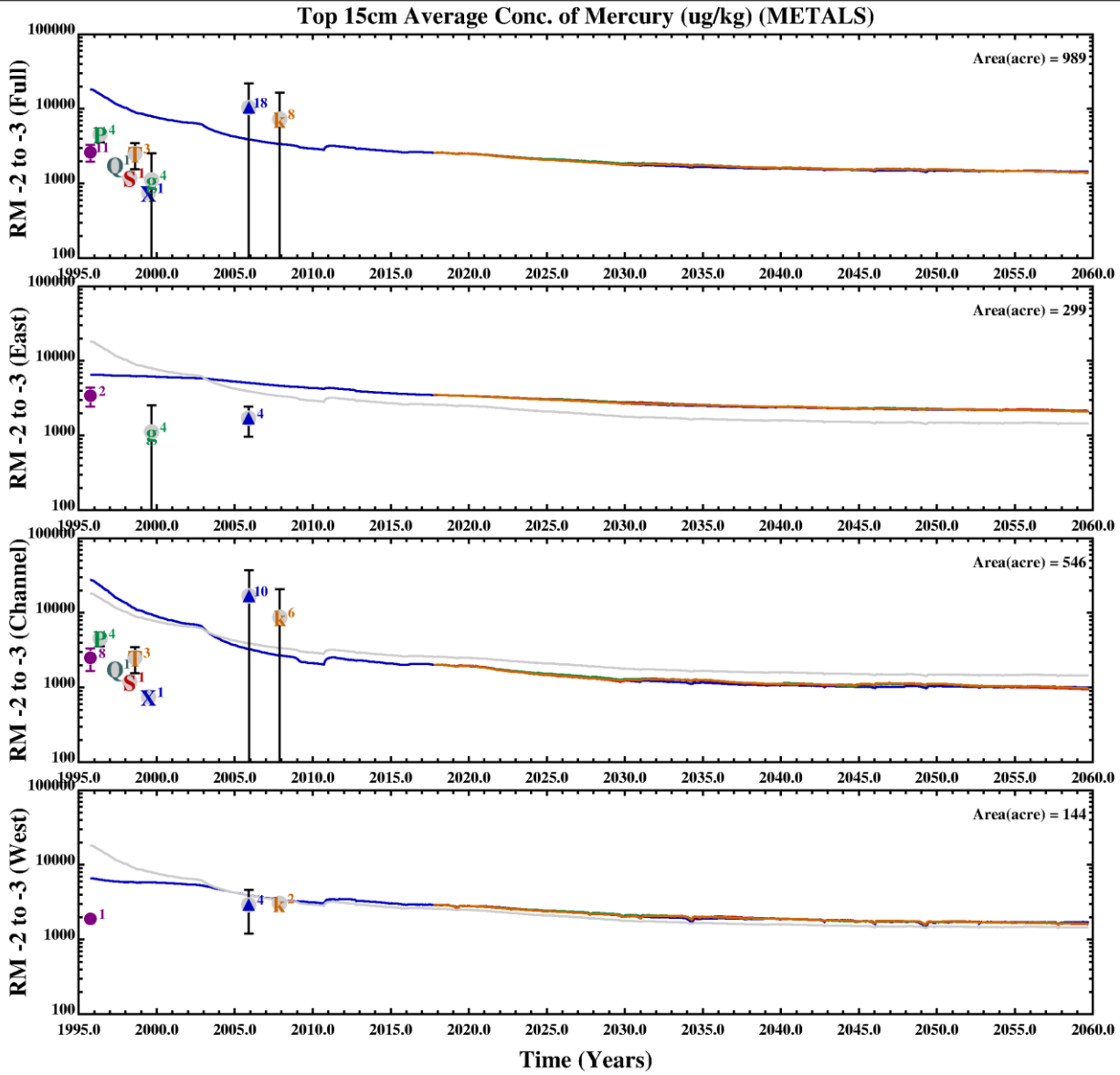
2014



- Data used for ICs
 - A 1990 Surficial Sediment Investigation
 - B EPA EMAP 90-92
 - C 1991 Core Sediment Investigation
 - D NOAA NS&T Hudson-Raritan Phase I, 1991
 - E 1992 Core Sediment Investigation
 - F 1993 Core Sediment Investigation - 01 (March)
 - G 1993 Core Sediment Investigation - 02 (July)
 - H 1993 USEPA Surficial Sediment Program
 - I NOAA NS&T Hudson-Raritan Phase II, 1993
 - J REMAP, 1993
 - K 1994 Surficial Sediment Investigation
 - L REMAP, 1994
 - M 1995 RI Sampling Program
 - N 1995 Sediment Grab Sampling Program
 - O 1995 USACE Minish Park Investigation
 - P 1996 Newark Bay Reach A Sediment Sampling Program
 - Q 1997 Newark Bay Reach B,C,D Sampling Program
 - S 1998 Newark Bay Elizabeth Channel Sampling Program
 - T REMAP, 1998
 - U 1999 Late Summer/Early Fall ESP Sampling Program
 - X 1999 Prelim Toxicity Identification Eval
 - Y 1999/2000 Minish Park Monitoring Program
 - a 2000 Spring ESP Sampling Program
 - b 2000 Toxicity Identification Evaluation
 - c 2005 MPI - Newark Bay Phase I Oversight
 - ▲ 2005 Newark Bay RIWP Phase I Sediment Investigation
 - d 2005 USEPA-MPI High Res Sediment Core
 - e 2006 HRSA RI Sampling Program
 - g 1999-2006 Honeywell Intl Sampling
 - i 2007 USEPA-MPI-EMBM Sediment Samples
 - j 2007 USEPA-MPI Dundee High Res Core
 - k 2007 Newark Bay Phase II TSI Sediment Samples
 - 2008 CPG Low Resolution Sediment Coring
 - m 2009 CPG Benthic Sediment Study
 - o 2009 USEPA-MPI Benthic Oversight
 - p 2010 CPG Benthic Sediment Sampling
 - q 2010 USEPA-CDM Benthic Oversight
 - 2011 CPG River Mile 10.9 Data
 - r 2012 CDMSmith Background Benthic Sediment
 - s 2012 CDMSmith Low Res Coring Supplemental
 - t 2012 CPG Background Benthic Sediment
 - v 2012 CPG Low Res Coring Supplemental
 - u 2012 CPG River Mile 10.9 Data
-
- No Action Gradient IC, Reach Scale Up
 - Deep Dredging
 - Full Capping
 - Focused Capping
 - No Action Gradient IC, Reach Scale Up (Full Reach)

Log Scale Temporal Plots of Total Mercury Sediment Concentrations for No Action and Three Remedial Alternatives (RM0 to -1.5)
Lower Eight Miles of the Lower Passaic River

Figure 6-29
 2014

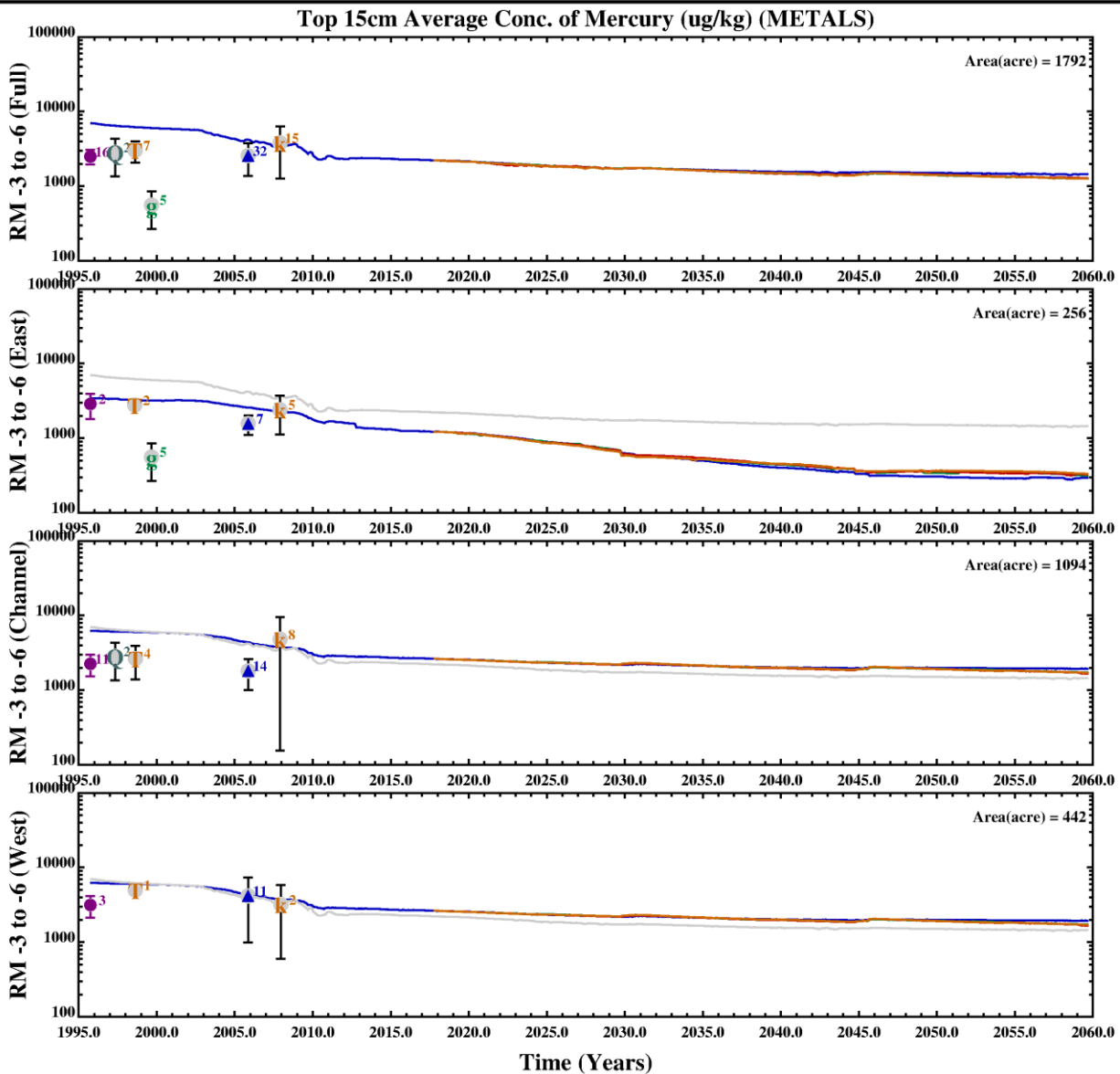


- Data used for ICs
 - A 1990 Surficial Sediment Investigation
 - B EPA EMAP 90-92
 - C 1991 Core Sediment Investigation
 - D NOAA NS&T Hudson-Raritan Phase I, 1991
 - E 1992 Core Sediment Investigation
 - F 1993 Core Sediment Investigation - 01 (March)
 - G 1993 Core Sediment Investigation - 02 (July)
 - H 1993 USEPA Surficial Sediment Program
 - I NOAA NS&T Hudson-Raritan Phase II, 1993
 - J REMAP, 1993
 - K 1994 Surficial Sediment Investigation
 - L REMAP, 1994
 - M 1995 RI Sampling Program
 - N 1995 Sediment Grab Sampling Program
 - O 1995 USACE Minish Park Investigation
 - P 1996 Newark Bay Reach A Sediment Sampling Program
 - Q 1997 Newark Bay Reach B,C,D Sampling Program
 - S 1998 Newark Bay Elizabeth Channel Sampling Program
 - T REMAP, 1998
 - U 1999 Late Summer/Early Fall ESP Sampling Program
 - X 1999 Prelim Toxicity Identification Eval
 - Y 1999/2000 Minish Park Monitoring Program
 - a 2000 Spring ESP Sampling Program
 - b 2000 Toxicity Identification Evaluation
 - c 2005 MPI - Newark Bay Phase I Oversight
 - ▲ 2005 Newark Bay RIWP Phase I Sediment Investigation
 - d 2005 USEPA-MPI High Res Sediment Core
 - e 2006 HRSA RI Sampling Program
 - g 1999-2006 Honeywell Intl Sampling
 - i 2007 USEPA-MPI-EMBM Sediment Samples
 - j 2007 USEPA-MPI Dundee High Res Core
 - k 2007 Newark Bay Phase II TSI Sediment Samples
 - 2008 CPG Low Resolution Sediment Coring
 - m 2009 CPG Benthic Sediment Study
 - o 2009 USEPA-MPI Benthic Oversight
 - p 2010 CPG Benthic Sediment Sampling
 - q 2010 USEPA-CDM Benthic Oversight
 - 2011 CPG River Mile 10.9 Data
 - r 2012 CDMSmith Background Benthic Sediment
 - s 2012 CDMSmith Low Res Coring Supplemental
 - t 2012 CPG Background Benthic Sediment
 - ▼ 2012 CPG Low Res Coring Supplemental
 - u 2012 CPG River Mile 10.9 Data
-
- No Action Gradient IC, Reach Scale Up
 - Deep Dredging
 - Full Capping
 - Focused Capping
 - No Action Gradient IC, Reach Scale Up (Full Reach)

Log Scale Temporal Plots of Total Mercury Sediment Concentrations for No Action and Three Remedial Alternatives (RM-1.5 to -2.6)
Lower Eight Miles of the Lower Passaic River

Figure 6-30

2014



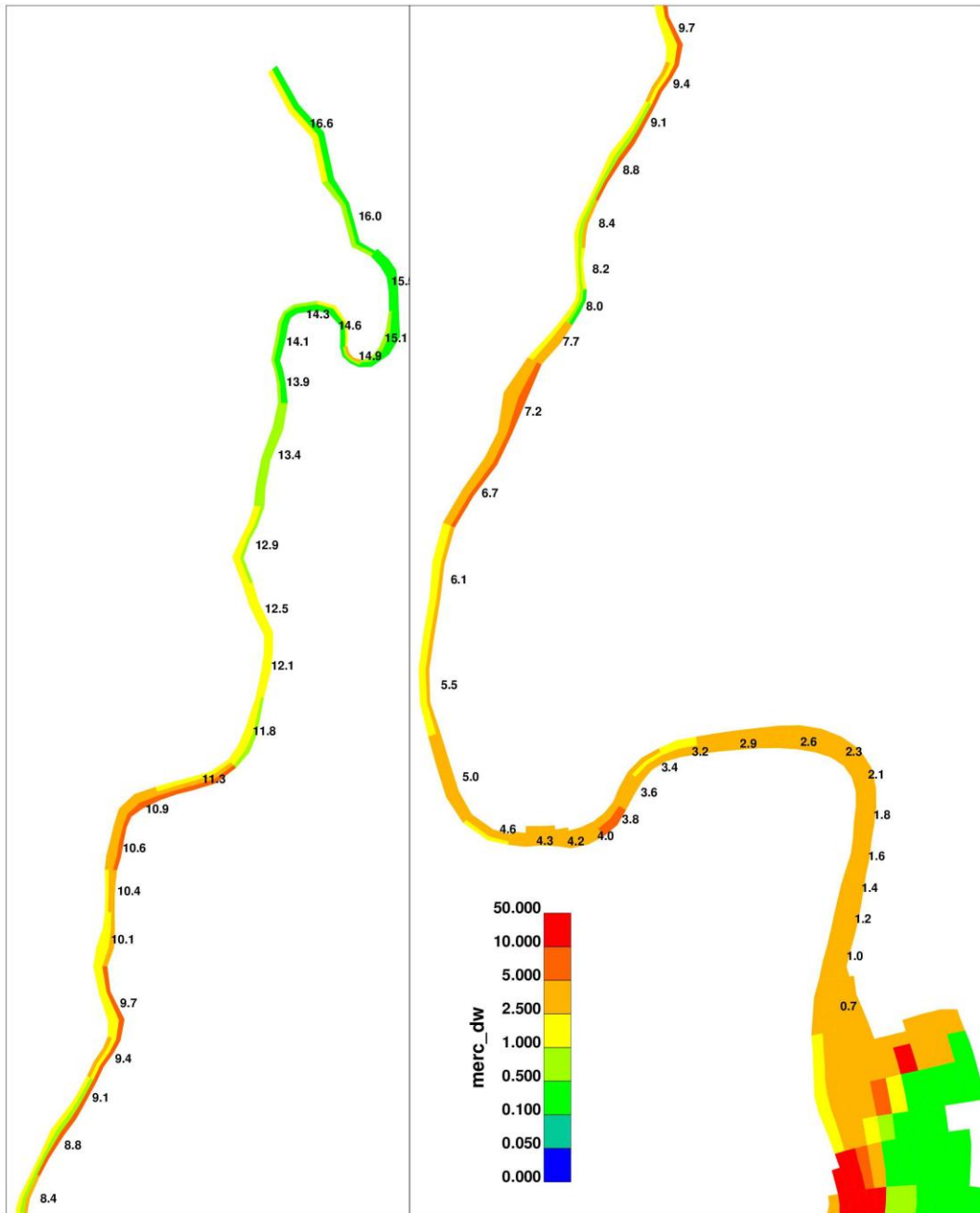
- Data used for ICs
 - A 1990 Surficial Sediment Investigation
 - B EPA EMAP 90-92
 - C 1991 Core Sediment Investigation
 - D NOAA NS&T Hudson-Raritan Phase I, 1991
 - E 1992 Core Sediment Investigation
 - F 1993 Core Sediment Investigation - 01 (March)
 - G 1993 Core Sediment Investigation - 02 (July)
 - H 1993 USEPA Surficial Sediment Program
 - I NOAA NS&T Hudson-Raritan Phase II, 1993
 - J REMAP, 1993
 - K 1994 Surficial Sediment Investigation
 - L REMAP, 1994
 - M 1995 RI Sampling Program
 - N 1995 Sediment Grab Sampling Program
 - O 1995 USACE Minish Park Investigation
 - P 1996 Newark Bay Reach A Sediment Sampling Program
 - Q 1997 Newark Bay Reach B,C,D Sampling Program
 - S 1998 Newark Bay Elizabeth Channel Sampling Program
 - T REMAP, 1998
 - U 1999 Late Summer/Early Fall ESP Sampling Program
 - X 1999 Prelim Toxicity Identification Eval
 - Y 1999/2000 Minish Park Monitoring Program
 - a 2000 Spring ESP Sampling Program
 - b 2000 Toxicity Identification Evaluation
 - c 2005 MPI - Newark Bay Phase I Oversight
 - ▲ 2005 Newark Bay RIWP Phase I Sediment Investigation
 - d 2005 USEPA-MPI High Res Sediment Core
 - e 2006 HRSA RI Sampling Program
 - g 1999-2006 Honeywell Intl Sampling
 - i 2007 USEPA-MPI-EMBM Sediment Samples
 - j 2007 USEPA-MPI Dundee High Res Core
 - k 2007 Newark Bay Phase II TSI Sediment Samples
 - 2008 CPG Low Resolution Sediment Coring
 - m 2009 CPG Benthic Sediment Study
 - o 2009 USEPA-MPI Benthic Oversight
 - p 2010 CPG Benthic Sediment Sampling
 - q 2010 USEPA-CDM Benthic Oversight
 - 2011 CPG River Mile 10.9 Data
 - r 2012 CDMSmith Background Benthic Sediment
 - s 2012 CDMSmith Low Res Coring Supplemental
 - t 2012 CPG Background Benthic Sediment
 - v 2012 CPG Low Res Coring Supplemental
 - u 2012 CPG River Mile 10.9 Data
- No Action Gradient IC, Reach Scale Up
 - Deep Dredging
 - Full Capping
 - Focused Capping
 - No Action Gradient IC, Reach Scale Up (Full Reach)

Log Scale Temporal Plots of Total Mercury Sediment Concentrations for No Action and Three Remedial Alternatives (RM-2.6 to -5.25)
Lower Eight Miles of the Lower Passaic River

Figure 6-31

2014

**No Action
Top 15 cm Mercury (mg/Kg-DW) in yr: 1995.75**



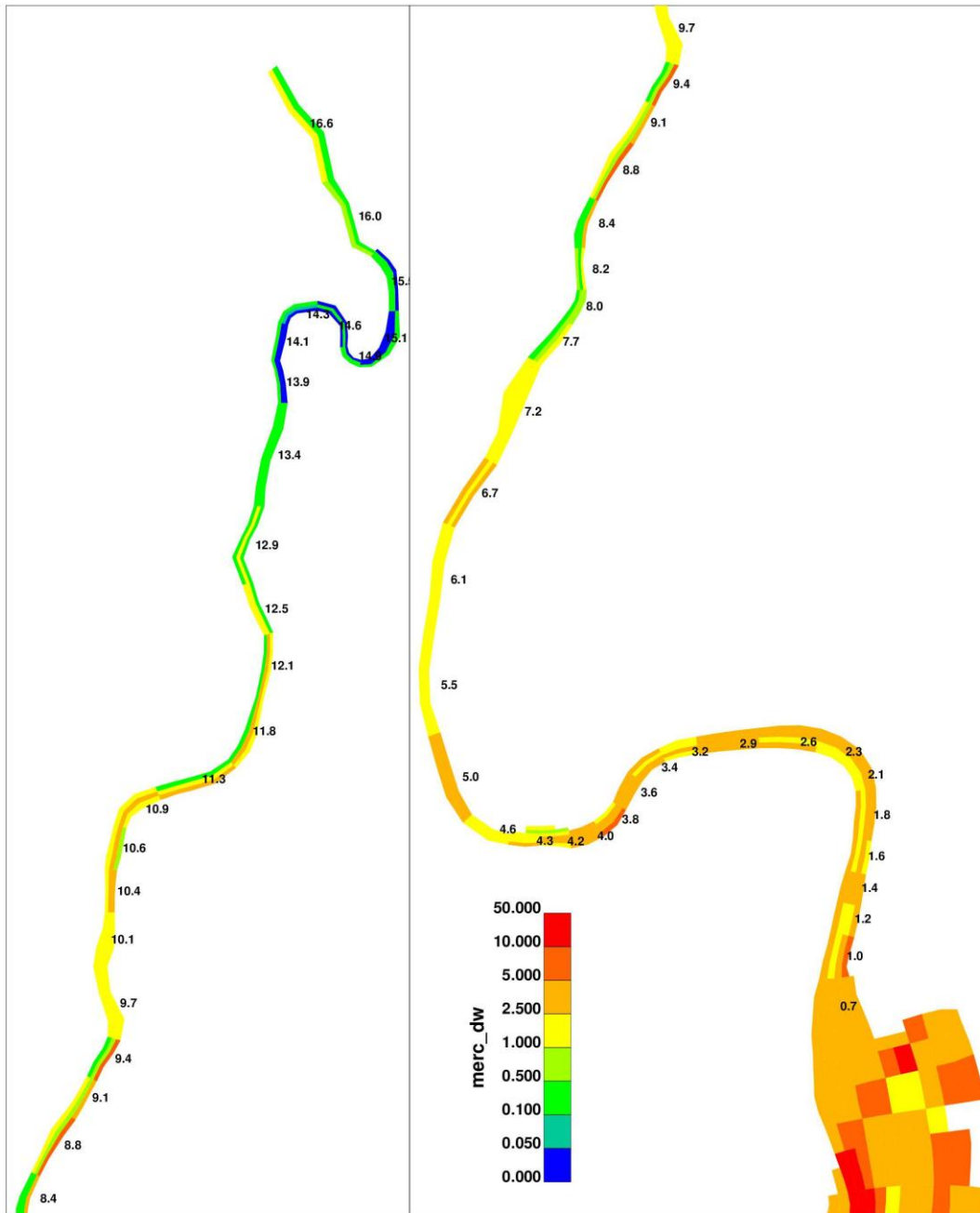
Spatial Distribution of Total Mercury in October 1995

Figure 6-32

Lower Eight Miles of the Lower Passaic River

2014

**No Action
Top 15 cm Mercury (mg/Kg-DW) in yr: 2005.04**



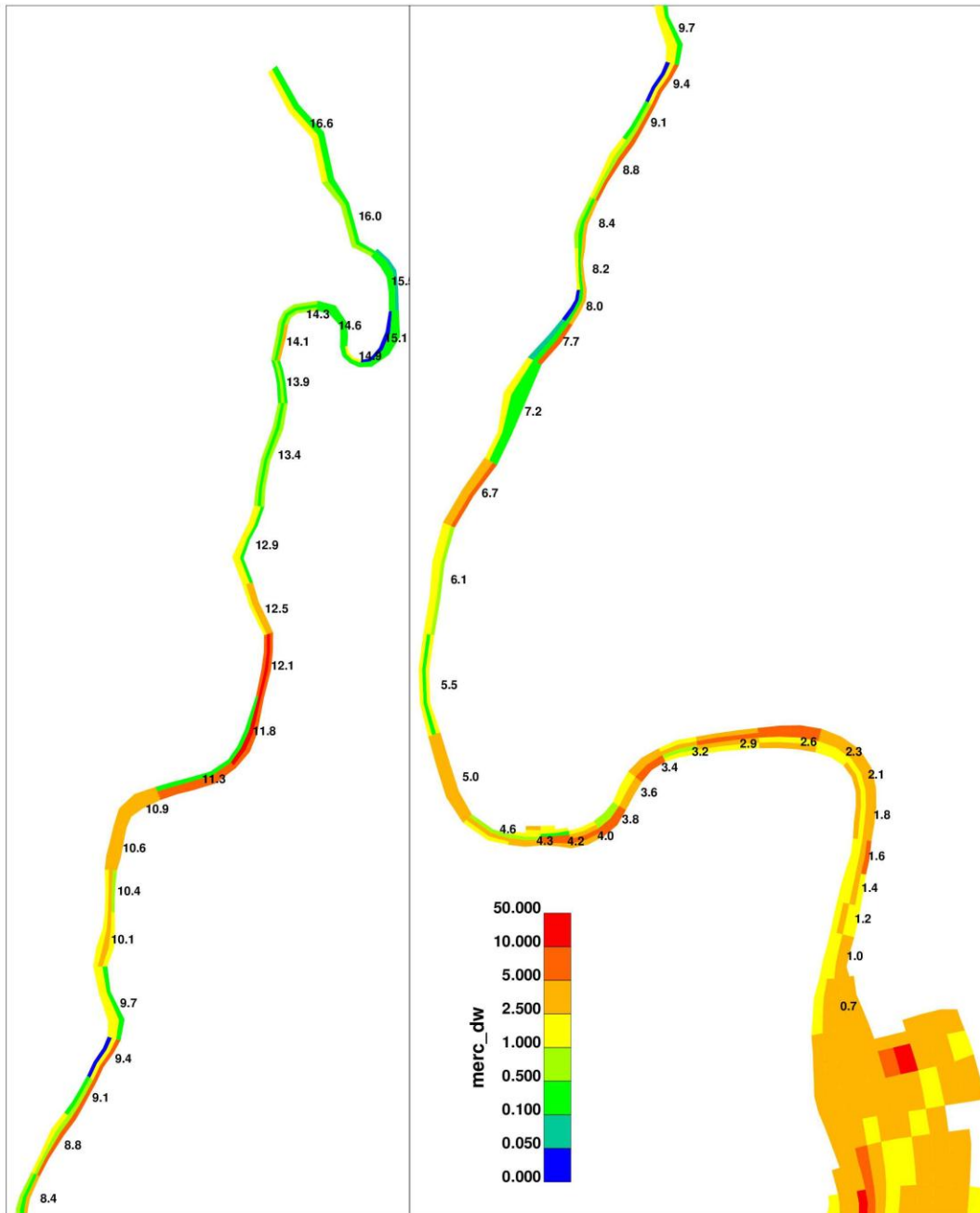
Spatial Distribution of Total Mercury in January 2005

Figure 6-33

Lower Eight Miles of the Lower Passaic River

2014

**No Action
Top 15 cm Mercury (mg/Kg-DW) in yr: 2012.04**



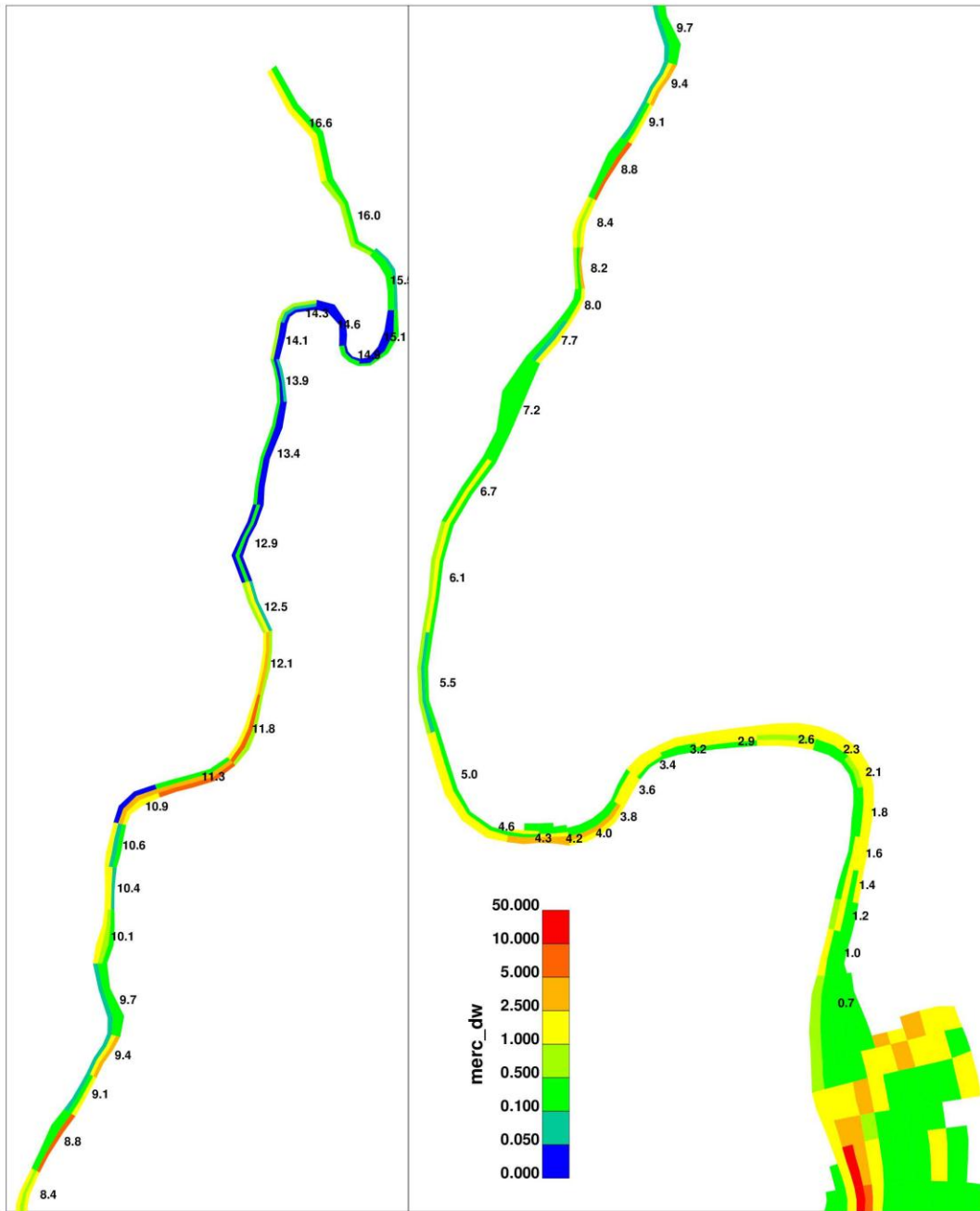
Spatial Distribution of Total Mercury in January 2012

Figure 6-34

Lower Eight Miles of the Lower Passaic River

2014

**No Action
Top 15 cm Mercury (mg/Kg-DW) in yr: 2059.74**



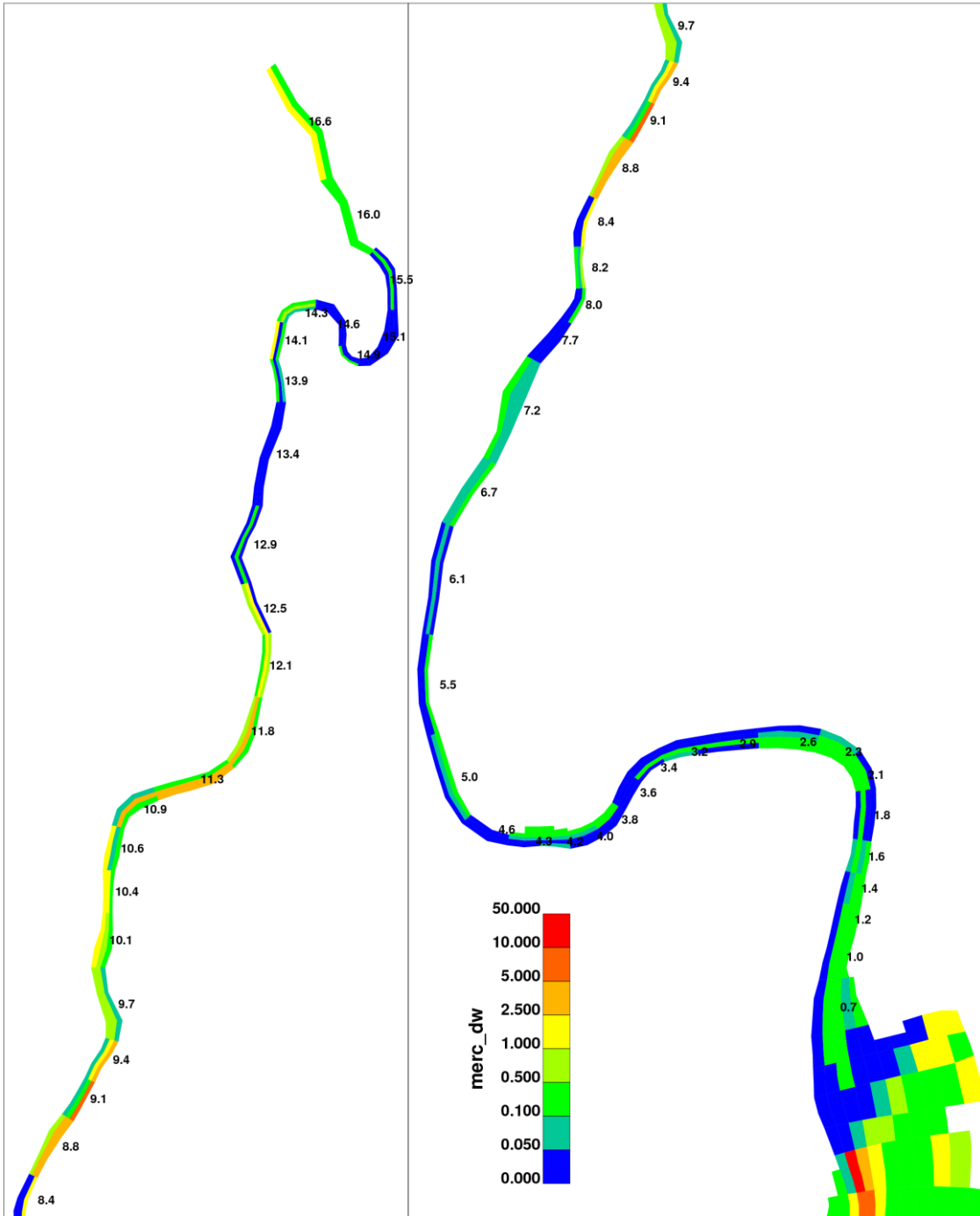
Spatial Distribution of Total Mercury in January 2059 - No Action Simulation

Lower Eight Miles of the Lower Passaic River

Figure 6-35

2014

Dredging
Top 15 cm Mercury (mg/Kg-DW) in yr: 2059.74



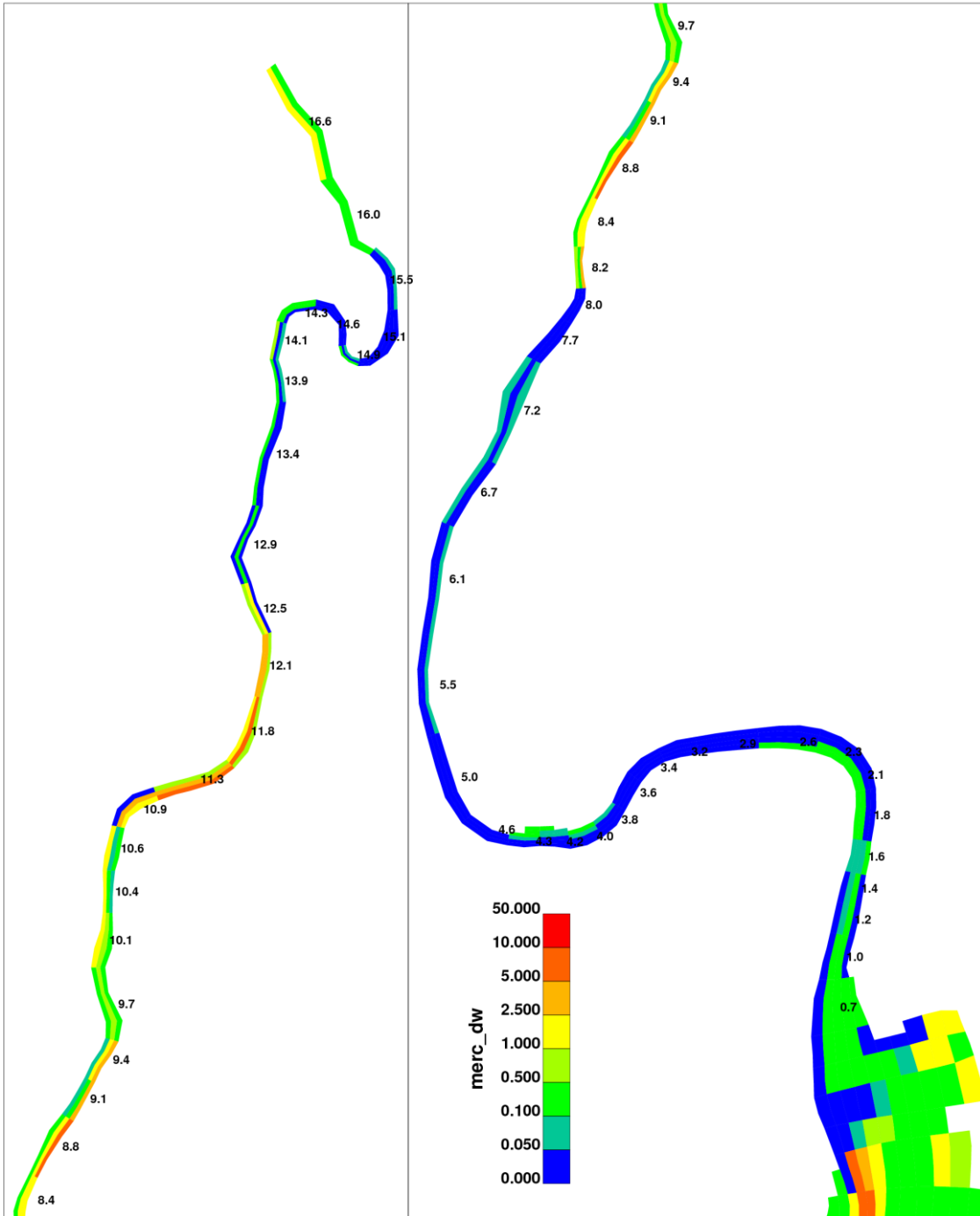
Spatial Distribution of Total Mercury in January 2059 - Deep Dredging Simulation

Lower Eight Miles of the Lower Passaic River

Figure 6-36

2014

Capping
Top 15 cm Mercury (mg/Kg-DW) in yr: 2059.74



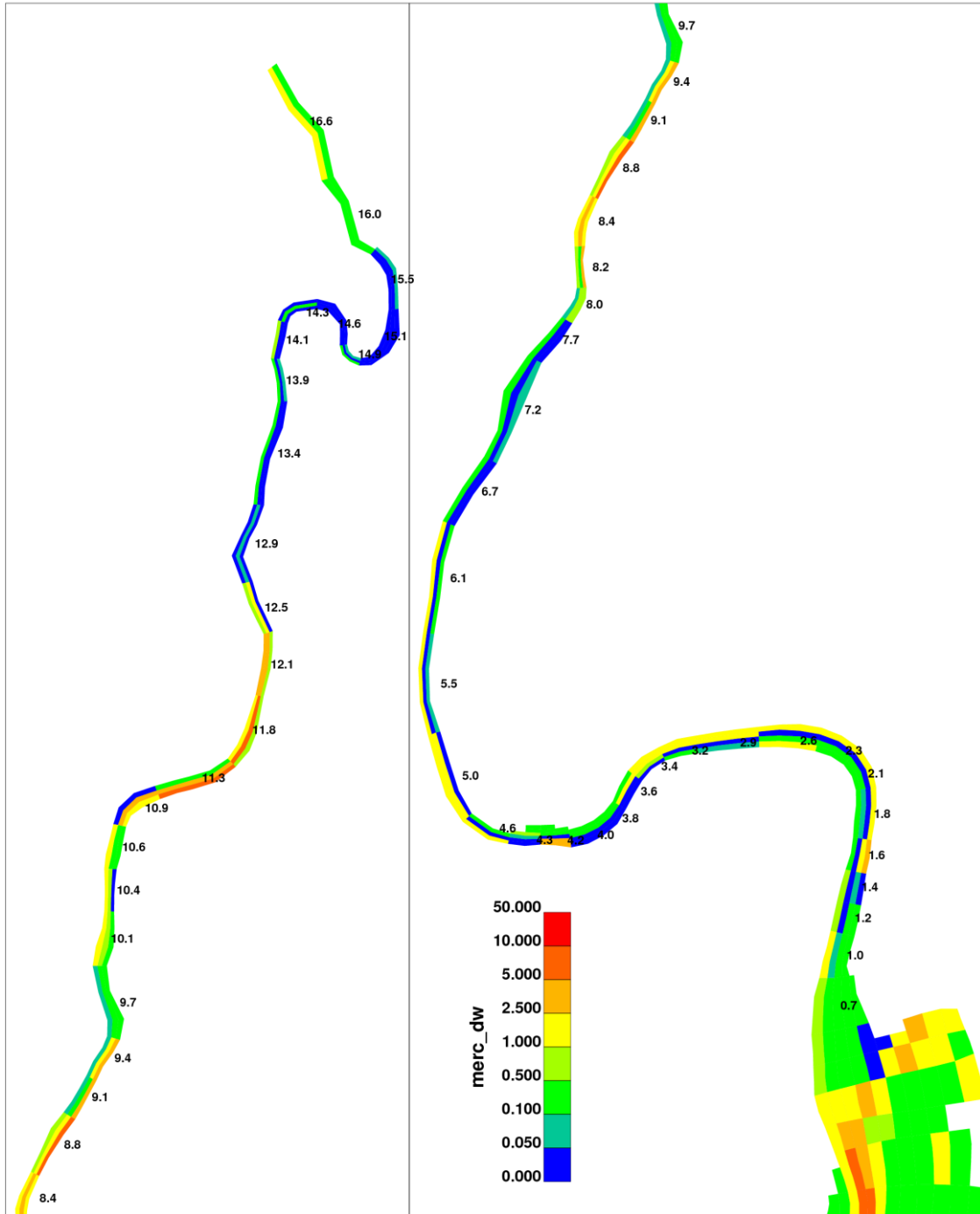
Spatial Distribution of Total Mercury in January 2059 - Full Capping Simulation

Lower Eight Miles of the Lower Passaic River

Figure 6-37

2014

Focused Capping
Top 15 cm Mercury (mg/Kg-DW) in yr: 2059.74

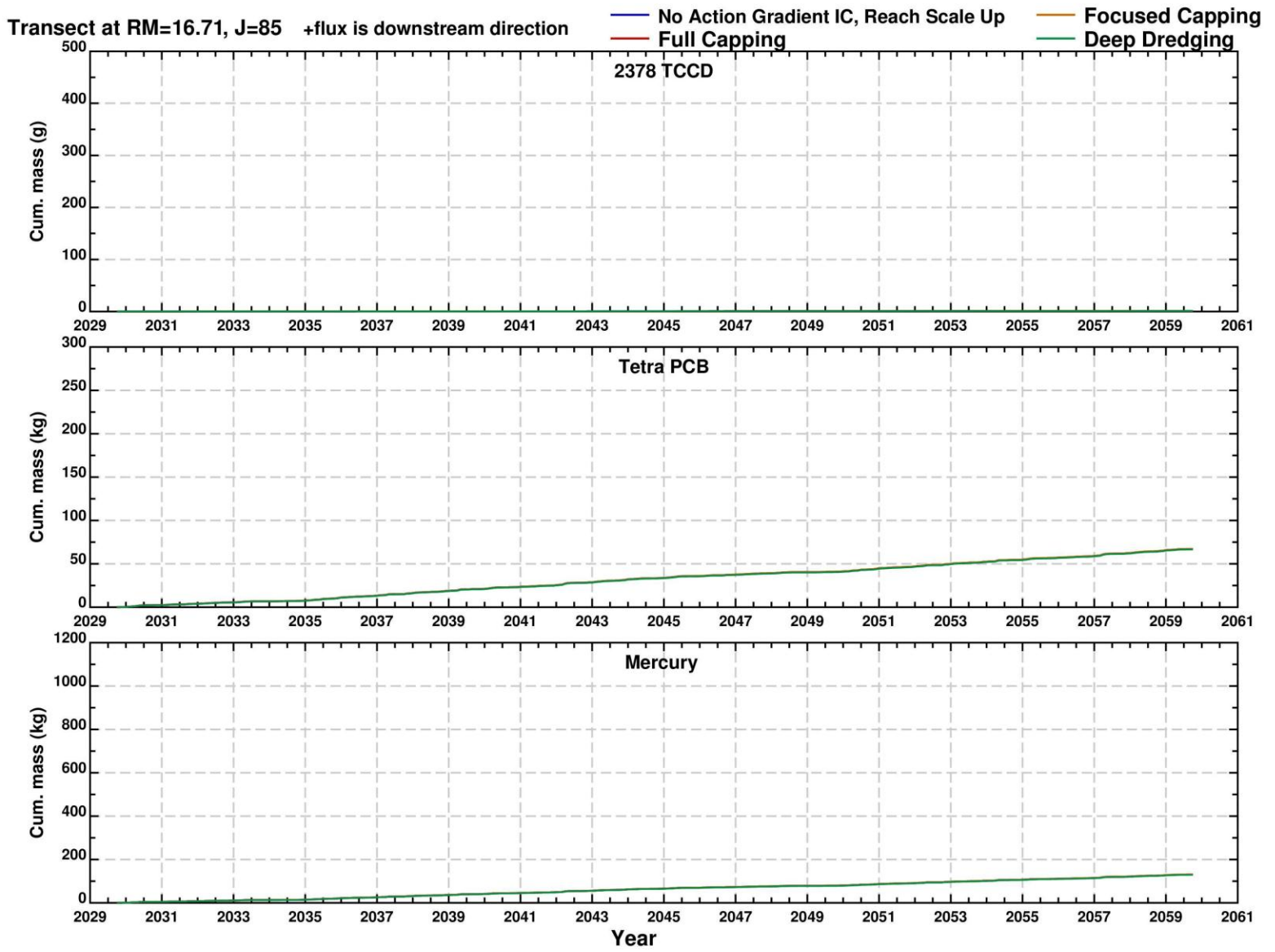


Spatial Distribution of Total Mercury in January 2059 - Focused Capping Simulation

Lower Eight Miles of the Lower Passaic River

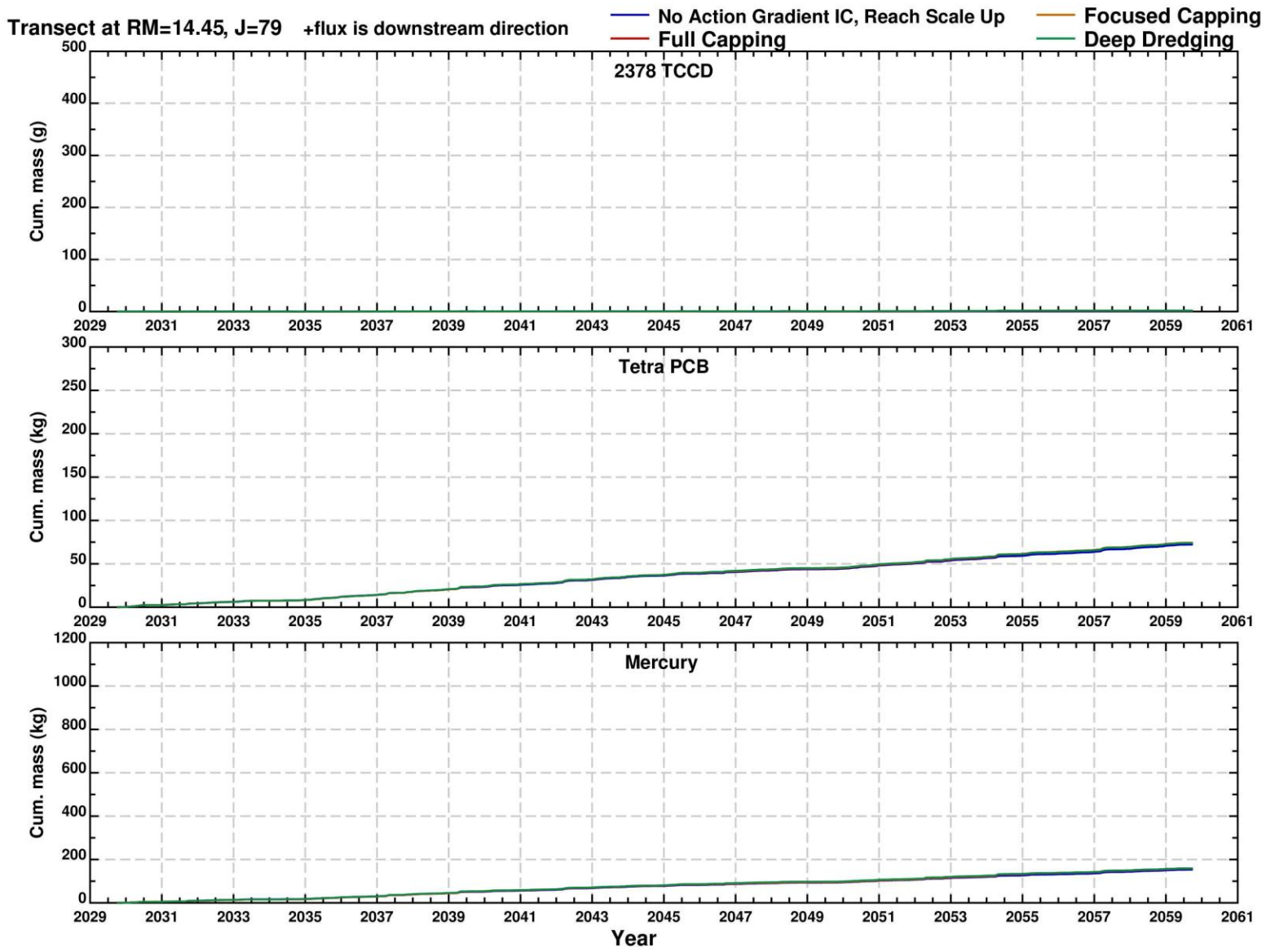
Figure 6-38

2014



Cumulative (from 2024) Water Column Contaminant Mass Transport at RM 16.7

Figure 6-39

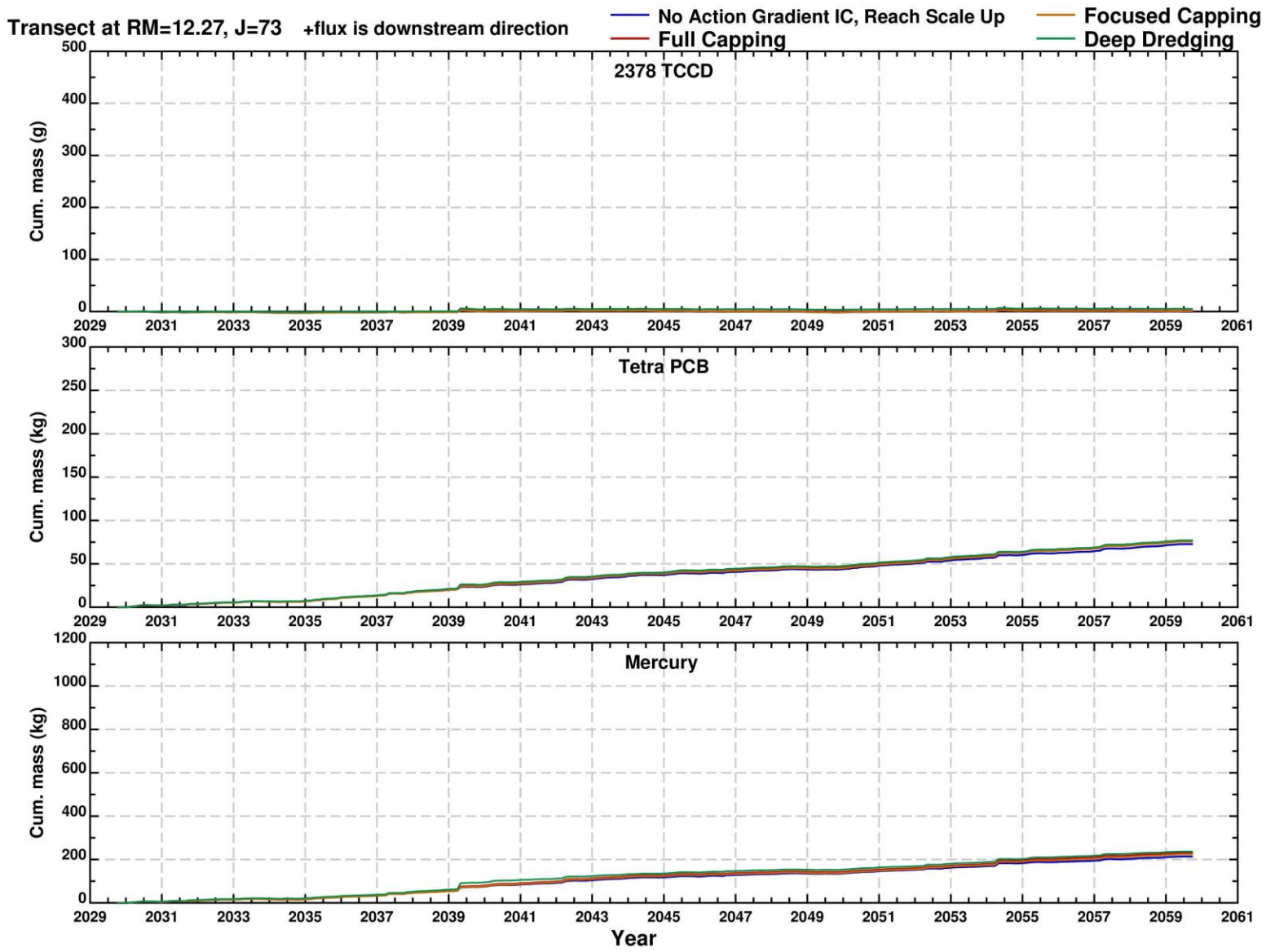


Cumulative (from 2024) Water Column Contaminant Mass Transport at RM 14.5

Figure 6-40

Lower Eight Miles of the Lower Passaic River

2014

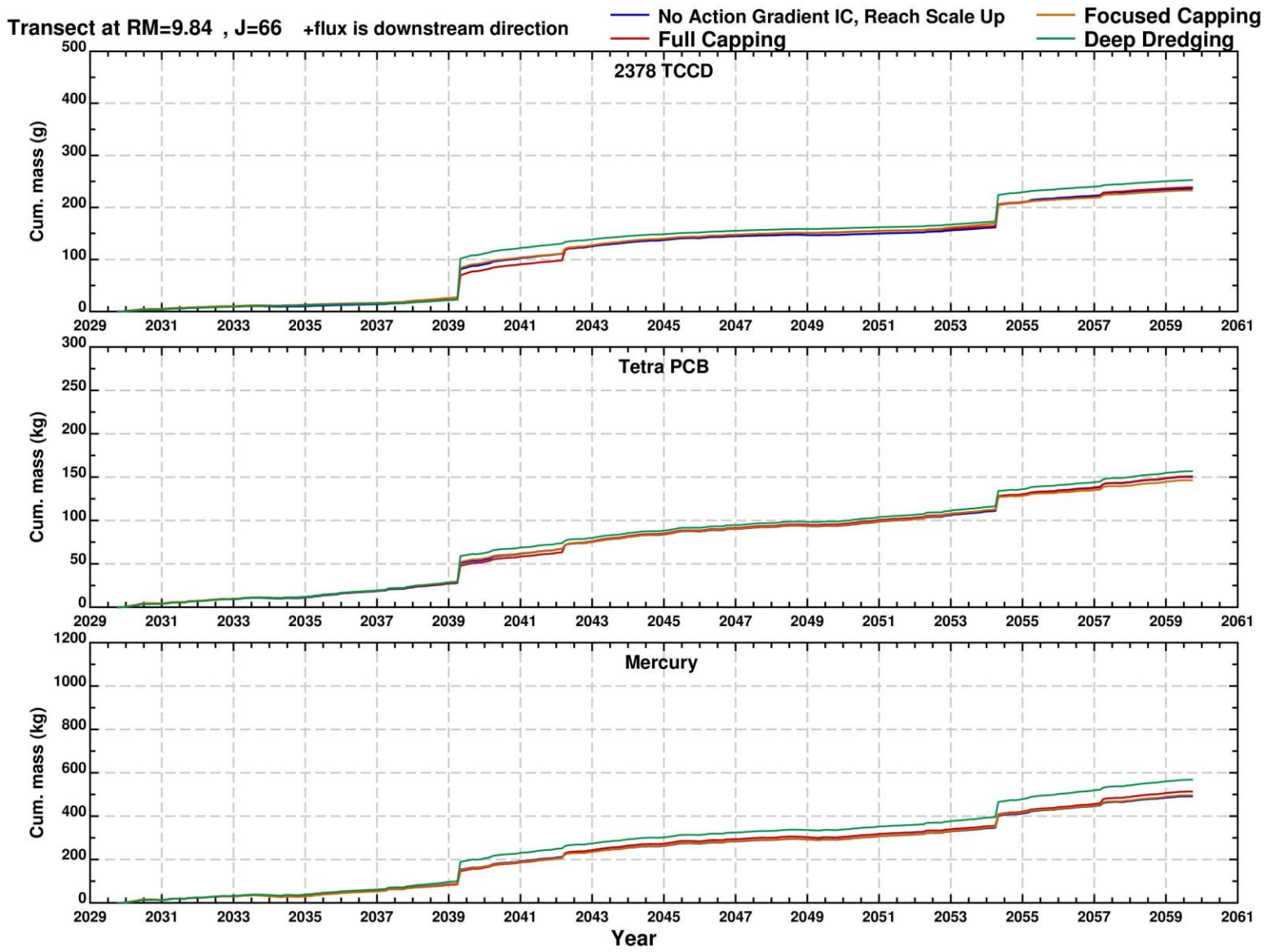


Cumulative (from 2024) Water Column Contaminant Mass Transport at RM 12.3

Figure 6-41

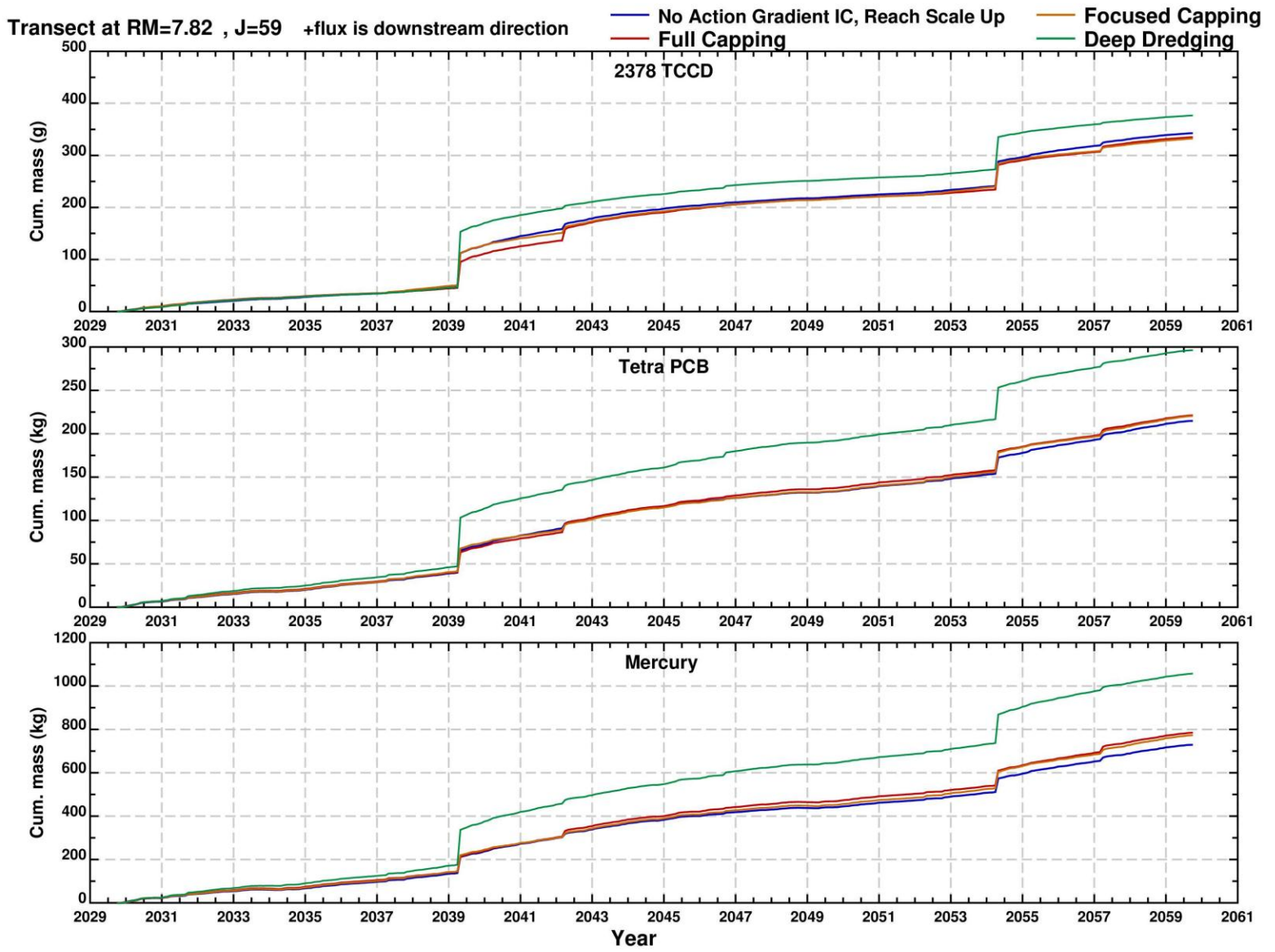
Lower Eight Miles of the Lower Passaic River

2014



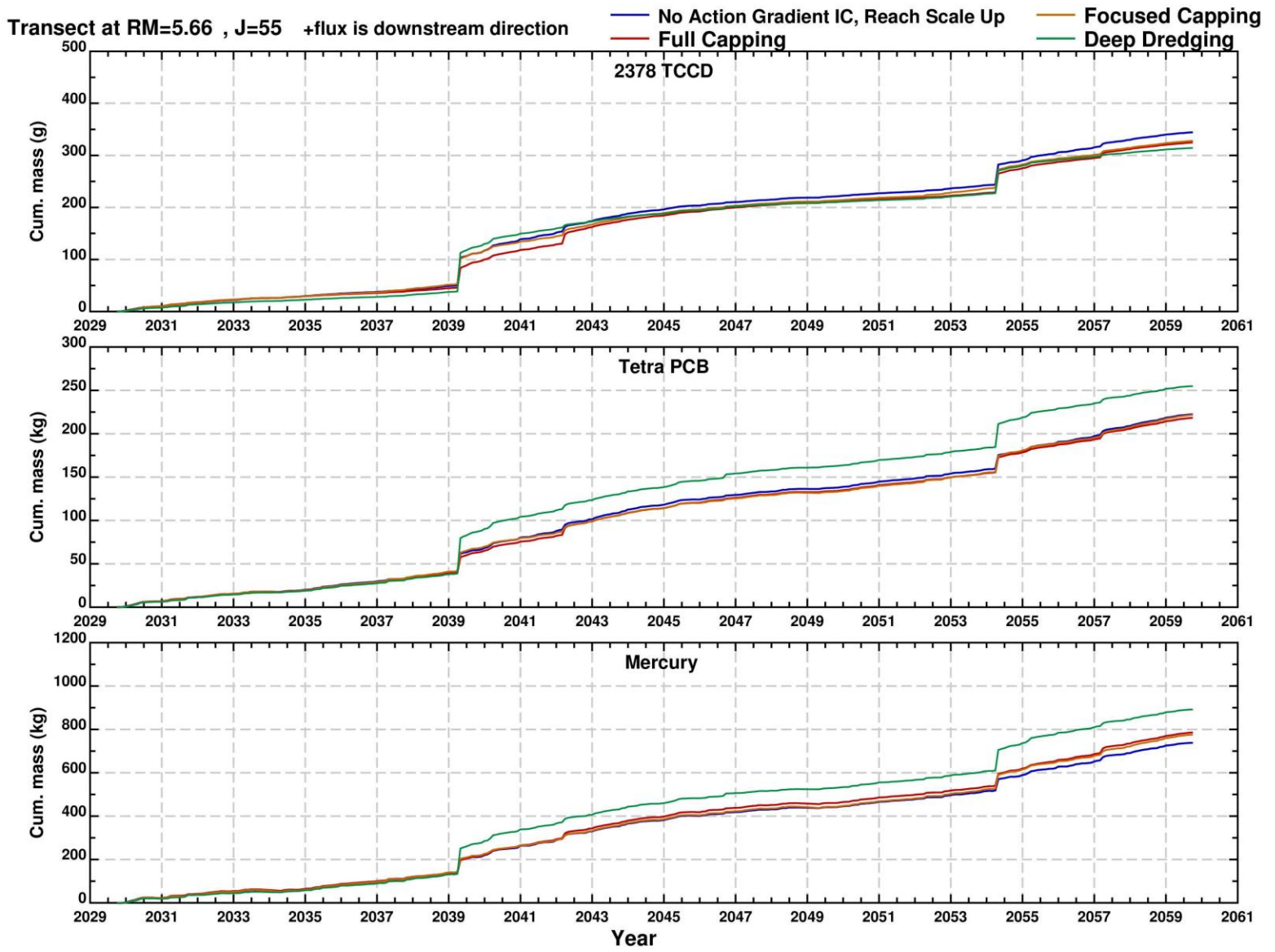
Cumulative (from 2024) Water Column Contaminant Mass Transport at RM 9.8

Figure 6-42



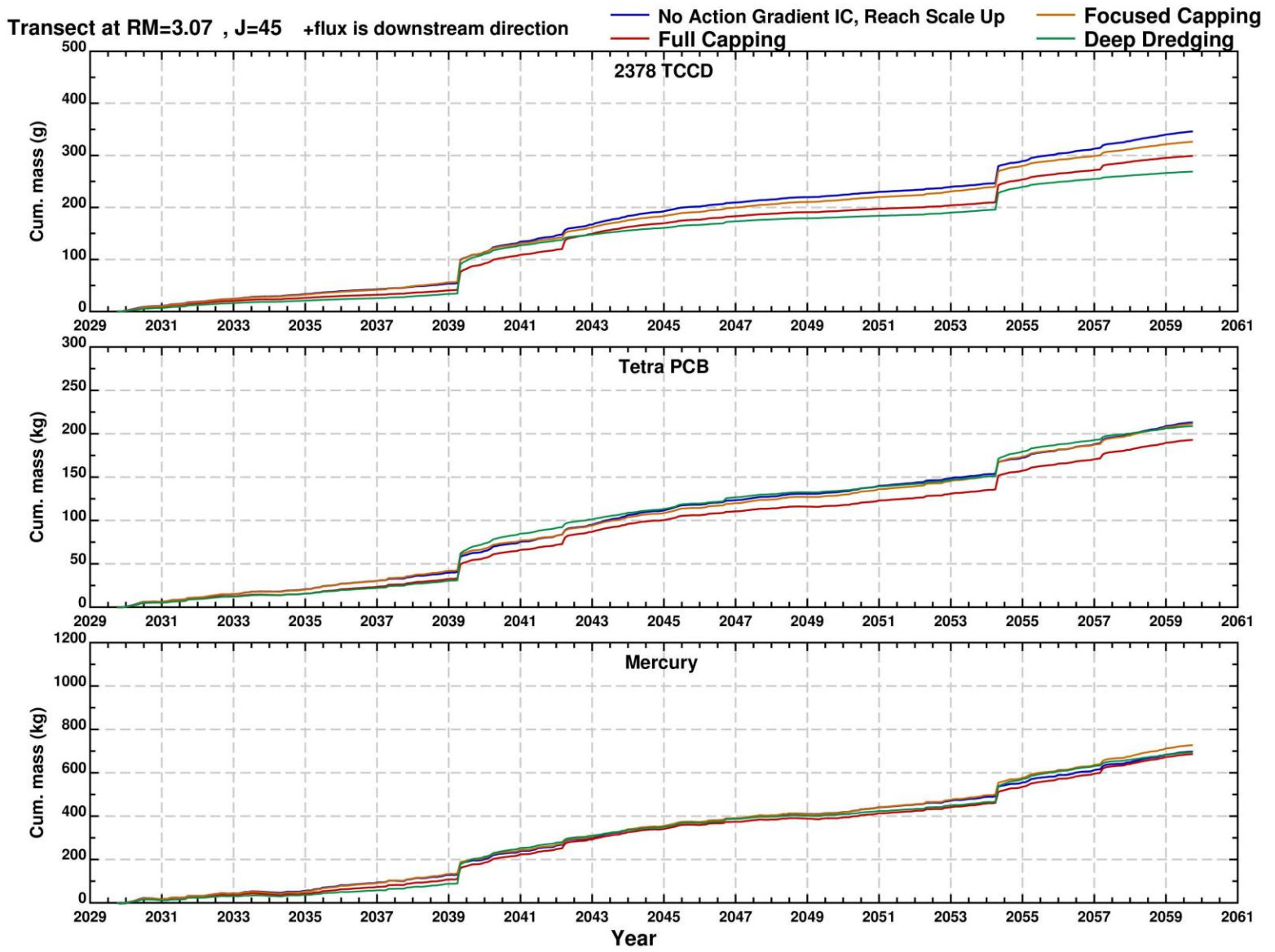
Cumulative (from 2024) Water Column Contaminant Mass Transport at RM 7.8

Figure 6-43



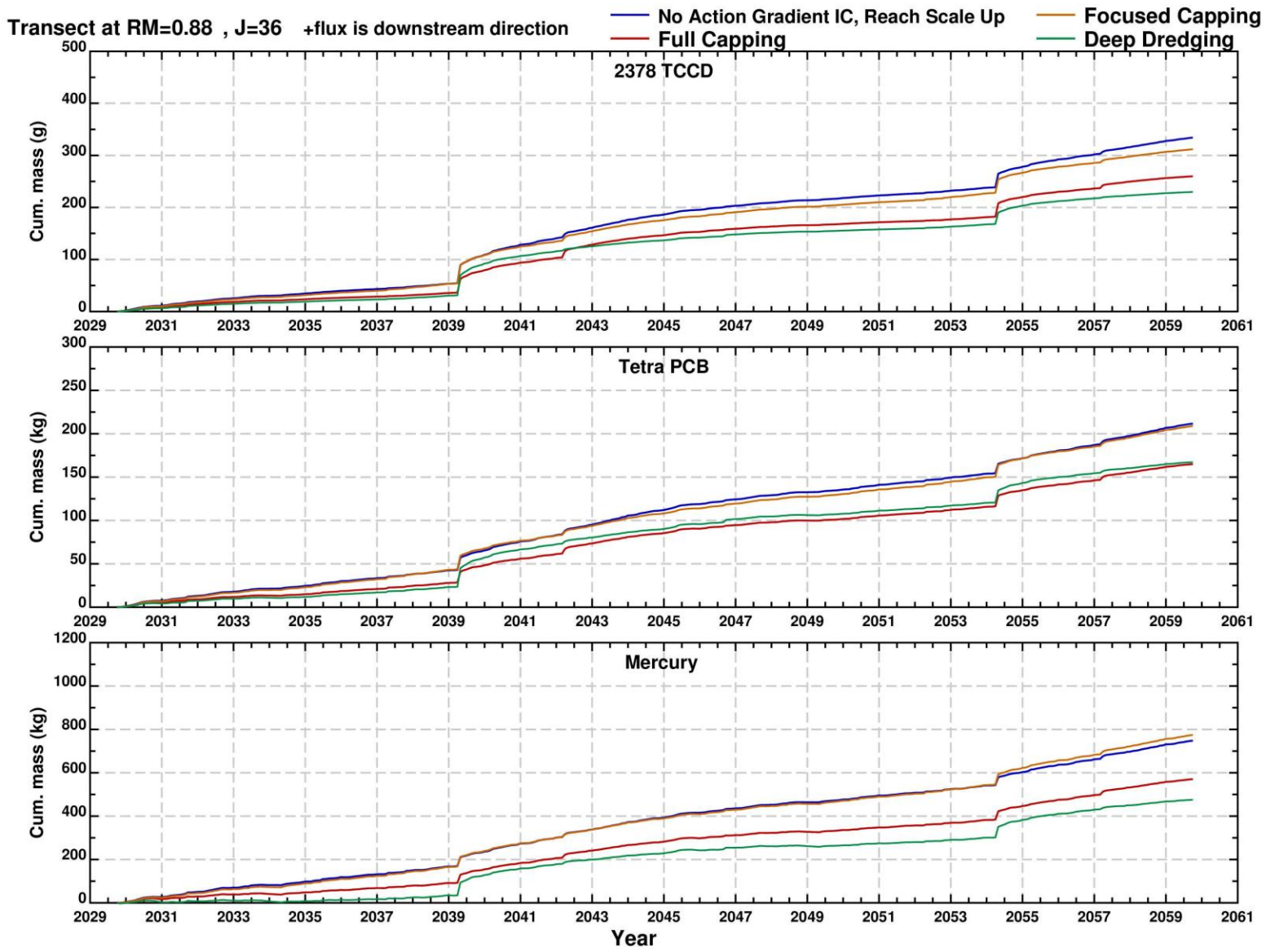
Cumulative (from 2024) Water Column Contaminant Mass Transport at RM 5.7

Figure 6-44



Cumulative (from 2024) Water Column Contaminant Mass Transport at RM 3.1

Figure 6-45

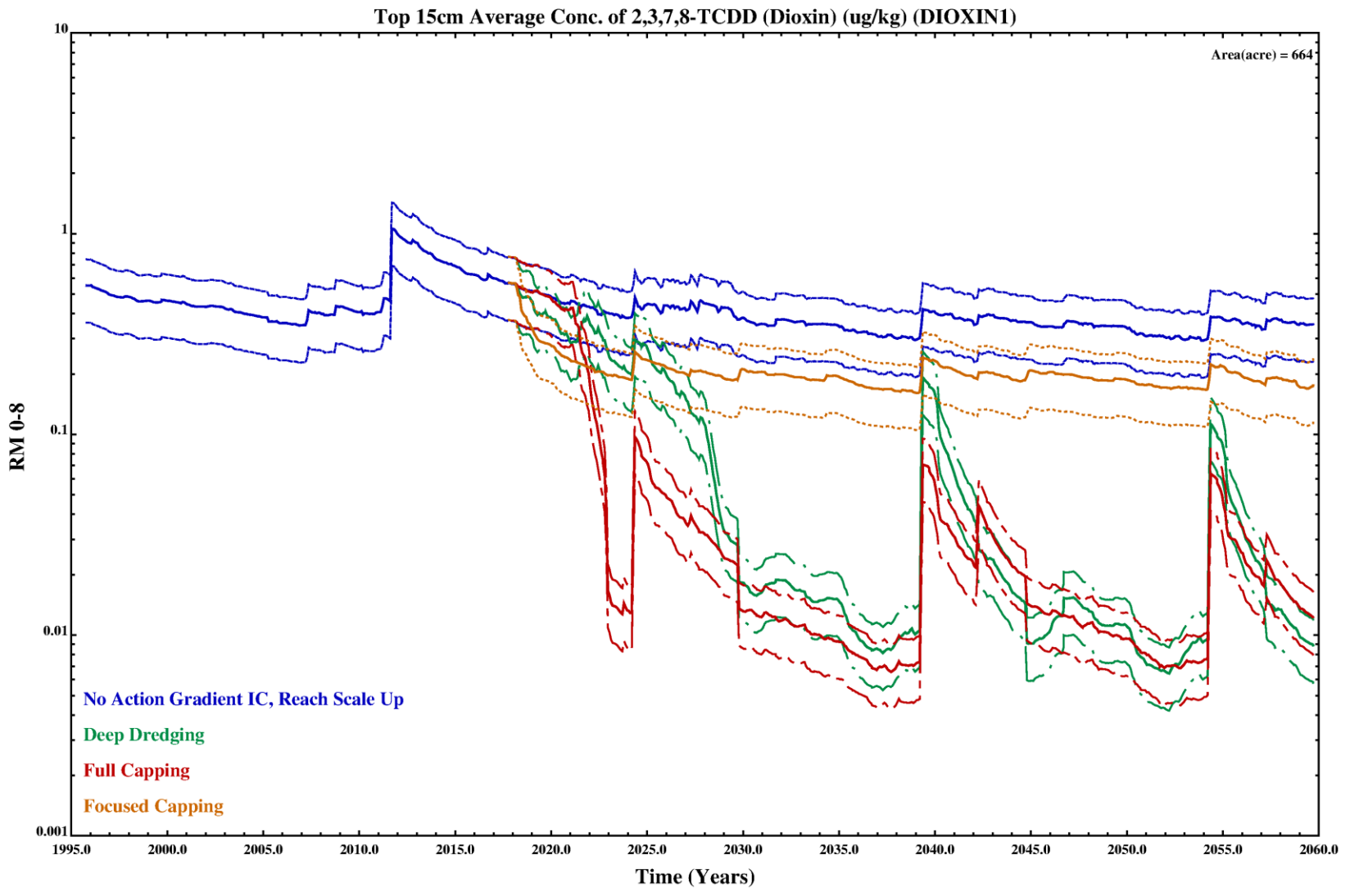


Cumulative (from 2024) Water Column Contaminant Mass Transport at RM 0.9

Figure 6-46

Lower Eight Miles of the Lower Passaic River

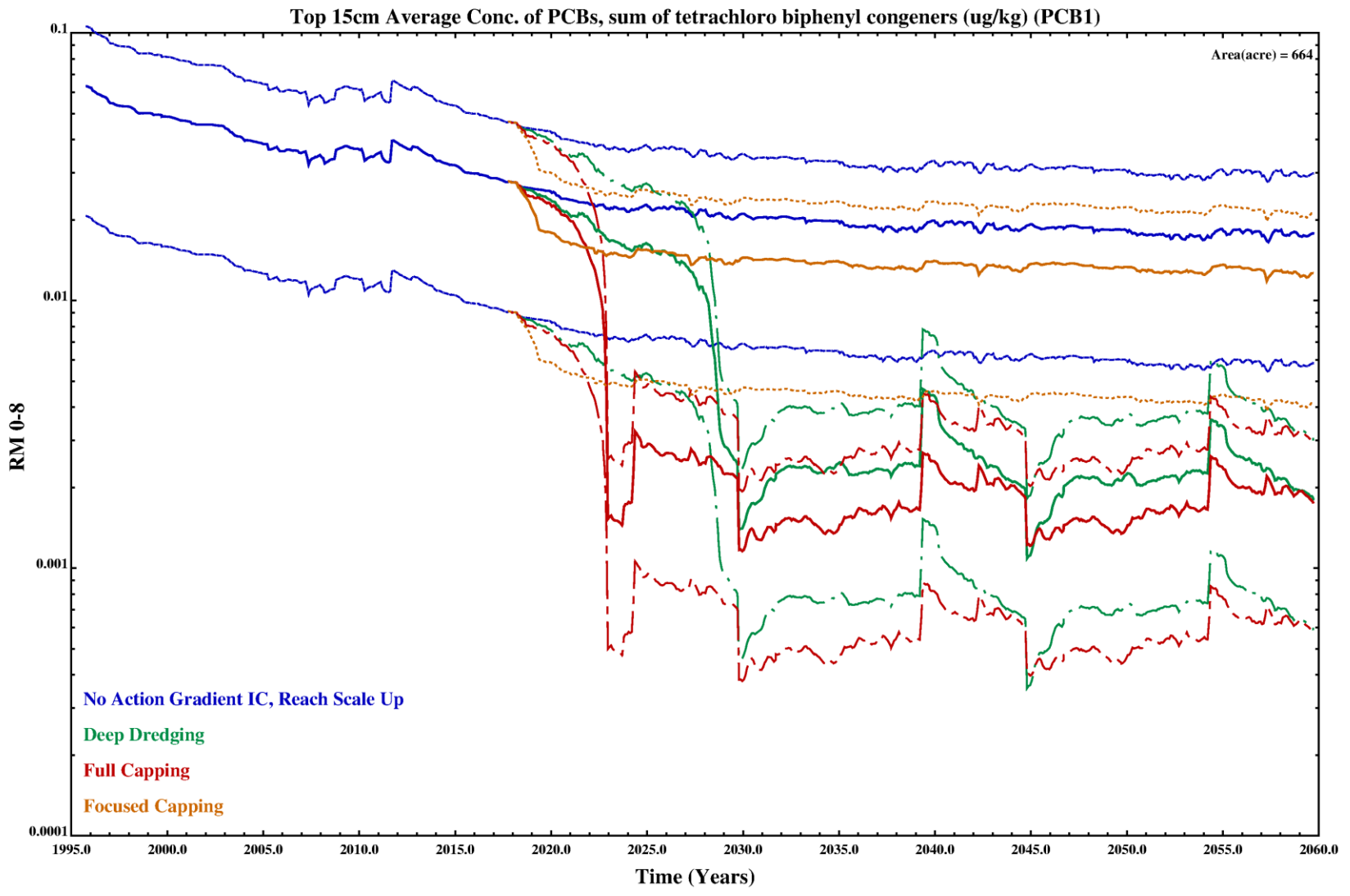
2014



Log Scale Temporal Plots of 2,3,7,8 TCDD Sediment Concentrations for No Action and Three Remedial Alternatives (RM0-8.3) with Uncertainty
Lower Eight Miles of the Lower Passaic River

Figure 6-47

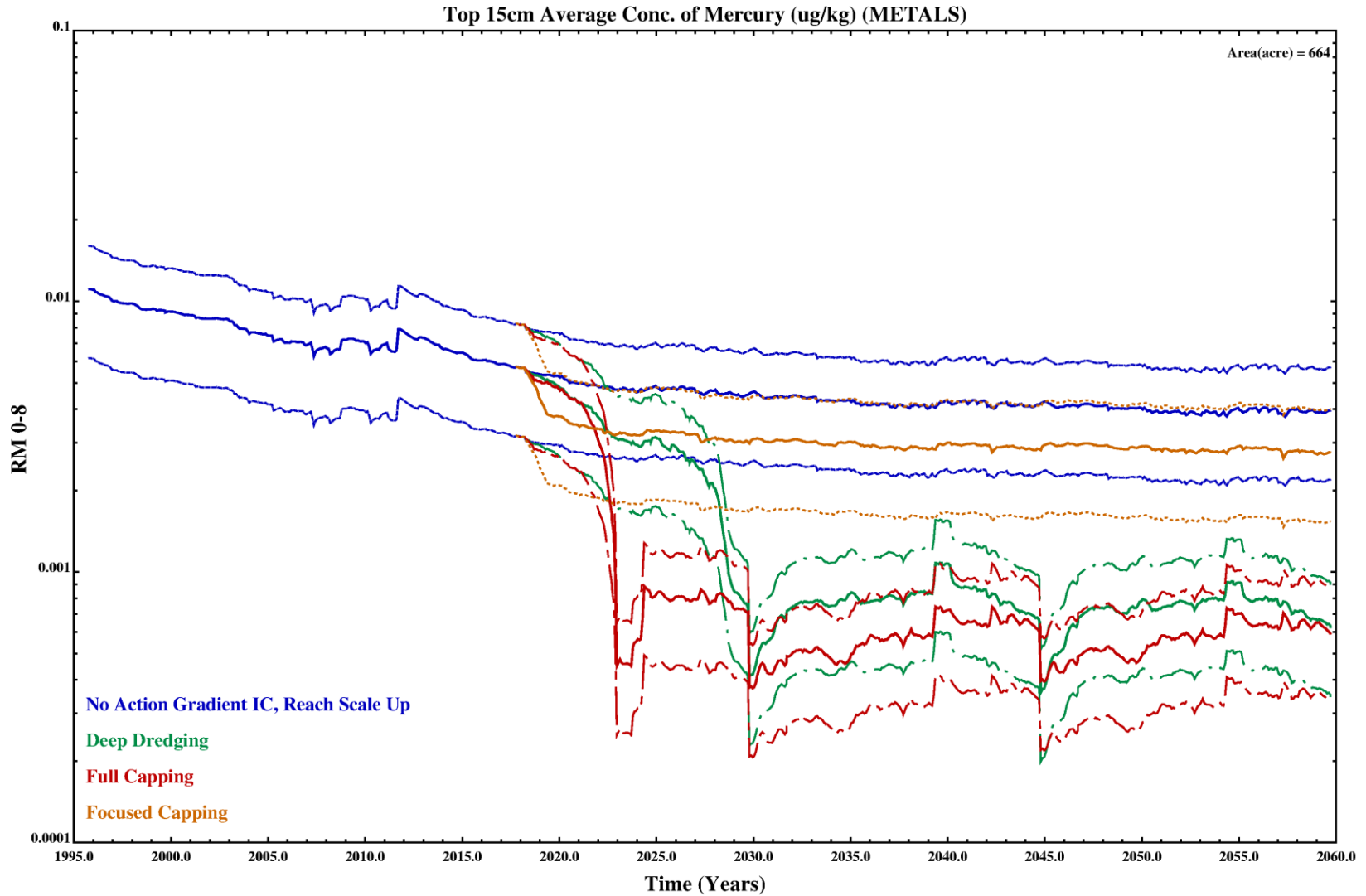
2014



Log Scale Temporal Plots of Tetra-PCB Sediment Concentrations for No Action and Three Remedial Alternatives (RM0-8.3) with Uncertainty
Lower Eight Miles of the Lower Passaic River

Figure 6-48

2014



Log Scale Temporal Plots of Total Mercury Sediment Concentrations for No Action and Three Remedial Alternatives (RM0-8.3) with Uncertainty Bounds

Lower Eight Miles of the Lower Passaic River

Figure 6-49

2014